


8-2015

Changes in Tall Shrub Abundance on the North Slope of Alaska, 2000-2010

Rocio Raquel Duchesne-Onoro
Montclair State University

Follow this and additional works at: <https://digitalcommons.montclair.edu/etd>

 Part of the [Earth Sciences Commons](#), and the [Environmental Sciences Commons](#)

Recommended Citation

Duchesne-Onoro, Rocio Raquel, "Changes in Tall Shrub Abundance on the North Slope of Alaska, 2000-2010" (2015). *Theses, Dissertations and Culminating Projects*. 81.
<https://digitalcommons.montclair.edu/etd/81>

This Dissertation is brought to you for free and open access by Montclair State University Digital Commons. It has been accepted for inclusion in Theses, Dissertations and Culminating Projects by an authorized administrator of Montclair State University Digital Commons. For more information, please contact digitalcommons@montclair.edu.

CHANGES IN TALL SHRUB ABUNDANCE ON THE NORTH SLOPE OF ALASKA,

2000-2010

A DISSERTATION

Submitted to the Faculty of
Montclair State University in partial fulfillment
of the requirements
for the degree of Doctor of Philosophy

by

ROCIO RAQUEL DUCHESNE-ONORO

Montclair State University

Montclair, NJ

2015

Dissertation Chair: Mark J. Chopping, PhD

Copyright © 2015 by *Rocio R. Duchesne-Onoro*. All rights reserved.

MONTCLAIR STATE UNIVERSITY
THE GRADUATE SCHOOL
DISSERTATION APPROVAL

We hereby approve the Dissertation
CHANGES IN TALL SHRUB ABUNDANCE ON THE
NORTH SLOPE OF ALASKA, 2000-2010

of

Rocio R. Duchesne-Onoro

Candidate for the Degree:

Doctor of Philosophy

Dissertation Committee:

Department of Earth &
Environmental Studies

Certified by:

[Redacted Signature]

Dr. Joan C. Ficke
Dean of The Graduate School

8/18/15

Date

[Redacted Signature]

Dr. Mark Chopping
Dissertation Chair

[Redacted Signature]

Dr. Sandra Passchier

[Redacted Signature]

Dr. Dirk Vanderklein

[Redacted Signature]

Dr. Marc Imhoff

ABSTRACT

CHANGES IN TALL SHRUB ABUNDANCE ON THE NORTH SLOPE OF ALASKA, 2000-2010

by Rocio Raquel Duchesne-Onoro

The observed greening of Arctic vegetation and the expansion of shrubs in the last few decades has likely had profound implications for the tundra ecosystem, including feedbacks to climate. Uncertainty surrounding the magnitude, direction, and implications of this vegetation shift calls for monitoring of vegetation structural parameters, such as fractional cover of shrubs. Due to the extent of the North Slope of Alaska and its extreme environments, remote sensing may be the most suitable tool to produce wall-to-wall fractional shrub cover maps for the entire region, however, most regional maps have relied on vegetation indices or needed many years worth of data to cover the whole region. Here, a new mapping approach is presented that uses satellite imagery from the Multi-angle Imaging SpectroRadiometer (MISR) sensor and some landscape variables to predict tall shrub (> 0.5 m) cover with the ultimate goal of evaluating temporal changes in tall shrub fractional cover during the period of 2010-2000. Specifically, we: 1) undertook two field surveys in the North Slope of Alaska to obtain estimates of tall shrub cover, canopy height, crown radius, and total number of shrubs at 26 sites (250 m × 250 m each); 2) evaluated the ability of the semi-automated image interpretation algorithm CANAPI - CANopy Analysis from Panchromatic Imagery, to derive structural data for tall (> 0.5 m) shrubs in the Arctic; 3) constructed a robust reference database with estimates of shrub structural parameters; 4) trained and validated the boosted regression

tree model to predict tall shrub fractional cover from moderate resolution imagery; 5) created the 2000 and the 2010 tall shrub fractional cover map for the North Slope of Alaska; and 6) evaluated the changes in shrub abundance during the period 2010-2000 in the North Slope of Alaska. Results from the field surveys suggested that tall shrub fractional cover was less than 5% at 250 m scales. The evaluation of the CANAPI algorithm showed that CANAPI could successfully retrieve fractional cover ($R^2 = 0.83$, $P < 0.001$), mean crown radius ($R^2 = 0.81$, $P < 0.001$), and total number of shrubs ($R^2 = 0.54$, $P < 0.001$) from very-high resolution imagery. As a result, a robust reference database was constructed with estimates of tall shrub fractional cover, canopy radius, and total number of shrubs for 1,039 sites across the domain of the North Slope. After the training and validation of the Boosted Regression Tree (BRT), the best model used 14 predictor variables and explained 52% of the variation in the response variable, fractional cover. The red reflectance, slope, nadir Bidirectional Reflectance Distribution Function (BRDF) adjusted weight of determination, and isotropic scattering kernel were the variables more often used to generate the regression trees, and therefore they contributed the most to the model. The trained BRT model was used to construct the tall shrub fractional cover map for the year 2000 and 2010 using moderate resolution imagery. The maps revealed that cover ranged from 0.00 to 0.21 and about 75% of the sites had a fractional cover less than 0.013. High cover values were predicted along floodplains, creeks, and sloped terrain. The 2000 MISR-derived fractional cover map presented here outperformed the 2000 Landsat-derived tall shrub fractional cover map when compared to the robust validation data set ($R^2 = 0.38$, Root Mean Square Error (RMSE) = 0.08).

Temporal comparisons of tall shrub abundance in the MISR-derived maps suggested that shrubs expanded during the period 2000-2010. The extent of the area that unequivocally experienced a robust change in tall shrub cover was less than 1 % (1,487 km²) of the total area of the North Slope of Alaska (213,090 km²). It is possible that tall shrubs may have expanded throughout a larger area but there is insufficient precision in the MISR-based estimates to make an unequivocal determination. Nevertheless, it seems that there was a positive trend toward an increase in shrub cover considering that 95% of the locations that had a robust change saw an increase. The tall shrub cover expansion rate varied between 0.006 yr⁻¹ and 0.017 yr⁻¹, being higher along the forest-tundra ecotone, north of the Brooks Range. More research is necessary to determine if the increase in cover corresponded to the advance of the tree line, or to the expansion of the tall shrubs, or both.

ACKNOWLEDGMENTS

This work was supported by two grants. The first one was a National Aeronautics and Space Administration (NASA) Terrestrial Ecology Program Award (NNX09AL03G "Mapping Changes in Shrub Abundance and Biomass in Arctic Tundra using NASA Earth Observing System Data: A Structural Approach") to the chair of my committee, Dr. Mark Chopping. Through this grant I received financial support for three and a half years as a research assistant to work on this project and conducted the first field campaign to Alaska. The second one was a Graduate Student Research grant awarded to me by the Geological Society of America (GSA). This grant, together with supporting funds from the NASA grant, allowed me to carry out a second field campaign to the study area. Financial support in the form of teaching assistantship was also received from Montclair State University to cover the fifth and last year of this study. High-resolution imagery for the training and validation of the boosted regression tree model was obtained from the National Geospatial-Intelligence Agency (NGA) website (cad4nasa.gsfc.nasa.gov).

Special thanks to Dr. Mark Chopping, my committee chair and advisor, for his constant support and words of encouragement. He gave me the opportunity to participate in a large scale project with NASA and help me network with top notch scientists. His constructive feedback enriched this dissertation. Thanks to the members of the dissertation committee Dr. Sandra Passchier, Dr. Dirk Vanderklein, and Dr. Marc Imhoff for their advice and guidance. They shared their views on the topic with me which helped to improve the quality of the dissertation as a whole. Thanks to field assistants Jesse

Carlstrom, Michael Cohrs, and Scott Buchanan, who participated in the data collection during the expeditions to the Arctic. Thanks to my colleagues in the doctoral program who made of my journey in Montclair State University a pleasant experience.

I would like to give thanks to God whom I love, the One who has shepherded me all the days of my life and without His grace and mercy I would not have had the strength to finish this research. Thanks to my beloved husband, Joel Colon, who supported me all the way during this process. He gave me words of encouragement when I thought it was not possible, and helped me in many practical ways while I was working in the dissertation. Thanks to my dear father, Paulo Duchesne, and my precious mother, Nieves Onoro, for instilling in me a spirit of self development from my childhood, they are role models to me.

DEDICATION

To Jesus Christ be the glory forever and ever, Amen.

TABLE OF CONTENTS

Content	Page
ABSTRACT	<i>iv</i>
ACKNOWLEDGEMENT	<i>vii</i>
DEDICATION	<i>ix</i>
LIST OF TABLES	<i>xv</i>
LIST OF FIGURES	<i>xvi</i>
LIST OF ABBREVIATIONS	<i>xxi</i>
CHAPTER 1	1
1.1. Introduction	1
1.2. Research Objectives	9
1.3. Organization of Thesis	11
1.4. References	13
CHAPTER 2	20
Construction of a Robust Reference Database with Estimates of Shrub Structure from Field Surveys and Very-High Resolution Imagery	20
Abstract	20
2.1. Introduction	22
2.2 Materials and Methods	25
2.2.1. Study Area and Site Selection	25
2.2.2. Target Shrub Population	32

Content	Page
2.2.3. Transect Method and Sampling Strategy	32
2.2.4. Optimizing Field Sampling	33
2.2.5. Sampling Shrub Parameters	35
2.2.6. Deriving Shrub Site Parameters using the Belt Transect	37
2.2.7. CANAPI Estimates and Calibration Equations	38
2.2.8. Expansion of the Reference Database	41
2.3. Results and Discussion	41
2.3.1. Optimizing Field Sampling	41
2.3.2. Shrub Estimates from Field Surveys	43
2.3.3. CANAPI Estimates and Calibration Equations	46
2.3.4. Enlargement of Reference Database	49
2.4. Conclusion	52
2.5. References	53
CHAPTER 3	60
Training and Validation of Boosted Regression Tree Model to Predict Shrub Cover from Moderate Resolution Imagery.....	60
Abstract	60
3.1. Introduction	62
3.2. Materials and Methods	67
3.2.1. Data Sources	67
3.2.2. MISR Data Processing	70

Content	Page
3.2.3. Training and Validation of the Boosted Regression Tree Model	71
3.3. Results and Discussion	74
3.3.1. Transformation of the Response Variable	74
3.3.2. Identification of Monotonic Variables and Simplification of the BRT Model	75
3.3.3. Relative Contribution of the Explanatory Variables to the BRT Model ...	81
3.3.4. Interaction Between Explanatory Variables in the Model	88
3.3.5. Validation of the BRT Model	90
3.4. Conclusion	91
3.5. References	92
CHAPTER 4	100
Construction of the 2000 Shrub Fractional Cover Map and Comparison to Existing Maps for the North Slope of Alaska	100
Abstract	100
4.1. Introduction	102
4.2. Materials and Methods	108
4.2.1. Data Sources	108
4.2.2. MISR Data Processing	110
4.2.3. Boosted Regression Tree	112
4.2.4. Work Flow for the Creation of the 2000 Shrub Cover Map of Arctic Alaska	113

Content	Page
4.2.5. Comparison of the Fractional Cover Map with the Arctic Bioclimatic Subzones Map	116
4.2.6. Comparison of the Fractional Cover Map with the 2000 Circa Fractional Cover Map	117
4.3. Results and Discussion	117
4.3.1. MISR-derived Tall Shrub Cover Map of Arctic Alaska for the Year 2000	117
4.3.2. Comparison of the 2000 MISR Map with the Arctic Bioclimatic Subzones	121
4.3.3. Comparison of Predicted Fractional Cover between the 2000 MISR Map and the 2000 Landsat Map	123
4.4. Conclusion	130
4.5. References	131
CHAPTER 5	138
The 2010 Tall Shrub Fractional Cover Map and Temporal Changes in Shrub Abundance in the North Slope of Alaska, 2000-2010	138
Abstract	138
5.1. Introduction	140
5.2. Materials and Methods	145
5.2.1. Data Sources	145

Content	Page
5.2.2. Production of the 2010 Tall Shrub Cover Map	146
5.2.3. Temporal Comparison of the 2000 and 2010 Fractional Cover Maps ...	148
5.3. Results and Discussion	149
5.3.1. Tall Shrub Fractional Cover Map of Arctic Alaska, 2010	149
5.3.2. Temporal Change in Tall Shrub Cover over the Last Decade	154
5.4. Conclusion	163
5.5 References	165
REFERENCES	172
LIST OF APPENDICES	189
Appendix A	190
Appendix B	191
Appendix C	240
Appendix D	241
Appendix E	244
Appendix F	246
Vita	247
Cover page	248

LIST OF TABLES

Table	Page
Table 2-1. Description of 26 field sites (250 m x 250 m each) surveyed during summer 2010 and 2011.....	27
Table 3-1. Relative contribution of the predictor variables to the BRT model. The sum of all the contributions adds to 100.....	82
Table 4-1. Summary of available MISR imagery for years 2000-2002.....	109
Table 4-2. Distribution of tall shrub fractional cover estimates from the MISR-derived map.....	118
Table 4-3. Comparison of tall shrub fractional cover by bioclimatic subzone using Dunn Test. Dunn's pairwise z test statistic followed by the P -value associated with the test in parenthesis.....	123
Table 5-1. Summary of available MISR imagery for years 2010-2011.....	145
Table 5-2. Distribution of fractional cover estimates from 2010 tall shrub cover map...	150
Table 5-3. Relative change in tall shrub cover in the North Slope of Alaska, 2000-2010. Only a significant change (greater than 0.06, the model RMSE was 0.03) is displayed.....	155

LIST OF FIGURES

Figure	Page
<p>Figure 2-1. Map of the North Slope of Alaska. Field sites surveyed during the Colville campaign in 2010 (red dots) and during the Dalton campaign in 2011 (blue dots). Albers Equal Area Conic projection, spheroid WGS 84, datum WGS 84. (Source: AlaskaMapped SDMI WCS layers [downloaded file]. Alaska Mapped, Statewide Digital Mapping Initiative. URL: http://www.alaskamapped.org/data/arcgis-layer-files: [20 February, 2015]).....</p>	26
<p>Figure 2-2. Aerial photograph of the Colville-07 field site and surrounding landscape. The top of the image is the north. Photo credit" Ken Tape (University of Alaska, Fairbanks).....</p>	29
<p>Figure 2-3. Quick Bird, IKONOS, and WorldView panchromatic subsets of the 26 field sampling sites. Each site has an area of 62,500 square meters.....</p>	30
<p>Figure 2- 4. Distribution of belt transects at site Colville-02 (250 m × 250 m) following a systematic sampling strategy with a randomly selected starting point. White dots represent shrubs observed in the QuickBird panchromatic subset.....</p>	36
<p>Figure 2-5. QuickBird panchromatic subsets with shrub crowns delineated by the CANAPI algorithm. Each site is 250 m × 250 m. a. Colville-02, b. Colville-06, c. Colville-10.....</p>	39
<p>Figure 2-6. Map of the physiognomic vegetation types (CAVM, 2003) for the North slope of Alaska. The black boxes represent available high resolution imagery and from which 250 m x 250 m subsets were selected for the reference database.</p>	42
<p>Figure 2-7. Field estimates at 26 sites: a. total number of shrubs, b. mean crown radius, c. fractional cover, and d. shrub height. Colville 2010 campaign (rhomboids) and Dalton campaign 2011 (squares).....</p>	44
<p>Figure 2-8. Plots display the relationship between a) mean shrub height and latitude and b) mean crown radius and latitude for both the Colville (rhomboids) and Dalton (squares) sites. Latitude is expressed in meters, projection Albers Conical Equal Area, Spheroid WGS 84, Datum WGS 84.....</p>	45

Figure	Page
Figure 2-9. Correlations between 'raw' CANAPI estimates and field estimates for four vegetation structural variables (a) fractional cover ($P < 0.001$), (b) mean crown radius ($P < 0.001$), (c) total number of shrubs ($P < 0.001$), and (d) mean height ($P = 0.57$).....	47
Figure 2-10. Histograms of frequency: a. total number of shrubs, b. fractional cover, and c. mean crown radius.....	50
Figure 2-11. Five-number summary. a. Total number of shrubs, b. mean crown radius in meters.....	51
Figure 3-1. Histogram of frequency of the response variable for 1,039 sites of 250 m × 250 m in the North Slope of Alaska. Bin width of 0.015. a. tall shrub fractional cover, b. arcsine transformed tall shrub fractional cover.....	74
Figure 3-2. Partial dependence plots depicting the marginal effect of latitude on the response after accounting for the average effect of all other variables in the model. The fitted function is centered by subtracting its mean: a. latitude was unrestricted, b. latitude was set to be monotonic. Contribution of the variable to the model is in parenthesis.....	76
Figure 3-3. Panchromatic subset of a fractional cover map: a. latitude was not restricted, b. the relationship between latitude and fractional cover was restricted to be monotonic.....	76
Figure 3-4. Partial dependence plot depicting the effect of elevation on the response after accounting for the average effect of all other variables in the model. The fitted function is centered by subtracting its mean: a. elevation was unrestricted, b. elevation was set to be monotonic. Contribution of the variable to the model is in parenthesis.....	77
Figure 3-5. Partial dependence plot depicting the marginal effect of near-infrared reflectance on the response after accounting for the average effect of all other variables in the model. The fitted function is centered by subtracting its mean: a. NIR was unrestricted, b. NIR was restricted. Contribution of the variable to the model is in parenthesis.....	79

Figure	Page
Figure 3-6. Comparison of predicted fractional cover with high resolution imagery: a. subset of Google Earth imagery, b. subset of a preliminary fractional cover map where NIR is unrestricted, c. subset of a second fractional cover map where NIR is restricted.....	80
Figure 3-7. Partial dependence plot depicting the effect of each independent variable on the response after accounting for the average effect of all other variables in the model. The fitted function is centered by subtracting its mean. Contribution of the variable to the model is in parenthesis. a. red reflectance, b. slope, c. NBAR_45W, d. isotropic scattering, e. volumetric scattering, f. geometric scattering, g. white-sky albedo, h. latitude, i. blue reflectance, j. green reflectance, k. black-sky albedo, l. northness, m. eastness, and n. NIR reflectance.....	85
Figure 3-8. Interaction plot depicting the effect of slope and green reflectance on the response variable, ArcFC.....	89
Figure 3-9. Interaction plot depicting the effect of latitude and slope on the response variable, ArcFC.....	89
Figure 3-10. Scatter plot of observed arcsine fractional cover derived from the CANAPI algorithm against the predicted arcsine fractional cover from the BRT model for 305 validation sites.....	90
Figure 4-1. Simplified land cover type for the North Slope of Alaska using the International Geosphere Biosphere Programme global vegetation classification scheme. Source: MODIS Land Cover Type Product, year 2001.....	104
Figure 4-2. Land cover for the North Slope of Alaska based on the National Land Cover Database. Spatial resolution of 30 m . Source: USGS website.....	105
Figure 4-3. Diagram illustrating the processing steps to generate the shrub fractional cover map. Abbreviations used are: HDF (Hierarchical Data Format), BGRN (Blue, Green, Red, and Near-infrared), BRF (Bidirectional Reflectance Factor), PRM (Parameters), ArcFC (Arcsine transformed fractional cover).....	115

Figure	Page
Figure 4-4. Tall shrub fractional cover map for the North Slope of Alaska, year 2000. Fractional cover values were derived from the Boosted Regression Tree model.....	119
Figure 4-5. Portion of the 2000 MISR-derived tall shrub fractional cover map depicting the correlation of high shrub cover along the floodplains of major rivers and water flow lines. Insect A: Major rivers of the North Slope, Insect B: Water flow lines west of the Colville river (source: USGS, The National Map, Hydrography).....	120
Figure 4-6. Section of the Noatak River in the southwestern portion of the North Slope of Alaska. The high values of cover corresponded to a forest of spruce, not shrubs.....	121
Figure 4-7. Boxplots depicting the five number summary (minimum, first quartile, median, third quartile, and maximum) for fractional cover in the three bioclimate subzones.....	122
Figure 4-8. Fractional cover map for the North Slope of Alaska: top, MISR 2000 map, bottom, Landsat 2000 map. Fractional cover was rescaled. Water and ice are not filtered for the Landsat 2000 map.....	124
Figure 4-9. Correlation between observed fractional cover derived from the CANAPI algorithm for 234 sites and the predicted fractional cover derived from the 2000 Landsat map re-projected onto a 250 m grid.	127
Figure 4-10. Correlation of the predicted fractional cover from the 2000 MISR map and the predicted fractional cover values from the 2000 Landsat map for the 234 validation sites.....	128
Figure 4-11. Comparison of predicted shrub cover from the 2000 Landsat map and the 2000 MISR map with false color and panchromatic QuickBird imagery for four selected sites along the Colville River with different shrub cover.....	129
Figure 5-1. Tall shrub fractional cover map for the North Slope of Alaska, year 2010. Fractional cover values derived from the Boosted Regression Tree model and it ranged from 0.0 to 0.2.....	151

Figure	Page
Figure 5-2. Section east of the Noatak River in the southwestern portion of the North Slope of Alaska (A). The high values of cover corresponded to a forest of spruce (C and D), and the transition between trees and shrubs (B).....	152
Figure 5-3. Portion of the 2010 fractional cover map depicting the correlation of high shrub cover along floodplains of major rivers and water tracks. Water flow lines west of the Colville river (source: USGS, The National Map, Hydrography).....	153
Figure 5-4. Change in tall shrub cover (CSC) for the North Slope of Alaska during the period 2000 - 2010. In the legend, the region between -0.06 and 0.06 represents locations where the direction of change is uncertain.....	157
Figure 5-5. Change in tall shrub cover (CSC) depicting increase of tall vegetation. In the legend, the region between -0.06 and 0.06 represents locations where the direction of change is uncertain. A. Noakat River and surrounding areas, B. Floodplains and river terraces, C. Southern boundary of the North Slope of Alaska.....	158
Figure 5-6. Change in tall shrub cover (CSC) depicting decrease of tall vegetation. In the legend, the region between -0.06 and 0.06 represents locations where the direction of change is uncertain. A. Residual effect of compositing technique in white polygon, B. Decrease in a few patches along the Colville River, C. Residual effect of compositing technique within the white polygon and decrease in vegetation cover along the Kiruktagiak River.....	160
Figure 5-7. Tall shrub growth rate against the initial fractional cover in year 2000.....	162

LIST OF ABBREVIATIONS

ArcFC (Arcsine Transform of Fractional Cover)
Arctic Climate Impact Assessment (ACIA)
Algorithm for Modeling Bidirectional Reflectance Anisotropies of the Land Surface (AMBRALS)
Canopy Analysis with Panchromatic Imagery (CANAPI)
Circumpolar Arctic Vegetation Map (CAVM)
Bidirectional Reflectance Distribution Function (BRDF)
Bidirectional Reflectance Factor (BRF)
Blue Reflectance (B)
Boosted Regression Tree (BRT)
Geological Society of America (GSA)
Geometrical Optical Model (GO model)
Green Reflectance (G)
Instantaneous Field of View (IFOV)
Leaf area index (LAI)
Nadir BRDF-adjusted reflectance at solar zenith angle of 45 degrees (NBAR_45)
National Aeronautics and Space Administration (NASA)
Near-infrared reflectance (NIR)
North America Datum of 1983 (NAD83)
National Elevation Dataset (NED)
National Geospatial-Intelligence Agency (NGA)
Neural Networks (NN)
Maximum Normalized Difference Vegetation Index (MaxNDVI)
Multi-angle Imaging SpectroRadiometer (MISR)
Moderate-Resolution Imaging Spectroradiometer (MODIS)
RossThick-LiSparse (RTLS)
Random Forest (RF)
Red Reflectance (R)
Root mean square error (RMSE)
Summer Warmth Index (SWI)
U.S. Geological Survey (USGS)
Weight of determination of the nadir BRDF-adjusted reflectance at solar zenith angle of 45 degrees (NBAR_45W)

CHAPTER 1

1.1. Introduction

There are many definitions of the word Arctic. One of them describes the Arctic as the region north of the Arctic Circle (66.5°N). However, this definition does not take into consideration the vegetation, hydrology, or topography of the area. A more appropriate definition of the Arctic, suitable for studying terrestrial processes, is the region at high northern latitudes which the southern limit extends until the discontinuous or sporadic permafrost (McGuire et al., 2006). This study focuses on the Arctic region of Alaska, also known as the North Slope. It extends north of the Brooks Range until the coast of the Arctic Ocean.

The Arctic landscape is a complex ecosystem composed of different landforms such as glaciers, rolling hills, flat plains, wetlands, and polar deserts. The Arctic climate varies by location and season. For instance, at Point Barrow, Alaska, the mean annual surface temperature is -12.2 °C and the average annual precipitation is of 100 mm or less (ACIA, 2004). Winters are long and bitter, while summers are short. Biodiversity of plants and animals is low and on land it decreases from the boreal forest to the coastal plain. About 3% of the world's plant species occur in the Arctic where lichens and mosses are abundant (Matveyeva & Chernov, 2000). About four million people inhabit the region including some aboriginal communities. The four major indigenous groups that reside in Alaska are the Yup'ik, the Inupiat, the Athabaskan, and the Tlingit and Haida Indians who live in remote villages.

While the global mean surface temperature has risen in the past seven decades by about 0.3-0.6 °C, the temperature increase in the Arctic has been more pronounced due to the effect of polar amplification (IPCC, 2013). In particular in the last 150 years, the Arctic has experienced the highest temperatures in 400 years (Overpeck et al., 1997). Over the last 30 years the Arctic has warmed about 2°C per decade (ACIA, 2004). However, the temporal and spatial scale of the warming has not been uniform (McGuire et al., 2006). While Alaska experienced an increase in surface temperature in the latter half of the 20th century, Greenland underwent a cooling period (Hinzman et al., 2005). Considering that temperature is a very important factor to maintain the equilibrium between solid and liquid water in the Arctic, small changes in the temperature threshold can cause shifts between the two water states with great consequences for physical and biological systems and for humans (Macdonald et al., 2005).

There are three major terrestrial factors that determine the feedbacks of the Arctic terrestrial ecosystems to climate systems: 1) emissions of greenhouse gases (methane and carbon dioxide), 2) energy partitioning which refers to the heat flux from the surface to the atmosphere as influenced, for example, by permafrost, and 3) albedo (McGuire, et al., 2006). In the case of emissions, tundra and wetlands in the Arctic have about 200 to 300 Gt of stored carbon in the soil (Post et al., 1982). This is equivalent to 600 ppm of atmospheric CO₂ (Adams et al., 1990). Under warmer and dryer climate conditions, the stored carbon could be released to the atmosphere as CO₂ and contribute to climate warming (IPCC, 2013). On the other hand, the Arctic wetlands are also one of the largest sources of methane (CH₄) and warmer moister conditions will enhance the release of CH₄

to the atmosphere (McGuire et al., 2006). In the case of energy partitioning, the role of permafrost is a key factor. In the North Slope of Alaska the temperature of permafrost in deep wells revealed that from 1950 until 1970, the permafrost cooled, and ever since then, the permafrost has warmed (Romanovsky & Osterkamp, 2000). The presence or absence of permafrost influences the local hydrological processes. Where a continuous layer of permafrost is present, soils are very wet because the water cannot infiltrate to deeper ground. When the superficial layer thaws thermokarst are formed and in the boreal forest it can cause the death of trees when their roots are flooded . This in turn may affect birds and mammals that depend on the forest (Hinzman et al., 2005). As permafrost continues thawing, soils can be quite dry as the water can penetrate deeper and a possible consequence is the drainage of lakes and changes in stream water chemistry. In the case of albedo, a shift in land surface vegetation towards shrubbier landscape will exert a positive feedback to radiative forcing and amplify climate warming as shrub tundra has a lower albedo than sedge tundra (Chapin et al., 2005; Hinzman et al., 2005). A shrub expansion could alter the surface energy balance of the tundra by reducing the albedo in both summer and winter (Bonan et al., 1992; Chapin et al., 2000; Euskirchen, 2009; Sturm et al., 2005).

Although the effects of increasing shrub cover in the Arctic are not well understood (Selkowitz, 2010), shrub encroachment may have many more implications for regional climate in the Arctic including changes in surface hydrology, energy and carbon budget, and the disturbance regime (Sturm et al., 2001). Shrub expansion would change the hydrology by increasing summer transpiration (Sturm et al., 2001). In winter, protruding

shrubs would trap snow drifted by ground-level winds which might reduce water losses caused by sublimation when the snow is carried away by the wind (Sturm et al., 2001). Furthermore, snow depth would not be uniformly distributed across the landscape, but rather deeper snow would surround the shrubs downwind (Sturm et al., 2001). In spite of the increase in snow depth, melting would only take 7-10 days (Hizman et al., 1996) in part because the timing of the snowmelt occurs close to the annual solar maximum. Moreover, deeper snow acts as an excellent insulator promoting an increase in subnival temperatures that could stimulate winter mineralization and support shrub growth (Sturm et al., 2001). According to Hizman et al. (2005) in Alaska there has been a trend toward an early snow free season stimulated by the high solar radiation. The early snowmelt favors soil microbial activity because of warmer ground temperatures which in turn promotes plant growth (Fahnestock et al., 1998). Simulations show that in a span of 100 years the snow free period might have enlarged by ~50 days (Euskirchen, 2009). The lengthening of the snow free period may also be a positive feedback to climate (Chapin et al., 2000) as more solar radiation could be absorbed by the surface thus promoting warming of the ground (Hinzman et al., 2005). Furthermore, an increase in shrubs could have a positive feedback effect on biogeochemical processes causing accelerated nutrient cycling which may favor deciduous shrub growth over other types of vegetation and active layer thickness (Sturm et al., 2001). An increase in primary production could be a major contributor to changes in the high-latitude carbon budget (Sturm et al., 2005). However, under warmer and dryer conditions plants may reduce photosynthetic carbon uptake (Gamon et al., 2013). Shrub encroachment would cause changes to the

disturbance regime such as increased fire occurrence and intensity as more flammable vegetation becomes available (Lloyd et al., 2003).

There are several lines of evidence for shrub expansion in the Arctic and its linkage to climate. An increase in shrub abundance has been observed across the Arctic using repeat aerial photography (Myers-Smith et al., 2011; Sturm et al., 2001). Observational and experimental studies have detected a recent increase in aboveground biomass, particularly for deciduous shrubs, linking it to recent climate warming (Elmendorf et al., 2012; Huemmrich et al., 2010). The first long-term observational study in the Arctic detected an amplification in aboveground biomass from 1981 to 2008 and a twofold boost in the mean canopy height in dwarf shrubs during a period of only 8 years (Hudson & Henry, 2009). Shrub rings also indicate that warming is a primary contributor to shrub expansion in the Arctic (Forbes et al., 2010; Tape et al., 2012). Regional assessment of shrub expansion has been done using remote sensing imagery to derive vegetation indices, the Normalized Difference Vegetation Index (NDVI) being the most widely used. The increasing trend of the NDVI derived from the Advanced Very High Resolution Radiometer (AVHRRs) and Landsat satellites is consistent with an increase in biomass and photosynthetic activity, also called 'greening'; a lengthening of the growing seasons; and an expansion of shrubs tundra (Jia & Howard, 2003; Myneni et al., 1997; Silapaswan et al., 2001; Stow et al., 2004). If the atmospheric heating in the region continues, a likely scenario may be the conversion of tundra to shrubland (Euskirchen et al., 2009). This theory is supported by the pollen record for the transition from glacial to

Holocene climatic conditions in northwestern Alaska, which showed that shrubs increased their dominance during a previous period of warming (Anderson et al., 1994).

Since shrub expansion will have significant implications for regional climate in the Arctic (Sturm et al., 2001), the Intergovernmental Panel on Climate Change (IPCC, 2013) and the Arctic Climate Impact Assessment (ACIA, 2004) recommended long-term (>10years) monitoring of changes in arctic vegetation and climate, particularly with respect to the increase in deciduous shrubs. The most feasible way to survey the entire extent of the Arctic is using remote sensing. However, creating fractional cover maps from remote sensing imagery faces many challenges. To start, tall shrub (>0.5 m) abundance is very low in the Arctic. For instance, at scales of 250 m, cover is mostly always less than 5% (Duchesne et al., 2015). Second, the Arctic has a persistent cloud cover, especially during the summer months, which makes it difficult to capture a cloud-free scene (Gamon et al., 2013). In addition, sampling is limited to the short summer season when shrubs have a full canopy and there is no snow on the ground (Stow et al., 2004). Finally, the incoming radiation has to travel a longer path in the atmosphere due to the low sun angles. As a consequence signal strength is reduced due to greater light scatter (Hinzman et al., 2005).

Most of the studies done on shrub expansion using satellite imagery have employed vegetation indices as proxies for plant growth. Vegetation indices, which have been widely used to detect changes in Arctic vegetation, frequently display non linear relationships with canopy attributes (i.e., fractional vegetation cover) and should be used only as an estimate for canopy light absorption instead of as a proxy for features of

canopy architecture (Glenn et al., 2008). NDVI maps, as many existing global land cover and vegetation maps derived from spaceborne remote sensing sensors are, do not adequately represent shrub cover characteristics across the arctic tundra biome (Selkowitz, 2010). Furthermore, the relationship between the vegetation indices and biophysical quantities of the vegetation vary with season, in proportion to dead material in plant canopy, vegetation type, and soil background (Sellers, 1985). NDVI is sensitive to the solar and illumination geometry and does not take into account the reflectance anisotropy characteristics of the surface. Up to this date the only fractional cover map for the North Slope of Alaska was developed for year 2000, as a baseline, using Landsat imagery (Beck et al., 2011). The map was made by exploiting the spectral signal in Landsat using an empirical canopy model but did not take into consideration the surface anisotropy reflectance and due to heavy cloud cover of the region, it required four years worth of imagery.

To pursue mapping of shrub fractional cover in order to assess temporal changes in shrub abundance, there is the need to use an adequate model. Physical or semi-empirical canopy reflectance models could be used but they require *a priori* information on the surface, which is a challenge since there is high variability in the composition of the background vegetation. Other kind of models, machine learning algorithms, have the advantage of learning the relationship between the response and the predictor variables to find prevailing patterns (Breiman, 2001; Elith et al., 2008) and they are not constrained by the need for realistic internal model parameters such as leaf reflectance, leaf angle distribution, plant number density, mean crown radius, height and so on. Beck's et al.

(2011) study used Random Forest, a machine learning algorithm, to predict shrub fractional cover, but this model is like a black box. It is not possible to know the role of the predictors in the model or to identify interaction effects. In contrast, the boosted regression tree (BRT) model, another machine learning algorithm, provides simple graphical and numerical representations of the predicted variation in the response variable in relation to the explanatory variables, of the relative influence of the predictors, and as well as of the interactions between the independent variables (De'Ath, 2007). Because of these main advantages, the BRT model was selected in this study over other models to predict fractional cover estimates from moderate spatial resolution imagery. The BRT is an ensemble method where a large number of simple models (regression trees) are fitted and then combined using a boosting algorithm to develop a final model (Leathwick et al., 2006).

In addition to the selection of a model, the other main aspect is the selection of the sensor. For regional studies moderate resolution sensors are ideal because of their wide swath and higher temporal resolution, which could increase the possibility of obtaining a cloud-free/snow-free scene. In this study, the Multi-angle Imaging SpectroRadiometer (MISR), a moderate resolution sensor, was selected to monitor changes in terrestrial vegetation because it provides data at large scales and at regular intervals, which improves the chances of getting more cloud-free scenes (Selkowitz, 2010). Furthermore, reflectance values from MISR have been used for mapping forest and shrub canopy structures with success (Chopping et al., 2007; Chopping et al., 2008; Nolin, 2004; Strahler et al., 2005). The multi-spectral and multi-angular information provided by

MISR may improve the predictive performance of the model (Selkowitz, 2011). The multi-spectral information from MISR's nadir camera and the multi-angular information in the red band from all its off nadir cameras were used together with ancillary terrain data to drive the boosted regression tree model (BRT) with the goal of creating two wall-to-wall tall shrub (>0.5 m) fractional cover maps for the North Slope of Alaska, one for the year 2000 and another for the year 2010. The ultimate goal was to assess the magnitude and direction of the shrub expansion in the North Slope.

1.2. Research Objectives

The first objective of this study was to conduct two field surveys in the North Slope of Alaska to collect structural information on the tall shrub (>0.5m) vegetation. The field survey data were used to calibrate fractional cover estimates from the semi-automated image interpretation algorithm, CANAPI - CANopy Analysis from Panchromatic Imagery (Chopping, 2011), with the goal of building a robust reference database with estimates of shrub fractional cover, mean crown radius, and total number of shrubs for 1,039 sites. Each site had an area of 62,500 m² (250 m x 250 m), projected onto an Albers Conical Equal Area grid (Appendix A).

The second objective was to train and to validate the BRT model by using the reference database as input data and to find the best set of explanatory variables for the model in order to predict shrub fractional cover. Many runs of the model were performed to find the ideal model parameters (i.e., learning rate, tree complexity). The evaluation of the model was carried out in order to establish the relative contribution of the variables to

the model and the role of the interaction terms. The model was validated using a fresh set of observations.

The third objective was to construct the year 2000 fractional cover map by using MISR multi-spectral and multi-angular reflectance values together with some ancillary terrain data and to compare the results with existing vegetation maps. Evaluation included comparisons of predicted cover with fractional cover estimates obtained from the Beck's et al. (2011) circa 2000 tall shrub fractional cover map. Fractional cover estimates were also compared to the bioclimatic subzones of the Circumpolar Arctic Vegetation Map (CAVM, 2003). All map products generated as part of this research were projected onto a 250 m Albers Conical Equal Area grid (Appendix A).

The fourth objective was twofold. First, to derive the 2010-2011 fractional cover map for the North Slope of Alaska using MISR's multi-spectral and multi-angular reflectance values together with some ancillary terrain data and the Boosted Regression Tree model previously derived. Second, to compare shrub fractional cover values for the years 2000 and 2010 in order to determine the magnitude and direction of the shrub expansion. All map products generated as part of this research were projected onto a 250 m Albers Conical Equal Area grid (Appendix A).

The information produced in this study is of particular importance to the scientific, international, and federal agency communities concerned with the past and potential future of the tundra vegetation and its feedback to climate. Dynamic large-scale vegetation maps could assist to elucidate the likelihood of rapid, large-scale shrub expansion in Arctic tundra and its climatic, environmental, and ecological impacts.

Furthermore, the shrub fractional cover maps could provide reliable vegetation input data to better inform ecological and climate models. These maps may shed light on how changes in shrub abundance affect albedo in the summer time in this important and increasingly dynamic biome.

1.3. Organization of Thesis

The above-mentioned research objectives were accomplished and the results and research findings were organized in the form of various chapters in this dissertation. Each chapter covers one objective as follows:

- Chapter 2 is entitled " Capability of CANAPI Algorithm to Derive Shrub Structural Parameters from Satellite Imagery in Alaskan Arctic - A Reference Database". This chapter provides a description of the shrub canopy structure at 26 sites in Arctic tundra surveyed during two field expeditions. It further explains the derivation of CANAPI estimates using very high-resolution satellite imagery from the same field sites. It continues with the calibration of the CANAPI estimates by establishing correlations with field estimates. Finally this chapter provides shrub fractional cover estimates for 1,013 additional sites dispersed across the North Slope. The final product is a robust reference database with cover estimates for 1,039 sites of 250 m × 250 m - aligned to an Albers Conical Equal Area grid. This database was recently published as a product of the North American Carbon Program (Duchesne et al., 2015).

- Chapter 3 is entitled 'Training and Validation of Empirical Canopy Model to Predict Estimates of Shrub Cover from Multi-angle Imaging SpectroRadiometer Imagery'. This chapter supplies a description of the process of training and validating the boosted regression tree model. First, it explains the procedure to identify the explanatory variables for the BRT model and to find the best parameters (i.e., learning rate and tree complexity). Second, it provides an explanation of the role of the predictor variables in the model. Third, it evaluates the interactions among explanatory variables and their marginal effect on the response.
- Chapter 4 is entitled 'Mapping Tall Shrub Fractional Cover in the North Slope of Alaska in year 2000 using MISR'. This chapter explains all the steps to prepare MISR data for the BRT model, from downloading files, to modeling of BRDF, to flagging, to compositing techniques used. Then, it describes the process by which the output of the BRT model was filtered and transformed into the shrub fractional cover map. It continues by comparing the predicted shrub cover with fractional cover estimates obtained from the 2000 baseline tall shrub fractional cover map (Beck et al., 2011), and with the bioclimatic subzones of the Circumpolar Arctic Vegetation Map (CAVM, 2003).
- Chapter 5 is entitled 'The 2010 Tall Shrub Fractional Cover Map and Temporal Changes in Shrub Abundance in the North Slope of Alaska, 2000-2010'. This chapter provides a brief explanation on the processes taken to build the 2010 tall shrub fractional cover map, given that many of the details were already described

in chapter 4. Then, it compares the 2000 and 2010 MISR-derived predicted tall shrub fractional cover maps by estimating the change in shrub cover, the relative change in shrub cover, and the growth rate.

1.4. References

Adams, J.M., Faure, H., Faure-Denard, L., Mcglade, J.M., & Woodward, F.L. (1990).

Increases in terrestrial carbon storage from the Last Glacial Maximum to the present. *Nature*, 348, 711-714.

Arctic Climate Impact Assessment (ACIA). (2004). Scientific Report. Cambridge University Press. 1020p

Anderson, P. M., Bartlein, P. J., & Brubaker, L. B. (1994). Late quaternary history of tundra vegetation in northwestern Alaska. *Quaternary Research*, 41(3), 306–315.

Beck, Pieter S. A., Horning, N., Goetz, S. J., Loranty, M. M., & Tape, K. D. (2011).

Shrub cover on the north slope of Alaska: a circa 2000 baseline map. *Arctic, Antarctic, and Alpine Research*, 43(3), 355–363.

Bonan, G. B., Pollard, D., & Thompson, S. L. (1992). Effects of boreal forest vegetation on global climate. *Nature*, 359, 716-718.

Breiman, L. (2001). Statistical modeling: the two cultures. *Statistical Science*, 16, 199–215.

- Chapin, F. S. III., Eugster, W., McFadden, J. P., Lynch, A. H., & Walter, D. A. (2000). Summer differences among Arctic ecosystems in regional climate forcing. *J. Climate*, 13, 2002-2010.
- Chapin, F.S. III., Sturm, M., Serreze, M.C., McFadden, J.P., Key, J.R., et al. (2005). Role of land-surface changes in Arctic summer warming. *Science*, 310,657–660.
- Chopping, M., Su, L., Kollikkathara, N., & Urena, L. (2007). Advances in mapping woody plant canopies using the NASA MISR instrument on Terra. Proceedings *IEEE International Geoscience and Remote Sensing Symposium*. Barcelona, Spain.
- Chopping, M., Moisen, G., Su, L., Laliberte, A., Rango, A., Martonchik, J., & Peters, D. (2008). Large area mapping of southwestern forest crown cover, canopy height, and biomass using MISR. *Remote Sensing of Environment*, 112, 2051-2063.
- Chopping, M. (2011). CANAPI: canopy analysis with panchromatic imagery. *Remote Sensing Letters*, 2(1), 21–29.
- De'Ath, G. (2007). Boosted trees for ecological modeling and prediction. *Ecology*, 88(1), 243–251.
- Duchesne, R.R., Chopping, M.J., & Tape, K.D. (2015). NACP woody vegetation characteristics of 1,039 sites across the North Slope, Alaska. Data set. Available online [<http://daac/ornl.gov/>] from Oak Ridge National Laboratory Distributed Active Archive Center, Oak Ridge, Tennessee, USA.
- Elith, J., Leathwick, J. R., & Hastie, T. (2008). A working guide to boosted regression trees. *Journal of Animal Ecology*, 77(4), 802–813.

- Elmendorf, S. C., Henry, Gregory H. R., Hollister, R. D., Björk, R. G., Boulanger-Lapointe, N., Cooper, E. J., . . . , & Wipf, S. (2012). Plot-scale evidence of tundra vegetation change and links to recent summer warming. *Nature Climate Change*, 2(6), 453–457.
- Euskirchen, E. S., McGuire, A. D., Chapin, F. S. III, Yi, S., & Thompson, C. C. (2009). Changes in vegetation in northern Alaska under scenarios of climate change, 2003-2100: implications for climate feedbacks. *Ecological Applications*, 19(4), 1022-1043.
- Fahnestock, J.T., Jones, M.H., Brooks, P.D., Walker, D. A., & Welker, J.M. (1998). Winter and Early Spring CO₂ Flux from tundra communities of northern Alaska. *Journal of Geophysical Research*, 102, 29925-29931.
- Forbes, B. C., Fauria, M. M., & Zetterberg, P. (2010). Russian Arctic warming and ‘greening’ are closely tracked by tundra shrub willows. *Global Change Biology*, 16(5), 1542–1554.
- Gamon, J. A., Huemmrich, K. F., Stone, R. S., & Tweedie, C. E. (2013). Spatial and temporal variation in primary productivity (NDVI) of coastal Alaskan tundra: decreased vegetation growth following earlier snowmelt. *Remote Sensing of Environment*, 129, 144–153.
- Glenn, E., Huete, A., Nagler, P., & Nelson, S. G. (2008). Relationship between remotely sensed vegetation indices, canopy attributes and plant physiological processes: what vegetation indices can and cannot tell us about the landscape. *Sensors*, 8, 2136-2160.

- Hinzman, L. D., Kane, D. L., Benson, C. S., & Everett, K. R. (1996). Energy balance and hydrological processes in an Arctic watershed. Vol. 120. *Ecologica Studies*. Reynolds, J.F. & Tenhunen, J.D. Eds., Springer-Verlag, 131-154.
- Hinzman, L. D., Bettez, N. D., Bolton, W. R., Chapin, F. S., Dyurgerov, M. B., Fastie, C. L., . . . , & Yoshikawa, K. (2005). Evidence and implications of recent climate change in northern Alaska and other Arctic regions. *Climatic Change*, 72(3), 251–298.
- Hudson, J. M. G., & Henry, G. H. R. (2009). Increased plant biomass in a High Arctic heath community from 1981 to 2008. *Ecology*, 90(10), 2657–2663.
- Huemmrich, K., Gamon, J. A., Tweedie, C. E., Oberbauer, S. F., Kinoshita, G., Houston, S., . . . , & Mano, M. (2010). Remote sensing of tundra gross ecosystem productivity and light use efficiency under varying temperature and moisture conditions. *Remote Sensing of Environment*, 114(3), 481–489.
- Intergovernmental Panel on Climate Change. (2014). Climate change 2013: the physical science basis: working group I contribution. IPCC Fifth Assessment Report. Cambridge: Cambridge University Press.
- Jia, G. J., & Howard, E. E. (2003). Greening of arctic Alaska, 1981–2001. *Geophysical Research Letters*, 30(20).
- Leathwick, J.R., Elith, J., Francis, M.P., Hastie, T., & Taylor, P. (2006). Variation in demersal fish species richness in the oceans surrounding New Zealand: an analysis using boosted regression trees. *Marine Ecology Progress Series*, 321, 267–281.

- Lloyd, A., Rupp, T., Fastie, C., & Starfield, A. (2003). Patterns and dynamics of treeline advance in the Seward Peninsula, Alaska. *Journal of Geophysical Research*, 108(8161).
- Macdonald, R. W., Harner, T., & Fyfe, J. (2005). Recent climate change in the Arctic and its impact on contaminant pathways and interpretation of temporal trend data. *The Science of the total environment*, 342(1-3), 5–86.
- McGuire, A. D., Chapin, F. S., Walsh, J. E., & Wirth, C. (2006). Integrated regional changes in Arctic climate feedbacks: implications for the global climate system. *Annual Review of Environment and Resources*, 31(1), 61–91.
- Matveyeva, N. & Chernov, Y. (2000). Biodiversity of terrestrial ecosystems. In: M. Nuttall and T.V. Callaghan (eds.). *The Arctic: Environment, People, Policy*, pp. 233–274. Harwood Academic Publishers.
- Myers-Smith, I. H., Forbes, B., Wilking, M., Hallinger, M., Lantz, T., Blok, D., Tape K., ..., & Hik, D.S. (2011). Shrub expansion in tundra ecosystems: dynamics, impacts, and research priorities. *Environmental Research Letters*, 6(4), 045509.
- Myneni, R. B., Keeling, C. D., Tucker, C. J., Asrar, G., & Nemani, R. R. (1997). Increased plant growth in the northern high latitudes from 1981 to 1991. *Nature*, 386(6626), 698–702.
- Nolin, A. (2004). Towards retrieval of forest cover density over snow from the Multi-angle Imaging SpectroRadiometer (MISR). *Hydrological Processes*, 18(18), 3623 – 3636.

- Overpeck, J., Hughen, K., Hardy, D., Bradley, R., Case, R., Douglas, M., ..., & Zielinski, G. (1997). Arctic environmental change of the last four centuries. *Science*, 278, 1251-1256.
- Post, W.M., Emanuel, W.R., Zinke, P.J., & Stangenberger, A.J. (1982). Soil carbon pools and world life zones. *Nature*, 298, 156-159.
- Romanovsky, V. E. & Osterkamp, T. E. (2000). Effects of unfrozen water on heat and mass transport processes in the active layer and permafrost. *Permafrost Periglacial Process*, 11, 219–239.
- Selkowitz, D. (2010). A Comparison of multi-spectral, multi-angular, and multi-temporal remote sensing datasets for fractional shrub canopy mapping in Arctic Alaska. *Remote Sensing of Environment*, 114 (2010), 1338–1352.
- Sellers, P.J. (1985). Vegetation-canopy spectral reflectance and biophysical processes. In: Asrar G. (Ed.), *Theory and applications of optical remote sensing* (p 297-335). New York: Wiley, Ch. 8
- Silapaswan, C.S., Verbyla, D.L., & McGuire, A.D (2001). Land cover change on the Seward Peninsula: the use of remote sensing to evaluate the potential influences of climate warming on historical vegetation dynamics. *Canadian Journal of Remote Sensing*, 27, 542-554.
- Stow, D., Hope, A., McGuire, D., Verbyla, D., Gamon, J., Huemrich, F., ..., & Myneni, R. (2004). Remote sensing of vegetation and land-cover change in Arctic tundra ecosystems. *Remote Sensing of Environment*, 89, 281–308.

- Strahler, A., Jupp, D., Woodcock, C., & Li, X. (2005). The discrete-object scene model and its application in remote sensing. *Proceedings 9th International Symposium on Physical Measurements and Signatures in Remote Sensing*, 1, 166 -168.
- Sturm, M., McFadden, J., Liston, G., Chapin, S. III., Racine, C., & Holmgren, J. (2001) Snow-shrub interactions in Arctic tundra: a hypothesis with climatic implications. *Journal of Climate*, 14(3), 336–344.
- Sturm, M., Douglas, T., Racine, R., & Liston, G. (2005). Changing snow and shrub conditions affect albedo with global implications. *Journal of Geophysical Research*, 110(G01004,), 1–13.
- Tape, K. D., Hallinger, M., Welker, J. M., & Ruess, R. (2012). Landscape heterogeneity of shrub expansion in Arctic Alaska. *Ecosystems*, 15(5), 711-724.

CHAPTER 2

Construction of a Robust Reference Database with Estimates of Shrub Structure from Field Surveys and Very-High Resolution Imagery for the Alaskan Arctic

Abstract

The observed greening of Arctic vegetation and the expansion of shrubs in the last few decades likely have profound implications for the tundra ecosystem, including feedbacks to climate. Uncertainty surrounding this vegetation shift and its implications calls for monitoring of vegetation structural parameters, such as fractional cover of shrubs. In this study, two field surveys were carried out in the North Slope of Alaska to obtain estimates of tall shrub cover, canopy height, crown radius, and total number of shrubs at 26 sites (250 m × 250 m each). The field estimates were used to evaluate the ability of CANAPI, a semi-automated image interpretation algorithm that identifies and traces crowns by locating their crescent-shaped sunlit portions, to derive structural data for tall (> 0.5 m) shrubs in the Arctic. CANAPI estimates of shrub canopy parameters were obtained from high-resolution imagery for the field sites by adjusting the algorithm's parameters and filter settings for each site, such that the number of crowns delineated by CANAPI roughly matched those observed in the high resolution imagery. The CANAPI estimates were then compared with the field measurements to evaluate the algorithm's performance. CANAPI successfully retrieved fractional cover ($R^2 = 0.83$, $P < 0.001$), mean crown radius ($R^2 = 0.81$, $P < 0.001$), and total number of shrubs ($R^2 = 0.54$,

$P < 0.001$). CANAPI performed best in sparse vegetation where shrub canopies were distinct, while it tended to underestimate shrub cover where shrubs were clustered. The CANAPI algorithm and the regression equations presented here were exploited to derive vegetation parameters for 1,013 sites of similar characteristics across the North Slope of Alaska from sub-meter panchromatic imagery in order to construct a robust, in the sense of accurate across a variety of conditions, reference database. CANAPI was sensitive enough to discriminate very low shrub cover values considering that about 75% of the 1,039 sampling plots had a fractional cover less than 2% at 250 m scales.

Keywords: CANAPI, fractional cover, crown radius, Arctic tundra, reference data, remote sensing

2.1. Introduction

Since 1875, the region north of 60°N has warmed at a rate of 1.36°C per century, which is about twice as fast as the global average temperature (IPCC, 2014). During the 1960s-2000s, temperature trends from Arctic Alaska indicated a pronounced warming over the region (Chapman & Walsh, 1993). During this period, an increase in shrub abundance was observed across the Arctic using repeat aerial photography (Myers-Smith et al., 2011; Sturm et al., 2001b). Observational and experimental studies also detected a recent increase in aboveground biomass, particularly for deciduous shrubs, linked to recent climate warming (Chapin et al., 1995; Elmendorf et al., 2012; Hudson & Henry, 2009; Huemmrich et al., 2010). The increasing trend of the Normalized Difference Vegetation Index (NDVI) in the Arctic, also known as 'greening', has been associated with a warming trend in the region (Jia & Howard, 2003; Myneni et al., 1997; Stow et al., 2004). Shrub rings indicate that warming is a primary contributor to shrub expansion in the Arctic (Forbes et al., 2010; Tape et al., 2012). If the atmospheric heating in the region continues, a likely scenario could be the conversion of tundra to shrubland (Euskirchen et al., 2009). The pollen record of shrub expansion during the transition from glacial to Holocene climatic conditions in northwestern Alaska provides an older example of warming concurrent with shrub expansion (Anderson et al., 1994).

The implications of increasing shrub abundance are complex (Selkowitz, 2010). An increase in shrubs may change the snow distribution pattern (Epstein et al., 2004; Liston et al., 2002; Sturm et al., 2001a) and, as a result, impact myriad ecological and hydrological processes in the region (Boelman et al., 2011; Liston et al., 2002). The

proliferation of shrubs may alter the energy exchange and regional climate by decreasing albedo (Blok et al., 2011; Hinzman et al., 2005; Sturm et al., 2001a). The expansion of shrubs may also increase the likelihood of fires as more woody vegetation becomes available (Higuera et al., 2008). Changes in wildlife distribution are also anticipated, as boreal species extend northward into shrub habitat and tundra specialists become constrained (Elmhagen et al., 2015). The uncertainty of events that can take place as a result of shrub expansion call for the construction of dynamic cover maps of the Arctic region to monitor changes in the tundra canopy structure (Euskirchen et al., 2009; Tape et al., 2006). Remote sensing is the only practical tool that can help in the generation of such maps given the extent and inaccessibility of the region, which prohibits field work as the sole source of regional estimates.

Regional mapping of fractional cover employing remote sensing imagery is only possible using physical, semi-empirical, or empirical models that retrieve cover estimates from radiance values. One of the basic requirements of such models is to have a robust reference database for training and validation purposes. Up to this date, the few remote sensing studies that have quantified fractional shrub canopy in Arctic Alaska have made use of machine learning algorithms, field observations, and high resolution imagery to build such reference databases (Beck et al, 2011; Selkowitz, 2010). For example, Beck et al (2011) used a regression tree classification model to construct high-resolution short and tall shrub presence/absence maps from SPOT and IKONOS imagery that were later aggregated to a Landsat 30 m resolution grid depicting total and tall shrub percent cover. Alternative methods such as spectral mixture analysis have shown some success in

estimating green vegetation, nonphotosynthetic vegetation, and soil fractions in savanna biomes (Meyer and Okin, 2015), but the approach does not seem feasible at this time due to insufficient spectra for all surface components and insufficient spectral information in available imagery (Asner & Heidebrecht, 2002). One particular challenge in the Arctic is that often the non-woody background is not bare soil but green vegetation. LiDAR (Light Detection and Ranging) is an alternative method for capturing vegetation height. However satellite lidar (i.e., the Geoscience Laser Altimeter System that was flown on ICESat) is inadequate for sampling shrubs heights as the error in tree height estimates is sometimes as large as the height of a shrub in the Arctic, rendering the shrub height estimates not quite accurate (Hopkinson et al.2005; Popescu et al., 2011; Rosette et al., 2008). Nevertheless, airborne lidar of high spatial resolution (footprint diameter of about 20 cm for each laser pulse) can provide the vertical accuracy necessary to sample shrub vegetation (Streutker & Glenn, 2006), but to the best of our knowledge lidar data are not yet available for much of the North Slope of Alaska. It is conceivable that CANAPI - CANopy Analysis from Panchromatic Imagery (hereafter CANAPI), a semi-automated image-interpretation algorithm that has been used effectively to generate estimates of woody vegetation structural parameters in forest ecosystems (Chopping, 2011; Chopping et al., 2012), could be complementary to lidar in quantifying shrub structural parameters (i.e., crown radius, plant height).

The CANAPI algorithm identifies and traces crowns by locating its crescent-shaped sunlit portion and can retrieve tree number density, fractional cover, height, and mean crown radius from subsets of a variety of high-resolution (≤ 1 m) panchromatic imagery

such as QuickBird (Chopping et al., 2011). For some forest canopies, CANAPI has been used over large areas with a single set of parameters and filter settings (Chopping et al., 2012), but in Arctic tundra the filter settings must vary from site to site. One advantage of CANAPI is that it identifies tree and shrub crown extents for precise estimation of cover across a range of crown sizes, which is of particular importance given that in Arctic tundra, the percent cover of shrubs taller than 0.5 m is usually less than 5% (Beck et al., 2011; Duchesne et al., 2015; Selkowitz, 2010).

This study extends the limits of the CANAPI algorithm by deploying it for the first time in Arctic shrub tundra, where shrubs are significantly smaller than trees. The main goal of this study was to create a robust reference database with estimates of shrub structure for the Alaskan Arctic. The specific objectives were to characterize shrub canopy structure at 26 sites in Arctic Alaska, to derive CANAPI estimates using very-high resolution satellite imagery from the same field sites, and to calibrate the CANAPI estimates by establishing correlations with field estimates in order to build a robust reference database.

2.2. Materials and Methods

2.2.1. Study Area and Site Selection

Two three-week field campaigns were undertaken on the Alaskan North Slope (the tundra region north of the Brooks Range mountains) during 24 July - 12 August 2010 and 20 July - 9 August 2011. The first campaign surveyed 14 sites along the Chandler and Colville Rivers from north of the Brooks Range to the Arctic Coastal Plain. The second

campaign surveyed 12 sites along the Dalton Highway from the Brooks Range to the Arctic Coast (Figure 2-1).

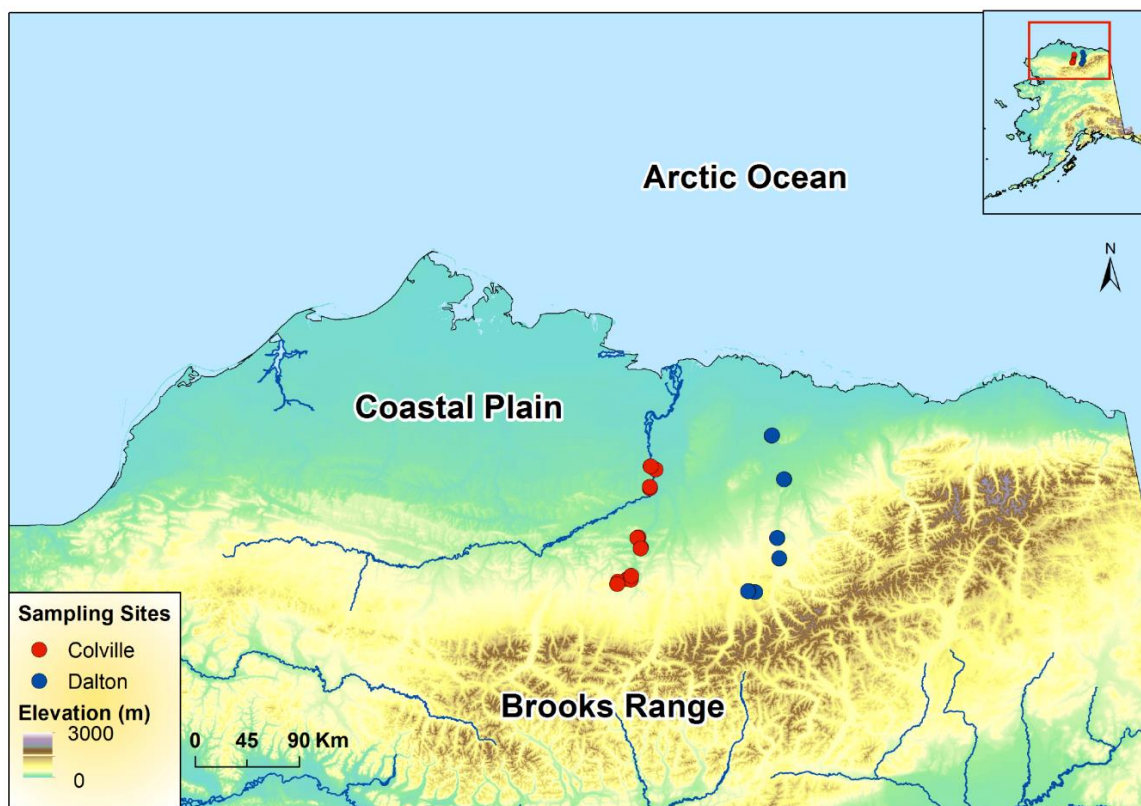


Figure 2-1. Map of the North Slope of Alaska. Field sites surveyed during the Colville campaign in 2010 (red dots) and during the Dalton campaign in 2011 (blue dots). Albers Equal Area Conic projection, spheroid WGS 84, datum WGS 84. (Source: AlaskaMapped SDMI WCS layers [downloaded file]. Alaska Mapped, Statewide Digital Mapping Initiative. URL: <http://www.alaskamapped.org/data/arcgis-layer-files>: [20 February, 2015]).

Sampling sites fell along an altitudinal and climatic gradient with the southernmost sites at higher elevation (~790 m) and influenced by the continental climate associated with the Brooks Range, while the northernmost sites were located at a much lower

elevation (~73 m), where maritime climate conditions prevailed (Table 2-1). Sites along the Chandler and Colville rivers were located either in the floodplain or along tributary creeks within 1 km of the floodplain. In contrast, sites along the Dalton Highway were located at least 1 km away from the road to avoid the effect of road dust on the vegetation. Each sampling site was 250 m × 250 m for a total site area of 62.5 km². This spatial resolution is adequate for regional studies as it corresponds to the spatial sampling of moderate resolution satellite imagers such as the Multi-angle Imaging SpectroRadiometer (MISR) and the Moderate Resolution Imaging Spectroradiometer (MODIS).

Table 2-1. Description of 26 field sites (250 m x 250 m each) surveyed during summer 2010 and 2011.

Site Name	Center Pixel Coordinate		Elevation	Date	Dominant
	(Albers Projection ¹ , m)		a.m.s.l.	Sampled	Vegetation
	X	Y	(m)	(d.m.y)	Type
Colville-01	98250	2190000	94	11.08.2010	Graminoid
Colville-02	102500	2187250	96	10.08.2010	Wetland
Colville-03	97750	2172250	96	09.08.2010	Erect-shrub
Colville-04	97750	2171000	96	09.08.2010	Erect-shrub
Colville-05	87750	2128750	150	05.08.2010	Graminoid
Colville-06	86750	2128250	145	05.05.2010	Graminoid

Colville-07	89750	2120000	143	03.08.2010	Graminoid
Colville-08	89500	2119000	222	03.08.2010	Graminoid
Colville-09	81500	2095500	249	08/02/2010	Graminoid
Colville-10	81000	2092000	249	08/01/2010	Graminoid
Colville-11	78000	2092500	297	30.07.2010	Graminoid
Colville-12	70000	2090500	287	29.07.2010	Graminoid
Colville-13	69750	2090000	289	28.07.2010	Graminoid
Colville-14	69250	2088250	290	29.07.2010	Graminoid
Dalton-01	203500	2216750	80	30.07.2011	Wetland
Dalton-02	203250	2216500	78	30.07.2011	Wetland
Dalton-03	213750	2178750	203	29.07.2011	Graminoid
Dalton-04	214000	2179000	225	29.07.2011	Graminoid
Dalton-05	207750	2128250	392	26.07.2011	Graminoid
Dalton-06	208250	2128000	392	26.07.2011	Graminoid
Dalton-07	209750	2110750	409	25.07.2011	Erect-shrub
Dalton-08	209750	2110250	438	25.07.2011	Erect-shrub
Dalton-09	188500	2081250	790	04.08.2011	Graminoid
Dalton-10	189000	2081250	790	04.08.2011	Graminoid
Dalton-11	183000	2082250	752	22.07.2011	Graminoid
Dalton-12	182750	2082000	768	22.07.2011	Graminoid

¹ Coordinates are for an instance of the Albers Conical Equal Area map projection; see Duchesne et al, 2015 for details and the map projection parameters used.

Field sites were selected using low-altitude aerial photographs and high-resolution satellite imagery (QuickBird, IKONOS, and WorldView) (Figure 2-2). Selected sites represented a variety of tall shrub distributions, from dense willow shrubs (*Salix spp.*) and alder shrubs (*Alnus viridis*) along water tracks to scattered well-defined shrub canopies (Figure 2-3). Each site was designated as either graminoid-dominated tundra, erect-shrub-dominated tundra, or wetland (CAVM, 2003), though riparian shrub sites are generally not represented in broad scale maps (Table 2-1). Graminoid tundra sites were typically dominated by sedges, dwarf shrubs less than 0.40 m tall, and a well-developed



Figure 2-2. Aerial photograph of the Colville-07 field site and surrounding landscape. The top is north, horizontal extent is about 550 m. Photo credit: Ken Tape (University of Alaska, Fairbanks).

organic layer. There were often tall willow thickets (>2 m) occurring along stream margins. Erect-shrub tundra sites were characterized by low shrubs greater than 0.40 m tall. Wetland sites were dominated by sedges, grasses, and mosses. At most sites shrubs were less than 0.40 m tall; however, some sites like Colville-02, hosted shrubs with an average height upwards of 1.5 m. Sites were sampled during the peak growing season when the shrub crown was at its fullest.

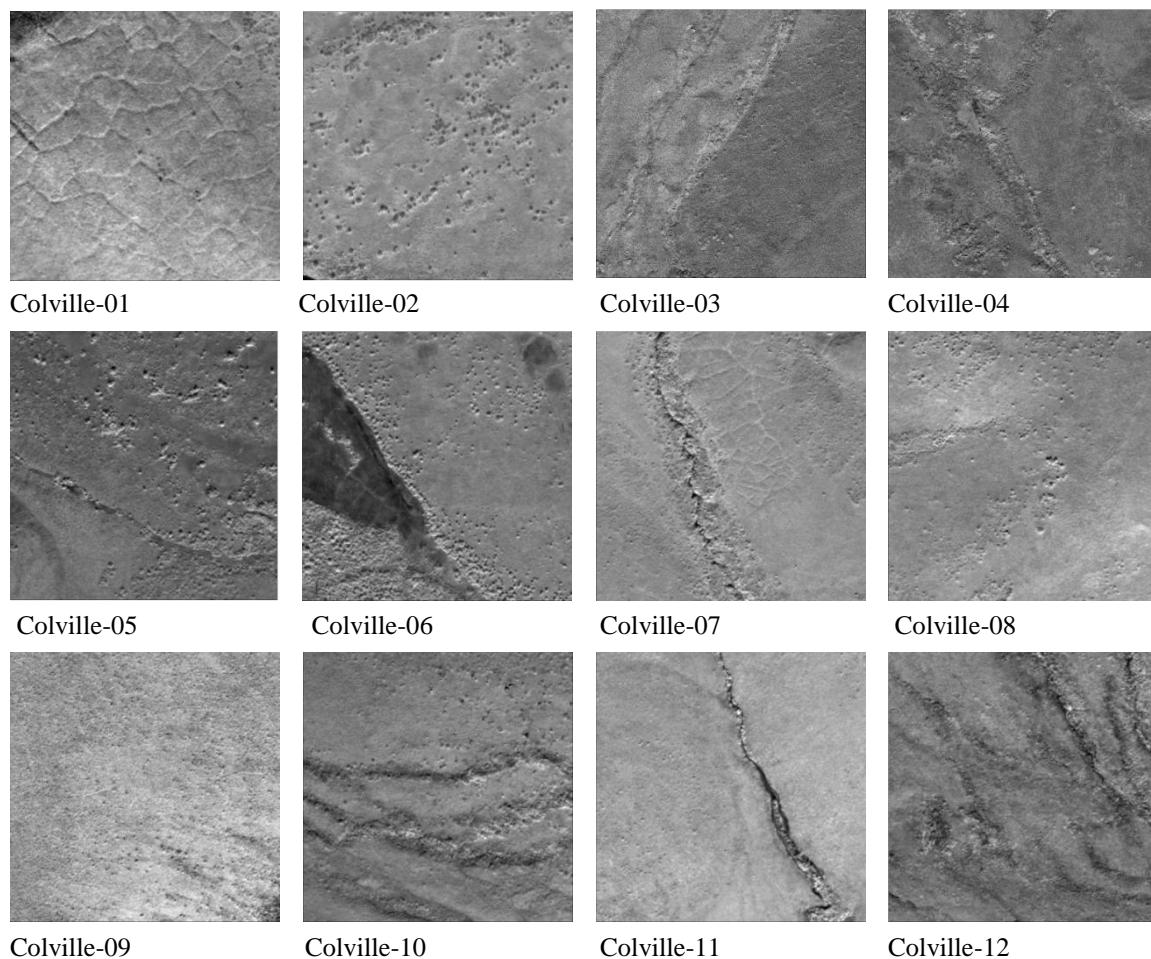


Figure 2-3. Quick Bird, IKONOS, and WorldView panchromatic subsets of the 26 field sampling sites. Spatial resolutions ranged from 0.46 m to 1 m. Each site has an area of 62,500 square meters.

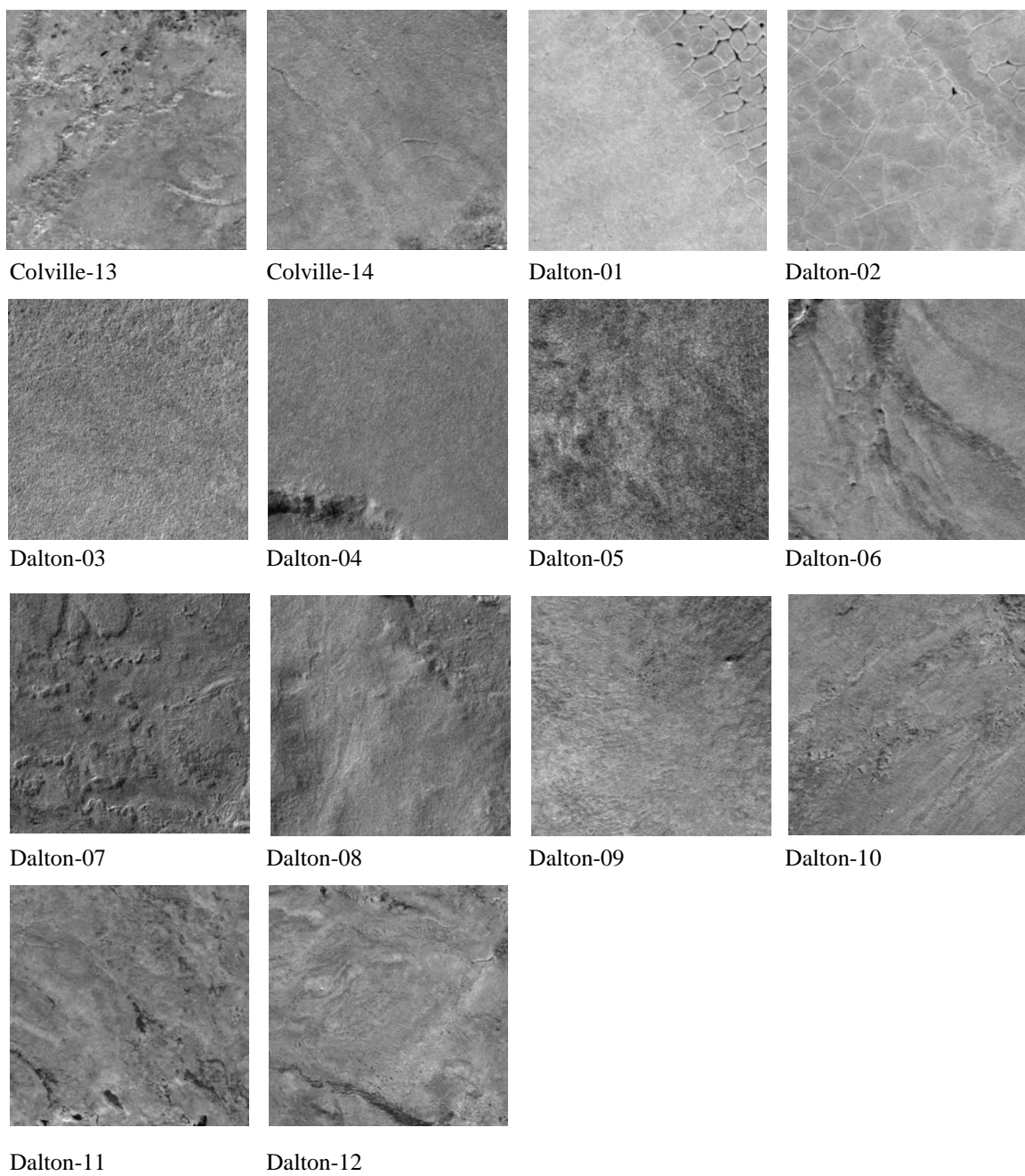


Figure 2-3 (continued). Quick Bird, IKONOS, and WorldView panchromatic subsets of the 26 field sampling sites. Spatial resolutions ranged from 0.46 m to 1 m. Each site has an area of 62,500 square meters.

2.2.2. Target Shrub Population

The target population was shrubs taller than 0.5 m, measured from the lowest detectable solid ground. This height threshold was selected because it represents the approximate height boundary between shrubs that grow mainly between tussocks and shrubs that protrude significantly above tussocks (Selkowitz, 2010). The same threshold has also been widely used in other vegetation studies on the North Slope of Alaska to distinguish shrubs that form a canopy from background vegetation (Liston et al, 2002; Tape et al, 2006). Canopy-forming shrubs play a different role in the ecosystem compared to inter-tussock shrubs. For instance, taller shrubs cast shadows on the background vegetation that in turn may change the micro-temperature around the shrub (Chapin et al., 2005). They also trap more blowing snow during winter (Sturm et al., 2001a). In addition, taller shrubs can be more readily identified in very-high resolution imagery, which allows the delineation of shrub crowns with greater ease.

2.2.3. Transect Method and Sampling Strategy

The belt transect method was selected to obtain precise estimates of cover, height, and crown radius of shrub vegetation to compare to and assess the accuracy of the CANAPI algorithm. This is a common technique used to estimate the cover and height of woody vegetation, along environmental gradients, by extrapolating measurements within each belt transect to the entire sampling site (Hill et al., 2005). Since this can be a laborious technique it is recommended for sparse vegetation, as is the case of most tall

shrub canopies in the Arctic. This method was used to survey all sites except Colville-01, where all shrubs were sampled since there were just a few.

The sampling strategy used to implement the belt transect method was systematic sampling with a randomly selected starting point. A baseline was placed along one side of the sampling sites and transects were laid perpendicular to the baseline. The first transect began at a randomly selected point along the baseline and transects thereafter were placed at regular intervals. In doing so, the sites were evenly sampled, the travel time and setup was reduced in comparison to random sampling, sampling units were better interspersed, and the same formulas inherent in simple random sampling were used (Elzinga et al., 1998).

Two Garmin Etrex Geo-positional System (GPS), each with a horizontal accuracy of 10 m, were used to record the sampling transects and the location of each shrub surveyed. A Canon PowerShot digital camera was used to take photographs of all shrubs, and a measuring rod was used to measure the height and crown width of each shrub.

2.2.4. Optimizing Field Sampling

Prior to the field surveys, there were two important considerations: first, to decide on the most favorable transect width; and second, to determine the optimum number of transects to sample. From the statistical standpoint, long, narrow transects systematically placed (with a random start) in the population to be sampled are more effective for estimating cover than square or wider rectangular transects (Elzinga et al., 1998). Therefore, the transects used were narrow rectangles of 250 m long by 5 m wide.

Although a 6 m belt width is suggested when plant density is less than 15% (Tazik, et al., 1992), which is the case for tall shrubs in Arctic tundra, a 5 m belt width still rendered reliable estimates of cover according to a pilot study carried out at site Colville-02.

The pilot study was performed with the aid of QuickBird high-resolution panchromatic imagery (250 m × 250 m) and an image processing program (ImageJ) to determine the ideal number of transects to sample per site (Figure 2-4). Sequential sampling was used to determine the initial sample size using the transect method described above, whereby the number of transects were increased monotonically from 3 to 15. With each iteration, the mean and standard deviation estimates were calculated. The sample size was plotted against the mean and standard deviation with the goal to identify the smallest sample size at which the curves began to smooth out. Finally, the mean and standard deviation values of the initial sample size were used to determine the ideal sample size for a site. This last process involved three steps (Elzinga et al., 1998):

(1) Calculating an uncorrected sample size estimate, n , by using Equation 2-1:

$$n = \frac{(Z_{\alpha})^2 \times (s)^2}{\beta^2} \quad \text{Eq. 2-1}$$

where n is the uncorrected sample size estimate, Z_{α} is the standard normal coefficient, s is the standard deviation, and β is the desired precision level expressed as half of the maximum acceptable interval width.

(2) Consulting the Sample Size Correction table to determine the corrected sample size estimate, n^* . This was necessary because Equation 2-1 underestimates the number of sampling units needed to meet the specified level of precision.

(3) Multiplying the corrected sample size estimate by the finite population correction factor when more than 5% of the population is being sampled using Equation 2-2:

$$n' = \frac{n^*}{\left(1 + \left(\frac{n^*}{N}\right)\right)} \quad \text{Eq. 2-2}$$

where n' is the new FPC-corrected sample size, n^* is the corrected sample size from the sample size correction table, and N is the total number of possible transect locations in the population. N is calculated by dividing the total area of the population by the size of one transect ($N = 62,500 \text{ m} / 1,250 \text{ m} = 50$).

2.2.5. Sampling Shrub Parameters

The four corners of the sampling site were located in the field using GPS. A baseline parallel to the terrain slope was laid along one of the sides of the site. The starting point of the first transect was randomly located within the first 50 m of the baseline and established perpendicular to it. The subsequent transects were located parallel to the first and equally spaced from each other (Figure 2-4).

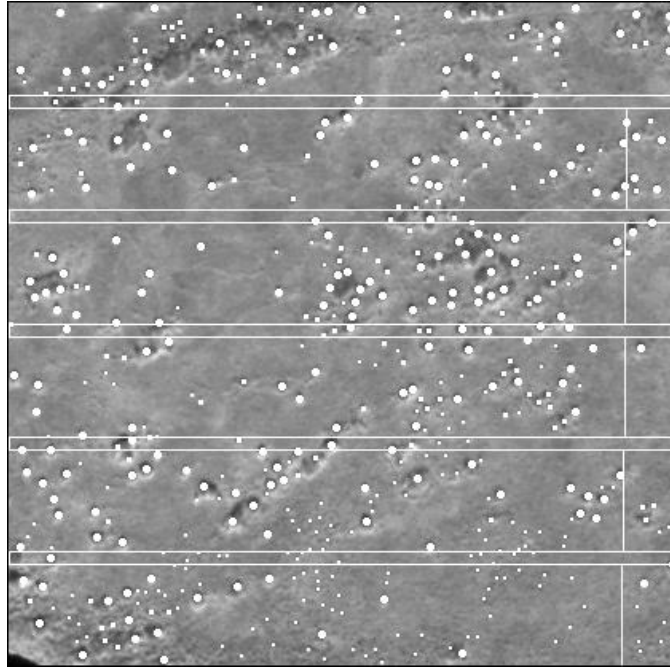


Figure 2- 4. Distribution of belt transects at site Colville-02 (250 m \times 250 m) following a systematic sampling strategy with a randomly selected starting point. White dots represent shrubs observed in the QuickBird panchromatic subset.

Three people did the sampling. The first person walked the transect using a GPS to mark the path with flags. The second person walked along the transect with a 5 m pole held horizontally (2.5 m on each side of the transect), stopping at every shrub taller than 0.5 m that had at least half of its base located within the belt. The third person recorded the GPS location of the shrub and took a digital photograph of it that included a 2 m scale rod (with 0.10 m increment marks) in the field-of-view. The process was repeated until all shrubs within the belt and all transects at a site were sampled.

Shrub genus was identified later using the photographic records and field notes. Photos were also used to estimate canopy width (horizontal extent from the left-most

branch to the right-most branch) and height (vertical extent from base to top of foliage) of the shrubs by calibrating distances in the photo using the 2 m scale rod placed beside each shrub.

2.2.6. Deriving Shrub Site Parameters using the Belt Transect

The belt transect method was used to determine fractional cover, total number of shrubs, shrub mean crown radius, and mean shrub height at each site. Mean crown radius was estimated using all measurements of individual shrubs but clusters of shrubs were omitted because the crown borders of each shrub could not be identified. Mean crown radius was defined as half of the mean crown diameter. Mean shrub height was estimated using all the observations, both individual shrubs and clusters of shrubs. Shrub height was defined as the length of the shrub from its base to the top branch. Fractional cover estimates included both surveyed individual shrubs and clusters of shrubs. The crowns that exceeded the belt width were adjusted to 5 m. Estimation of fractional cover was a two-step process:

(1) Estimation of shrub/cluster cover area (*SCCA*), which assumes that the crown was circular:

$$SCCA = \sum \pi (r_i)^2 \quad \text{Eq. 2-3}$$

where r_i is the individual shrub or shrub cluster crown radius (m),

(2) Estimation of fractional cover (*FC*):

$$FC = \frac{SCCA}{TBA} \quad \text{Eq. 2-4}$$

where $SCCA$ is shrub cover area (m^2) and TBA is the sum of the area covered by all belt transects sampled at a site ($1,250 m^2$ /transect). Fractional cover values range from 0 to 1, with 1 being 100% shrub cover.

Total number of shrubs (TNS) in the sampling site was estimated using records of individual and cluster of shrubs where each shrub or shrub cluster was considered one individual:

$$TNS = \frac{A \times S}{TBA} \quad \text{Eq. 2-5}$$

where A is the site area ($62,500 m^2$), and S is the total number of shrubs and clusters surveyed in all belt transects.

2.2.7. CANAPI Estimates and Calibration Equations

CANAPI is a user-tunable algorithm that can be run in ImageJ and uses high resolution panchromatic imagery to analyze tree and shrub canopies (Chopping, 2011). The CANAPI algorithm operates in two steps: first, it identifies crowns by locating the crescent-shaped sunlit portion of the crown; and second, it attempts to estimate tree or shrub height using the length of the shadow cast by each crown, where the shadow is not truncated by another crown or the edge of the image. For application in Arctic tundra, CANAPI's parameters and filter settings were adjusted for each site separately, until the number of crowns delineated by CANAPI roughly matched those observed in the high resolution imagery (Figure 2-5).

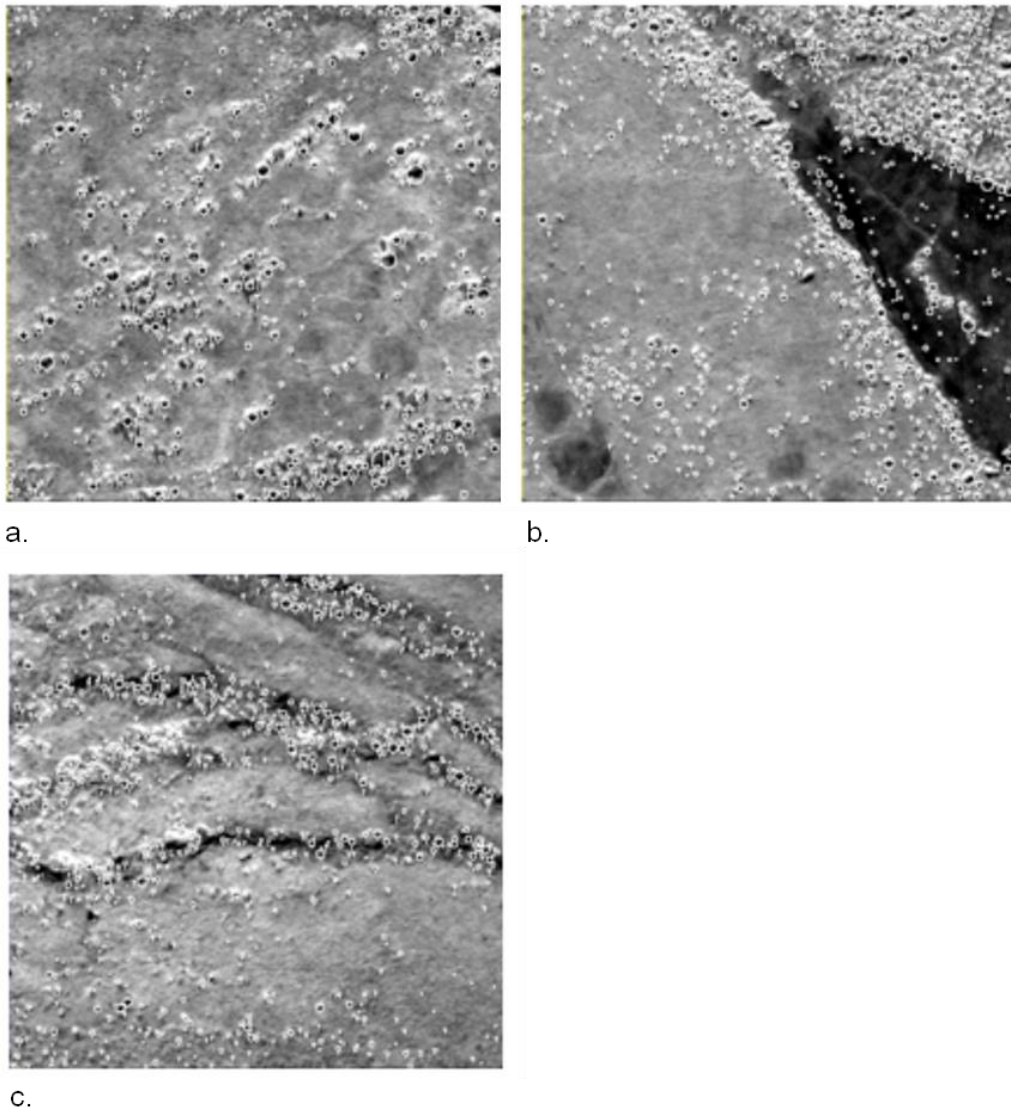


Figure 2-5. QuickBird panchromatic subsets with shrub crowns delineated by the CANAPI algorithm. Each site is 250 m \times 250 m. a. Colville-02, b. Colville-06, c. Colville-10.

The CANAPI algorithm was used here to derive shrub fractional cover, canopy crown radius, total number of shrubs, and shrub height estimates for the field sites (Figure 2-2). The CANAPI algorithm estimates were derived from image subsets of 250

m × 250 m, corresponding to the field sites – aligned with the Albers Equal Area Conic grid – selected from sub-meter high resolution panchromatic scenes from the QuickBird, WorldView, and GeoEye sensors (0.6 m, 0.5m, and 0.5 m spatial resolution, respectively). Some imagery was purchased, while some was obtained through the National Geospatial-Intelligence Agency Commercial Archive Data (<http://cad4nasa.gsfc.nasa.gov/>), both through the NASA Terrestrial Ecology project NNX09AL03G "Mapping Changes in Shrub Abundance and Biomass in Arctic Tundra using NASA Earth Observing System Data". Field data were considered more reliable than CANAPI estimates because shrubs were measured *in situ*. Thus, field data were used in validation of image-based estimates of fractional cover, mean crown radius, mean height, and total number of shrubs via linear regressions.

Sites with indiscrete shrubs were not suitable for the CANAPI algorithm and were not included in the regression analysis. CANAPI requires shrub crowns to be well defined in order to identify them in the high-resolution satellite imagery. Four CANAPI estimates of fractional cover were omitted from the analysis because at those sites shrubs formed a homogeneous layer that made it impossible to delineate shrub crowns. Similarly, five CANAPI estimates of total shrub were excluded from the analysis because of the homogeneous layer of shrubs (4 sites) and almost leafless shrub crowns (1 site). Two CANAPI estimates of mean crown radius were not included in the analysis because at those sites there was either no shrub in the field or detected by CANAPI. Three CANAPI estimates of mean shrub height were omitted from the analysis because at one

site there were no shrubs in the field, and at the other two sites the few shrubs detected by CANAPI had their shadows truncated by other shrubs.

2.2.8. Expansion of the Reference Database

A total of 1,013 high resolution panchromatic subsets of 250 m × 250 m - aligned with the Albers Conical Equal Area grid onto which the MISR data are mapped - were obtained across the North Slope of Alaska. These sites were explicitly chosen to include representatives from all four physiognomic vegetation types present in the region and they were spread across the entire domain, covering a wide latitudinal and longitudinal range (Figure 2-6). Image-based estimates were obtained for those sites using the CANAPI algorithm and were later adjusted using the regression coefficients previously derived, thus a solid reference database of 1,039 data points was built.

2.3. Results and Discussion

2.3.1. Optimizing Field Sampling

The mean number of shrubs and standard deviation values became rather stable once at least nine transects were sampled (mean = 10.3, SD = 2.29). According to Equation 2-1, the uncorrected sample size estimate (n) should be 1 ($Z_{\alpha} = 1.64, \beta = 3.8$). Consistent with the Sample Size Correction table, the corrected sample size estimate for a 90% confidence interval should be 5 ($n^* = 5$). Since sampling five belts (6,250 m²) means sampling more than 5% of the area (62,500 m²), the correction to a sample size estimate that incorporates the finite population correction (FPC) factor was applied. The minimum

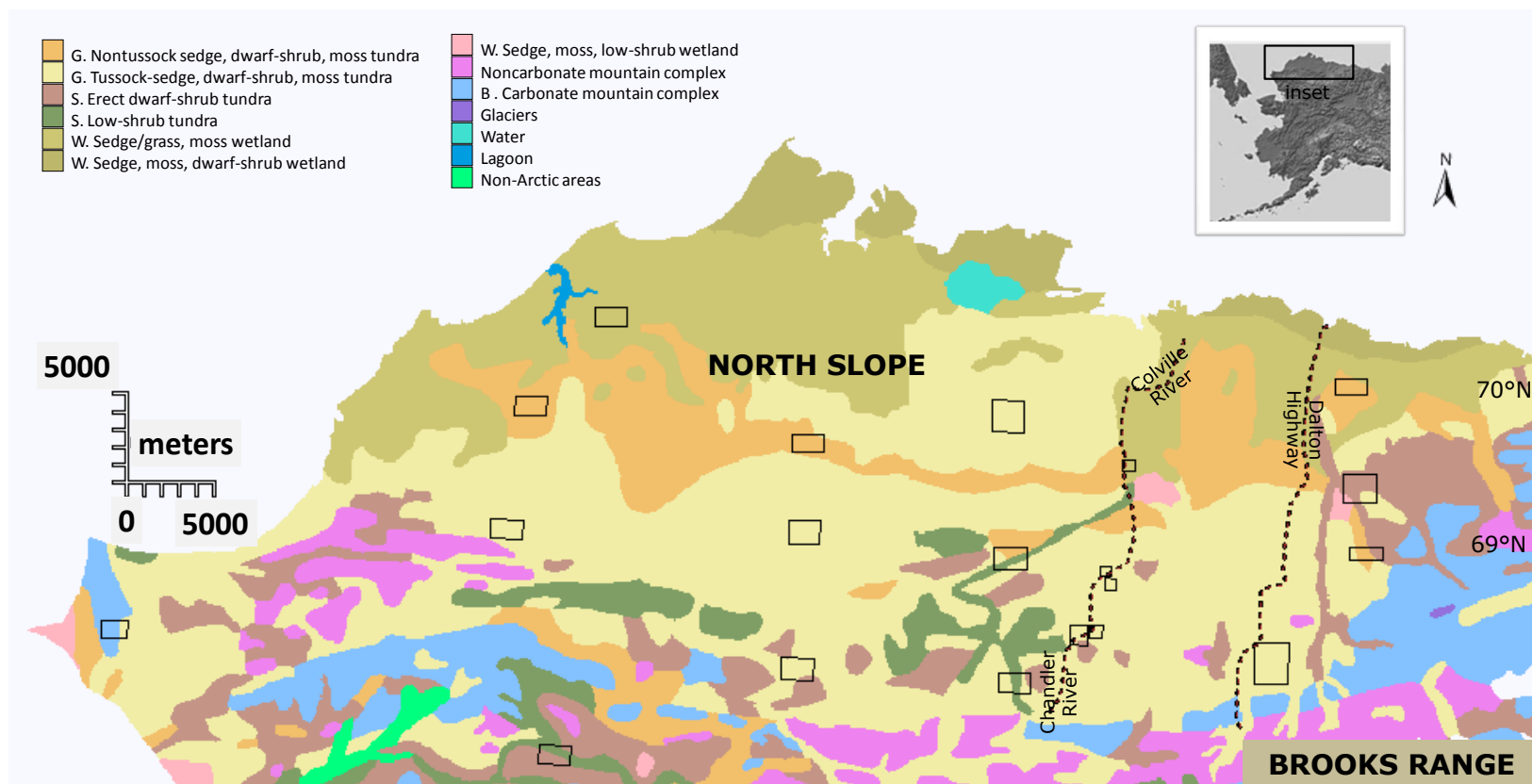


Figure 2-6. Map of the physiognomic vegetation types (CAVM, 2003) for the North slope of Alaska. The black boxes represent available high resolution imagery and from which 250 m x 250 m subsets were selected for the reference database.

number of transects to sample to be 90% confident that the estimate of the population mean was within +/- 4 shrubs of the true mean was 5.

2.3.2. Shrub Estimates from Field Surveys

Analysis of the shrub structural estimates at the 26 field sites revealed that there seemed to be a distinction between the Colville and Dalton sites with respect to the mean shrub height and the mean shrub crown radius (Figure 2-7 d and 2-7 b). Shrubs in the Colville sites were taller (0.77 m - 1.98 m) and had a wider crown (0.67 m - 1.21m), while shrubs in the Dalton sites were shorter (0.57m - 0.80 m) and had a narrower crown (0.36 m - 0.92 m). Shrub fractional cover was no greater than 13% at the sampling sites (Figure 2-7c). The total number of shrubs taller than 0.5 m ranged from 0 to 1520 and there was no difference between the Colville and Dalton sites (Figure 2-7a). It is possible that the observed differences in shrub height, mean crown radius, and fractional cover between the Dalton and Colville sites might be related to the geomorphology of the landscape. For instance, the Colville sites were located on floodplains and steeper slopes with water tracks running downhill, while the Dalton sites were not.

Ratio comparison of the mean height and mean crown radius measurements showed that the shrubs' shape tended to be elongated in the Colville sites (1.43 m: 0.97 m) and more circular in the Dalton sites (0.63 m: 0.51 m). *Alder sp* was the dominant species in 13 out of the 14 plots of the Colville sites (percentage dominance > 67%), while *Willow sp* was the dominant species in all the Dalton sites (percentage dominance > 53%) except

in Dalton-09 where there were no shrubs at all. It is important to note that about 0.2 m of the shrubs' stem was usually hidden between tussocks.

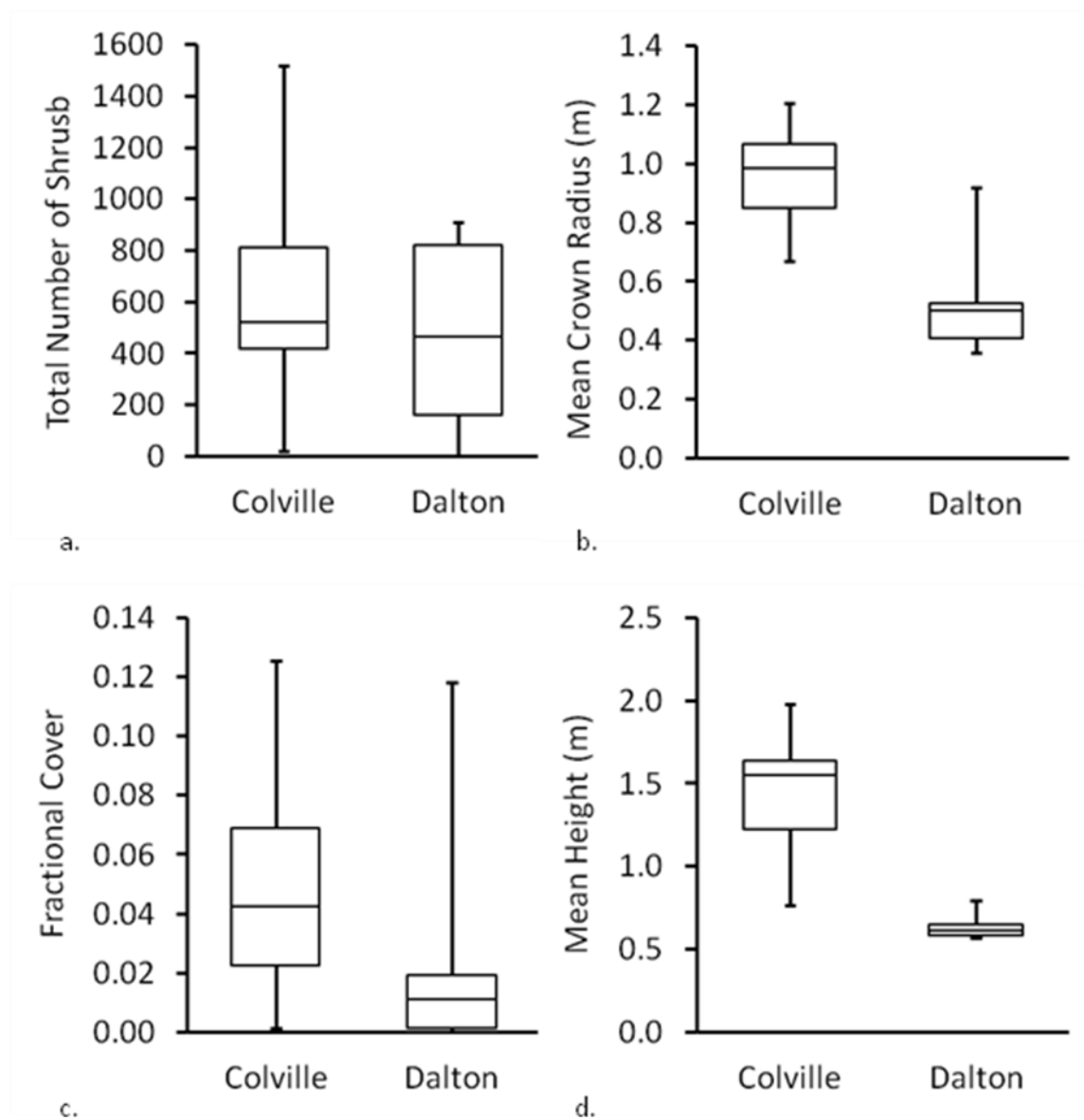


Figure 2-7. Box plots with field estimates at 26 sites (minimum, first quartile, median, third quartile, and maximum): a. total number of shrubs, b. mean crown radius, c. fractional cover, and d. shrub height. Colville 2010 campaign (rhomboids) and Dalton campaign 2011 (squares).

Mean shrub height slowly decreased with increasing latitude in both the Colville and Dalton sites (Figure 2-8a). In contrast, a divergent pattern is observed in the shrubs' mean crown radius with respect to latitude. In the Colville sites, the canopy width increased with increasing latitude, while in the Dalton sites, it decreased with increasing latitude (Figure 2-8b). These patterns may be related to the inherent ability of certain species of shrubs to acclimate to the environment. It appears that *Alder sp.* would be taller and have thinner canopy at lower latitudes but towards the coastal plain it becomes shorter but widens its canopy. *Willow sp.* seems to decrease its crown width towards the coastal plain. There was not a definite pattern between latitude - fractional cover and latitude - total number of shrubs (omitted here).

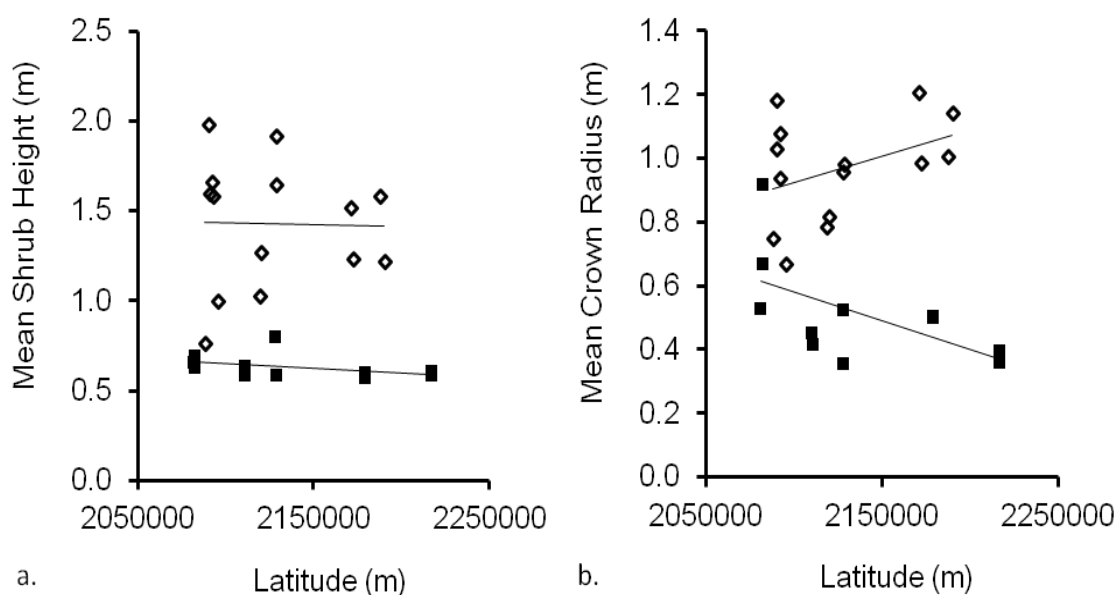


Figure 2-8. Plots display the relationship between a) mean shrub height and latitude and b) mean crown radius and latitude for both the Colville (rhomboids) and Dalton (squares) sites. Latitude is expressed in meters, projection Albers Conical Equal Area, Spheroid WGS 84, Datum WGS 84.

2.3.3. CANAPI Estimates and Calibration Equations

Regression equations between field and CANAPI estimates for four vegetation structural variables were estimated. The coefficients of determination for fractional cover and mean crown radius revealed a strong positive relationship between field and CANAPI estimates ($R^2 = 0.83$ and 0.80 , respectively; $RMSE = 0.009$ and 0.17 m; $P < 0.001$) (Figure 2-9a and 2-9b). The relationship between field and CANAPI estimates for the total number of shrubs was also positive but not as strong ($R^2 = 0.54$; $RMSE = 334$ shrubs; $P < 0.001$) (Figure 2-9c), whereas the coefficient of determination for shrub height showed that there was no correlation between field and CANAPI estimates ($R^2 = 0.02$; $RMSE = 0.67$ m; $P = 0.57$) (Figure 2-9d).

Further exploration of these relationships revealed that CANAPI tended to underestimate fractional cover when there were cluster of shrubs, because CANAPI was unable to identify the shrub crowns in the cluster. Wherever vegetation was sparse, CANAPI estimates were consistent with field data because CANAPI could identify the individual shrub crowns. Similar relationships applied to the estimates of the total number of shrubs. Mean crown radius CANAPI estimates were often lower than the corresponding field estimates. This might also be an effect of the lower spatial resolution of the panchromatic images used to derive the CANAPI estimates in comparison to the finely resolved field measurements. The CANAPI mean shrub height estimates tended to be lower than the field values, but there was not a clear pattern, resulting in a poor coefficient of determination.

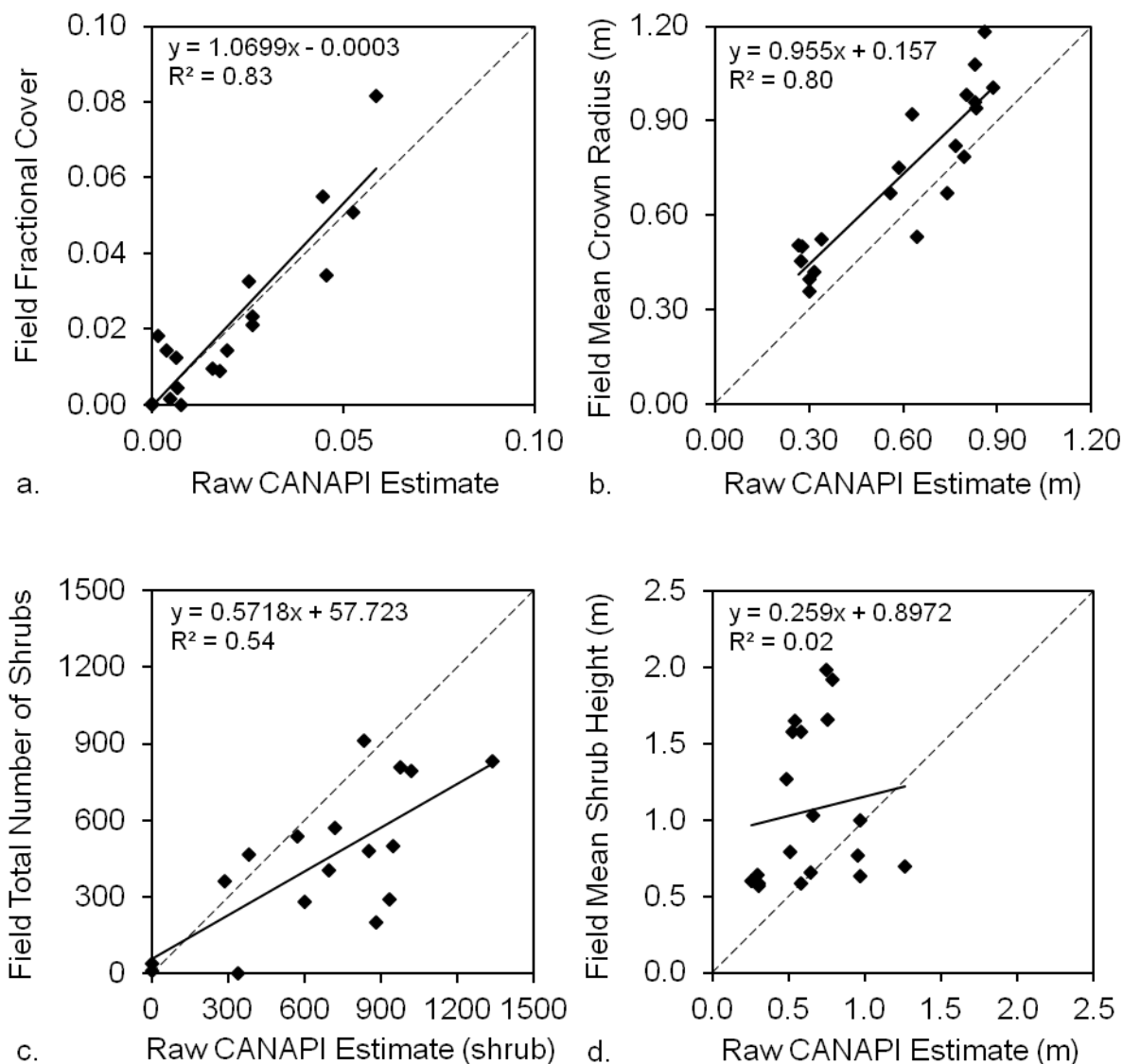


Figure 2-9. Correlations between 'raw' CANAPI estimates and field estimates for four vegetation structural variables (a) fractional cover ($P < 0.001$), (b) mean crown radius ($P < 0.001$), (c) total number of shrubs ($P < 0.001$), and (d) mean height ($P = 0.57$).

CANAPI predicts the height of an object by measuring the length of the shadow cast (in pixels) and by multiplying it by the tangent of the sun elevation angle. This means that there are at least three sources of error that may account for the differences between the

field and CANAPI estimates: 1) the lower spatial resolution of the sensors compared to the precise measurements made in the field; 2) different sensor-object geometries from the different high resolution sensors used (QuickBird, GeoEye, WorldView 1 and 2) that were not accounted for by the CANAPI algorithm used to derive the height estimates; 3) error from field measurements and subsequent calculations, though this is thought to be a much smaller term.

The high coefficient of determination values for fractional cover and mean crown radius (0.83 and 0.80 respectively) suggest that it is appropriate to use the regression coefficients to adjust shrub CANAPI estimates in Arctic tundra (Equations 2-6 and 2-7). Although the coefficient of determination was not low for total number of shrubs (0.53), the regression coefficients must be used with caution (Equation 2-8). It is not recommended that the regression equation be used to adjust CANAPI estimates of mean shrub height due to the poor correlation found with the field estimates.

The CANAPI algorithm is sensitive to small changes in woody vegetation cover and consistently detects a wide size range of erect shrubs. The sensitivity of the algorithm is a key factor given that at a spatial resolution of 250 m tall shrub cover is usually less than 5% in the Arctic (Beck et al., 2011; Selkowitz, 2010). Results showed that when adjusting the algorithm's parameters and filter settings for each site, CANAPI can provide good estimates of fractional cover, crown radius, and total number of shrubs with remarkable confidence in spite of the important limiting factors: 1) the surrounding background is composed of mixed vegetation (tussocks, moss, and lichens), and therefore there is less contrast between shrubs and their background; 2) the signal is quite small

since 75 percent of the time cover is less than 0.02 in the Arctic landscape at 250 m scales; and 3) shrubs are considerably smaller than trees (the target population where CANAPI has been previously used successfully) and thus more difficult to detect.

2.3.4. Enlargement of Reference Database

CANAPI estimates were derived for 1,013 subsets across the entire domain of the North Slope of Alaska (Appendix B). Those estimates were adjusted using the following regression equations:

$$\text{Fractional Cover} = (1.0699 \times \text{CANAPI estimate}) - 0.0003 \quad (\text{Eq. 2-6})$$

$$\text{Mean Crown Radius} = (0.955 \times \text{CANAPI estimate}) + 0.157 \quad (\text{Eq. 2-7})$$

$$\text{Shrub Total} = (0.5718 \times \text{CANAPI estimate}) + 57.723 \quad (\text{Eq. 2-8})$$

The final reference database had 1,039 sites including the field plots surveyed in 2010 and 2011. Exploratory analysis of this dataset showed that the mean crown radius estimates were normally distributed and that it ranged from 0.3 m to 1.5 m (Figure 2-10c). The distribution of the total number of shrubs and fractional cover were highly skewed to the left (Figure 2-10a and 2-10b). Out of the 1,039 sampled sites, 717 sites had less than 400 shrubs and 755 sites (~75%) had a fractional cover less than 0.02. Thus, the population of tall shrubs (0.5 m) was quite small and therefore, the more challenging it is to detect a small signal. These results agreed with Selkowitz's (2010) study in the North Slope, in which, at the 250 m spatial resolution, more than 80% of the training pixels had a fractional cover value less than 0.05.

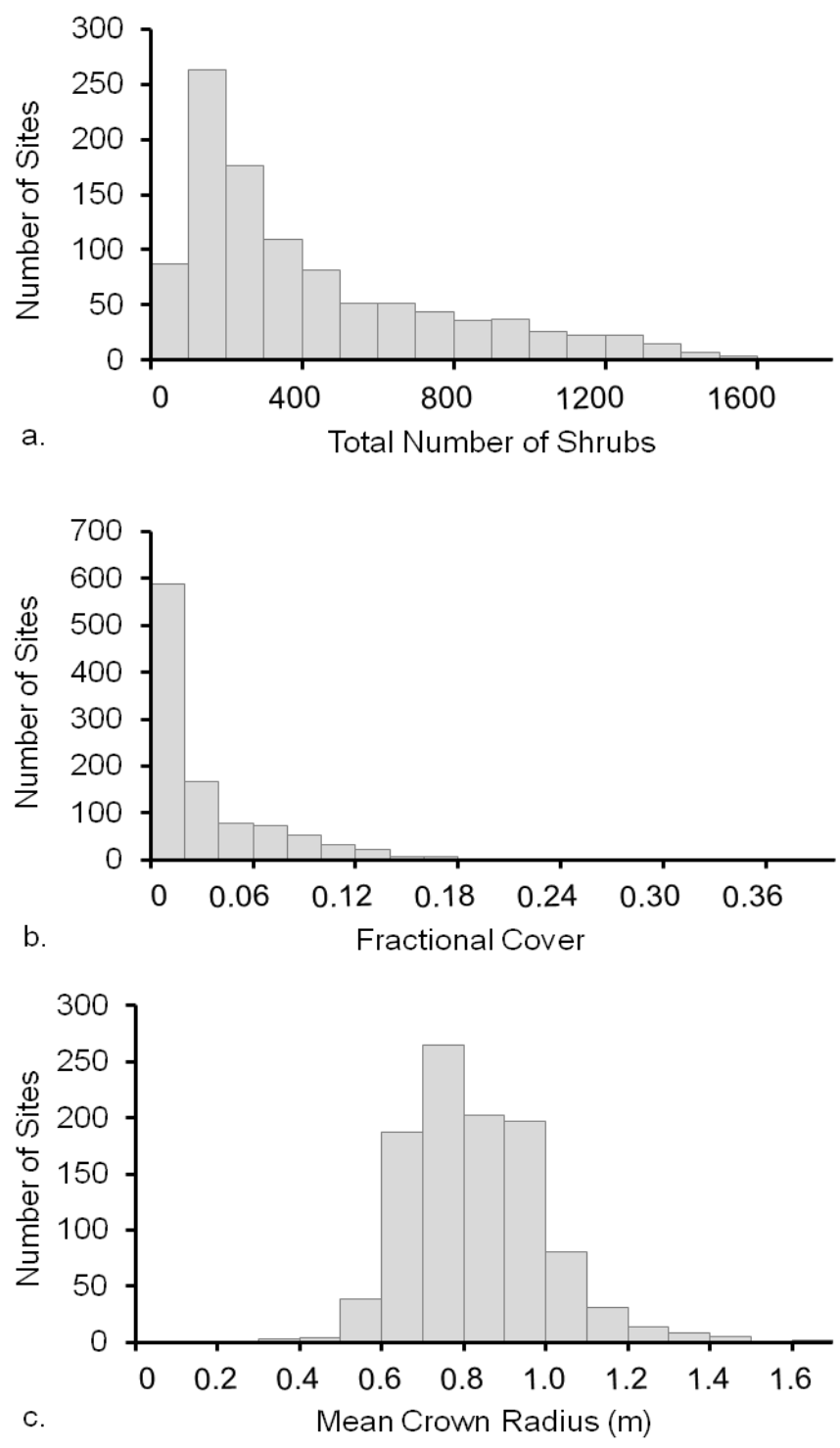


Figure 2-10. Histograms of frequency: a. total number of shrubs, b. fractional cover, and c. mean crown radius.

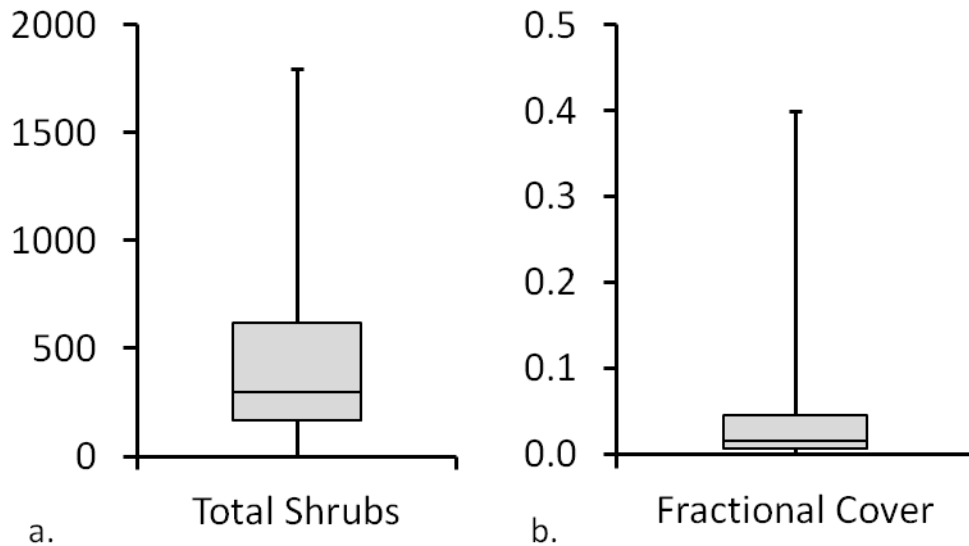


Figure 2-11. Five-number summary. a. Total number of shrubs, b. fractional cover.

Due to the different distributions presented in the histograms, the five-number summary was used to describe the fractional cover and total number of shrubs, while the mean and standard deviation were used to describe the mean crown radius. The medians of the total number of shrubs and of the fractional cover was 296 and 0.02 respectively, while the maximum total number of shrubs and fractional cover was 1,794 and 0.40 respectively (Figure 2-11). The histogram of fractional cover showed that there was a gap between 0.40 and 0.22, and suggested that the extreme value could have been an outlier, however, a visual inspection of the site showed that it was a valid entry. The mean crown radius of all sites in the reference database was 0.8 m with a standard deviation of 0.17 m.

2.4. Conclusion

CANAPI is a user friendly, user-adjustable algorithm that can perform well under different scenarios, in particular, with sparse woody vegetation. The results obtained in this study show that CANAPI provides a way to build reference datasets for some important structural characteristics of the woody vegetation directly from high-resolution panchromatic imagery. CANAPI provides data that can be used to assess the results of other mapping or estimation approaches, though the regression equations developed here for Arctic Alaska will apply most accurately in similar tundra landscapes. A comprehensive data set “Woody Vegetation Characteristics of 1,039 Sites across the North Slope, Alaska” was derived in this way as part of the NASA Terrestrial Ecology project "Mapping Changes in Shrub Abundance and Biomass in Arctic Tundra using NASA Earth Observing System Data: A Structural Approach" for the North American Carbon Program (NACP; Wofsy & Harriss (2002)) and has been made available at the Oak Ridge National Laboratory (ORNL) Distributed Active Archive Center (DAAC) (Duchesne et al., 2015a). A copy of the CANAPI algorithm is included along with shrub canopy statistics for 26 field sites that might be useful if adjustment of the equations is desired in order to help account for user bias. A peer-reviewed paper is also available with details on the capability of the CANAPI algorithm to derive shrub structural parameters from satellite imagery in the Alaskan Arctic (Duchesne et al., 2015b). Future research projects and campaigns such as the upcoming NASA-sponsored Arctic-Boreal Vulnerability Experiment (ABOVE; Kasischke et al., 2010) that require data on shrub abundance in Arctic tundra may opt to use the NACP database. For example it could be

used to assess the results of ABoVE remote sensing initiatives that attempt to exploit imagery acquired at lower spatial resolutions (e.g., from Landsat, or NASA's Multi-angle Imaging SpectroRadiometer (MISR) and Moderate Resolution Imaging Spectroradiometer (MODIS)); or by using CANAPI with earlier and/or more current imagery to assess changes in cover through time. This database could also be used with recently-developed allometric equations (Berner et al., 2015) to provide tall shrub aboveground biomass estimates for all sites.

2.5. References

- Anderson, P. M., Bartlein, P. J., & Brubaker, L. B. (1994). Late quaternary history of tundra vegetation in northwestern Alaska. *Quaternary Research*, 41(3), 306–315.
- Asner, G. P., & Heidebrecht, K. B. (2002). Spectral unmixing of vegetation, soil and dry carbon cover in arid regions: comparing multispectral and hyperspectral observations. *International Journal of Remote Sensing*, 23(19), 3939–3958.
- Beck, P. S. A., Horning, N., Goetz, S. J., Loranty, M. M., & Tape, K. D. (2011). Shrub cover on the north slope of Alaska: a circa 2000 baseline map. *Arctic, Antarctic, and Alpine Research*, 43(3), 355–363.
- Berner, L. T., Alexander, H. D., Loranty, M. M., Ganzlin, P., Mack, M., Davydov, S. P., & Goetz, S. J. (2015). Biomass allometry for alder, dwarf birch, and willow in boreal forest and tundra ecosystems of far northeastern Siberia and north-central Alaska. *Forest Ecology and Management*, 337, 110–118.

- Blok, D., Schaepman-Strub, G., Bartholomeus, H., Heijmans, M. M. P. D., Maximov, T., & Berendse, F. (2011). The response of Arctic vegetation to the summer climate: relation between shrub cover, NDVI, surface albedo, and temperature. *Environmental Research Letters*, 6(3): 035502.
- Boelman, N. T., Gough, L., McLaren, J. R., & Greaves, H. (2011). Does NDVI reflect variation in the structural attributes associated with increasing shrub dominance in arctic tundra? *Environmental Research Letters*, 6(3), 35501.
- CAVM Team. (2003). Circumpolar Arctic Vegetation Map. (1:7,500,000 scale), Conservation of Arctic Flora and Fauna (CAFF) Map No. 1. U.S. Fish and Wildlife Service, Anchorage, Alaska. ISBN: 0-9767525-0-6.
- Chapin, F. S., Shaver, G. R., Giblin, A. E., Nadelhoffer, K. J., & Laundre, J. A. (1995). Responses of Arctic tundra to experimental and observed changes in climate. *Ecology*, 76(3), 694.
- Chapin, F. S., Sturm, M., Serreze, M. C., McFadden, J. P., Key, J. R., Lloyd, A. H., . . . , & Welker, J. M. (2005). Role of land-surface changes in arctic summer warming. *Science (New York, N.Y.)*, 310(5748), 657–660.
- Chapman, W.L., & Walsh, J.E. (1993). Recent variations of sea ice and air temperatures in high latitudes. *Bulletin American Meteorological Society*, 74: 33-47.
- Chopping, M. (2011). CANAPI: canopy analysis with panchromatic imagery. *Remote Sensing Letters*, 2(1), 21–29.

- Chopping, M., North, M., Chen, J., Schaaf, C. B., Blair, J. B., Martonchik, J. V., & Bull, M. A. (2012). Forest canopy cover and height from MISR in topographically complex southwestern US landscapes assessed with high quality reference data. *IEEE Journal of Selected Topics in Applied Earth Observations and Remote Sensing*, 5(1), 44–58.
- Duchesne, R.R., Chopping, M.J., & Tape, K.D. (2015a). NACP woody vegetation characteristics of 1,039 sites across the North Slope, Alaska. Data set. Available online [<http://daac/ornl.gov/>] from Oak Ridge National Laboratory Distributed Active Archive Center, Oak Ridge, Tennessee, USA. URL: <http://dx.doi.org/10.3334/ORNLDAAC/1270>, last access April 17, 2015.
- Duchesne, R.R., Chopping, M.J., & Tape, K.D. (2015b). Capability of the CANAPI algorithm to derive shrub structural parameters from satellite imagery in the Alaskan Arctic. *Polar Record*. [In press].
- Elmendorf, S. C., Henry, G. H. R., Hollister, R. D., Björk, R. G., Boulanger-Lapointe, N., Cooper, E. J., . . . , & Wipf, S. (2012). Plot-scale evidence of tundra vegetation change and links to recent summer warming. *Nature Climate Change*, 2(6), 453–457.
- Elmhagen, B., Kindberg, J., & Hellstrom, P. (2015). A boreal invasion in response to climate change? Range shifts and community effects in the borderland between forest and tundra. *AMBIO*, 44(1), 39-50.
- Elzinga, C.L., Salzer, D.W., & Willoughby, J. W. (1998). Measuring and monitoring plant populations. BLM Technical Reference 1730-1.

- Epstein, H. E., Beringer, J., Gould, W. A., Lloyd, A. H., Thompson, C. D., Chapin, F. S., . . ., & Walker, D. A. (2004). The nature of spatial transitions in the Arctic. *Journal of Biogeography*, 31(12), 1917–1933.
- Euskirchen, E. S., McGuire, A. D., Chapin, F. S., Yi, S., & Thompson, C. C. (2009). Changes in vegetation in northern Alaska under scenarios of climate change, 2003–2100: implications for climate feedbacks. *Ecological Applications*, 19(4), 1022–1043.
- Forbes, B. C., Fauria, M. M., & Zetterberg, P. (2010). Russian Arctic warming and ‘greening’ are closely tracked by tundra shrub willows. *Global Change Biology*, 16(5), 1542–1554.
- Hill D., Fasham M., Tucker G., Shewry M, & Shaw P. (Eds.). (2005). Handbook of Biodiversity Methods: Survey, Evaluation, and Monitoring. New York, NY: Cambridge University Press.
- Higuera, P. E., Brubaker, L. B., Anderson, P. M., Brown, T. A., Kennedy, A. T., & Hu, F. S. (2008). Frequent fires in ancient shrub tundra: implications of paleorecords for arctic environmental change. *PloS one*, 3(3), e0001744.
- Hinzman, L. D., Bettez, N. D., Bolton, W. R., Chapin, F. S., Dyrurgerov, M. B., Fastie, C. L., . . ., & Yoshikawa, K. (2005). Evidence and implications of recent climate change in northern Alaska and other Arctic regions. *Climatic Change*, 72(3), 251–298.
- Hopkinson, C., Chasmer, L. E., Sass, G., Creed, I. F., Sitar, M., Kalbfleisch, W., & Treitz, P. (2005). Vegetation class dependent errors in lidar ground elevation and

- canopy height estimates in a boreal wetland environment. *Canadian Journal of Remote Sensing*, 31(2), 191-206.
- Hudson, J. M. G., & Henry, G. H. R. (2009). Increased plant biomass in a High Arctic heath community from 1981 to 2008. *Ecology*, 90(10), 2657–2663.
- Huemmrich, K., Gamon, J. A., Tweedie, C. E., Oberbauer, S. F., Kinoshita, G., Houston, S., . . . , & Mano, M. (2010). Remote sensing of tundra gross ecosystem productivity and light use efficiency under varying temperature and moisture conditions. *Remote Sensing of Environment*, 114(3), 481–489.
- Intergovernmental Panel on Climate Change. (2014). Climate change 2013: the physical science basis: working group I contribution. IPCC Fifth Assessment Report. Cambridge: Cambridge University Press.
- Jia, G. J., & Howard E. E. (2003). Greening of arctic Alaska, 1981–2001. *Geophysical Research Letters*, 30(20).
- Kasischke, E. S., Goetz, S. J., Kimball, J. S., & Mack, M. M. (2010). The Arctic-Boreal Vulnerability Experiment (ABoVE): A concise plan for a NASA-sponsored field campaign. Final Report on the VuRSAL/ABoVE Scoping Study.
- Liston, G. E., Mcfadden, J. P., Sturm, M., & Pielke, R. A. (2002). Modelled changes in arctic tundra snow, energy and moisture fluxes due to increased shrubs. *Global Change Biology*, 8(1), 17–32.
- Meyer T., & Okin G. S. (2015). Evaluation of spectral unmixing techniques using MODIS in a structural complex savanna environment for retrieval of green

- vegetation, non photosynthetic vegetation, and soil fractional cover. *Remote Sensing of Environment*, 161, 122-130.
- Myers-Smith, I. H., Forbes, B., Wilmking, M., Hallinger, M., Lantz, T., Blok, D., Tape, K., ..., & Hik, D.S. (2011). Shrub expansion in tundra ecosystems: dynamics, impacts, and research priorities. *Environmental Research Letters*, 6(4): 045509.
- Myneni, R. B., Keeling, C. D., Tucker, C. J., Asrar, G., & Nemani, R. R. (1997). Increased plant growth in the northern high latitudes from 1981 to 1991. *Nature*, 386(6626), 698–702.
- Popescu, S. C., Zhao, K., Neuenschwander, A., & Lin, C. (2011). Satellite lidar vs. small footprint airborne lidar: comparing the accuracy of aboveground biomass estimates and forest structure metrics at footprint level. *Remote Sensing of Environment*, 115, 2786-2797.
- Rosette, J.A.B., North, P. R. J., & Suarez, J. C. (2008). Vegetation height estimates for a mixed temperate forest using satellite laser altimetry. *International Journal of Remote Sensing*, 29(5), 1475-1493.
- Selkowitz, D. J. (2010). A comparison of multi-spectral, multi-angular, and multi-temporal remote sensing datasets for fractional shrub canopy mapping in Arctic Alaska. *Remote Sensing of Environment*, 114(7), 1338–1352.
- Stow, D. A., Hope, A., McGuire, D., Verbyla, D., Gamon, J., Huemmrich, F., . . . , & Myneni, R. (2004). Remote sensing of vegetation and land-cover change in Arctic Tundra Ecosystems. *Remote Sensing of Environment*, 89(3), 281–308.

- Streutker, D., & Glenn, N. F. (2006). LiDAR measurement of sagebrush steppe vegetation height. *Remote Sensing of Environment*, 102(1-2), 135-145.
- Sturm, M., Jon Holmgren, Mcfadden, J. P., Liston, G. E., Chapin, F. S., & Racine, C. H. (2001a). Snow-shrub interactions in arctic tundra: a hypothesis with climatic implications. *J. Climate*, 14, 336–344.
- Sturm, M., Racine, C., & Tape, K. (2001b). Climate change: increasing shrub abundance in the Arctic. *Nature*, 411(6837), 546–547.
- Tape, K., Sturm, M., & Racine, C. (2006). The evidence for shrub expansion in Northern Alaska and the Pan-Arctic. *Global Change Biology*, 12(4), 686–702.
- Tape, K. D., Hallinger, M., Welker, J. M., & Ruess, R. (2012). Landscape heterogeneity of shrub expansion in Arctic Alaska. *Ecosystems*, 15(5): 711-724.
- Tazik, D., Warren, S., Diersing, V., Shaw, R., Brozka, R., Bagley, C., & Whitworth, W. (1992). U.S. Army Land Condition-Trend Analysis (LCTA) Plot Inventory Field Methods. Champaign, IL. US Army Corps of Engineers: Construction Engineering Research Laboratory Technical Report N-92/03.
- Wofsy, S. C., & Harriss, R. C. (2002). The North American Carbon Program (NACP). Report of the NACP Committee of the US Interagency Carbon Cycle Science Program. US Global Change Research Program, Washington, DC, 59.

CHAPTER 3

Training and Validation of the Boosted Regression Tree Model to Predict Shrub Cover from Moderate Resolution Imagery

Abstract

In the past few decades shrubs have expanded in the North Slope of Alaska. An increase in shrub abundance could potentially affect the regional climate, terrestrial ecosystem, hydrology, and energy partitioning at the surface. In order to assess the extent of the environmental impact, it is imperative to know the direction and magnitude of the shrub expansion. Vegetation indices have shown a greening trend in Arctic Alaska, but the indices are proxies only of vegetation photosynthetic activity and not of canopy architecture. Machine learning algorithms like the Random Forest (RF) model have been used to map shrub cover in northern Alaska, however, little can be inferred about the role of the predictor variables. Therefore, the Boosted Regression Tree (BRT), an ensemble machine-learning algorithm that can provide graphical and numerical representations of the relative influence of the predictors and the interactions among them, was trained and validated to predict tall shrub cover (>0.5 m) in the North Slope of Alaska from moderate resolution satellite images. The BRT model used 14 explanatory variables: four spectral bands from the nadir camera of the Multi-angle Imaging SpectroRadiometer (MISR) sensor, six parameters that resulted from the inversion of the RossThick-LiSparse Reciprocal (RTLS-R) model (a canopy reflectance model that takes into consideration the multi-angular information provided by MISR's nine cameras), and four terrain variables.

The final model explained 52% of the variation in the response variable, fractional cover, and had a tree complexity of three and a learning rate of 0.005. The red reflectance, slope, nadir BRDF-adjusted reflectance weight, and isotropic scattering kernel were the variables more often used to generate the regression trees, and therefore they contributed the most to the model. Since the boosted regression tree is an empirical model, its application is limited to the prediction of tall shrub fractional cover in Arctic landscapes.

Keywords: Booster Regression Tree, RossThick-LiSparse Reciprocal model, Multi-angle Imaging SpectroRadiometer, shrub fractional cover, North Slope of Alaska.

3.1 Introduction

The region north of the Brooks Range in Alaska, also known as the North Slope, is dominated by tundra. By definition, the tundra is a treeless land dominated by sedges, grasses, mosses, lichens, and scattered shrubs. However, in the past few decades, an expansion of shrubs northward has been underway and linked to recent warming trends (Chapin et al., 1995; Elmendorf et al., 2012; Hudson & Henry, 2009; Huemmrich et al., 2010). Shrubs have the potential to influence climate by changing the regional albedo, the energy partitioning at the surface, and the emission of greenhouse gases (McGuire et al., 2006). Until the direction and magnitude of the shrub expansion is known, it would be impossible to assess the extent of their impact on the climate (Hinzman et al., 2005).

Due to the vastness of the North Slope and the relative inaccessibility of the region, remote sensing may be the most appropriate method to quantify and monitor shrub cover changes in the Arctic (Jia & Epstein, 2003; Selkowitz, 2010). Nevertheless, mapping shrubs in the Arctic comes with many challenges. First, collection of satellite imagery is limited to the short summer season when there is no snow on the ground and the shrubs have a fuller canopy (Stow et al., 2004). Second, the probability of getting a cloud-free scene is low considering the persistent cloud cover, especially during the summer months (Gamon et al., 2013). Third, due to the low sun angles at high latitudes, the incoming and outgoing radiation is more scattered as it travels through a longer path in the atmosphere; thus, the signal-to-noise ratio at the sensor is reduced (Hinzman et al., 2005). And fourth, tall shrub cover at moderate spatial resolution (~250 m) is usually less than 5% in the North Slope (Duchesne et al., 2015; Selkowitz, 2010).

Multi-spectral remote sensing has been frequently used to determine greening trends in the Arctic by exploiting differences in the spectral signal of the vegetation (Bi et al., 2013; Jia & Epstein, 2003; McManus et al., 2012; Myneni et al., 1997; Raynolds et al., 2013; Stow et al., 2003; Zhou et al., 2001). However, vegetation indices are proxies of vegetation photosynthetic activity but not of canopy architecture parameters, such as cover (Glenn et al., 2008). The relationship between the vegetation indices and biophysical quantities of the vegetation varies with season, proportion of dead material in plant canopy, vegetation type, and soil background (Sellers, 1985). The Normalized Difference Vegetation Index (NDVI), in particular, is sensitive to the solar and illumination geometry. Besides using vegetation indices, machine-learning algorithms have been employed to map shrub cover in the North Slope of Alaska by exploiting the spectral information in the six bands (blue, green, red, two near-infrared bands, and a mid-infrared band) of the Landsat 7 satellite at 30 m spatial resolution (Beck et al., 2011).

Although less commonly used, multi-angular remote sensing has also been recognized as a source of information for mapping vegetation (Chopping et al., 2006; Chopping et al., 2008; Lacaze et al., 2002; Nolin, 2004). Multi-angular remote sensing exploits the variations in surface reflectance from different sun-target-sensor geometry, which is described by the bidirectional reflectance distribution function (BRDF) (Nicodemus et al., 1997). The BRDF is an intrinsic property of the surface and it provides the reflectance of a target as a function of the viewing and illumination geometry. BRDF effects should be taken into account for any remote sensing land surface study. Even though the BRDF cannot be directly obtained from multi-angular measurements, models

like the RossThick-LiSparse Reciprocal (Wanner et al., 1995) can be used to obtain bidirectional reflectance factors and the BRDF (Martonchik et al., 1998).

A pivotal study conducted by Selkowitz (2010) used regression trees to determine the potential of multi-spectral, multi-angular, and multi-temporal remote sensing datasets for mapping shrub fractional cover (>0.5 m) in Arctic Alaska. Results showed that higher spatial resolution datasets (i.e., from Landsat) produce more accurate shrub cover estimates than lower spatial resolution datasets (i.e., from MISR, flying on NASA's Terra satellite). However, shrub cover estimates from MISR came very close to those from Landsat when using MISR's multi-angular red band data together with the multi-spectral information at nadir. MISR has nine viewing cameras with four spectral bands (blue, green, red, near-infrared) each and it has a swath width of 360 km. At high latitudes, like the North Slope, MISR has a revisit time of 1 or 2 days. Considering that the persistent cloud cover in the region challenges mapping efforts—for instance, the 2000 circa map needed imagery from four years to cover the entire North Slope (Beck et al., 2010)—MISR can be a better sensor for mapping shrub cover in Arctic Alaska because of its higher temporal resolution and wider swath (Selkowitz, 2010).

In this study, the MISR sensor, which was launched in 1999, was selected as the source of multi-spectral and multi-angular information to support mapping efforts because of its many advantages. First, multi-angular observations, such as those from MISR, contain unique additional information beyond that provided by sensors with nadir or single-angle spectral measurements (Asner et al., 1998; Chen et al., 2003). For instance, multi-angular observations provide the means to derive the BRDF, which

describes the anisotropic behavior of reflected light as a result of surface 3-D structure and the optical properties of surface components. Second, the smaller ground-projected instantaneous field of view of MISR's nadir spectral bands and off-nadir red bands (spatial resolution of 275 m) may be an advantage for mapping vegetation in comparison to coarser spatial resolution sensors like the Advanced Very High Resolution Radiometers (AVHRRs) (spatial resolution of 1 km) (Selkowitz, 2010). Third, mapping efforts in the North Slope are often limited to the short summer season with its persistent cloud cover (Hope & Stow, 1995). The high temporal resolution and wide swath of MISR increases the likelihood of obtaining cloud-free scenes in this region (Selkowitz, 2010). Sensors with lower temporal resolution, such as Landsat, would require many years of data to cover the entire North Slope (Beck et al., 2011 ; Muller et al., 1999). Fourth, the concurrent use of multi-angular and multi-spectral information from MISR for the retrieval of shrub cover has shown promising results (Selkowitz, 2010).

Besides the selection of the sensor, it is also necessary to select the most appropriate model to pursue mapping efforts of shrub fractional cover. Physical or semi-empirical canopy reflectance models could be used but they require *a priori* information on the surface, which is a challenge since there is a high variability in the composition of the background vegetation. Other kind of models, machine learning algorithms, have the advantage of learning the relationship between the response and the predictor variables to find prevailing patterns (Breiman, 2001; Elith et al., 2008) and they are not constrained by the need for realistic internal model parameters such as leaf reflectance, leaf angle distribution, plant number density, mean crown radius, height and so on. Algorithms,

such as ensemble trees, neural nets, and support vector machines belong to the machine-learning group. Ensemble methods, like the Boosted Regression Tree (BRT) and Random Forest (RF), were initially used in ecological studies (De'Ath, 2007; Leathwick et al., 2006), but in recent years there has been an increase in their use in remote sensing studies (Beck et al., 2011; Raynolds et al., 2013). Preliminary tests were run using the semi-empirical modified Simple Geometric Model (SGM, Chopping et al., 2003) and the empirical Neural Networks (NN) and Random Forest models. The modified SGM model describes the reflectance anisotropy properties of the background by using the RossThick-LiSparse kernel weights (isotropic, geometric, and volumetric kernels). Since the volume scattering kernel weight could not be predicted accurately, it was not feasible to predict the contribution of the background with sufficient precision. This might have been due to the small contrast between the background and the shrubs and to the high variability in the background composition (lichens, mosses, tussock, rocks, etc). NN and RF models produced better results but had the shortcoming of being considered black boxes where no information was provided on the contribution and role of the explanatory variables in the model.

In this study, the Boosted Regression Tree model was selected to map shrub fractional cover in the North Slope of Alaska due to its several advantages over other models. The BRT model can work with categorical as well as with numerical explanatory variables (Leathwick et al., 2006). It can handle missing data with minimal loss of information. The model is unaffected by extreme outliers. It can fit a complex nonlinear distribution of the explanatory variables (Elith et al., 2008). But, most importantly, unlike

the neural network and the random forest models, the BRT model provides simple graphical and numerical representations of the predicted variation in the response variable in relation to the explanatory variables, of the relative influence of the predictors, and of the interactions between the independent variables (De'Ath, 2007).

Having selected the MISR sensor and Boosted Regression Tree model to map shrub fractional cover in the North Slope of Alaska, this study focused on the training and validation of the model. Specific objectives were to obtain MISR imagery for the year 2010—the year for which fractional cover estimates in the reference database were obtained, to invert the RossThick-LiSparse reciprocal model using the red reflectance values of MISR's nine cameras in order to account for the anisotropic properties of the surface, to identify suitable predictor variables and their relative contribution to the model, to simplify the BRT model by dropping variables that did not improve its predictive performance, to identify interactions between predictor, and to evaluate the predictive performance of the BRT model.

3.2. Materials and Methods

3.2.1. Data Sources

A robust reference database was used to train the boosted regression tree model and to validate the results. The database consisted of tall shrub cover estimates for 1,039 sites across the North Slope of Alaska, as described in Chapter 2. Each site was aligned with a 250 m Albers Conical Equal Area grid, onto which the MISR data were mapped, and had an area of 62.5 km². The sites included representatives from all four physiognomic

vegetation types present in the region (CAVM, 2003) and they covered a wide latitudinal and longitudinal range. Shrub cover estimates for 2010 were obtained from very high resolution imagery using the CANAPI algorithm (Duchesne et al., 2015). The CANAPI estimates were assumed to be reliable since they were previously calibrated with field estimates via regression equations ($R^2 = 0.83$, $P < 0.001$).

For the training and validation of the BRT model, MISR data corresponding to 21 paths (P065-P085) and 59 orbits were downloaded for the period June 15 - July 31 2010 (Appendix C). This period matched the peak of the growing season when the shrub crowns were at their fullest and minimal changes in reflectance were observed. The MISR data were downloaded from the NASA Langley Atmospheric Science Data Center using the MISR Order and Customization Tool (<http://10dup05.larc.nasa.gov/MISR/cgi-bin/MISR/main.cgi>).

MISR is a sun-synchronous moderate resolution sensor on board of the Terra satellite and was launched in December 1999 (Diner et al., 1999). Besides its nadir camera, it has eight more pointing at fixed angles (± 26.1 , ± 45.6 , ± 60.0 , and ± 70.5 degrees) and each camera has four optical channels (blue, green, red, and near-infrared). Thus, MISR can provide simultaneous multi-angular calibrated images in four spectral bands. For this study, the red band at all off-nadir angles and the four spectral bands at nadir were used in the analysis. Only these spectral bands have a spatial resolution of 275 m while the other off-nadir spectral bands have a spatial resolution of 1 km.

Other explanatory variables in the model included elevation, latitude, aspect, northness, and eastness. Elevation data for the North Slope of Alaska were obtained from

the National Elevation Dataset (NED) produced by the U.S. Geological Survey (USGS). The data were originally available at a spatial resolution of 2 arc-second (approximately 60 m) and were distributed in geographic coordinates in conformance with the North American Datum of 1983 (NAD83). Elevation was provided in units of meters. Latitude (m), slope (degrees), and aspect were derived from the elevation data. Considering that aspect is a circular variable, it was linearized by creating new two variables: northness and eastness:

$$Northness = \cos\left(\frac{aspect * \pi}{180}\right) \quad \text{Equation 3-1}$$

$$Eastness = \sin\left(\frac{aspect * \pi}{180}\right) \quad \text{Equation 3-2}$$

A value of 1 for northness indicated a north facing slope and a value of -1 a south facing one. Similarly, a value of 1 for eastness represented a slope facing directly east while a value of -1 a slope facing directly west.

Modeling was pursued in the statistical analysis and modeling package R (v3.0.1, 2013) using the 'gbm' library (Ridgeway, 2004) and the 'brt' functions (Elith & Leathwick, 2008). Data visualization was done in ERDAS Imagine 2014. All imagery used was projected unto a 250 m Albers Conical Equal Area grid.

3.2.2. MISR Data Processing

This study used four MISR products: the MISR Level 1B2 Terrain Data-MI1B2T, the MISR Level 2 Land Surface Parameters-MIL2ASLS, the MISR Geometric Parameters-MIB2GEOP, and the Ancillary Geographic Product-MIANCAGP. The MISR Level 1B2 Terrain Data contained the terrain-projected top of atmosphere radiance, resampled at the surface, and topographically corrected. The MISR Level 2 Surface Parameters contained information on land directional reflectance properties (BRFs), albedos and associated radiation, and terrain-referenced geometric parameters on a 1.1 km grid. The MISR Geometric Parameters supplied the solar azimuth, solar zenith, and nine viewing azimuth and zenith angles at a spatial resolution of 17.6 km on the reference WGS84 ellipsoid. The Ancillary Geographic Product consisted of eleven fields of geo-location data, such as digital terrain elevation, on a SOM grid. With the aid of custom MISR Toolkit routines the data in the Hierarchical Data Format (HDF) were extracted, and the surface reflectance estimates were obtained and mapped onto the Albers Conical Equal Area map projection, with a grid interval of 250 m.

The MISR red band bidirectional reflectance factors (BRFs) in all nine cameras were used to invert the RossThick-LiSparse Reciprocal (RTLS-R) model, using the Algorithm for Modeling Bidirectional Reflectance Anisotropies of the Land Surface (AMBRALS) code (Wanner et al., 1997). The RTLS-R model is a kernel-driven semi-empirical BRDF model (Wanner et al., 1995), suitable for scenes with high values of the leaf area index (LAI) (Roujean et al., 1992) and sparse spacing of shrub or tree crowns (Li & Strahler, 1992). Inversion of this model resulted in 13 parameters for each location (or raster cell):

three kernels functions (isotropic, volumetric, and geometric) that describe the BRDF shape, the weight of determination of these functions, the black-sky (directional) and white-sky (diffuse) albedos with their respective weight of determination, the RMSE, number of observations, and the weight of determination of the nadir BRDF-adjusted reflectance at solar zenith angle of 45 degrees (NBAR_45W). Five variables from the RTLS-R model (the isotropic, volumetric, and geometric kernels; the white and black sky albedo; and the nadir BRDF-adjusted weight) together with the surface reflectance from MISR's four spectral bands at nadir were used as initial explanatory variables to predict shrub fractional cover in the BRT model.

3.2.3. Training and Validation of the Boosted Regression Tree Model

The boosted regression tree (BRT) was used in this study to retrieve fractional cover estimates from moderate resolution imagery. The BRT model, sometimes called 'stochastic gradient boosting', is an ensemble method in which a large number of simple models (regression trees) are fit and then combined using a boosting algorithm to develop a final model (Leathwick et al., 2006). The trees are added to the final model in a forward stage-wise fashion, emphasizing observations poorly predicted by the previous trees (Friedman et al., 2000). Thus, the final BRT model can be seen as an additive regression model in which each of the individual terms is a simple regression tree (Elith et al, 2008).

The BRT model has several advantages that favor its selection over other models for this study. However care should be taken to avoid an over-fitted or complex model. In the first case, as more explanatory variables are added to the BRT model, eventually the

model can become over-fitted to the training data (Leathwick et al., 2006). To minimize this probability, Elith and Leathwick (2008) wrote code to simplify the model by performing backward elimination of explanatory variables that do not give evidence of improving the model's predictive performance. In the second case, the model complexity can be controlled by keeping the size of the individual regression trees low. The greater the tree size, the more complex the model becomes.

Several models were run by adjusting two parameters: the learning rate, also known as shrinkage rate, and the size of the individual trees. The learning rate was used to reduce the contribution of each tree as it was added to the model; smaller rates were preferred because they increased the predictive performance of the final model (Elith et al., 2008). The size of the individual trees regulated the number of splits and controlled the complexity of the model. A value of 1 meant that the individual trees consisted of a single decision rule, while a value of 2 signified that two decisions rules were used, which allowed for two-way interactions, and so on (Leathwick et al., 2006). Additional parameters included: the loss function, the number of trees, and the bag fraction. The purpose of the Gaussian loss function was to minimize the square error (Ridgeway, 2006). The Gaussian function was used because the response was a continuous variable. Since fractional cover was heavily skewed, it was necessary to transform the response using the arcsine transform, a transformation commonly used in ecological studies to better distribute proportions (Read et al., 2011):

$$ArcFC = \sin^{-1}(\sqrt{fc}) \quad \text{Equation 3-3}$$

where *ArcFC* is the transformed fractional cover, and *fc* is the original fractional cover value.

Cross-validation was used to determine the number of trees that minimize the predictive error. This method was deployed because the training dataset was relatively small (<1,000 observations). Cross-validation was accomplished by dividing the training data into 10 subsets to construct 10 training data sets, each of which omitted one of the 10 subsets; then, 10 BRT were grown, one for each training data set; the predictive error was calculated for each BRT for tree sizes 1 to m ; the BRT with the minimum predictive error was selected together with the optimum number of trees m^* ; lastly, a BRT was grown of m^* trees from the whole training data set. The bag fraction controlled the stochasticity of the model, in other words, it set the proportion of observations used in selecting variables when constructing the trees. The bag fraction was set to 0.5 (the default), which meant that at each iteration, 50% of the data from the training set were drawn at random, without replacement.

There were a total of 15 explanatory variables used in the initial BRT model: six parameters that resulted from the inversion of the RTLS-R model (three kernels functions, the black-sky and white-sky albedos, and NBAR_45W), four spectral bands from MISR's nadir camera (blue, green, red, and near-infrared), and five terrain variables (latitude, elevation, slope, northness, and eastness). The response variable was the transformed shrub fractional cover, ArcFC.

The database, which had 1,039 observations, was randomly divided into training and validation data sets (734 and 305 observations, respectively). Several BRT models were

run with different combinations of learning rates (0.1, 0.05, 0.01, 0.005, 0.001, 0.0005) and tree complexities (1 to 5) using the training dataset. For each model, changes of the predictive deviance and the coefficient of determination with respect to the number of trees were evaluated. Once the best model was selected, it was simplified by dropping explanatory variables that did not significantly change the initial predictive deviance of the model. The contribution of the explanatory variables to the simplified model was evaluated as well as the interactions between predictor variables. Lastly, the model was evaluated using the validation dataset that was not used during the training of the model.

3.3. Results and Discussion

3.3.1. Transformation of the Response Variable

Fractional cover estimates from the reference database revealed that about 67% of the sites had a shrub cover lower than 3% (Figure 3-1a). The distribution of the shrub cover estimates showed that the values were strongly skewed to the left and more than 50% of the sites fell within the first bin. Although the BRT model can handle this distribution, a smoother spread of the response can render better results. Transformation of the fractional cover values using the arcsine transform rendered a more even distribution of the estimates (Figure 3-1b).

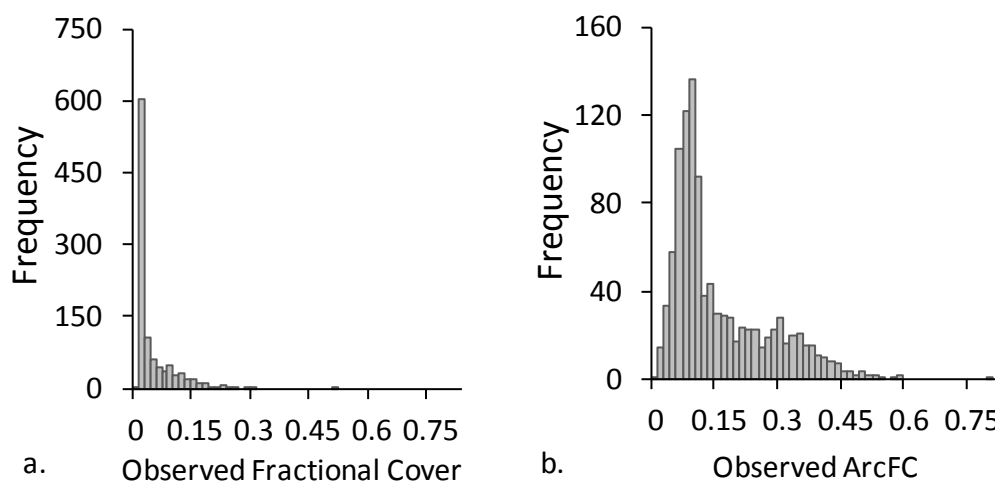


Figure 3-1. Histogram of frequency of the response variable for 1,039 sites of 250 m \times 250 m in the North Slope of Alaska. Bin width of 0.015. a. tall shrub fractional cover, b. arcsine transformed tall shrub fractional cover.

3.3.2. Identification of Monotonic Variables and Simplification of the BRT Model

Initial modeling efforts included all predictor variables without any restriction. Examination of the partial dependence plots showed that shrub fractional cover was lower in the foothills of the Brooks Range and in the coastal plain, but quite high in the mid latitude of the domain (Figure 3-2a). This pattern did not correspond to the one observed in the field in which the vegetation size increases from the coastal plain to the foothills of the Brooks Range, from prostrate dwarf shrubs (< 0.15 m in height), to erect dwarf shrub (0.15 m to 0.40 m in height), to low shrubs (>0.4 m in height) (Epstein et al., 2004). Since this study focused on shrubs taller than 0.5 m, it was expected to observe higher shrub cover values southward (lower latitude values). Thus, the relationship between fractional cover and latitude was restricted to be monotonic. The new partial

dependence plots showed that once latitude was restricted, fractional cover was lower towards the coastal plain and higher towards the Brooks Range (Figure 3-2b). The effect of using latitude unrestricted and restricted in the model was observed in preliminary fractional cover maps. When latitude was unrestricted, the fractional cover map suffered from whiter bands across the image. The problem was solved once latitude was restricted (Figure 3-3).

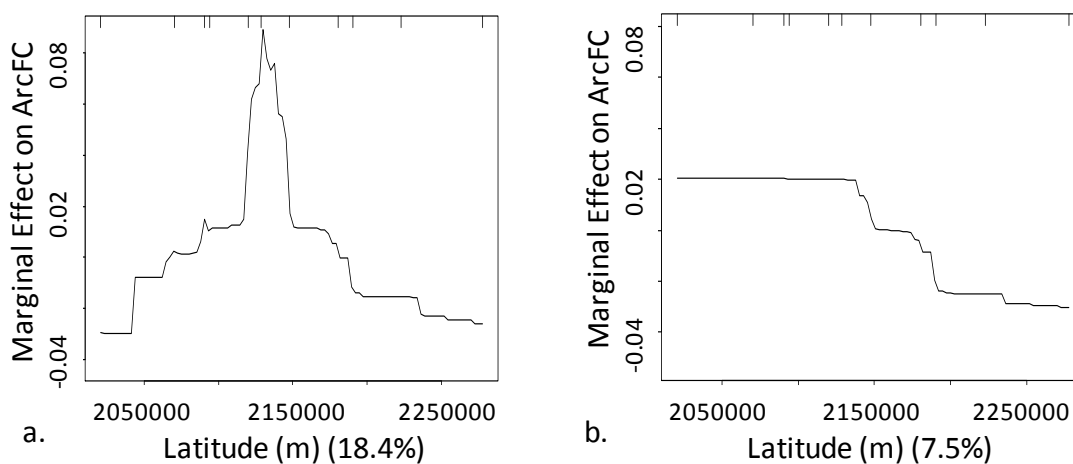


Figure 3-2. Partial dependence plots depicting the marginal effect of latitude on the response after accounting for the average effect of all other variables in the model. The fitted function is centered by subtracting its mean: a. latitude was unrestricted, b. latitude was set to be monotonic. Contribution of the variable to the model is in parenthesis.

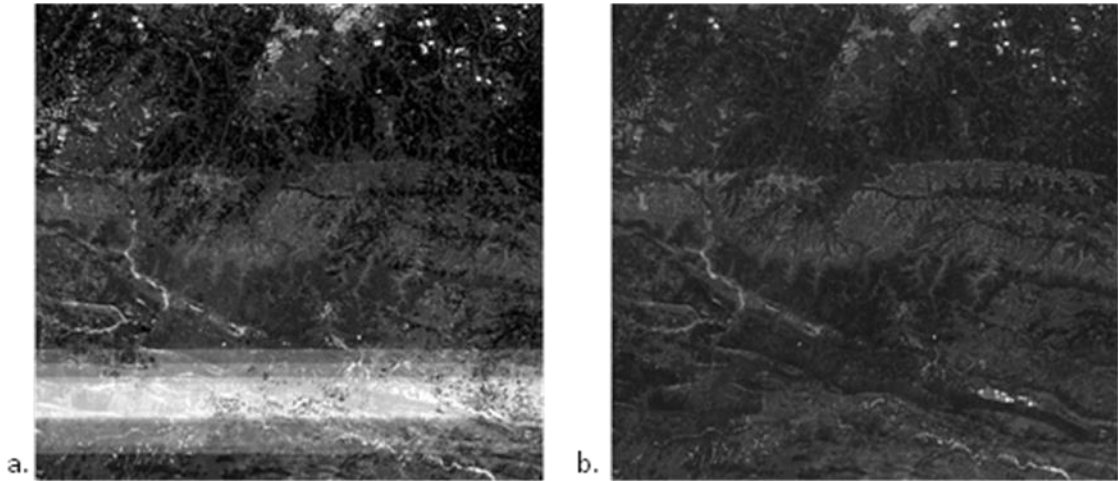


Figure 3-3. Panchromatic subset of a fractional cover map: a. latitude was not restricted, b. the relationship between latitude and fractional cover was restricted to be monotonic.

Similarly, the partial dependence plots showed that predicted shrub cover was higher at lower elevations (< 200 m), and then it decreased rapidly as elevation increased (Figure 3-4a). Although field observations show that fractional cover is higher on floodplains (lower elevations) compared to interfluves (higher elevations) (Tape et al., 2006), this pattern is relevant when considering the distribution of shrubs at a large scale. This study, on the contrary, used a coarser scale and therefore elevation was more aligned to represent the regional elevation gradient (from higher elevations at the Brooks Range to lower elevations at the coastal plain). Consequently, shrub cover was expected to decrease at lower elevations (i.e., coastal plain). In order to account for these considerations, the relationship between elevation and shrub cover were set to be monotonic (Figure 3-4b).

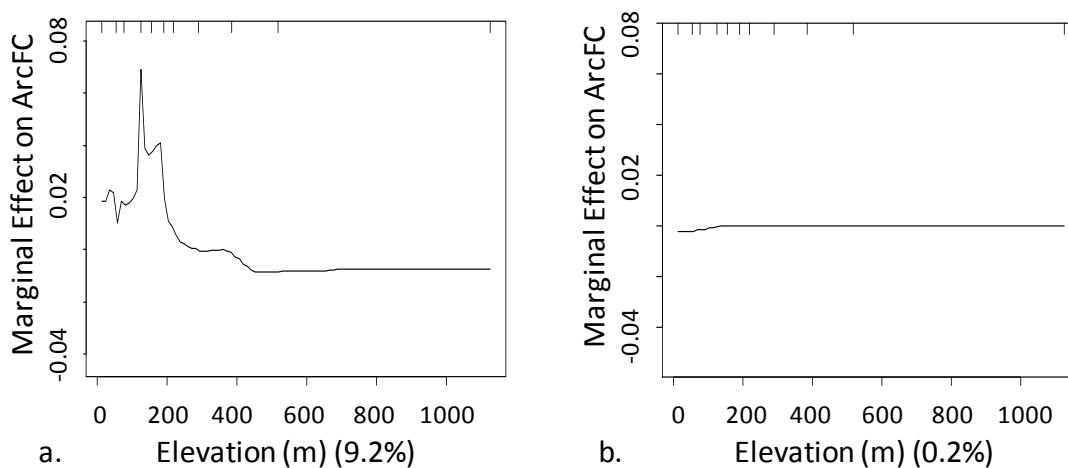


Figure 3-4. Partial dependence plot depicting the effect of elevation on the response after accounting for the average effect of all other variables in the model. The fitted function is centered by subtracting its mean: a. elevation was unrestricted, b. elevation was set to be monotonic. Contribution of the variable to the model is in parenthesis.

Also, the partial dependence plots showed that as near-infrared reflectance (NIR) decreased, shrub cover increased (Figure 3-5a). This relationship was not quite what was expected. The proportion of NIR energy that is reflected from the surface is a function of moisture content and of the intrinsic properties of the elements on the ground (i.e., vegetation, rocks, water). Vegetation in the Arctic is mainly composed of deciduous shrubs, lichens, mosses, tussock, and grasses. Lichens and mosses are brighter (~35%) than shrubs (~20%), while water strongly absorbs near-infrared radiation (<14%) (Bubier et al., 1997; Vierling et al., 1997). Therefore it was expected that areas that had a high content of moisture (i.e., wet sedges (~13%)), which usually also have a lower shrub abundance, would relate to lower values of near-infrared reflectance. Similarly, it was expected that sites with lower values of shrub abundance—and therefore a greater

proportion of background vegetation (i.e., lichens)—would correlate with higher values of NIR reflectance; whereas, sites with higher shrub cover—and therefore less bright background vegetation—would correlate with mid NIR reflectance values. Furthermore, comparisons of a preliminary shrub fractional cover map with high resolution imagery showed that there was no correspondence between observed and predicted shrub cover when NIR was unrestricted (Figure 3-6a and Figure 3-6b). Therefore, the relation between NIR and cover was also adjusted to better model the relationship observed in the field (Figure 3-5b). After this adjustment, the new shrub cover map better represented the shrub cover pattern in the high resolution imagery (Figure 3-6a and Figure 3-6c).

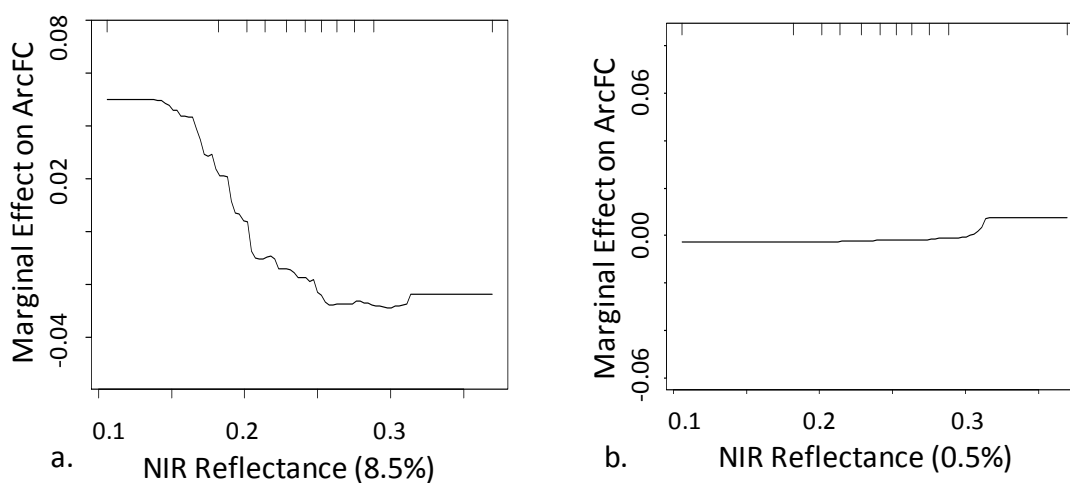


Figure 3-5. Partial dependence plot depicting the marginal effect of near-infrared reflectance on the response after accounting for the average effect of all other variables in the model. The fitted function is centered by subtracting its mean: a. NIR was unrestricted, b. NIR was restricted. Contribution of the variable to the model is in parenthesis.

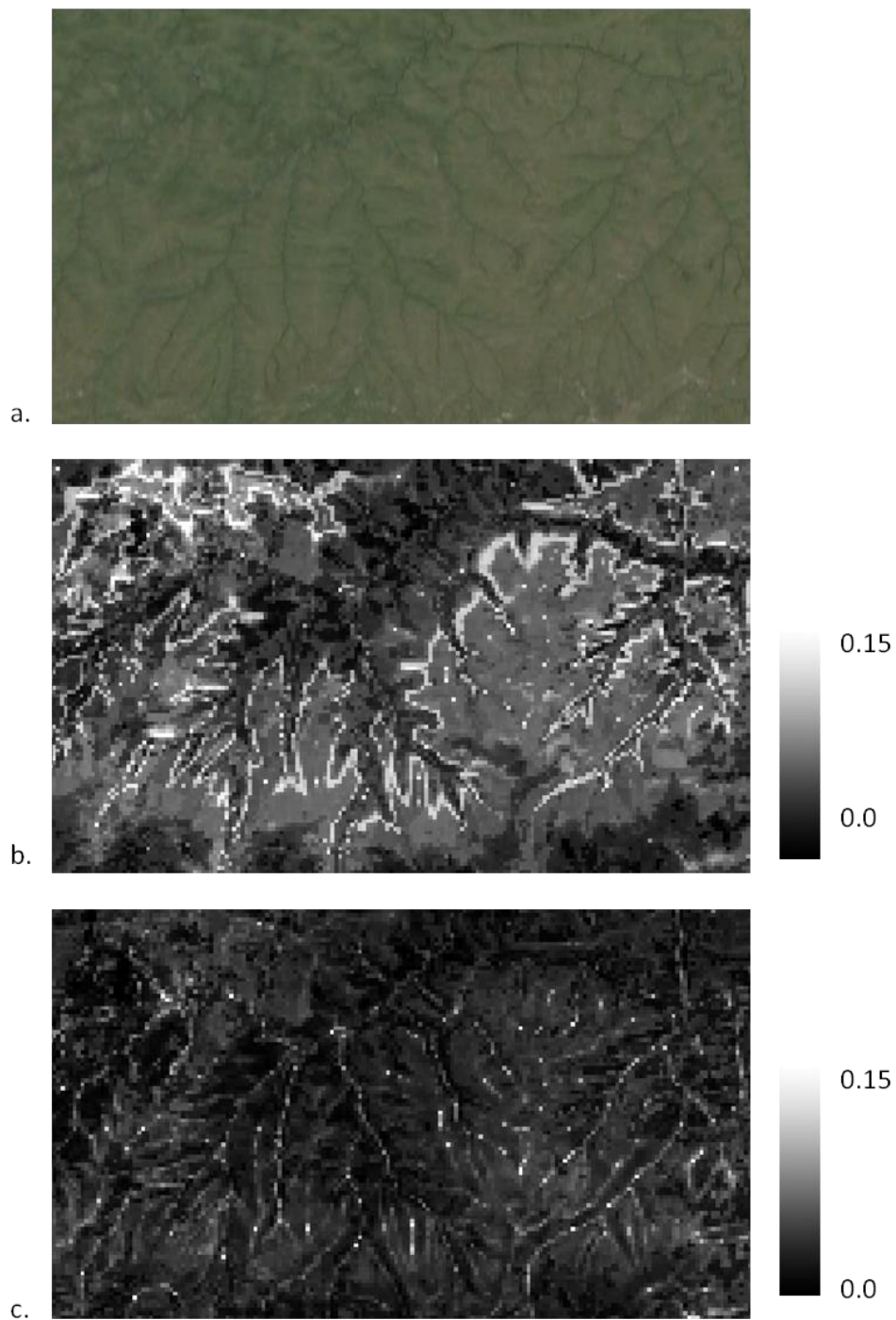


Figure 3-6. Comparison of predicted fractional cover with high resolution imagery: a. subset of Google Earth imagery, b. subset of a preliminary fractional cover map where NIR is unrestricted, c. subset of a second fractional cover map where NIR is restricted.

After latitude, elevation, and NIR reflectance were adjusted, the BRT model was run several times with different combinations of learning rate and tree complexity. The best model had a learning rate of 0.005 and a tree complexity of three. Simplification of the model was explored using backward elimination. Elevation was dropped because it did not contribute enough to the predictive performance of the model (Figure 3-4b).

3.3.3. Relative Contribution of the Explanatory Variables to the BRT Model

The relative importance of the variables was assessed on a scale of 0 to 100, with the higher number indicating a stronger influence on the response (Elith et al., 2008). In order of importance, the six variables that contributed to the model the most were the red surface reflectance (14.7), the slope (13.9), NBAR_45W (12.7), and the isotropic (11.2), volumetric (7.2), and geometric (6.9) kernels from the RTLS-R model (Table 3-1). These variables were frequently used for splitting during the creation of the regression trees and helped improve the predictive performance of the model.

The partial response plots suggested that the percentage of red reflectance was lower when woody vegetation was higher (Figure 3-7a), which agreed with the theory. During the summer months, deciduous shrubs in the North Slope grow green leaves after a long leafless winter, and leaves are the primary photosynthesizing organ. The healthy green foliage, which is rich in chlorophyll, absorbs wavelengths of light in the visible region of the spectrum. Strong absorption is noticeable between the 600 and 700 nm wavelength range, which corresponds to the red absorption band. Thus, an increase in shrub cover

would imply that more radiation in the red portion of the electromagnetic spectrum would be absorbed and less would be reflected.

Table 3-1. Relative contribution of the predictor variables to the BRT model. The sum of all the contributions adds to 100.

Variable	Relative Contribution (%)
Red reflectance	14.7
Slope	13.9
Nadir BRDF-adjusted reflectance WoD*	12.7
Isotropic kernel	11.23
Volumetric kernel	7.23
Geometric kernel	6.92
White-sky albedo	6.51
Latitude	6.17
Blue reflectance	6.00
Green reflectance	5.78
Black-sky albedo	3.69
Northness	2.39
Eastness	2.19
Near-infrared reflectance	0.54

* Weight of Determination

The characteristics of the terrain also seem to influence shrub abundance (Figure 3-7 b). For instance, as the slope of the terrain increased ($5^\circ < \text{slope} < 12^\circ$ degrees), so did the shrub cover. Flat areas (slope $< 1^\circ$ degree) also were characterized by high values in shrub cover, while in semi-flat areas ($1^\circ \leq \text{slopes} \leq 5^\circ$ degrees) the presence of shrubs was considerably lower. This pattern agrees with that described by Tape et al.'s (2006) study in which floodplains and slopes had more abundant shrub cover in comparison to interfluves.

The weight of determination of the nadir BRDF-adjusted reflectance at solar zenith angle of 45 degrees increased with shrub abundance (Figure 3-7c). Quite the opposite relation is observed between the isotropic scattering kernel and shrub cover. The isotropic kernel is a constant term from the RTLS-R model that compensates for the multiple scattering not accounted for by the volumetric and geometric scattering kernels (Wanner et al., 1995). The isotropic scattering describes the "brightness" of the surface, and as expected, the "brightness" decreased with more shrubs, as they are darker than the background vegetation (Figure 3-7d).

The volumetric scattering kernel seemed to decrease with higher estimates of shrub cover (Figure 3-7e). Estimation of the volume scattering assumes a homogeneous medium (canopy) of a given volume density made of randomly located scattering parts (leaves). The medium rests on a flat surface and its height is a function of the leaf-area index (LAI) (Roujean et al., 1992). Although shrubs have a high LAI (Epstein et al., 2004), volume scattering effects are significant for both vegetated and non vegetated surfaces regardless of their LAI value (Roujean et al., 1992). Thus, it seems that in areas

with low shrub cover, the background vegetation has a stronger volume effect on the reflectance.

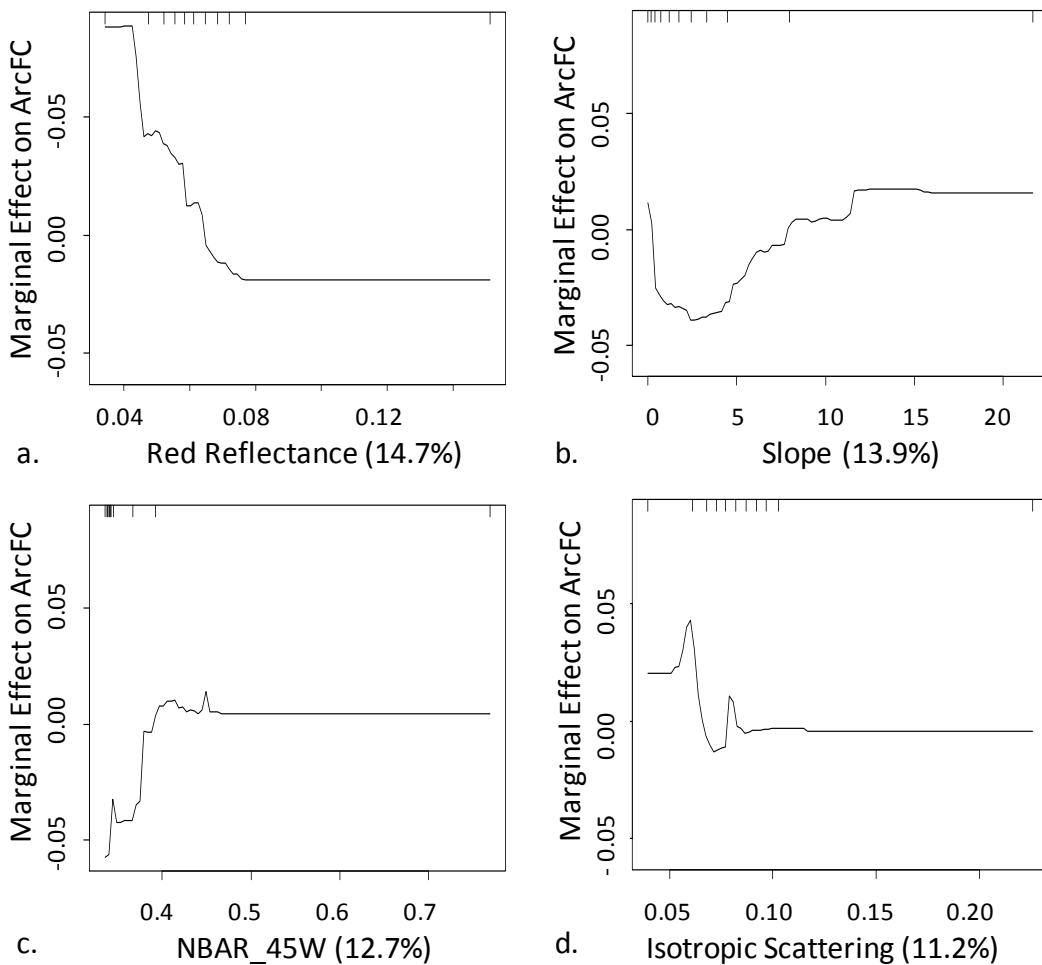
The geometric scattering seems to decrease with higher estimates of shrub cover (Figure 3-7f). The geometric kernel describes the reflectance of a surface as a function of the areal proportion of the sunlit and shaded canopy and ground (Wanner et al., 1995). At high latitudes, shadows cast by protruding shrubs are more pronounced due to the low solar angle. These shadows may reduce the scattering effect of the brighter background vegetation, thus resulting in lower values of geometric scattering.

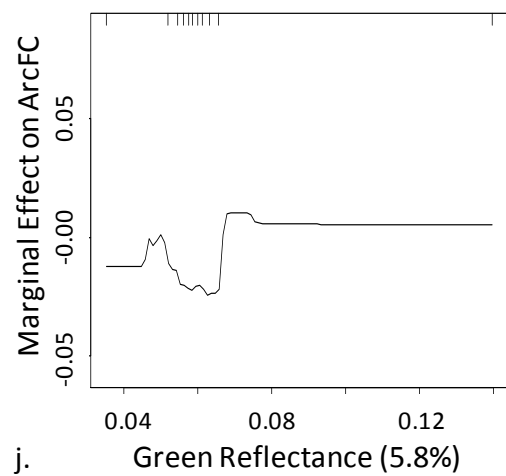
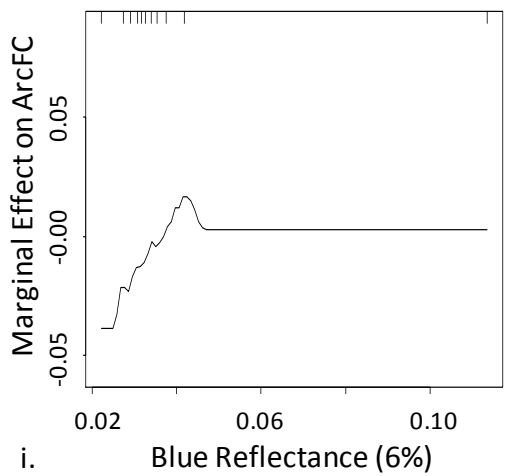
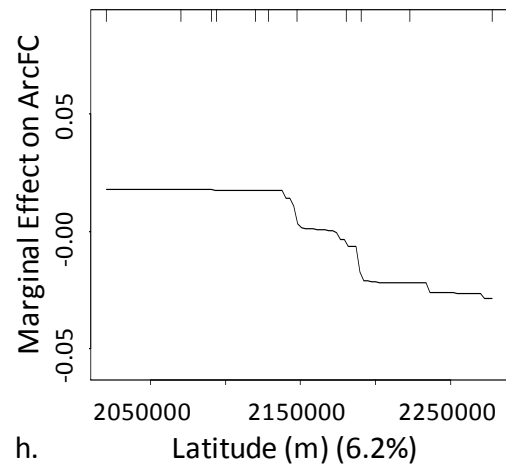
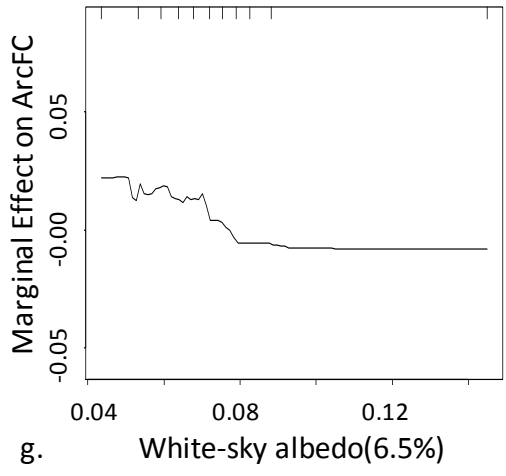
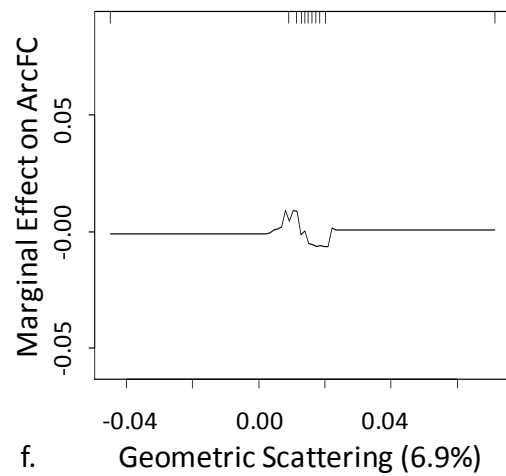
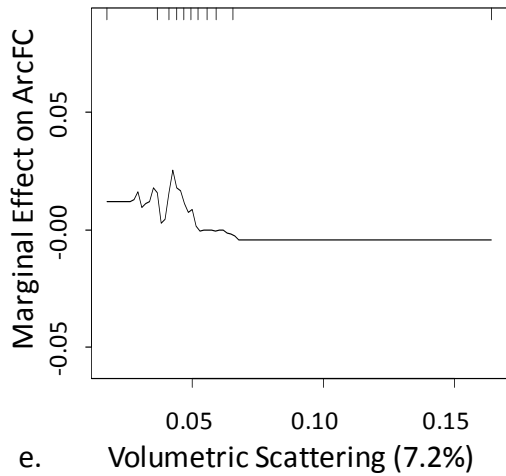
The white-sky albedo (Figure 3-7g), which is the bihemispherical reflectance under isotropic illumination conditions, and the black-sky albedo (Figure 3-7k), which is the directional hemispherical reflectance computed at local solar noon, decreased with higher shrub cover values. This is expected as shrubs are darker than the background vegetation and contribute to lower albedo values.

After latitude was adjusted, the dependence plot showed a better relationship between latitude and shrub cover (Figure 3-7h). There are no tall shrubs on the coastal plain of Alaska where wet sedges and prostrate dwarf shrubs (<0.15 m in height) are dominant. Shrub abundance increased towards the foothills of the Brooks Range (lower latitude) where low shrubs (>0.4 m in height) dominate the landscape (Epstein et al., 2004).

Blue reflectance seemed to decrease with higher values of shrub cover (Figure 3-7i). Although blue light is strongly absorbed by shrubs and perhaps an inverse relationship than the one found was expected, light in the blue spectrum is highly scattered in the

atmosphere. At higher latitudes, where the sun angle is much lower, the light goes through a longer path in the atmosphere and the scattering of the blue light is more pronounced. It may be possible that the blue reflectance that reached the sensor may be more noise than signal. On the other hand, it seems like two peaks on green reflectance correlate to higher values of shrub cover (Figure 3-7j). It may be that this corresponded to the reflective properties of two dominant species of shrub. The remaining three variables (northness, eastness, and near-infrared reflectance) had a much lower contribution to the model.





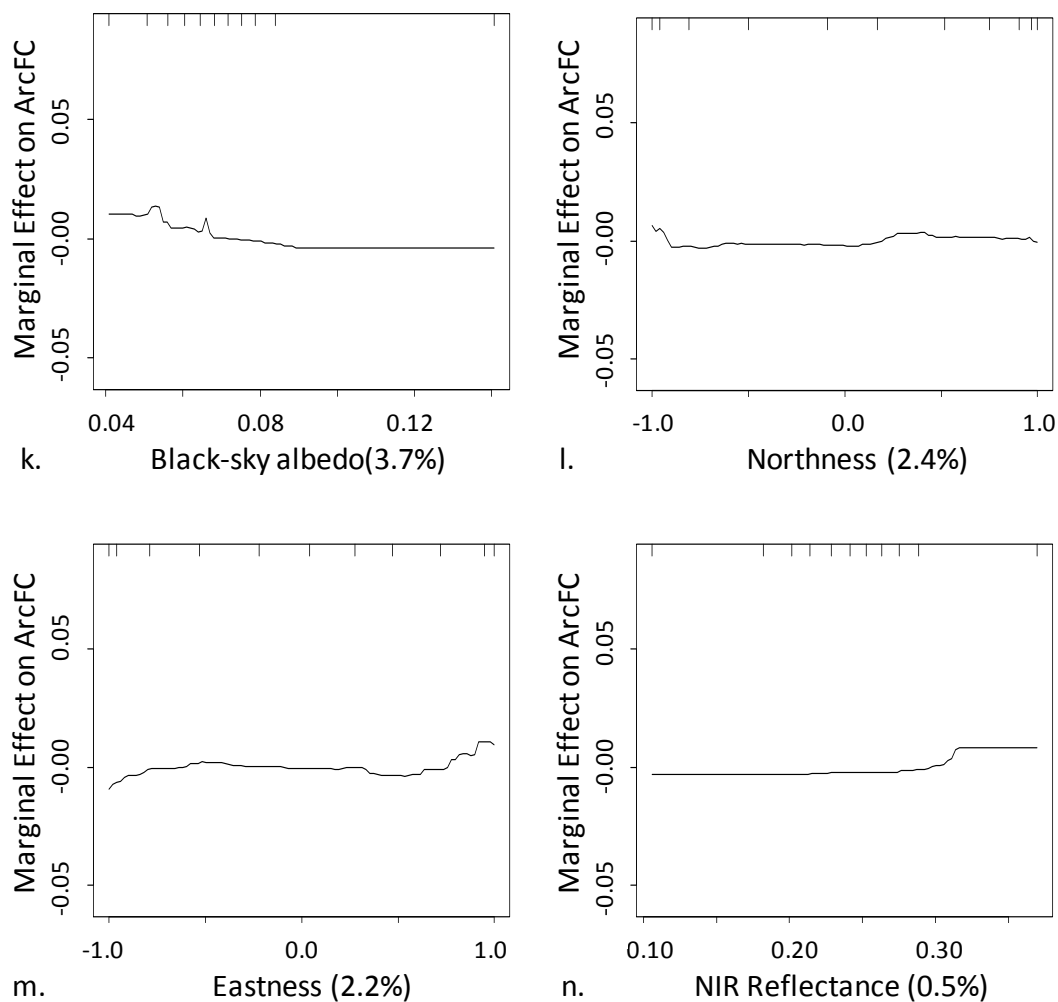


Figure 3-7. Partial dependence plot depicting the effect of each independent variable on the response after accounting for the average effect of all other variables in the model. The fitted function is centered by subtracting its mean. Contribution of the variable to the model is in parenthesis. a. red reflectance, b. slope, c. NBAR_45W, d. isotropic scattering, e. volumetric scattering, f. geometric scattering, g. white-sky albedo, h. latitude, i. blue reflectance, j. green reflectance, k. black-sky albedo, l. northness, m. eastness, and n. NIR reflectance.

3.3.4. Interaction Between Explanatory Variables in the Model

Interaction plots show the relation between two explanatory variables and the response while setting all other variables to their respective means. The two most important interactions were between the slope and green reflectance and between the slope and latitude. The first interaction revealed that sites with slope near to zero had higher shrub abundance, and this effect was more pronounced with higher green reflectance values (Figure 3-8). This is the case along floodplains and river terraces where the terrain is flat and shrubs are abundant (Tape et al., 2006). As the number of shrubs with a healthy canopy increases in flat areas, so does the green reflectance. This agrees with the fact that vegetation reflects slightly more green than blue or red electromagnetic energy. Although cover also increased with the steepness of the terrain, shrub abundance was overall much lower compared to the flat areas. Also, it seemed that on steeper terrains, lower values of green reflectance correlated with higher values of cover.

The second interaction depicts the relationship between latitude, slope, and shrub cover (Figure 3-9). Similarly to the previous interaction, nearly flat terrains (slope < 1) have higher shrub abundance, and this effect is enhanced toward the foothills of the Brooks Range. Equally, as the terrain is steeper and the latitude decreases, shrub cover increases. This behavior was observed on valley slopes (Tape et al., 2006).

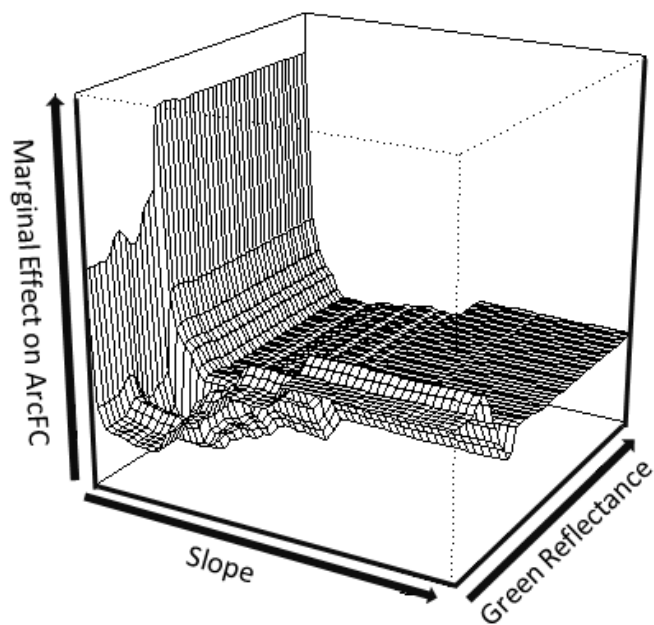


Figure 3-8. Interaction plot depicting the effect of slope and green reflectance on the response variable, ArcFC.

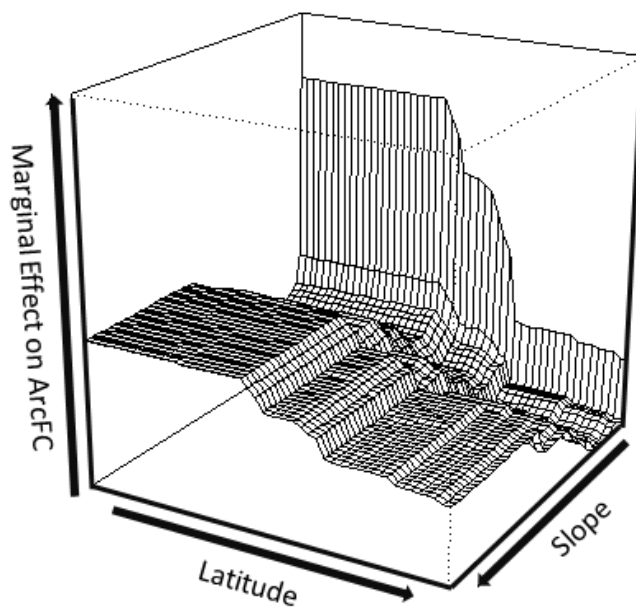


Figure 3-9. Interaction plot depicting the effect of latitude and slope on the response variable, ArcFC.

3.3.5. Validation of the BRT model

The validation dataset, consisting of tall shrub fractional cover estimates for 305 sites, was used to evaluate the predictive performance of the model. This dataset was not used during the training of the BRT. The predicted arcsine fractional cover values obtained from the BRT model for the new validation sites were converted back to fractional cover and compared to the validation dataset. The BRT model explained 52% of the variation in the response variable fractional cover (RMSE of 0.03) (Figure 3-10). This result is very reasonable considering the spatial resolution of the data (250 m × 250 m).

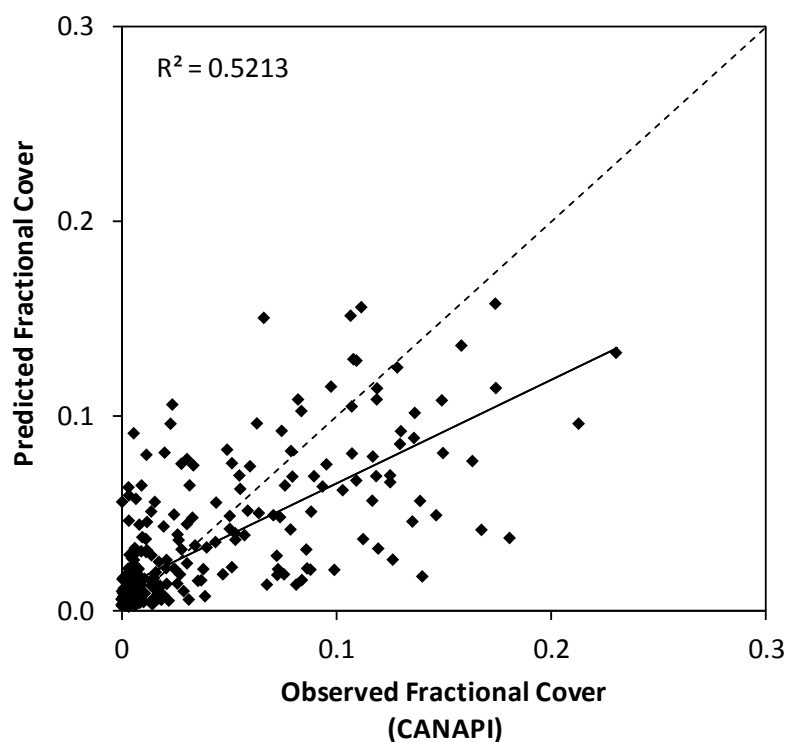


Figure 3-10. Scatter plot of observed fractional cover derived from the CANAPI algorithm against the predicted fractional cover from the BRT model for 305 validation sites.

Selkowitz (2010) found a similar coefficient of determination when evaluating regression tree models to predict tall shrub fractional cover from MISR imagery using the four spectral bands from the nadir camera and the red band data from all off-nadir cameras (average R^2 of 0.59, and average RMSE of 0.046 for models using data from June and July at a spatial resolution of 500 m). His study covered an area of 1,067 km² of tundra in northern Alaska and the regression tree model utilized to predict fractional shrub cover was trained and validated using a high resolution fractional shrub cover reference map built from field measurements and swath of IKONOS imagery. The BRT model overestimated fractional cover when the observed value was lower than 0.025 and underestimated cover when the observed value was higher than 0.025 (Figure 3-10). The underestimation of cover may be partially related to the clumping of tall shrubs, which hinder the identification of single canopies. The BRT model made use of the geometric kernel, which takes into consideration the sunlit and shaded portion of the canopy crown and background. When tall shrub are clustered, as happens along water tracks and floodplains, the shaded crowns are truncated by neighboring shrubs.

3.4. Conclusion

The boosted regression tree model was able to explain 52% of the variability in the response variable, fractional cover, using 14 predictor variables (red, blue, green, and near-infrared reflectance; slope; NBAR_45W; isotropic, volumetric, and geometric kernels; white- and black- sky albedo; latitude; northness; and eastness). It seemed that sites with lower red reflectance values and on hilly terrains had higher shrub cover

values. Similarly, the presence of more shrubs suggested a decrease in albedo. Near-infrared reflectance seemed to be a function not only of the composition of the vegetation but also of moisture content. After adjusting this variable, NIR reflectance ended up providing the least information to the model. The shrub cover pattern observed on preliminary fractional cover maps showed a good agreement with high resolution imagery. Multi-spectral and multi-angular data from MISR together with the use of terrain variables provided good results for mapping shrub cover in the Arctic. Since the training and validation of the BRT model was done using a wide range of sites that covered the entire domain of the North Slope of Alaska, the model can be readily applied to generate tall shrub fractional cover maps. However, because of its empirical nature, it can only be used to predict shrub abundance in similar Arctic tundra environments. The trained and validated BRT model presented here could be used to analyze temporal changes in tall shrub cover in the North Slope of Alaska with the goal of assessing the magnitude and direction of the ongoing shrub expansion.

3.5. References

- Asner, G. P., Braswell, B. H., Schimel, D. S., & Wessman, C. A. (1998). Ecological research needs from multiangle remote sensing data. *Remote Sensing of Environment*, 63(2), 155-165.
- Beck, P. S. A., Horning, N., Goetz, S. J., Loranty, M. M., & Tape K. D. (2011). Shrub cover on the North Slope of Alaska: a circa 2000 baseline map. *Arctic, Antarctic, and Alpine Research*, 43(3), 355–363.

- Breiman, L. (2001). Statistical modeling: the two cultures. *Statistical Science*, 16, 199–215.
- Bi, J., Xu, L., Samanta, A., Zhu, Z., & Myneni, R. (2013). Divergent Arctic-Boreal vegetation changes between North America and Eurasia over the past 30 years. *Remote Sensing*, 5(5), 2093–2112.
- Bubier, J., Rock, B., & Crill, P. (1997). Spectral reflectance of boreal wetland and forest mosses. *Journal of Geophysical Research*, 102(D24), 29483-29494.
- CAVM Team. (2003). Circumpolar arctic vegetation map. (1:7,500,000 scale), Conservation of Arctic Flora and Fauna (CAFF) Map No. 1. U.S. Fish and Wildlife Service, Anchorage, Alaska. ISBN: 0-9767525-0-6.
- Chapin, F. S., Shaver, G. R., Giblin, A. E., Nadelhoffer, K. J., & Laundre, J. A. (1995). Responses of Arctic tundra to experimental and observed changes in climate. *Ecology*, 76(3), 694.
- Chen, J. M., Liu, J., Leblanc, S. G., Lacaze, R., & Roujean, J-L. (2003). Multi-angular optical remote sensing for assessing vegetation structure and carbon absorption. *Remote Sensing of Environment*, 84(4), 516–525.
- Chopping, M.J., Rango, A., Havstad, K.M., Schiebe, F., Ritchie, J., Schmugge, T., ... & Davis, M.R. (2003). Canopy attributes of desert grassland and transition communities derived from multiangular airborne imagery. *Remote Sensing of Environment*, 85, 339-354.

- Chopping, M. J., Su, L., Laliberte, A., Rango, A., Peters, D. P. C., & Martonchik, J. V. (2006). Mapping woody plant cover in desert grasslands using canopy reflectance modeling and MISR data. *Geophysical Research Letters*, 33, L17402.
- Chopping, M., Moisen, G. G., Su, L., Laliberte, A., Rango, A., Martonchik, J. V., & Peters, D. P. C. (2008). Large area mapping of southwestern forest crown cover, canopy height, and biomass using the NASA Multiangle Imaging Spectro-Radiometer. *Remote Sensing of Environment*, 112(5), 2051–2063.
- De'Ath, G. (2007). Boosted trees for ecological modeling and prediction. *Ecology*, 88(1), 243–251.
- Diner, D. J., Asner, G. P., Davies, R., Knyazikhin, Y., Muller, J. P., Nolin, A. W., Pinty, B., Schaaf, C., & Stroeve, J. (1999). New directions in Earth observing: scientific applications of multi-angle remote sensing. *Bulletin of the American Meteorological Society*, 80 (11), 2209–2229.
- Duchesne, R.R., Chopping, M.J., & Tape, K.D. (2015). NACP woody vegetation characteristics of 1,039 sites across the North Slope, Alaska. Data set. Available online [<http://daac/ornl.gov/>] from Oak Ridge National Laboratory Distributed Active Archive Center, Oak Ridge, Tennessee, USA.
- Elith, J., Leathwick, J. R., & Hastie, T. (2008). A working guide to boosted regression trees. *Journal of Animal Ecology*, 77(4), 802–813.
- Elith, J., & Leathwick, J. R. (2008). Tutorial for running boosted regression trees. [Appendix S3 of the article *A working guide to boosted regression trees*, by J. Elith, J. R. Leathwick, and T. Hastie]. *Journal of Animal Ecology*, 77(4), 1-15.

- Elmendorf, S. C., Henry, G. H. R., Hollister, R. D., Björk, R. G., Boulanger-Lapointe, N., Cooper, E. J., . . . , & Wipf, S. (2012). Plot-scale evidence of tundra vegetation change and links to recent summer warming. *Nature Climate Change*, 2(6), 453–457.
- Epstein, H. E., Beringer, J., Gould, W. A., Lloyd, A. H., Thompson, C. D., Chapin, F. S., . . . & Walker, D. A. (2004). The nature of spatial transitions in the Arctic. *Journal of Biogeography*, 31(12), 1917–1933.
- Friedman, J.H., Hastie, T., & Tibshirani, R. (2000). Additive logistic regression: a statistical view of boosting. *Annals of Statistics*, 28, 337–407.
- Gamon, J. A., Huemmrich, K. F., Stone, R. S., & Tweedie, C. E. (2013). Spatial and temporal variation in primary productivity (NDVI) of coastal Alaskan tundra: Decreased vegetation growth following earlier snowmelt. *Remote Sensing of Environment*, 129(15), 144–153.
- Glenn, E. P., Huete, A. R., Nagler, P. L., & Nelson, S. G. (2008). Relationship between remotely-sensed vegetation indices, canopy attributes and plant physiological processes: what vegetation indices can and cannot tell us about the landscape. *Sensors*, 8(4), 2136–2160.
- Hinzman, L. D., Bettez, N. D., Bolton, W. R., Chapin, F. S., Dyurgerov, M. B., Fastie, C. L., . . . & Yoshikawa, K. (2005). Evidence and implications of recent climate change in northern Alaska and other Arctic regions. *Climatic Change*, 72(3), 251–298.
- Hope, A., & Stow, D. (1995). Shortwave reflectance properties of Arctic tundra. In Reynolds J. and Tenhuenen J. (Eds.), *Landscape function and disturbance in Arctic*

- tundra. *Ecological Studies* 120: 155– 164. Heidelberg: Springer.
- Hudson, J. M. G., & Henry, G. H. R. (2009). Increased plant biomass in a High Arctic heath community from 1981 to 2008. *Ecology*, 90(10), 2657–2663.
- Huemmrich, K., Gamon, J. A., Tweedie, C. E., Oberbauer, S. F., Kinoshita, G., Houston, S., . . . , & Mano, M. (2010). Remote sensing of tundra gross ecosystem productivity and light use efficiency under varying temperature and moisture conditions. *Remote Sensing of Environment*, 114(3), 481–489.
- Jia, G. J., & Epstein, H. E. (2003). Greening of Arctic Alaska, 1981–2001. *Geophysical Research Letters*, 30(20), 2067.
- Lacaze, R., Chen, J.M., Roujean, J.L., & Leblanc, S.G. (2002). Retrieval of vegetation clumping index using hotspot signatures measured by POLDER instrument. *Remote Sensing of Environment*, 79(1), 84-95.
- Leathwick, J.R., Elith, J., Francis, M.P., Hastie, T., & Taylor, P. (2006). Variation in demersal fish species richness in the oceans surrounding New Zealand: an analysis using boosted regression trees. *Marine Ecology Progress Series*, 321, 267–281.
- Li, X., & Strahler, A. H. (1992). Geometric-optical bidirectional reflectance modeling of the discrete crown vegetation canopy: effect of crown shape and mutual shadowing. *IEEE Transactions on Geoscience and Remote Sensing*, 30, 276-292.
- Martonchik, J.V., Diner, D.J., Pinty, B., Verstraete, M.M., Myneni, R.B., Knyazikhin, Y., & Gordon, H.R. (1998). Determination of land and ocean reflective, radiative, and biophysical properties using multiangle imaging. *IEEE Transactions on Geoscience and Remote Sensing*, 36, 1266–1281.

- McGuire, A. D., Chapin, F. S., Walsh, J. E., & Wirth, C. (2006). Integrated regional changes in Arctic climate feedbacks: implications for the global climate system. *Annual Review of Environment and Resources*, 31(1), 61–91.
- McManus, K. M., Morton, D. C., Masek, J. G., Wang, D., Sexton, J. O., Nagol, J. R., Ropars, P. & Boudreau, S. (2012). Satellite-based evidence for shrub and graminoid tundra expansion in northern Quebec from 1986 to 2010. *Global Change Biology*, 18, 2313–2323.
- Muller, S. V., Racoviteanu, A. E., & Walker, D. A. (1999). Landsat MSS-derived land-cover map of northern Alaska: extrapolation methods and a comparison with photointerpreted and AVHRR-derived maps. *International Journal of Remote Sensing*, 20, 2921–2946.
- Myneni, R. B., Keeling, C. D., Tucker, C. J., Asrar, A., & Nemani, R. R. (1997). Increased plant growth in the northern high latitudes from 1981 to 1991. *Nature*, 386, 698–702.
- Nicodemus, F. E., Richmond, J. C., Hsia, J. J., Ginsberg, I. W., & Limperis, T. (1977). Geometrical considerations and nomenclature for reflectance. *U.S.A. Department of Commerce/ National Bureau of Standards, NBS Monogr.*, No. 160, 1-52.
- Nolin, A. (2004). Towards retrieval of forest cover density over snow from the Multiangle Imaging SpectroRadiometer (MISR). *Hydrological Processes*, 18, 3623–3636.
- R Core Team. (2013). R: A language and environment for statistical computing. R Foundation for Statistical Computing. (Version 3.0.1) [Software]. Available from

<http://www.R-project.org>.

- Raynolds, M. K., Walker, D. A., Verbyla, D., & Munger, C. A. (2013). Patterns of change within a tundra landscape: 22-year Landsat NDVI trends in an area of the northern foothills of the Brooks Range, Alaska. *Arctic, Antarctic, and Alpine Research*, 45(2), 249–260.
- Read, C., Duncan, D., Vesk, P., & Elith, J. (2011). Surprisingly fast recover of biological soil crusts following livestock removal in southern Australia. *Journal of Vegetation Science*, 22, 905-916.
- Ridgeway, G. (2006). Generalized boosted models: a guide to the gbm package. Retrieved from <http://citeseerx.ist.psu.edu/viewdoc/summary?doi=10.1.1.113.9298>
- Roujean, J., Leroy, M., & Deschamps, P. (1992). A bidirectional reflectance model of the Earth's surface for the correction of remote sensing data. *Journal of Geophysical Research*, 97(D18), 20455-20468.
- Selkowitz, D. J. (2010). A comparison of multi-spectral, multi-angular, and multi-temporal remote sensing datasets for fractional shrub canopy mapping in Arctic Alaska. *Remote Sensing of Environment*, 114(7), 1338–1352.
- Sellers, P. J. (1985). Vegetation-canopy spectral reflectance and biophysical processes. In G. Asrar (Ed.), *Theory and applications of optical remote sensing* (pp. 297– 335). New York: Wiley, Ch. 8.
- Stow, D., Daeschner, S., Hope, A., Douglas, D., Petersen, A., Myneni, R., Zhou, L., & Oechel, W. (2003). Variability of the seasonally integrated normalized difference

- vegetation index across the North Slope of Alaska in the 1990s. *International Journal of Remote Sensing*, 24(5), 1111 – 1117.
- Stow, D. A., Hope, A., McGuire, D., Verbyla, D., Gamon, J., Huemmrich, F., . . . , & Myneni, R. (2004). Remote sensing of vegetation and land-cover change in Arctic tundra Ecosystems. *Remote Sensing of Environment*, 89(3), 281–308.
- Tape, K., Sturm, M., & Racine, C. (2006). The evidence for shrub expansion in northern Alaska and the Pan-Arctic. *Global Change Biology*, 12(4), 686–702.
- Vierling, L., Deering, D., & Eck, T. (1997). Differences in Arctic tundra type and phenology as seen using bidirectional radiometry in the early growing season. *Remote Sensing of Environment*, 60(1),71-82.
- Wanner, W., Li, X., & Strahler, A. H. (1995). On the derivation of kernels for kernel-driven models of bidirectional reflectance. *Journal of Geophysical Research*, 100(D10), 21077-21089.
- Wanner, W., Strahler, A. H., Hu, B., Lewis, P., Muller, J. P., Li, X., Schaaf, C. L. B., & Barnsley, M. J. (1997). Global retrieval of bidirectional reflectance and albedo over land from EOS MODIS and MISR data: theory and algorithm. *Journal of Geophysical Research*, 102(D14), 17143-17161.
- Zhou, L., Tucker, C. J., Kaufmann, R. K., Slayback, D., Shabanov, N. V., & Myneni, R. B. (2001). Variations in northern vegetation activity inferred from satellite data of vegetation index during 1981 to 1999. *Journal of Geophysical Research*, 106, 20069– 20083.

CHAPTER 4

Construction of the 2000 Shrub Fractional Cover Map and Comparison to Existing Maps for the North Slope of Alaska.

Abstract

The warming experienced in the North Slope of Alaska over the last few decades has brought a series of changes in the landscape, the most noticeable being the spreading of shrubs in the region. An increase in shrub cover may lead to a lower albedo, affect the energy and carbon budget, and alter the disturbance regime. In order to understand the magnitude and direction of this change, it is important to go back as much as possible in time to assess the initial condition of the landscape. Due to the extent of the North Slope and its extreme environments, remote sensing may be the most suitable tool to produce wall-to-wall fractional shrub cover maps for the entire region. Most regional maps have relied on the Normalized Difference Vegetation Index (NDVI) to track changes in the photosynthetic activity of the vegetation over the last few decades. However, vegetation indices tell little information about the structural characteristics of the vegetation. The only wall-to-wall fractional cover maps for the North Slope needed four years worth of data and still did not cover the entire region. Here, a new mapping approach is presented that uses satellite imagery from the Multi-angle Imaging SpectroRadiometer (MISR) sensor and some landscape variables to predict tall shrub (> 0.5 m) cover. The new tall shrub fractional cover map for the year 2000 revealed that cover ranged from 0.00 to 0.21 and about 75% of the sites had a fractional cover less than 0.013. High cover values were

predicted along floodplains, creeks, and sloped terrain. The fractional cover estimates related well with the bioclimatic subzones, showing that in warmer environments, shrub cover was higher. The map presented here outperformed the Landsat-derived tall shrub fractional cover map when compared to the robust validation data set ($R^2= 0.38$, RMSE = 0.08). Both maps, however, agreed on the fact that tall shrub cover was quite low in the North Slope of Alaska in 2000 and that it was restricted to a few areas in the domain.

Keywords: Fractional cover map, tall shrub, North Slope of Alaska, Multi-angle Imaging SpectroRadiometer (MISR), bioclimatic subzones, Landsat.

4.1 Introduction

Over the last few decades, average surface temperatures in the Arctic have increased and this has led to a series of changes in the terrestrial and aquatic ecosystems (IPCC, 2013). A noticeable change on land has been the proliferation of shrubs in the North Slope of Alaska. The link between shrub expansion and warmer temperatures has been established by a large volume of research. Observational studies and warming experiments have linked warming with an increase in shrub cover (Chapin et al., 1995; Elmendorf et al., 2012; Hudson & Henry, 2009; Huemmrich et al., 2010). Shrub rings have also suggested that warming was a primary contributor to shrub expansion in the Arctic (Forbes et al., 2010; Tape et al., 2012). Repeat aerial photography studies have detected an increase in shrub cover over five decades and attributed it to an increase in temperature in the region (Myers-Smith et al., 2011; Sturm et al., 2001). Remote sensing studies has shown that the greening in the Arctic is well correlated with the warming trend in the region (Jia & Howard, 2003; Myneni et al., 1997; Stow et al., 2004; Zhou et al., 2001). Although the greening is a function of the proportion of dead material in the plant canopy, the vegetation type, and the soil background (Sellers, 1985), it has been used as a proxy of biomass (Jia & Howard, 2003; Myneni et al., 1997).

An increase in shrub cover may affect the environment in several ways. For instance, an increase in shrubs may decrease the albedo as their leaves are darker than those of the grasses and because of the shadows thrown. Furthermore, the probability that the energy reflected from one canopy element will be absorbed by another is higher with an increase in leaf area and biomass (Oke, 1987). Similarly, if shrub cover increases, more incoming

radiation may be absorbed near the surface and a potential consequence could be the increase in surface temperature, which could encourage earlier snow thawing in spring (Chapin et al., 2005; Hinzman et al., 2005). Also, an increase in woody vegetation coupled with warm surface temperature and low moisture may increase fire frequencies and intensity as more fuel would become available (Higuera et al., 2008). In 2007, the largest recorded tundra fire in the Arctic burned 1,039 km² of Alaska's tundra and released 2,016 g of carbon per square meter into the atmosphere (Mack et al., 2011). Because an increase in shrub cover may alter both local and global carbon budgets, and have an effect on the Arctic climate and the ecosystem, it is important to monitor changes in vegetation, particularly with respect to increases in deciduous shrubs in the tundra (Euskirchen et al., 2009; Tape et al., 2006).

There are several global vegetation maps available, but they do not satisfactorily characterize shrub cover in the Arctic tundra biome (Selkowitz, 2010): 1) For instance, the Circumpolar Arctic Vegetation Map (CAVM) describes five physiognomic categories subdivided into 15 vegetation mapping units that depict the dominant plant functional type within the mapped polygon (CAVM, 2003). The scale used was 1:7.5 million which is not suitable for regional studies. 2) The MODIS Land Cover Type product (MCS12Q1) had a spatial resolution of 500 m and used five land cover classification schemes to describe land cover properties. The main classification scheme identified 17 land cover classes defined by the International Geosphere Biosphere Programme (NASA LPDAAC, 2001). In the North Slope there were only 14 land cover classes from which open shrublands and grasslands occupied most of the domain (Figure 4-1). 3) The Landsat

Multispectral Scanner System (MSS)-derived land cover map of northern Alaska had a spatial resolution of 100 m and it classified land cover type into eight broad categories (Muller et al., 1999). The map showed that 69% of the domain was covered by moist dwarf-shrub and tussock-graminoid tundra (28%), moist graminoid and prostrate-shrub tundra (22%), and moist low-shrub tundra and other shrublands (19%). 4) The National Land Cover Database (NLCD) of 2001 was another land cover map derived from Landsat imagery at a 30 m spatial resolution (Figure 4-2) (USGS, 2001). This map used 16 classes for the North Slope of Alaska and was derived using a decision-tree classification.

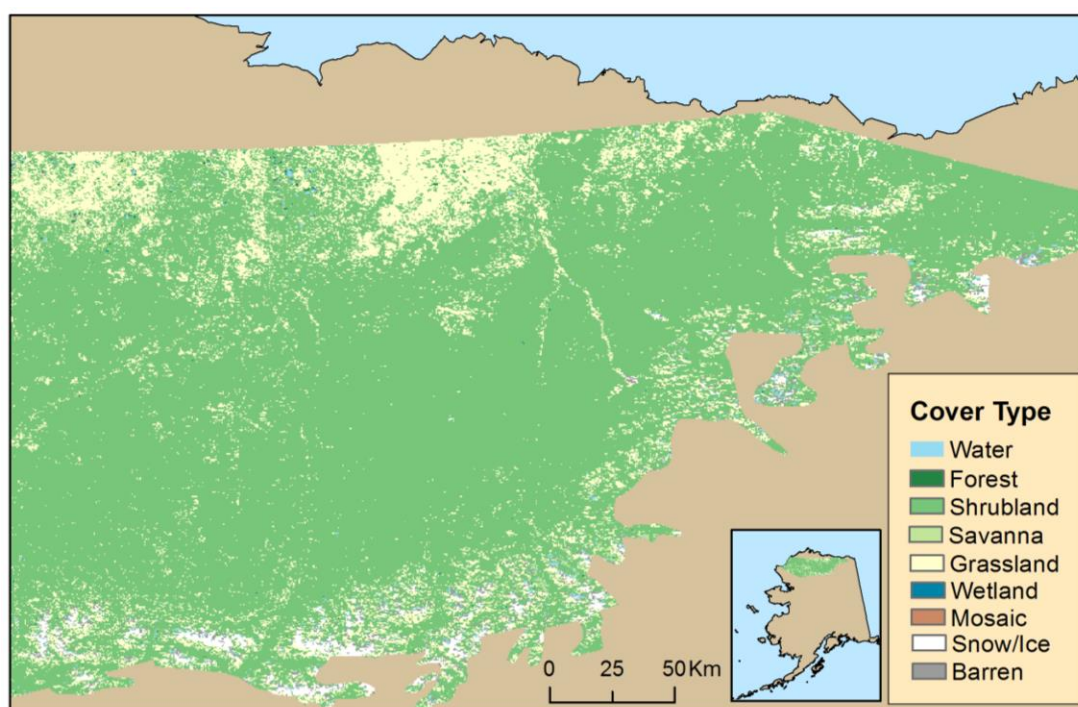


Figure 4-1. Simplified land cover type for the North Slope of Alaska using the International Geosphere Biosphere Programme global vegetation classification scheme. Source: MODIS Land Cover Type Product, year 2001.

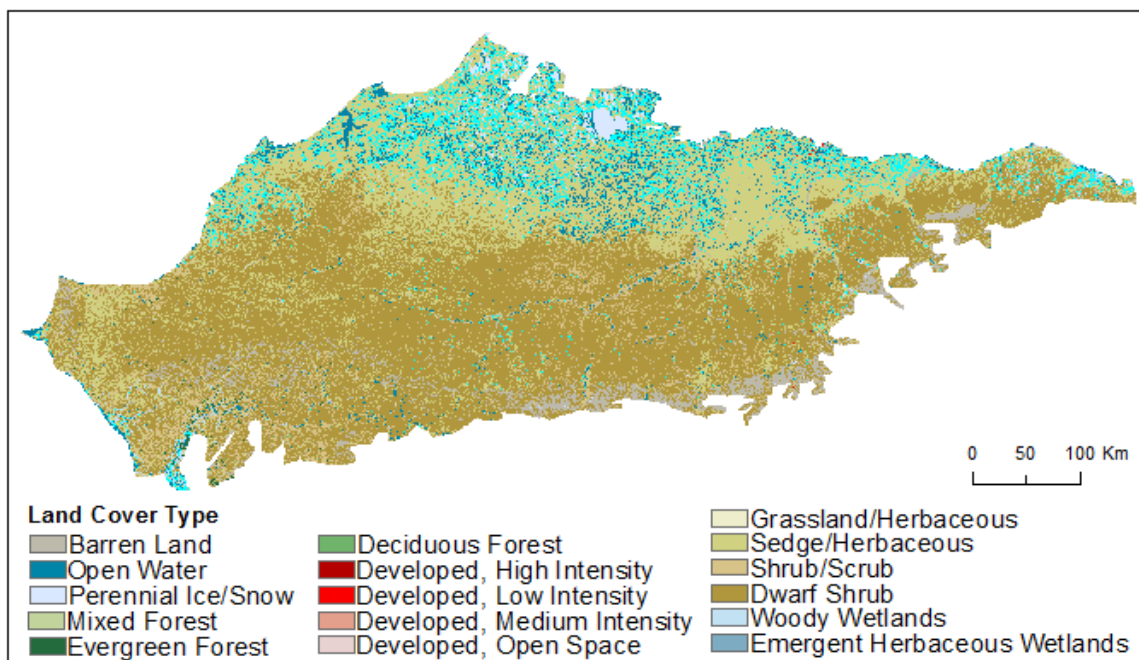


Figure 4-2. Land cover for the North Slope of Alaska based on the National Land Cover Database. Spatial resolution of 30 m . Source: USGS website.

Although it had a high spatial resolution and the vegetation classes were very specific, it did not provide estimates of shrub cover.

The only maps that provided shrub cover estimates for the North Slope of Alaska are the ones created by Beck et al. (2011). Their 2000 total and tall shrub fractional cover maps were produced using Landsat 7 imagery and the machine-learning algorithm called Random Forest. Their results were validated by comparing predicted shrub cover with field observations at 24 sites ($R^2 = 0.63$, $RMSE = 23\%$). Although the Landsat-derived shrub fractional cover maps provided estimates for the North Slope, they required imagery from four years to cover the region and yet there were large portions of the domain without data available. This was due to the fact that the North Slope has a short

snow-free season and is frequently covered by clouds, especially during summer (Stow et al., 2004). In order to increase the chances of capturing a cloud-free/snow-free scene, it is necessary that the sensor has a high temporal resolution and a large field-of-view.

Comparison of predicted shrub fractional cover derived from Landsat, the Multi-angle Imaging SpectroRadiometer (MISR), and Moderate Resolution Imaging Spectroradiometer (MODIS)—for the North Slope of Alaska—showed that when only the spectral information is exploited, sensors with higher spatial resolution provided the highest accuracy in the regression tree models (Selkowitz, 2010). On the other hand, when using both the angular and spectral information provided by MISR, estimates of shrub fractional cover came as accurate as those derived from Landsat data (Selkowitz, 2010). Therefore, MISR is a promising sensor for mapping shrub cover in Arctic Alaska because it can provide fractional cover estimates of similar accuracy to that of higher resolution sensors and its higher temporal resolution (1-2 days) and wider swath (360 km) can increase the likelihood of capturing more cloud-free scenes.

Besides persistent cloud cover, some of the other challenges of mapping shrub abundance in the Arctic are the low solar angle and the low shrub cover. In the Arctic, the effect of the low sun angles affect quality of the radiometric measurements in at least two ways: first, the incoming and outgoing radiation must travel a longer path in the atmosphere which translates into more energy that is scattered and less reaching the sensor; second, shadows make an important contribution to the total reflected energy even with the low stature shrubs and gentle rolling hills of the Arctic landscape (Stow et al., 2004). Regarding the low shrub cover, at the 250 m spatial resolution, the North

Slope has for the most part, a tall shrub cover less than 5% (Duchesne et al., 2015; Selkowitz, 2010). Thus, the sensor must be sensitive enough to pick up this very small signal. Perhaps the additional information provided by the off-nadir cameras of MISR may help to discriminate low shrub cover values.

One particular advantage of MISR is that its multi-angular measurements of reflectance could be used together with the RossThick-LiSparse Reciprocal (RTLS-R) model to obtain the bidirectional reflectance distribution function (BRDF) (Martonchik et al., 1998; Wanner et al., 1995). The BRDF is a function that describes the differences in the direction of reflected radiance with respect to the direction of irradiance incident to a surface (Nicodemus et al., 1997). These variations on surface reflectance due to the different sun-sensor geometry, should be accounted for in any study of the Earth's surface.

One of the considerations in mapping fractional cover in the Arctic is the selection of a model that would be sensitive to the small radiometric signal coming from the low shrub cover and to the low spectral contrast between the background vegetation and the tall shrubs. Today, more studies are using machine-learning algorithms (Beck et al., 2011; Raynolds et al., 2013; Selkowitz, 2010) because they learn the relationship between the predictors and the response and find prevailing patterns (Breiman, 2001; Elith et al., 2008). Some machine-learning algorithms like the Neural Nets (preliminary modeling efforts) and Random Forest (Beck et al., 2011) provided reasonable shrub cover estimates; however these models are considered black boxes because no information is provided on the contribution and role of the explanatory variables. In this study, the

Boosted Regression Tree model was used to map shrub fractional cover in the North Slope of Alaska because besides its many advantages, it provided simple graphical and numerical representations of the predicted variation in the response variable in relation to the explanatory variables, of the relative influence of the predictors, and of the interactions between the independent variables (De'Ath, 2007).

The main goal of this study was to create a tall shrub fractional cover map for the North Slope of Alaska for year the 2000 using moderate resolution imagery and the boosted regression tree model. Specific objectives were to obtain MISR imagery for the years 2000 to 2002, to invert the RossThick-LiSparse reciprocal model using the red reflectance values of MISR's nine cameras in order to account for the anisotropic properties of the surface, to mosaic all MISR paths into one multi-layer map with all the surface reflectance-derived predictor variables for the region, to retrieve shrub fractional cover using the BRT model, to filter map outputs, and to compare the new map with existing shrub cover maps for the North Slope.

4.2. Materials and Methods

4.2.1 Data Sources

The creation of the 2000 tall shrub fractional cover map used MISR data collected in years 2000, 2001, and 2002 during the period June 1 - August 15 (Appendix D). This period matched the growing season when the shrub crowns were at their fullest and minimal changes in reflectance were observed. A total of 22 paths (P065-P086) were necessary to cover the entire North Slope of Alaska; each path had five potential orbits

within the sampling time range. Out of the 330 possible orbits, only 225 had imagery available (Table 4-1). Year 2000 had the lowest number of good imagery, probably because of adjustments made to the sensor during its first year of orbit. The MISR data were downloaded from the NASA Langley Atmospheric Science Data Center using the MISR Order and Customization Tool (<http://10dup05.larc.nasa.gov/MISR/cgi-bin/MISR/main.cgi>).

Table 4-1. Summary of available MISR imagery for years 2000-2002.

Status	2000	2001	2002
Good Imagery	61	76	86
Bad Imagery	49	32	24
Total	110	110	110

Elevation data for the North Slope of Alaska were obtained from the National Elevation Dataset (NED) produced by the U.S. Geological Survey (USGS). The data were available at a spatial resolution of 2 arc-second (approximately 60 m). A total of 99 NED subsets were necessary to cover the entire study area. Latitude (m), slope (degrees), and aspect were derived from the elevation map. Considering that aspect is a circular variable, it was linearized by creating two variables: northness and eastness:

$$Northness = \cos\left(\frac{aspect * \pi}{180}\right) \quad \text{Eq. 4-1}$$

$$Eastness = \sin\left(\frac{aspect * \pi}{180}\right) \quad \text{Eq. 4-2}$$

A value of 1 for northness indicated a north facing slope and a value of -1 a south facing one. Similarly, a value of 1 for eastness represented a slope facing directly east while a value of -1 a slope facing directly west.

The MODIS Collection 5 Burned Area Product (MCD45) was used to identify burned areas. This product uses MODIS Aqua and Terra as input data and it is defined on a global 483 m sinusoidal grid. The monthly Geotiffs from year 2000 to 2002 (36 tiles) were downloaded from the University of Maryland website; just one tile was necessary to cover the entire study area (window 1).

All data processing was carried out using several software and utility scripts. Software included ERDAS Imagine 2014, ArcGIS 10.2.1. , Pythonwin - Python IDE and GUI Framework for Windows, and R v3.0.1. All data used were projected unto a 250 m Albers Conical Equal Area grid.

4.2.2. MISR Data Processing

MISR was launched in December 1999 and it is a sun-synchronous moderate resolution sensor on board of the Terra satellite (Diner et al., 1999). It has nine cameras pointing at fixed angles and each camera has four optical channels (blue, green, red, and near-infrared). MISR can provide simultaneous multi-angular calibrated images in four spectral bands. For this study, the red band at all off-nadir cameras and the four spectral bands at the nadir camera were used in the analysis. Only these spectral bands have a

spatial resolution of 275 m while the other off-nadir spectral bands have a spatial resolution of 1 km.

This study used four MISR products: the MISR Level 1B2 Terrain Data-MI1B2T, the MISR Level 2 Land Surface Parameters-MIL2ASLS, the MISR Geometric Parameters-MIB2GEOP, and the Ancillary Geographic Product-MIANCAGP. With the aid of the MISR Toolkit the MISR files that came in the Hierarchical Data Format (HDF) were extracted and the surface reflectance estimates were obtained and mapped onto the Albers Conical Equal Area map projection with a grid interval of 250 m. The MISR red band bidirectional reflectance factors (BRFs) in all nine cameras were used to invert the RossThick-LiSparse Reciprocal (RTLS-R) model, using the Algorithm for Modeling Bidirectional Reflectance Anisotropies of the Land Surface (AMBRALS) code (Wanner et al., 1997). The RTLS-R model is a kernel-driven semi-empirical bidirectional reflectance distribution function (BRDF) model, suitable for scenes with low values of the leaf area index (LAI) (Wanner et al., 1995) and sparse spacing of shrub or tree crowns (Li & Strahler, 1992). This step was necessary in order to account for the variations in surface reflectance as a result of differences in viewing and illumination geometries. Unless corrections for the BRDF are made, comparisons of surface reflectance observations across images from MISR are difficult or impossible (Wanner et al., 1997). Inversion of this model resulted in 13 parameters: three kernels functions (isotropic, volumetric, and geometric) that described the BRDF shape, the weights of these functions, the black-sky (directional) and white-sky (diffuse) albedos with their respective weights, the RMSE, number of observations, and the weight of determination

of the nadir BRDF-adjusted reflectance at solar zenith angle of 45 degrees (NBAR_45W). A few of the 13 variables from the RTLS-R model plus the surface reflectance from MISR's four spectral bands at nadir were some of the predictor variables used in the BRT model to predict shrub fractional cover.

4.2.3. Boosted Regression Tree

The boosted regression tree (BRT), which had been previously trained and validated, was used in this study to predict fractional cover for the North Slope of Alaska. The BRT model, sometimes called 'stochastic gradient boosting', is an ensemble method where a large number of simple models (regression trees) are fit and then combined using a boosting algorithm to develop a final model (Leathwick et al., 2006). The trees are added to the final model in a forward stage-wise fashion, emphasizing observations poorly predicted by the previous trees (Friedman et al., 2000). Thus, the final BRT model can be seen as an additive regression model in which each of the individual terms is a simple regression tree (Elith et al, 2008).

The BRT model (learning rate of 0.005 and a tree complexity of three) was fitted in R (v3.0.1, 2013) using the 'gbm' library (Ridgeway, 2004) and the 'brt' functions (Elith & Leathwick, 2008). Predicted arcsine tall shrub cover values (ArcFC) were obtained by using 14 explanatory variables: six parameters that resulted from the inversion of the RTLS-R model (three kernels functions, the black-sky and white-sky albedos, and NBAR_45W), four spectral bands of MISR at nadir (blue, green, red, and near-infrared),

and four terrain variables (latitude, slope, northness, and eastness). The response variable was the transformed shrub fractional cover which was later converted to fractional cover.

4.2.4. Work Flow for the Creation of the 2000 Shrub Cover Map of Arctic Alaska

MISR data was initially processed using the MISR toolkit routines in order to obtain surface reflectance values for the four spectral bands at nadir and the red spectral band at all nine angles. When the number of blocks to process in a given orbit was greater than 4, MISR data had to be processed in two batches due to limits in the system capacity and the MISR toolkit routines. BRDF values for the red spectral band were used to invert the RTLS-R model using the AMBRALS algorithm. The output of the AMBRALS included 13 parameters including the kernel weights and albedos. Following, the reflectance values of the four nadir spectral bands and the 13 parameters of AMBRALS were stacked in single files of 17 layers each, one file per orbit (Figure 4-3).

Several filters were applied in order to clean the data before compositing it. Pixels that used less than 8 multi-angular observations for the inversion of the RTLS-R model were flagged with a value of -999. Clouds were also flagged using the RMSE value from the RTLS-R model as a criterion. If the RMSE was equal or greater than 0.15, then a value of -999 was assigned to that pixel. In terrestrial ecosystems, surface reflectance is always positive and greater than zero. Thus, pixels with negative or zero surface reflectance values for the blue, green, red, or near-infrared bands or for the isotropic kernel, which is the diffuse reflectance from the RTLS-R model, were flagged with a -999 value. On the contrary, a negative volumetric or geometric kernel weight indicates

that the shape of the function is inverted. Although they no longer have physical interpretation, they still have meaning and were used in the analysis. However, since the compositing algorithm used was the mean and this statistical parameter is sensitive to negative values, the absolute values of the volumetric and geometric kernel weights were used instead (Figure 4-3). Flagged pixels were not included in further analysis.

The next phase was compositing all the filtered MISR orbits that encompassed the study area. This was accomplished in three steps. First, each orbit file (which had 17 layers) was split in 17 files, one file per parameter. In other words, one file would contain the blue band reflectance values, other file the green band reflectance values, and so on. At this point, only 10 parameters were used in the following steps: the four spectral bands at nadir, the three kernel functions, the two albedos, and the weight of determination of the nadir BRDF-adjusted reflectance. Second, all valid values for a given parameter were averaged on a pixel-per-pixel basis in the study area. Third, the mean values of each of the 10 parameters were stacked together in one single file with 10 layers; this was the composite data map for the entire North Slope of Alaska.

Following, the variables latitude, slope, northness and eastness were added as layers to the composite data map. This final version contained 14 variables which were the input data to the BRT model. This file was converted to ASCII to several comma-delimited files, which were run in R in order to obtain arcsine fractional cover (ArcFC). The BRT model outputs were put back together again to form the ArcFC map for the North Slope of Alaska. No data values, burned areas, and water/ice pixels in the map were flagged

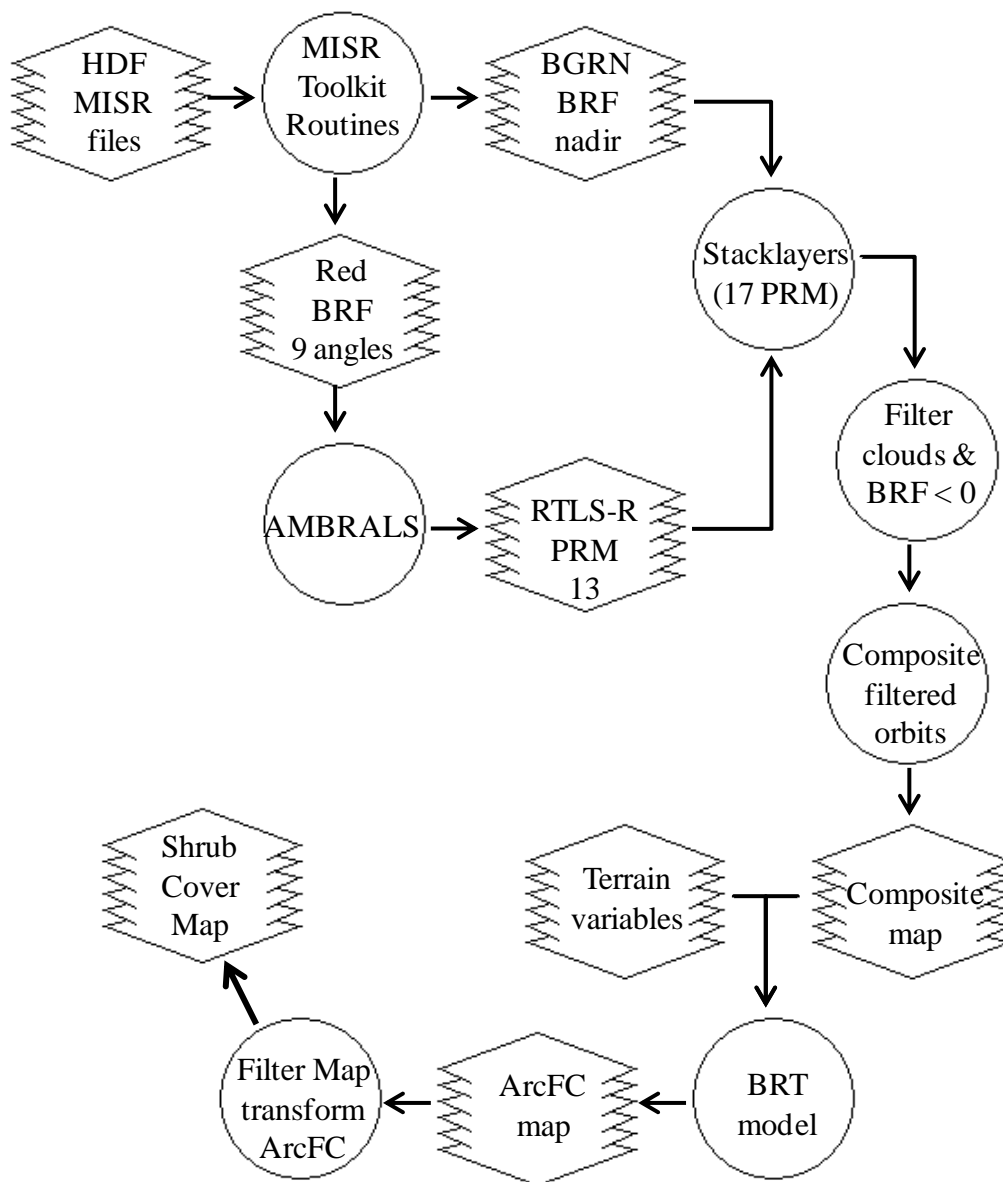


Figure 4-3. Diagram illustrating the processing steps to generate the shrub fractional cover map. Abbreviations used are: HDF (Hierarchical Data Format), BGRN (Blue, Green, Red, and Near-infrared), BRF (Bidirectional Reflectance Factor), PRM (Parameters), ArcFC (Arcsine transformed fractional cover).

by comparing the ArcFC map with different parameter values from the composite data map. For example, pixels containing water were identified by near-infrared values lower than 0.14, while RMSE values higher than 0.15 were used to identify pixels with ice content. Burned areas were masked using the MODIS burned area product. Finally, the ArcFC values were transformed back to fractional cover (Figure 4-3):

$$\text{Shrub Fractional Cover} = (\sin(\text{ArcFC}))^2 \quad \text{Eq. 4-3}$$

4.2.5. Comparison of the Fractional Cover Map with the Arctic Bioclimatic Subzones Map

The Arctic can be divided in five regions (A through E) where subzone A is the coldest one and subzone E is the warmest (CAVM, 2003). In the North Slope of Alaska, three subzones can be identified from north to south: subzone C, subzone D, and subzone E. The mean July temperature in subzone C is about 7°C, in subzone D it is about 9°C, and in subzone E it is about 12°C (CAVM, 2003). Therefore, in this section, the median of the predicted fractional cover values for each of the three subzones were compared to determine if the bioclimatic conditions had an effect on tall shrub cover. Non-parametric methods were used since fractional cover estimates within each subzone were not normally distributed and each group had different sample sizes. The Kruskal-Wallis, the one-way analysis of variance by ranks, was used to test whether the samples originated from the same distribution. Rejection of the null hypothesis meant that at least one population median of one group was different from the population median of at least one

other group. The Bonferroni-Dunn test, a post-hoc method used following a significant Kruskal-Wallis test, was deployed to identify which medians differed.

4.2.6. Comparison of the Fractional Cover Map with the 2000 Circa Fractional Cover Map

Estimates of fractional cover for 234 sites across the entire domain of the North Slope of Alaska were obtained for the year 2010 from the CANAPI-derived validation data (Duchesne et al., 2015). These sites were selected because they were not used to train the BRT model and fractional cover estimates were available for the Landsat derived map. The predicted fractional cover from the 2000 baseline map (Beck et al., 2011), and hereafter referred to as the 2000 Landsat map, was re-projected onto a 250 m Albers Conical Equal Area grid and compared to the validation data set. Then, the predicted cover derived from the BRT model, and hereafter referred to as the 2000 MISR map, was compared to the 2000 Landsat map using simple linear regression. Visual comparison with high-resolution imagery was also performed on a case-by-case basis.

4.3. Results and Discussion

4.3.1. MISR-derived Tall Shrub Cover Map of Arctic Alaska for the Year 2000

Predicted tall shrub fractional cover values for the North Slope of Alaska were derived from moderate resolution imagery using a BRT model with a tree size of three and a learning rate of 0.005 (Figure 4-4). Predicted shrub cover ranged from 0 to 0.21 and at a spatial resolution of 250 m, 75% of the sites had a fractional cover less than 0.013 (Table 4-2). This agreed with Selkowitz's research (2010) in the North Slope of Alaska,

in which at the same spatial resolution, 80% of the sites in the study area had a cover less than 0.05. In the 2000 MISR map, higher shrub fractional cover occurred along floodplains, in particular in the southern portion of the Colville, Chandler, Anaktuvuk, Nanushuk, Itkillik, and Kuparuk rivers, decreasing as the rivers descended to the coastal plain (Figure 4-5). Higher shrub cover also occurred along water tracks, creeks, and sloped terrain (Figure 4-5). This distribution also corresponded to the one of erect dwarf-shrub and low-shrub tundra (CAVM, 2003). Very high fractional cover values were also found along the Noatak River, but this corresponded to spruce trees and not shrubs (Figure 4-6). As a general pattern, shrub cover drastically decreased toward the coastal plain.

Table 4-2. Distribution of tall shrub fractional cover estimates from the MISR-derived map.

Minimum	First Quartile	Median	Third Quartile	Maximum
0	0.0054	0.0084	0.0135	0.2066

Low values of shrub cover were correlated with higher values of red reflectance from MISR's nadir camera and with higher albedo values. Shrubs were more abundant where the slope was less than 2° degrees, and again where the slope ranged between 5° and 10° degrees. The exception to this pattern was the very flat terrain on the coastal plain where severe climatic conditions prevent the growth of tall shrubs.

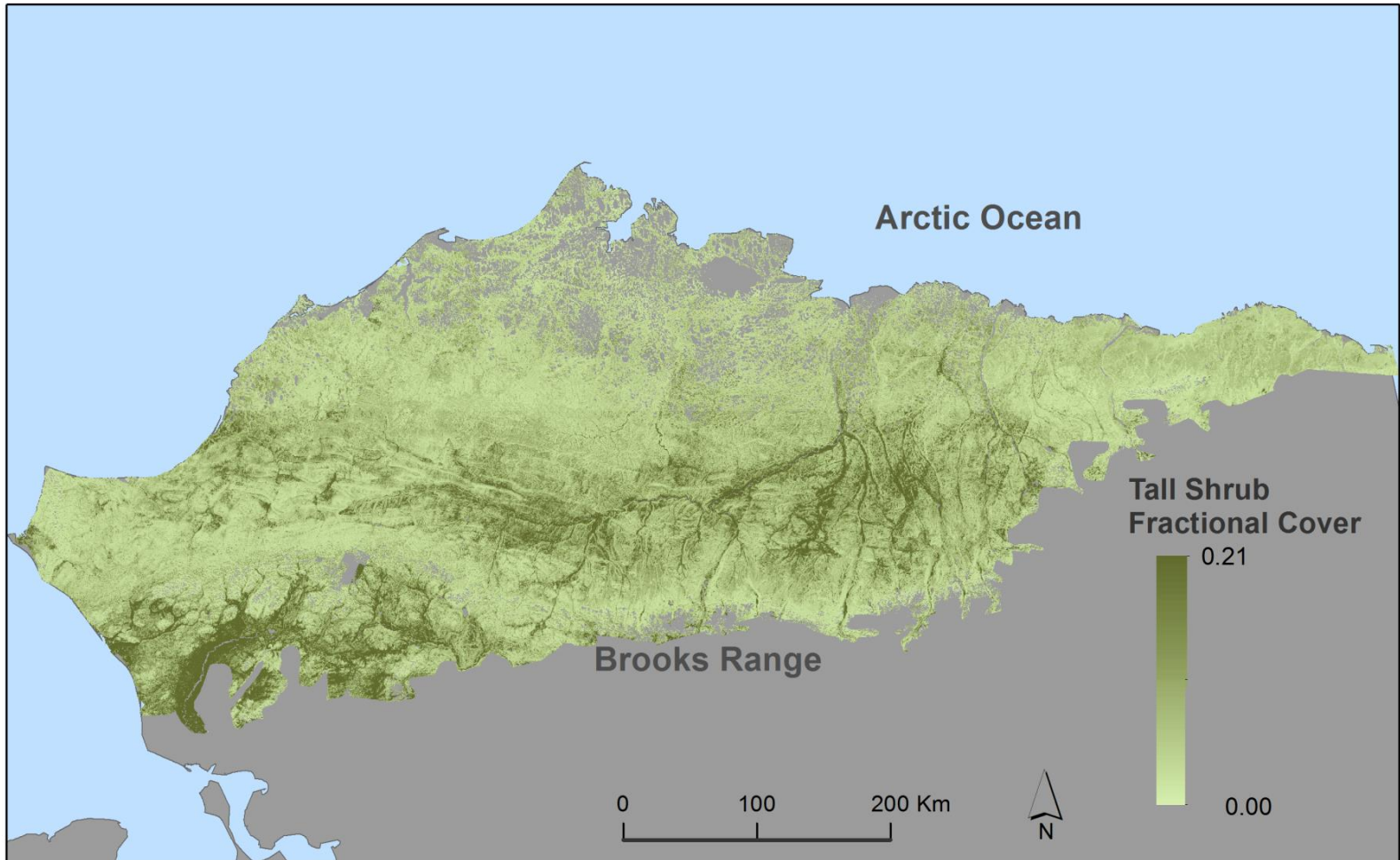


Figure 4-4. Tall shrub fractional cover map for the North Slope of Alaska, year 2000. Fractional cover values were derived from the Boosted Regression Tree model.

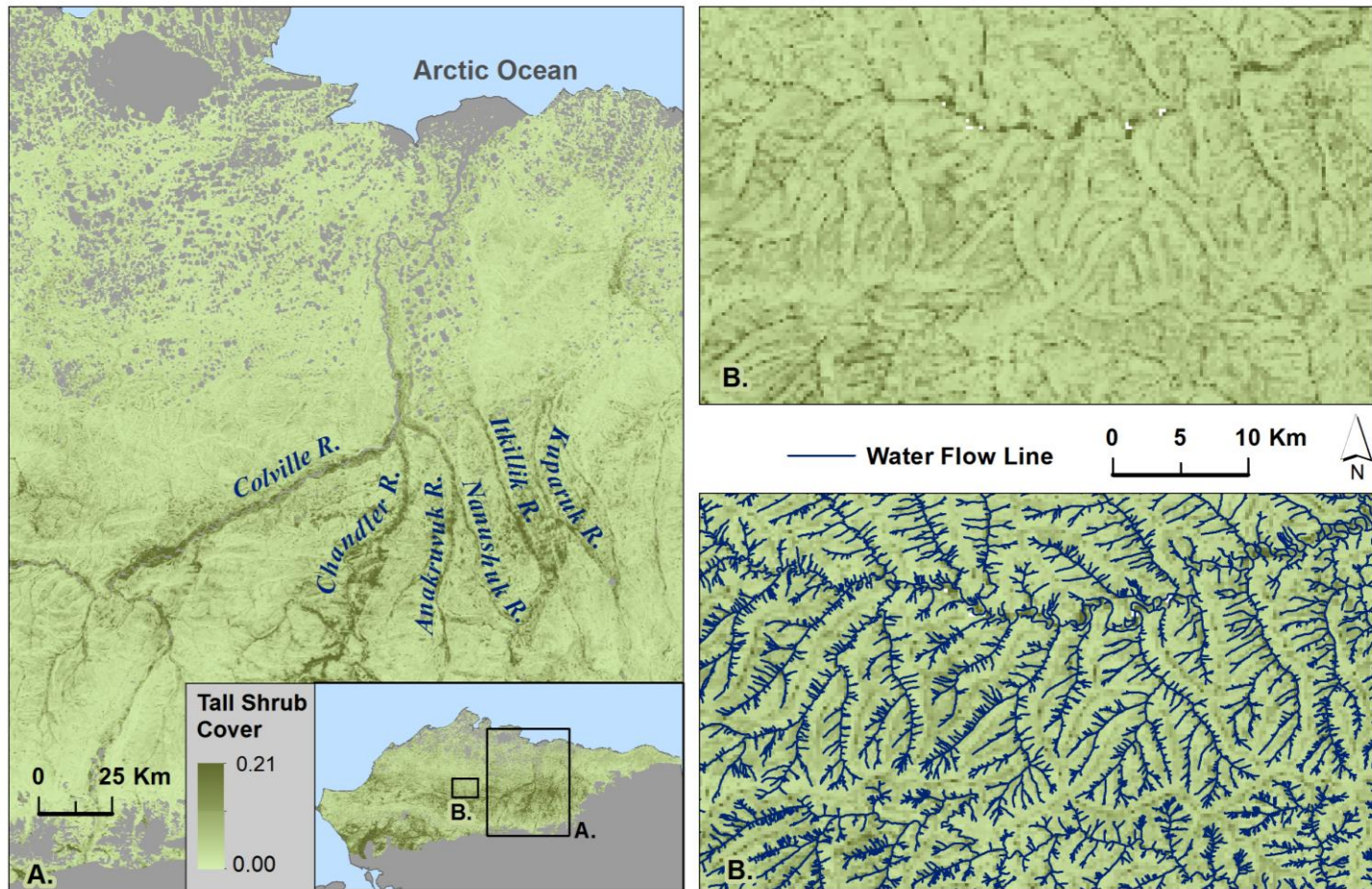


Figure 4-5. Portion of the 2000 MISR-derived tall shrub fractional cover map depicting the correlation of high shrub cover along the floodplains of major rivers and water flow lines. Inset A: Major rivers of the North Slope, Inset B: Water flow lines west of the Colville river (source: USGS, The National Map, Hydrography).

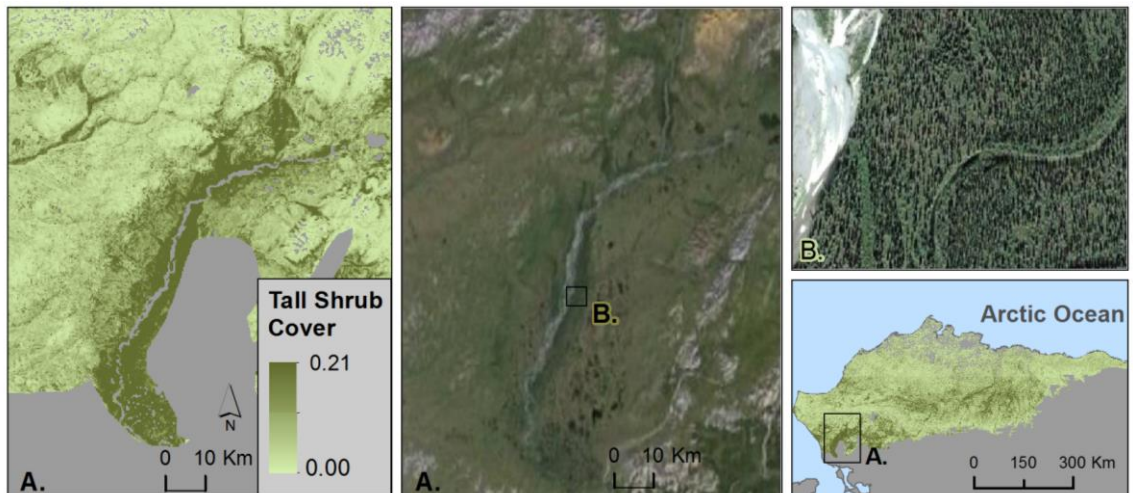


Figure 4-6. Section of the Noatak River in the southwestern portion of the North Slope of Alaska. The high values of cover corresponded to a forest of spruce, not shrubs.

4.3.2. Comparison of 2000 MISR Map with the Arctic Bioclimatic Subzones

The distribution of fractional cover in the three subzones was highly skewed to the left. The highest shrub fractional cover value in Subzone C was remarkably smaller than in Subzone E (0.04 and 0.21, respectively) (Figure 4-7). Similarly, the median shrub cover was higher in Subzone E (0.009), followed by Subzone D (0.007) and Subzone C (0.006). These results agree with the distribution of shrubs among the bioclimatic subzones in the Arctic (CAVM, 2003). The harsh conditions and strong winds in Subzone C limits the growth to hemi-prostrate dwarf-shrub. Subzone D is dominated by prostrate and erect dwarf shrubs (<0.4 m). Subzone E is the warmest one and is dominated by hypo-arctic low shrubs often greater than 0.4 m tall. Birch or willow thickets in subzone E can reach 0.8 to 2 m in height (CAVM, 2003).

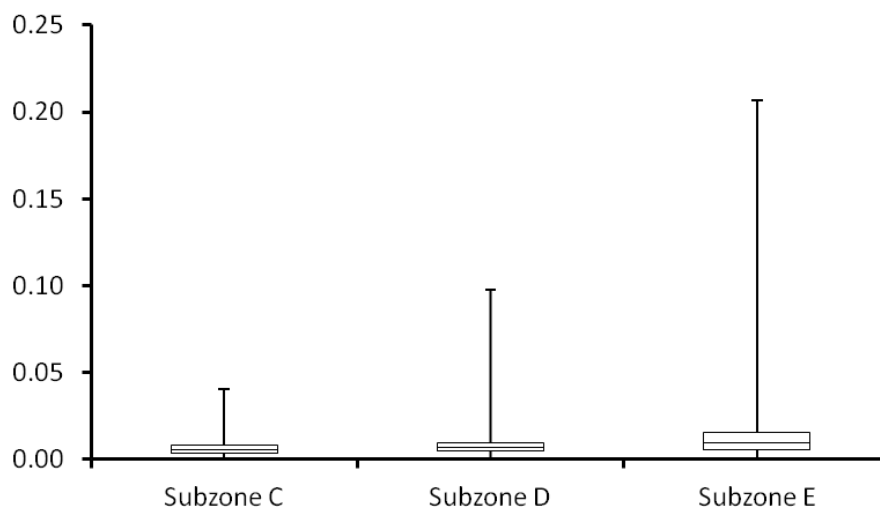


Figure 4-7. Boxplots depicting the five number summary (minimum, first quartile, median, third quartile, and maximum) for fractional cover in the three bioclimate subzones.

The Kruskal-Wallis test showed that at least one pair of medians was significantly different ($\chi^2 = 184055$, $P < 2.2e-16$). The Dunn test showed that the median fractional shrub cover of Subzone C and Subzone D are statistically different ($P < 0.001$), as well as the median shrub cover of Subzone C and Subzone E ($P < 0.001$), and the median shrub cover of Subzone D and Subzone E ($P < 0.001$) (Table 4-3). The test suggested that the prevailing climatic conditions in each subzone may have an effect on tall shrub fractional cover. Nevertheless, the RMSE (0.03) of the predicted fractional cover values is greater than the differences between any given pair of medians. Also to consider is the possibility that tall shrub cover estimates could have been overestimated where dwarf shrubs are dominant (Subzone C and Subzone D) because their spectral characteristics are similar to that of erect and low shrub.

Table 4-3. Comparison of tall shrub fractional cover by bioclimatic subzone using Dunn Test. Dunn's pairwise z test statistic followed by the P -value associated with the test in parenthesis.

Bioclimate Subzone	Subzone C	Subzone D
Subzone D	63.93 ($P < 0.001$)	
Subzone E	182.70 ($P < 0.001$)	401.29 ($P < 0.001$)

4.3.3. Comparison of Predicted Fractional Cover Between the 2000 MISR Map and the 2000 Landsat Map

The 2000 Landsat map, which used 4 years worth of imagery, covered most of the North Slope of Alaska with some portions of data not available in the southwest, probably due to the lack of suitable imagery (Figure 4-8). At a spatial resolution of 250 m, fractional cover estimates ranged from 0.00 to 0.83. Only a very small proportion of sites (49,965 out of 2,613,653) had values of fractional cover greater than 0.21, and most were limited to the floodplains and to patches of erect shrub tundra according to the CAVM map (2003). The vast majority of sites (about 80%) had fractional cover less than 0.02. The 2000 MISR map, which used 3 years worth of imagery, covered the entire domain of the North Slope except for very small areas with no available data. Tall fractional cover ranged from 0.00 to 0.21, and about 88% of the sites had a cover less than 0.02 (Figure 4-8). Both maps represented predicted fractional cover, but the 2000 Landsat map focused on shrubs taller than 1 m height, while the 2000 MISR map

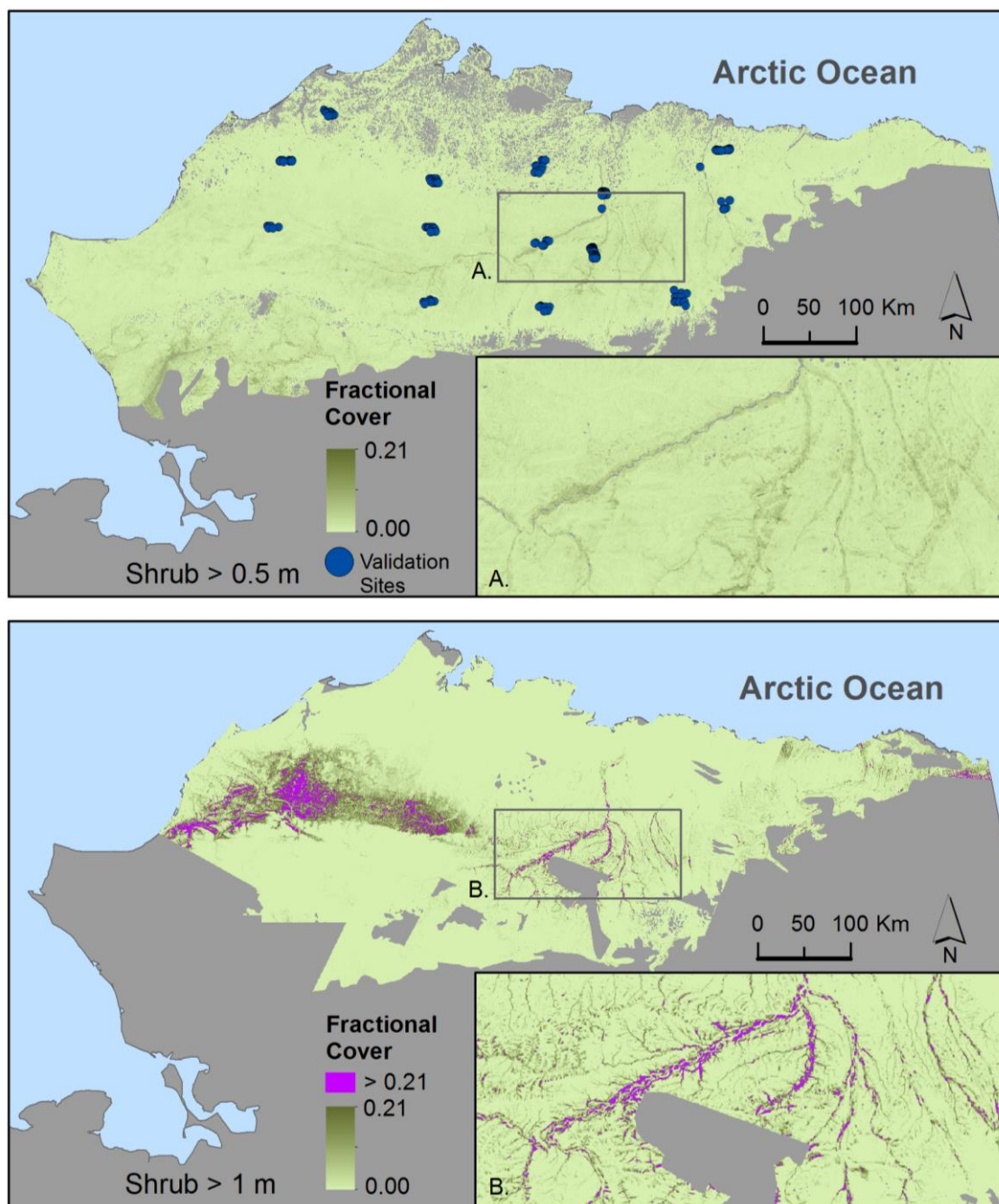


Figure 4-8. Fractional cover map for the North Slope of Alaska: top, MISR 2000 map, bottom, Landsat 2000 map. Fractional cover was rescaled. Water and ice are not filtered for the Landsat 2000 map.

focused on shrubs taller than 0.5 m height. The findings from both maps agreed with what has been reported by other authors for the region. At a spatial resolution of 250 m, most of the sites in the North Slope had a cover less than 0.05 (Duchesne et al., 2015; Selkowitz, 2010). However, considering that tall shrub cover (> 0.5 m in height) is usually less than 5%, it is very unlikely to have sites with very high shrub cover values, especially if shrub height is greater than 1 m. Perhaps those sites with very high cover were artifacts of the model used in the 2000 Landsat map.

The 2000 MISR map seemed to be more sensitive than the 2000 Landsat map to small changes in cover. This is particularly observed north of $70^{\circ} 25'$ degrees and south of $69^{\circ} 2'$ degrees where in the 2000 MISR map fractional cover values varied dynamically, while in the 2000 Landsat map the vast majority of sites had a predicted cover value of zero (Figure 4-8).

The predictive performance of the BRT model used to generate the 2000 MISR map ($R^2 = 0.52$, $RMSE = 0.03$) was much better than the one for the re-projected 2000 Landsat map ($R^2 = 0.38$, $RMSE = 0.08$). The original 2000 Landsat map which had a spatial resolution of 30 m, was able to explain 70% of the variation in the response variable, fractional cover (Beck et al., 2011), but the new 2000 Landsat map, re-projected onto a 250 m grid, could only explain 38% of the variation in the response variable. The decrease in accuracy in the 2000 Landsat map when aggregated to a coarser grid may be expected. Selkowitz (2010) found that a decrease in the spatial resolution of the input variables decreased the accuracy of the model. Nevertheless, there are two important considerations, besides the difference in spatial resolution, that could have contributed to

the decrease in the predictive performance of the re-projected 2000 Landsat map: 1) the original evaluation of the model was done at 20 sites where three observers visually assessed tall shrub cover while the new assessment was done using semi-automatic fractional cover estimates derived from the CANAPI algorithm at 234 sites; 2) there is a temporal gap between the CANAPI estimates derived from imagery for year 2010, and the Landsat-derived predicted values obtained for year 2000. The predicted cover from the 2000 Landsat map was overestimated with respect to the observed CANAPI estimates (Figure 4-9), which may be due to the spectral similarity between tall shrubs—the target population, and dwarf shrubs (<0.5 m in height)—the background vegetation (Selkowitz, 2010).

The correlation between both maps was poor ($R^2 = 0.18$). The fractional cover estimates from the 2000 Landsat map were consistently higher with respect to the estimates from the 2000 MISR map (Figure 4-10). Higher fractional cover values in the 2000 Landsat map can be identified along the floodplains of major rivers and in the area confined between $69^{\circ} 2'$ and $70^{\circ} 25'$ degrees latitude and $-163^{\circ} 28'$ and $-155^{\circ} 1'$ degrees longitude. The latest one, corresponding to some patches of erect dwarf-shrub and low-shrub tundra in subzone E according to the CAVM (2003) map although it is not as extensive as predicted by the 2000 Landsat map. Our findings agreed with what has been reported in the literature. Selkowitz (2010) found that Landsat-derived models had the tendency to overestimate shrub canopy across much of the study area, in particular in moist non-acidic tundra.

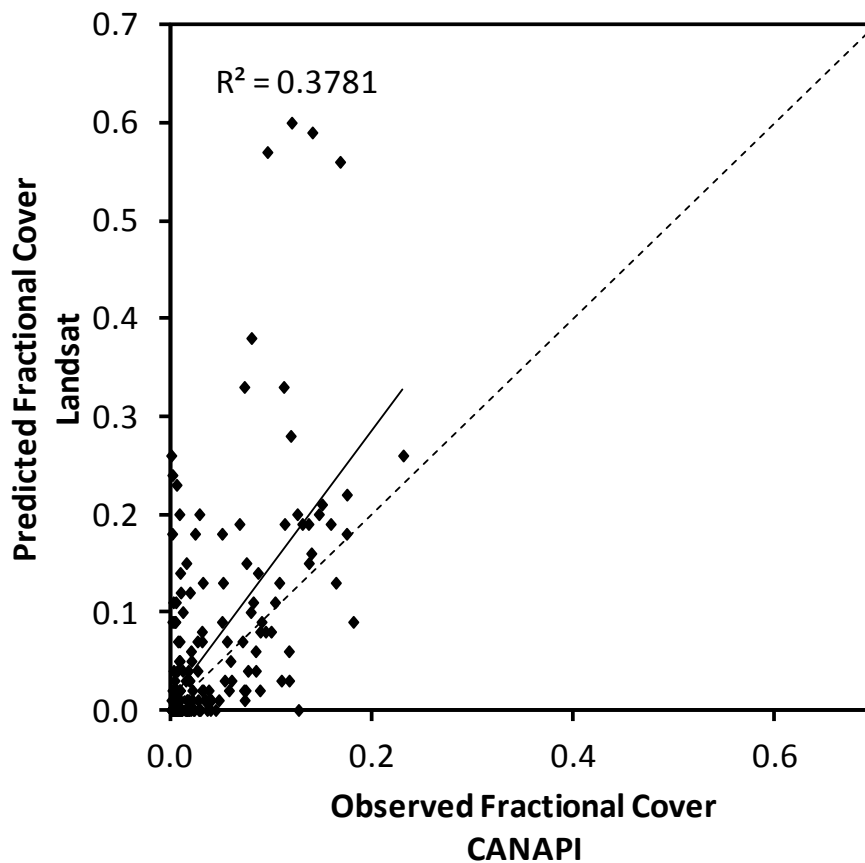


Figure 4-9. Correlation between observed fractional cover derived from the CANAPI algorithm for 234 sites and the predicted fractional cover derived from the 2000 Landsat map re-projected onto a 250 m grid.

A closer inspection at four of the validation sites revealed that the 2000 MISR map provided estimates that were closer to the observed values after taking into consideration the RMSE. For example, at site A (Figure 4-11), the observed cover was 0.12, while the 2000 Landsat map predicted 0.60 and the 2000 MISR map predicted 0.05. Taking into

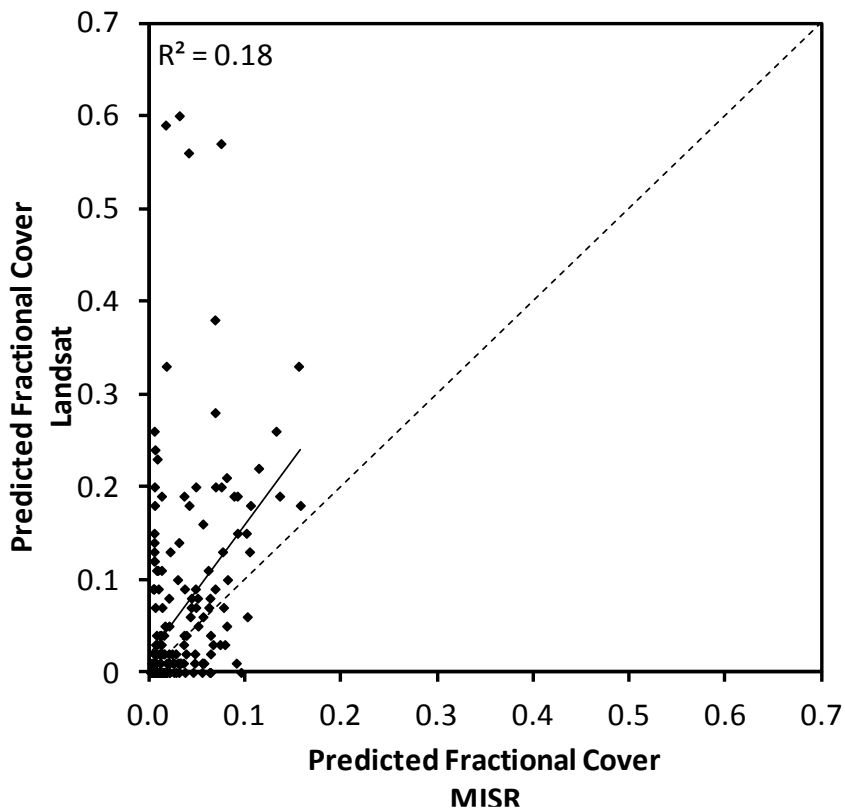


Figure 4-10. Correlation of the predicted fractional cover from the 2000 MISR map and the predicted fractional cover values from the 2000 Landsat map for the 234 validation sites.

consideration the RMSE values for both maps (0.08 and 0.03 respectively), it was clear that the 2000 MISR estimates were closer to the observed values. From the QuickBird imagery it can be seen that where there was an abundant background vegetation that added some roughness to the surface (sites A and B), the 2000 Landsat map seemed to be more sensitive to it and tended to overestimate fractional cover (Figure 4-11). Where the surface was smoother (sites C and D), both the 2000 MISR map and the 2000 Landsat map produced predicted fractional cover estimates that were within the expected margin

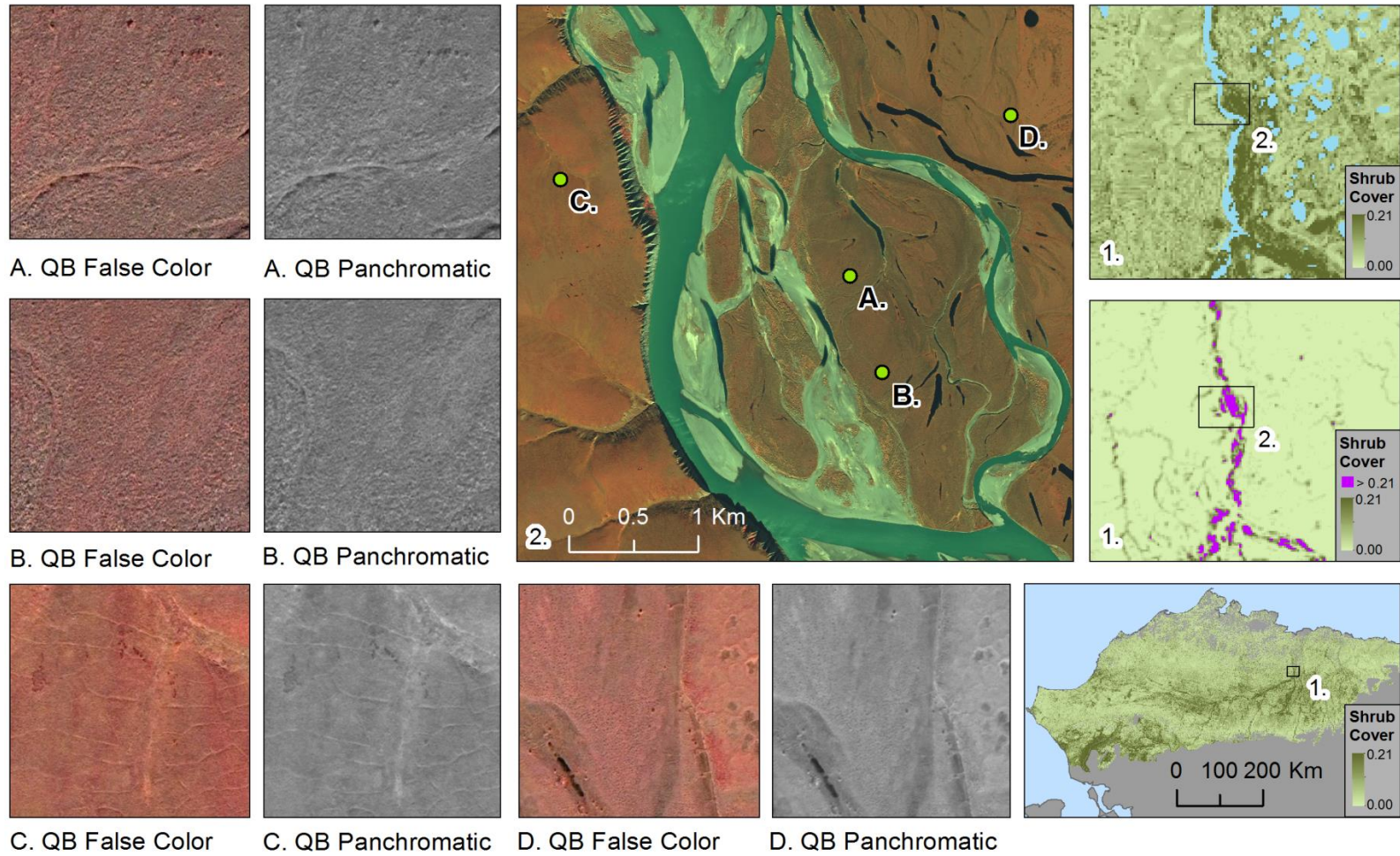


Figure 4-11. Comparison of predicted shrub cover from the 2000 Landsat map and the 2000 MISR map with false color and panchromatic QuickBird imagery for four selected sites along the Colville River with different shrub cover.

of error. For example, at site D where the observed cover was 0.008, the 2000 Landsat map predicted a cover of 0.00 and the 2000 MISR map a cover of 0.01. After taking into consideration the RMSE values, the predicted values from both maps fell within the expected range (Figure 4-11).

4.4 Conclusion

The boosted regression tree has been used to generate the 2000 MISR map with predicted fractional cover values for the North Slope of Alaska. The high temporal resolution and larger swath of the MISR sensor reduced the number of years worth of data needed to create the regional map and had a better coverage in comparison to higher resolution sensors (i.e., Landsat). Predicted fractional cover ranged from 0.00 to 0.21 and about 75% of the sites had a fractional cover less than 0.01. Higher fractional cover was found along rivers, creeks, and sloped terrain. The 2000 MISR map related well to the Arctic bioclimate subzones. It seems to be a positive relationship between tall shrub cover and mean temperature. Subzone E, the warmest one, had the highest shrub cover (0.21), while Subzone C, the coldest one in Alaska, had the lowest shrub cover (0.04).

Comparison of the 2000 MISR map with validation data revealed that the model could explain 52% of the variation in the response variable, fractional cover. The model was sensitive to low fractional cover values (< 0.03) and tended to underestimate cover when the observed values were greater than 0.03. However, underestimation may not be a problem considering that the vast majority of the North Slope has a fractional cover less than 0.01. The 2000 Landsat map had a small dynamic range for low estimates of shrub

cover and when observed fractional cover was greater than 0.01, fractional cover was overestimated. The correlation between estimates from the 2000 MISR map and the 2000 Landsat map was very poor ($R^2 = 0.18$). However, both models agreed that tall shrub fractional cover is very low in the North Slope of Alaska (< 0.05). For regional studies, where the overall abundance of shrub cover across the landscape is more relevant than to know the precise location of pockets with high shrub cover, the 2000 MISR map is the tool for such assessment. The 2000 MISR map had a better coverage, needed less years worth of imagery, and performed better ($R^2 = 0.52$, $RMSE = 0.03$) than the 2000 Landsat map re-projected onto a 250 m grid ($R^2 = 0.38$, $RMSE = 0.08$).

4.5 References

- Beck, P. S. A., Horning, N., Goetz, S. J., Loranty, M. M., & Tape, K. D. (2011). Shrub cover on the North Slope of Alaska: a circa 2000 baseline map. *Arctic, Antarctic, and Alpine Research*, 43(3), 355–363.
- Breiman, L. (2001). Statistical modeling: the two cultures. *Statistical Science*, 16, 199–215.
- CAVM Team. (2003). Circumpolar Arctic Vegetation Map. (1:7,500,000 scale), Conservation of Arctic Flora and Fauna (CAFF) Map No. 1. U.S. Fish and Wildlife Service, Anchorage, Alaska. ISBN: 0-9767525-0-6.
- Chapin, F. S., Shaver, G. R., Giblin, A. E., Nadelhoffer, K. J., & Laundre, J. A. (1995). Responses of Arctic tundra to experimental and observed changes in climate. *Ecology*, 76(3), 694.

- Chapin, F. S., Sturm, M., Serreze, M. C., McFadden, J. P., Key, J. R., Lloyd, A. H., . . . , & Welker, J. M. (2005). Role of land-surface changes in arctic summer warming. *Science (New York, N.Y.)*, *310*(5748), 657–660.
- De'Ath, G. (2007). Boosted trees for ecological modeling and prediction. *Ecology*, *88*(1), 243–251.
- Diner, D. J., Asner, G. P., Davies, R., Knyazikhin, Y., Muller, J. P., Nolin, A. W., . . . , & Strove, J. (1999). New directions in Earth observing: scientific applications of multiangle remote sensing. *Bulletin of the American Meteorological Society*, *80*, 2209–2228.
- Duchesne, R.R., Chopping, M.J., & Tape, K.D. (2015). NACP woody vegetation characteristics of 1,039 sites across the North Slope, Alaska. Data set. Available online [<http://daac/ornl.gov/>] from Oak Ridge National Laboratory Distributed Active Archive Center, Oak Ridge, Tennessee, USA.
- Elith, J., Leathwick, J. R., & Hastie, T. (2008). A working guide to boosted regression trees. *Journal of Animal Ecology*, *77*(4), 802–813.
- Elith, J., & Leathwick, J. R. (2008). Tutorial for running boosted regression trees. [Appendix S3 of the article *A working guide to boosted regression trees*, by J. Elith, J. R. Leathwick, and T. Hastie]. *Journal of Animal Ecology*, *77*(4), 1-15.
- Elmendorf, S. C., Henry, G. H. R., Hollister, R. D., Björk, R. G., Boulanger-Lapointe, N., Cooper, E. J., . . . , & Wipf, S. (2012). Plot-scale evidence of tundra vegetation change and links to recent summer warming. *Nature Climate Change*, *2*(6), 453–457.

- Euskirchen, E. S., McGuire, A. D., Chapin, F. S., Yi, S., & Thompson, C. C. (2009). Changes in vegetation in northern Alaska under scenarios of climate change, 2003–2100: implications for climate feedbacks. *Ecological Applications*, 19(4), 1022–1043.
- Friedman, J.H., Hastie, T., & Tibshirani, R. (2000). Additive logistic regression: a statistical view of boosting. *Annals of Statistics*, 28, 337–407.
- Forbes, B. C., Fauria, M. M., & Zetterberg, P. (2010). Russian Arctic warming and ‘greening’ are closely tracked by tundra shrub willows. *Global Change Biology*, 16(5), 1542–1554.
- Higuera, P. E., Brubaker, L. B., Anderson, P. M., Brown, T. A., Kennedy, A. T., & Hu, F. S. (2008). Frequent fires in ancient shrub tundra: implications of paleorecords for arctic environmental change. *PloS one*, 3(3), e0001744.
- Hinzman, L. D., Bettez, N. D., Bolton, W. R., Chapin, F. S., Dyurgerov, M. B., Fastie, C. L., . . . , & Yoshikawa, K. (2005). Evidence and implications of recent climate change in northern Alaska and other Arctic regions. *Climatic Change*, 72(3), 251–298.
- Hudson, J. M. G., & Henry, G. H. R. (2009). Increased plant biomass in a High Arctic heath community from 1981 to 2008. *Ecology*, 90(10), 2657–2663.
- Huemmrich, K., Gamon, J. A., Tweedie, C. E., Oberbauer, S. F., Kinoshita, G., Houston, S., . . . , & Mano, M. (2010). Remote sensing of tundra gross ecosystem productivity and light use efficiency under varying temperature and moisture conditions. *Remote Sensing of Environment*, 114(3), 481–489.

- IPCC. (2013). *Climate Change 2013: The physical science basis. Contribution of Working Group I to the Fifth Assessment Report of the Intergovernmental Panel on Climate Change* [Stocker, T.F., D. Qin, G.-K. Plattner, M. Tignor, S.K. Allen, J. Boschung, A. Nauels, Y. Xia, V. Bex and P.M. Midgley (eds.)]. Cambridge University Press, Cambridge, United Kingdom and New York, NY, USA, 1535 pp.
- Jia, G. J., & Howard, E. E. (2003). Greening of Arctic Alaska, 1981–2001. *Geophysical Research Letters*, 30(20), 2067.
- Leathwick, J.R., Elith, J., Francis, M.P., Hastie, T., & Taylor, P. (2006). Variation in demersal fish species richness in the oceans surrounding New Zealand: an analysis using boosted regression trees. *Marine Ecology Progress Series*, 321, 267–281.
- Li, X., & Strahler, A. H. (1992). Geometric-optical bidirectional reflectance modeling of the discrete crown vegetation canopy: effect of crown shape and mutual shadowing. *IEEE Trans. Geosci. Remote Sensing*, 30, 276–292.
- Mack, M.C., Bret-Harte, M.S., Hollingsworth, T. N., Jandt, R. R., Shuur, E. A. G., Shaver, G. R., & Verbyla, D. L. (2011). Carbon loss from an unprecedented Arctic tundra wildfire. *Nature*, 475, 489-492.
- Martonchik, J.V., Diner, D.J., Pinty, B., Verstraete, M.M., Myneni, R.B., Knyazikhin, Y., & Gordon, H.R. (1998). Determination of land and ocean reflective, radiative, and biophysical properties using multiangle imaging. *IEEE Transactions on Geoscience and Remote Sensing*, 36, 1266–1281.

- Muller, S.V., Racoviteanu, A. E., & Walker, D.A. (1999). Landsat MSS-derived land-cover map of northern Alaska: extrapolation methods and a comparison with photo-interpreted and AVHRR-derived maps. *International Journal of Remote Sensing*, 20(15-16), 2921-2946.
- Myers-Smith, I. H., Forbes, B., Wilmking, M., Hallinger, M., Lantz, T., Blok, D., Tape, K., ..., & Hik, D.S. (2011). Shrub expansion in tundra ecosystems: dynamics, impacts, and research priorities. *Environmental Research Letters*, 6(4), 045509.
- Myneni, R. B., Keeling, C. D., Tucker, C. J., Asrar, G., & Nemani, R. R. (1997). Increased plant growth in the northern high latitudes from 1981 to 1991. *Nature*, 386(6626), 698–702.
- NASA Land Processes Distributed Active Archive Center (LP DAAC). (2001). MODIS Land Cover Type Product. USGS/Earth Resources Observation and Science (EROS) Center, Sioux Falls, South Dakota. Retrieved on April 2015 from https://lpdaac.usgs.gov/products/modis_products_table/mcd12q1.
- Nicodemus, F. E., Richmond, J. C., Hsia, J. J., Ginsberg, I. W., & Limperis, T. (1977). Geometrical considerations and nomenclature for reflectance. *U.S.A. Department of Commerce/ National Bureau of Standards, NBS Monogr.*, No. 160, 1-52.
- Oke, T.R. (1987). *Boundary layer climates*. Methuen, London, UK.
- R Core Team. (2013). *R: A language and environment for statistical computing*. R Foundation for Statistical Computing. (Version 3.0.1) [Software]. Available from <http://www.R-project.org>.

- Raynolds, M. K., Walker, D. A., Verbyla, D., & Munger, C. A. (2013). Patterns of change within a tundra landscape: 22-year Landsat NDVI trends in an area of the northern foothills of the Brooks Range, Alaska. *Arctic, Antarctic, and Alpine Research*, 45(2), 249–260.
- Ridgeway, G. (2006). Generalized boosted models: a guide to the gbm package. Retrieved from <http://citeseerx.ist.psu.edu/viewdoc/summary?doi=10.1.1.113.9298>
- Selkowitz, D. J. (2010). A comparison of multi-spectral, multi-angular, and multi-temporal remote sensing datasets for fractional shrub canopy mapping in Arctic Alaska. *Remote Sensing of Environment*, 114(7), 1338–1352.
- Sellers, P. J. (1985). Vegetation-canopy spectral reflectance and biophysical processes. In G. Asrar (Ed.), *Theory and applications of optical remote sensing* (pp. 297– 335). New York: Wiley, Ch. 8.
- Stow, D. A., Hope, A., McGuire, D., Verbyla, D., Gamon, J., Huemmrich, F., . . . , & Myneni, R. (2004). Remote sensing of vegetation and land-cover change in Arctic Tundra Ecosystems. *Remote Sensing of Environment*, 89(3), 281–308.
- Sturm, M., Racine, C., & Tape, K. (2001). Climate change. Increasing shrub abundance in the Arctic. *Nature*, 411(6837), 546–547.
- Tape, K., Sturm, M., & Racine, C. (2006). The evidence for shrub expansion in Northern Alaska and the Pan-Arctic. *Global Change Biology*, 12(4), 686–702.
- Tape, K. D., Hallinger, M., Welker, J. M., & Ruess, R. (2012). Landscape heterogeneity of shrub expansion in Arctic Alaska. *Ecosystems*, 15(5), 711-724.

- U.S. Geological Survey. (2001). NLCD 2001 Land cover Alaska - National Geospatial Data Asset (NGDA) Land Use Land Cover. Edition 1.0.
- Wanner, W., Li, X., & Strahler, A. H. (1995). On the derivation of kernels for kernel-driven models of bidirectional reflectance. *Journal of Geophysical Research*, 100(D10), 21077-21089.
- Wanner, W., Strahler, A. H., Hu, B., Lewis, P., Muller, J. P., Li, X., Schaaf C. L. B., & Barnsley, M. J. (1997). Global retrieval of bidirectional reflectance and albedo over land from EOS MODIS and MISR data: Theory and algorithm. *Journal of Geophysical Research*, 102, 17143–17162.
- Zhou, L., Tucker, C. J., Kaufmann, R. K., Slayback, D., Shabanov, N. V., & Myneni, R. B. (2001). Variations in northern vegetation activity inferred from satellite data of vegetation index during 1981 to 1999. *Journal of Geophysical Research*, 106, 20069– 20083.

CHAPTER 5

The 2010 Tall Shrub Fractional Cover Map and Temporal Changes in Shrub Abundance in the North Slope of Alaska, 2000-2010

Abstract

Several lines of evidence point to a shrub expansion in the North Slope of Alaska. In order to understand the impact of the many implications that an increase in shrub abundance could have on the environment and regional climate, it is necessary to assess the direction and magnitude of the vegetation shift at a regional scale. In this study, the boosted regression tree model was used to predict tall shrub (> 0.5 m) fractional cover change from moderate resolution imagery for the North Slope of Alaska for the year of 2010. Estimates of change in shrub cover, relative change in shrub cover, and expansion rate were obtained by comparing predicted tall shrub cover values from the year 2010 and 2000. Results showed that shrubs were more abundant along floodplains, river terraces of major rivers, and hill slopes. Temporal comparisons of tall shrub abundance in the MISR-derived maps revealed that shrubs expanded during the period 2000-2010. The extent of the area that unequivocally experienced a robust change in tall shrub cover was less than 1 % (1,487 km²) of the total area of the North Slope of Alaska (213,090 km²). It is possible that tall shrubs may have expanded throughout a larger area but there is insufficient precision in the MISR-based estimates to make an unequivocal

determination. Nevertheless, it seems that there was a positive trend toward an increase in shrub cover considering that 95% of the locations that had a robust change saw an increase. Most of the shrub expansion was observed along the forest-tundra ecotone, north of the Brooks Range, especially along the Naokat River and surrounding areas. It is possible that the observed increase in cover indicates that the tree line is slowly moving northward, although this process could take many decades or centuries. More research is necessary to infer the potential impacts of canopy-forming shrubs on the regional climate and ecological processes in view of the findings in this study.

Keywords: Fractional cover map, tall shrub, North Slope of Alaska, Multi-angle Imaging SpectroRadiometer (MISR), temporal change, shrub expansion rate.

5.1. Introduction

Several lines of evidence point to a shrub expansion in the North Slope of Alaska over the past few decades (Myneni et al 1997; Stow et al., 2004; Sturm et al., 2001; Tape et al., 2006) and changes in the Arctic vegetation can affect the ecosystem in many different ways. A shrubbier tundra can influence climate (Hinzman et al., 2005) by altering the albedo, the emission of greenhouse gases, and the energy partitioning at the surface (McGuire et al., 2006). The vegetation shift could also affect the distribution of wildlife by modifying the availability of quality food sources and shelter. For instance, Porcupine Caribou herds find mosses and evergreen shrubs to be less digestible than willows and immature cotton-grass flowers (Griffith et al., 2002), early bird migrants survive by feeding on protruding willow branches when the ground is still covered by snow, and passerine migrants prefer nesting near willows as the wind speed is attenuated almost completely within 0.1 m of the ground (Wingfield et al., 2004). In addition, an increase in shrub density could affect the length of time the snow remains on the ground, the depth of the snow pack, and the snow distribution pattern (Liston et al., 2002). Snow-shrub interactions could affect climate in four ways: by increasing winter efflux of carbon dioxide, by reducing runoff during spring melt, by reducing winter sensible heat losses, and by reducing the winter albedo (Sturm et al., 2001). A shift toward a shrubbier Arctic could alter the nitrogen (N) and carbon (C) cycles and vice-versa (Chapin et al., 2005). Warmer winter temperature beneath the snow pack surrounding the shrubs could enhance N mineralization, which in turn may promote shrub expansion (Sturm et al., 2005). Furthermore, an increase in woody vegetation may increase the likelihood of fires. In

Alaska, 232 tundra fires were reported between 1950 and 2005 and most of the cases corresponded to warmer and dryer environments (Higuera et al., 2008).

In order to understand the impact of the many implications that a shrub expansion could have on the environment, it is necessary to assess the direction and magnitude of the vegetation shift at a regional scale. Many temporal studies on vegetation change are based on discrete observations that impede a thorough assessment across the landscape (Myers-Smith et al., 2011). For example, the first plot-based study, carried out from 1981 to 2008 in the Canadian High Arctic, covered an area of 8 km² (Hudson & Henry, 2009). Another plot-based study evaluated vegetation change in 48 locations spread across the pan-Arctic during 1980 and 2010 (Elmendorf et al., 2012). Repeat photography assessed shrub expansion in Alaska, during a 50 years span, in an area of about 320 km² (Sturm et al., 2001). Dendrochronology studies in the Russian Arctic showed an increase in shrub willow growth for the period 1981-2005 and covered an area of 7.5 km² (Forbes et al., 2010). A similar study in Arctic Alaska surveyed 26 transects of 80 m each and found that expansion of shrub patches in the last 50 years was associated with floodplains, outcrops, and stream corridors (Tape et al., 2012). On the other hand, most of the regional temporal studies are inadequate to assess the magnitude and direction of a possible shrub expansion because for the most part they are based on vegetation indices, with the Normalized Difference Vegetation Index (NDVI) being the most widely used. However, vegetation indices are merely proxies of photosynthetic activity and do not adequately represent shrub cover characteristics across the arctic tundra biome (Selkowitz, 2010). Furthermore, the relationship between the vegetation indices and

biophysical quantities of the vegetation varies with season, proportion of dead material in plant canopy, vegetation type, and soil background (Sellers,1985). Nevertheless, these kind of studies have shown that the vegetation is changing. For example, an increase in NDVI, also called greening, has been observed in the pan-Arctic between 1981 and 1991 and associated with an increase in plant growth (Myneni et al., 1997). A related study in the Arctic Slope of Alaska found a greening trend between 1981 and 2001 and it was correlated to an increase in aboveground plant biomass (Jia & Howard, 2003). A second study in the same region confirmed an increase in the greenness rate of change during the 1990s (Stow et al., 2004).

Due to the extent of the North Slope of Alaska, harsh weather conditions, and relative inaccessibility of the region, remote sensing seems to be a suitable approach for mapping regional vegetation changes (Selkowitz, 2010; Stow et al., 2004), as evidenced by the success of the greening studies mentioned above. Evaluation of temporal changes in shrub abundance calls for sensors with an extensive temporal coverage and for a robust canopy model able to predict tall shrub cover. Among the sensors with a long record of free data available are Landsat, the Advanced Very High Resolution Radiometer (AVHRR), the Moderate-resolution Imaging Spectroradiometer (MODIS), and the Multi-angle Imaging SpectroRadiometer (MISR). Landsat was launched in 1972 and it is the oldest land-surface observation satellite system. The advantage of Landsat is its finer spatial resolution in comparison to AVHRR, MISR, and MODIS. Landsat 1, 2, 3, 4, and 5 had a spatial resolution of 79 m, while Landsat 7—the latest satellite successfully launched—had a resolution of 30 m in its multi-spectral bands. The downside of using

this satellite for mapping Arctic vegetation is that it has a revisit cycle of 16 days. Using Landsat to create wall-to-wall vegetation maps in the Arctic would require many years worth of data because the collection of satellite scenes is limited to the summer months with its constant cloud cover (Beck et al., 2011; Selkowitz, 2010). The first AVHRR sensor was launched in 1978. Many have been launched thereafter and their records extend until present. One advantage is its high frequency of coverage as it acquires images of the entire Earth twice a day, which increases the likelihood of obtaining cloud-free scenes—specially for a region like the Arctic that has a persistent cloud cover. In spite of its long record and short revisit cycle, the AVHRRs have a coarse spatial resolution (local area coverage) of 1.1 km. Since shrub fractional cover is already very low (<5%) at a spatial resolution of 250 m (Duchesne et al., 2015) in the North Slope, using a coarser resolution implies detecting a much smaller signal. More importantly, post-launch degradation and anomalies observed with the change in satellites affects the consistency of measured vegetation parameters (Myneni et al., 1997). Besides the aforementioned sensors, MODIS and MISR follow with the longest temporal coverage available. MODIS is a multi-spectral sensor launched in 1999 on board of the Terra satellite, and in 2002 on board of the Aqua satellite. MISR was launched in 1999 together with MODIS on the Terra satellite. Both MODIS and MISR have a repeat coverage of about two days in the northern latitudes, but MODIS has a lower spatial resolution (500 m, depending on the band) than MISR (250 m). Besides, MISR offers near-simultaneous multi-angular observations of the land surface, which provides additional information

that can improve the predictive performance of canopy models (Selkowitz, 2010). Thus, MISR was selected as the sensor of choice in this study.

For consistency and in order to reduce bias in evaluating temporal changes in shrub abundance, it is better to deploy the same canopy model for every year of analysis. Since the year 2000 tall shrub fractional cover map was derived using the Boosted Regression Tree (BRT) model, it is reasonable to use the same model to construct the 2010 tall shrub fractional cover map. The BRT model is a machine learning algorithm able to explain 52% of the variability in tall shrub abundance in the North Slope of Alaska. The model successfully described the shrub cover pattern observed in high resolution imagery and in field plots (Duchesne et al., 2015). Thus, with the aid of this model, it may be possible to assess the changes in tall shrub abundance experienced over the last decade in the region.

The main goal of this study was twofold: to create a wall-to-wall map of tall shrub abundance for the North Slope of Alaska for the year 2010 using moderate resolution imagery and the BRT model, and to assess changes in shrub abundance during the period 2000-2010 in the region. Specific objectives were to obtain MISR imagery for the years 2010 to 2011, to invert the RossThick-LiSparse reciprocal model using the red reflectance values of MISR's nine cameras in order to account for the anisotropic properties of the surface, to mosaic all MISR paths into one multi-layer map with all the surface reflectance-derived predictor variables for the region, to retrieve shrub fractional cover using the BRT model, to filter map outputs, and to evaluate temporal changes in woody vegetation by comparing the new map with the previously created one for the year 2000.

5.2. Materials and Methods

5.2.1. Data Sources

The creation of the 2010 tall shrub fractional cover map used MISR data collected in the years 2010 and 2011 during the period June 1 - August 15 (Appendix E). This period matched the growing season when the shrub crowns were at their fullest and minimal changes in reflectance were observed. A total of 22 paths (P065-P086) were necessary to cover the entire North Slope of Alaska. Out of the 220 potential orbits, only 141 had imagery available after processing (Table 5-1). The MISR data were downloaded from the NASA Langley Atmospheric Science Data Center using the MISR Order and Customization Tool (<http://10dup05.larc.nasa.gov/MISR/cgi-bin/MISR/main.cgi>).

Table 5-1. Summary of available MISR imagery for years 2010-2011.

Status	2010	2011
Good Imagery	69	72
Bad Imagery	41	38
Total	110	110

Elevation data for the North Slope of Alaska were obtained from the National Elevation Dataset (NED) produced by the U.S. Geological Survey (USGS). The data were available at a spatial resolution of 2 arc-second (approximately 60 m). A total of 99 NED subsets mosaic were necessary to cover the entire study area. Latitude (m), slope (degrees), and aspect were derived from the elevation map. Considering that aspect is a

circular variable, it was linearized by creating two variables: 'northness' and 'eastness'.

Detailed explanation on the last two variables is provided in chapter 4.

The MODIS Collection 5 Burned Area Product - MCD45 was used to identify burned areas. The monthly Geotiffs from year 2000 to 2011 (132 tiles) were downloaded from the University of Maryland website; just one tile was necessary to cover the entire study area (window 1). In addition, the area burned during the Anaktuvuk fire of 2007, the largest fire during the last decade, was digitized since the MODIS product did not cover its entire extent.

All data processing was carried out using several software and utility scripts. Software included ERDAS Imagine 2014, ArcGIS 10.2.1. , Pythonwin - Python IDE and GUI Framework for Windows, and R v3.0.1. All data used were projected onto a 250 m Albers Conical Equal Area grid (Appendix A).

5.2.2. Production of the 2010 Tall Shrub Cover Map

The same steps taken to construct the tall shrub fractional cover map for the year 2000 were followed in order to produce the 2010 tall shrub fractional cover map. Chapter 4 provides a detailed explanation of the processing of MISR imagery, the BRT model, and the work flow for the creation of the shrub cover map of Arctic Alaska. This study used MISR's red band from all off-nadir cameras and the four spectral bands from the nadir camera. With the aid of the MISR Toolkit the MISR files that came in the Hierarchical Data Format (HDF) were extracted, and the surface reflectance estimates were obtained and mapped onto the Albers Conical Equal Area map projection. The

MISR red band bidirectional reflectance factors (BRFs) in all nine cameras were used to invert the RossThick-LiSparse Reciprocal (RTLS-R) model, using the Algorithm for Modeling Bidirectional Reflectance Anisotropies of the Land Surface (AMBRALS) code (Wanner et al., 1997). Inversion of this model resulted in 13 parameters but only 6 were used in the canopy model.

Clouds and invalid surface reflectance values were removed from the MISR data using several criteria. Then, the MISR orbits were composited by averaging all valid values for a given parameter on a pixel-per-pixel basis. Following, the variables latitude, elevation, slope, northness and eastness were added as layers to the composite data map. This final version contained 15 variables: six parameters that resulted from the inversion of the RTLS-R model (three kernels functions, the black-sky and white-sky albedos, and the weight of determination of the nadir BRDF-adjusted reflectance at solar zenith angle of 45 degrees), MISR's four spectral bands at nadir (blue, green, red, and near-infrared), and five terrain variables (latitude, elevation, slope, northness, and eastness), which were the input data to the Boosted Regression Tree model. The model, which had been previously trained and validated (see chapter 3), was fitted in R (v3.0.1, 2013) using the 'gbm' library (Ridgeway, 2004) and the brt.functions (Elith and Leathwick, 2008). The response variable was the arcsine transformed shrub fractional cover, which was later converted to fractional cover. No data values and water/ice pixels in the map were flagged using multiple criteria. Burned areas were masked using the MODIS burned area product and a mask of the Anaktuvuk fire.

5.2.3. Temporal Comparison of the 2000 and 2010 Fractional Cover Maps

Estimates of tall shrub cover obtained for the years 2000 and 2010 across the entire domain of the North Slope of Alaska were compared in order to assess the magnitude and direction of the vegetation change. Two measures of change: the change in tall shrub cover (CSC) and the relative change in tall shrub cover (RSC), also called percent change, were computed on a pixel-by-pixel basis:

$$CSC = \text{Fractional Cover in 2010} - \text{Fractional Cover in 2000} \quad \text{Eq. 5-1}$$

$$RSC = \left(\frac{\text{Fractional Cover in 2010} - \text{Fractional Cover in 2000}}{\text{Fractional Cover in 2000}} \right) \times 100 \% \quad \text{Eq. 5-2}$$

Negative values of CSC indicated a decrease in cover, while positive values of CSC showed an increase in cover. Considering that the root mean square error (RMSE) of the 2000 and 2010 fractional cover maps was 0.03, the direction of the change in cover (CSC) was uncertain within the bracket -0.06 to 0.06. Change in shrub cover outside of this bracket was considered trustworthy.

The annual expansion rate was determined for the pixels showing a reliable increase in tall shrub cover and it was calculated as the ratio of the change in shrub cover by the number of years in the temporal range, which in this study was 10 years (2000-2010):

$$\text{Expansion Rate} = \frac{CSC}{\text{Number of years}} \quad \text{Eq. 5-3}$$

5.3. Results and Discussion

5.3.1. *Tall Shrub Fractional Cover Map of Arctic Alaska, 2010*

Similar to the construction of the 2000 fractional cover map of the North Slope of Alaska, the spatial prediction of tall shrub fractional cover for the year 2010 was obtained using the trained and validated boosted regression tree model with the same input parameters and settings as for the 2000 map (Fig 5-1). The Anaktuvuk fire of 2007, which extended from the margins of the Nanushuk River to the margins of the Itkillik River, was flagged in the map. Predicted fractional cover in 2010 ranged from 0 to 0.21 (RMSE of 0.03) and 52 % of the variation in the response, fractional cover, was explained by the predictor variables of the model (see Chapter 3; Table 5-2). At a spatial resolution of 250 m, 75% of the sites had a fractional cover less than 0.015. Similarly, Selkowitz (2010) found that at the same spatial resolution, 80% of his sites had a cover less than 0.05 . Very high fractional cover was found along the Noatak River and it extended east of it (Fig 5-2). This mainly corresponded to spruce trees and the tree-shrub transition. Spruce trees grew more abundantly on the south-west side of the mountains and on the floodplains. High fractional cover occurred along floodplains, in particular in the southern portion of the Colville, Chandler, Anaktuvuk, Nanushuk, Itkillik, and Kuparuk rivers, decreasing as the rivers descended to the coastal plain (Fig 5-3). This distribution pattern also corresponded to the one of the erect dwarf-shrub and low-shrub tundra, which is dominated by tall shrubs (Walker et al., 2003). Slightly lower fractional cover occurred along water tracks, creeks, and sloped terrain (Fig 5-3), but it drastically decreased toward the coastal plain (Fig. 5-1). The patchy distribution of tall shrubs agrees

with similar studies that documented tall shrub cover in floodplains and terraces of major rivers, steeper hill slopes, and stream drainages (Selkowitz, 2010; Tape et al., 2006). The availability of water carrying sediment and nutrients seemed to enhance shrub expansion.

Table 5-2. Distribution of fractional cover estimates from 2010 tall shrub cover map.

Minimum	First Quartile	Median	Third Quartile	Maximum
0	0.0056	0.0086	0.0148	0.2077

Low values of shrub cover were correlated with higher values of red reflectance from MISR's nadir camera. Shrubs were more abundant where the slope was lower than 2° degrees (i.e., floodplains), and again where the slope ranged between 5° and 10° degrees (i.e., hillslopes). The exception to this pattern was the very flat terrain on the coastal plain where severe climatic conditions prevail. Sites with low shrub cover also exhibited higher albedo values, which is expected given that the shrubs are darker than the background vegetation. Tall shrub cover also decreases when latitude increases, which agrees with the observation that shrub abundance declines northward. The strong winds, cold conditions, low soil moisture, and dry climate in the High Arctic (Epstein et al., 2004) may hinder the expansion of tall shrubs in the coastal plain.

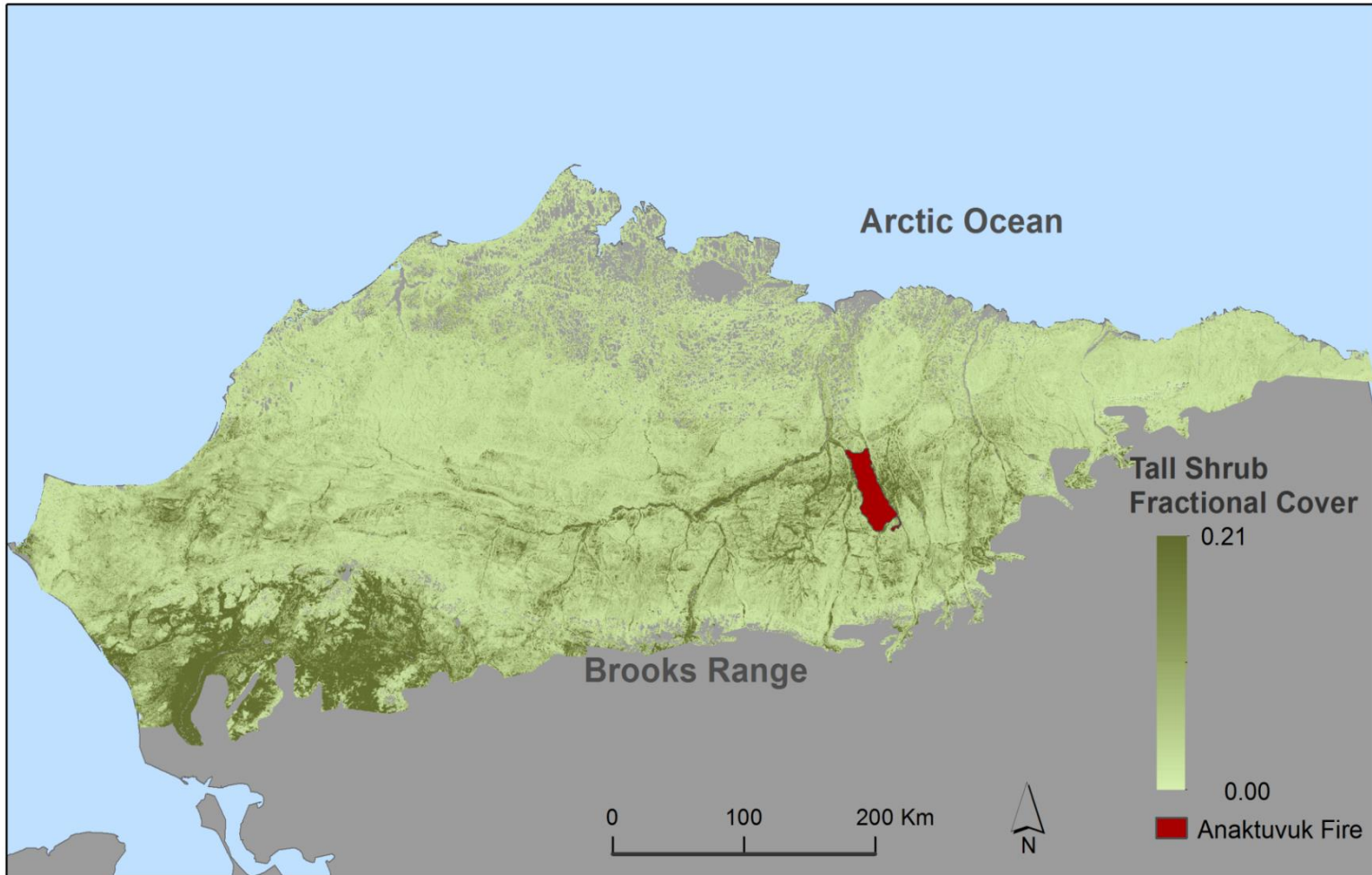


Figure 5-1. Tall shrub fractional cover map for the North Slope of Alaska, year 2010. Fractional cover values derived from the Boosted Regression Tree model and it ranged from 0.0 to 0.2.

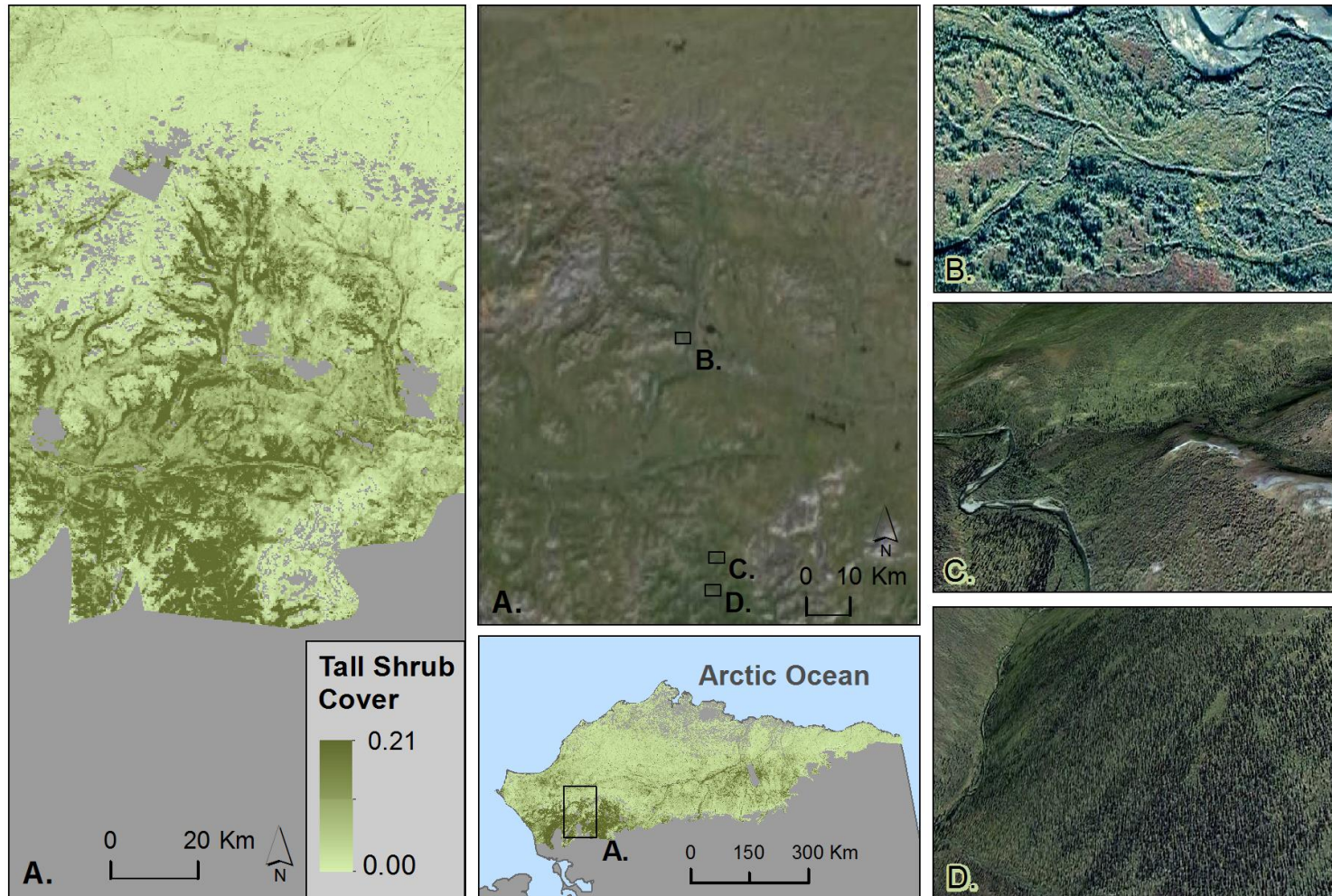


Figure 5-2. Section east of the Noatak River in the southwestern portion of the North Slope of Alaska (A). The high values of cover corresponded to a forest of spruce (C and D), and the transition between trees and shrubs (B).

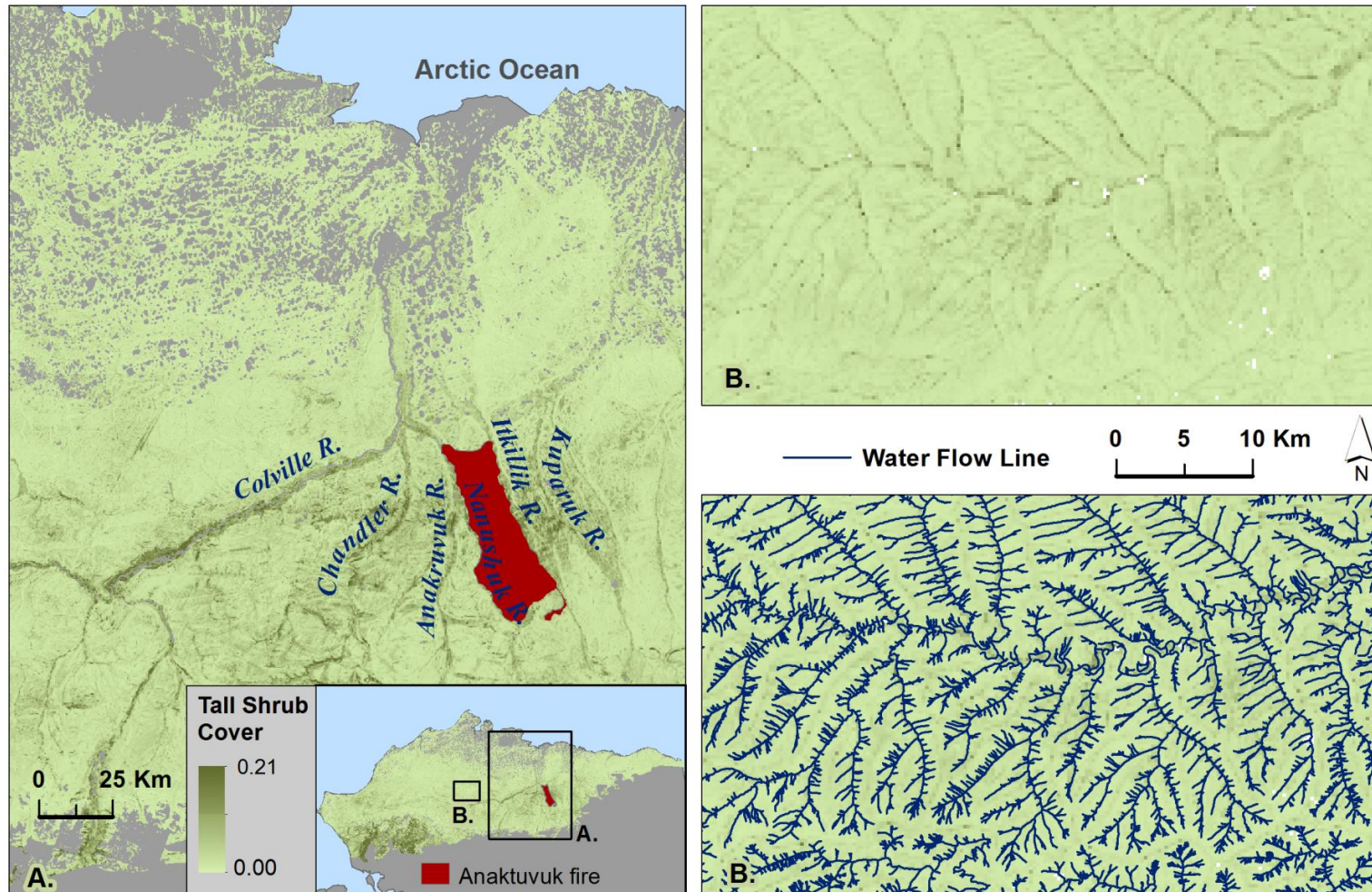


Figure 5-3. Portion of the 2010 fractional cover map depicting the correlation of high shrub cover along floodplains of major rivers and water tracks. Water flow lines west of the Colville river (source: USGS, The National Map, Hydrography).

5.3.2. Temporal Change in Tall Shrub Cover over the Last Decade

The predicted tall shrub cover map of the year 2010, and hereafter the 2010 MISR map, had a similar pattern of shrub abundance distribution as of the predicted tall shrub cover map of the year 2000, and hereafter the 2000 MISR map. The similarity in the tall shrub spatial distribution pattern in the 2000 and 2010 MISR maps indicates that the boosted regression tree model is consistent in predicting estimates of tall shrub cover. Shrubs were more abundant along floodplains, terraces, and water tracks on the hill slopes, which indicates that water may be a limiting factor for shrub expansion. There was a marked increase of shrubs southward, closer to the Brooks Range.

During the short period of the study (10 years), the extent of the area that unequivocally experienced a change in tall shrub cover was less than 1 % (1,487 km²) of the total area of the North Slope of Alaska (213,090 km²). It is possible that tall shrubs may have expanded throughout a larger area but there is insufficient precision in the MISR-based estimates to make an absolute determination. On the other hand, this study was limited to the mapping of tall shrubs but it is all together possible that smaller shrubs may be expanding even faster. Although Pattison et al., (2015) found that at 27 pairs of field plots that represented five different tundra types, deciduous and evergreen shrubs did not have an important change in cover during the period 1984-2009, other studies support the widespread shrub expansion (Elmendorf et al., 2012; Tape et al., 2006). This study showed that shrubs are expanding, but the propagation is site specific. The number of pixels that unequivocally exhibited an increase in tall shrub cover (greater than 0.06 considering that the model had an RMSE of 0.03; 22,603 pixels) was twenty times more

than the pixels where vegetation decreased. In about 90% of the pixels that showed an unequivocally increase in cover, tall vegetation increased by more than 100% (Table 5-3). In many of the cases, vegetation went from virtually zero canopy cover to 10% or more. On the other hand, there were a total of 1,200 pixels that displayed a decrease in tall shrub cover, which represented a total area of 75 km² (Table 5-3). Vegetation canopy decreased by 60% or more in 1,026 pixels.

Table 5-3. Relative change in tall shrub cover in the North Slope of Alaska, 2000-2010. Only an unequivocally change (greater than 0.06, model RMSE of 0.03) is displayed.

Percentage Change	Number of Pixels	Area (km²)
-98 to -80	695	43.44
-79.9 to -60	331	20.69
-59.9 to -40	165	10.31
-39.9 to -20	9	0.56
-19.9 to < 0	0	0
> 0 to 100	489	30.56
100.01 to 500	9922	620.12
500.01 to 1,000	7191	449.44
1,000.01 to 2,000	4072	254.5
2,000.01 to 5,297	929	58.06
Total	23,803	1,487.69

A map of the change in shrub cover revealed the direction of the change in tall shrub cover over the last decade (Fig. 5-4). The map showed that tall vegetation has expanded immediately north of the Brooks Range, in particular near the Noatak River in the southwestern portion of the North Slope of Alaska (Fig. 5-5). This region is dominated by spruce trees and it is the transition zone between the tree line and the tundra (Fig. 5-3 and Fig. 5-5). It is possible that the observed increase in cover indicates that the tree line is slowly moving northward. Nevertheless, the conversion of the forest-tundra ecotone is a slow process that could take many decades or centuries (Macdonald et al., 2005). Suarez et al. (1999) documented an invasion of white spruce into adjacent tundra ecosystems in the same region—the Noatak National Preserve—by about 100 m in the past 200 years and it seemed to be influenced by climate. Temperature is the main factor that determines location of the boundary between the boreal forest and the tundra ecosystems, but other factors like wind and precipitation also influence the rate of change of the treeline (Hinzman et al., 2005). On the other hand, the North Slope of Alaska has experienced an increase in summer temperature—Summer Warmth Index (SWI)—and vegetation productivity—Maximum Normalized Difference Vegetation Index (MaxNDVI)—as a result of declining sea ice levels (Bhatt et al., 2013), but the observed increase in shrub cover is not homogeneous across the landscape, which suggests that other factors may influence the distribution and expansion of shrubs. The patchy distribution of shrubs seems to respond more to indirect effects of warming such as nutrient availability (Chapin, 1983). It seems that shrubs are slowly expanding along some floodplains and

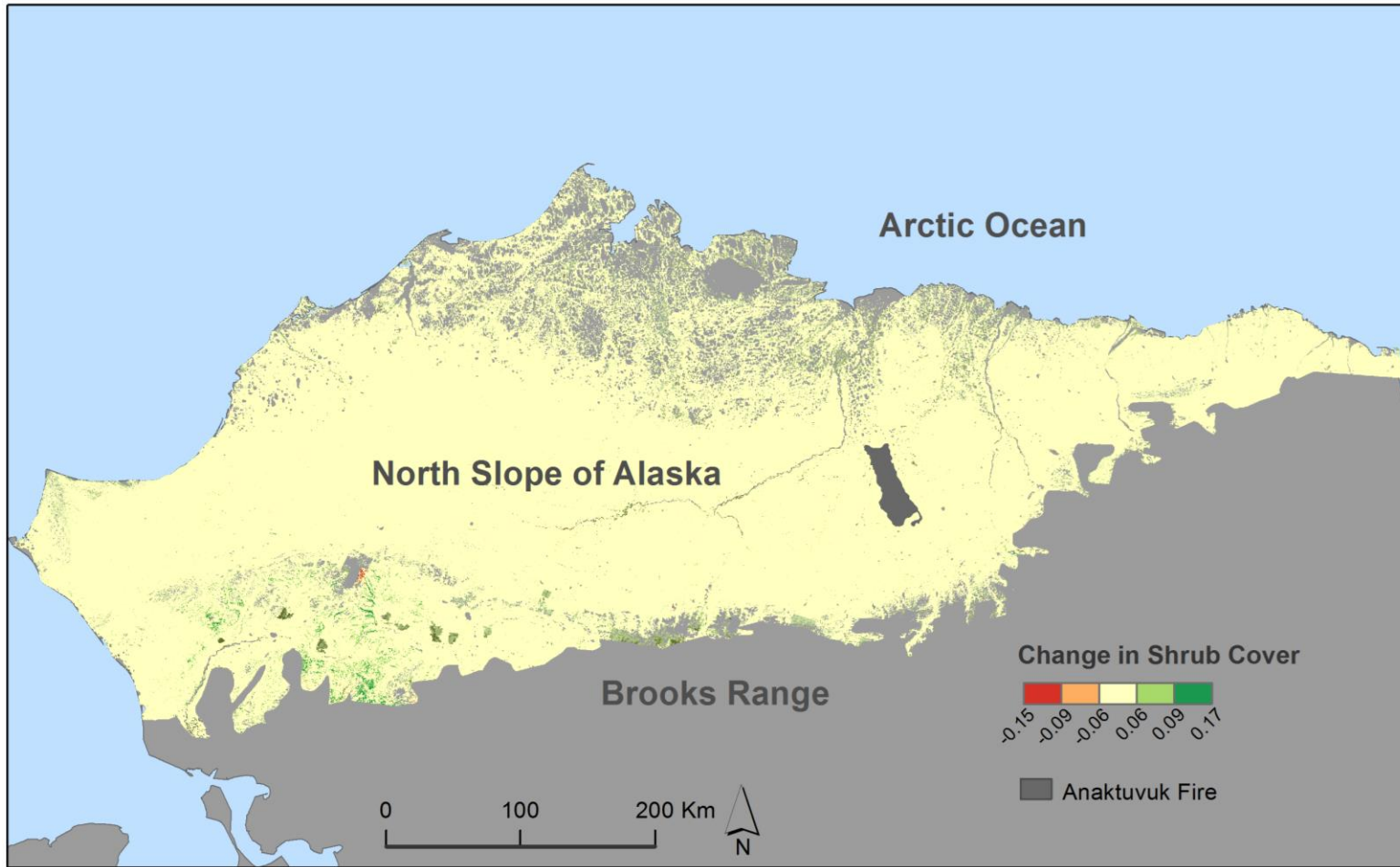


Figure 5-4. Change in tall shrub cover (CSC) for the North Slope of Alaska during the period 2000 - 2010. In the legend, the region between -0.06 and 0.06 represents locations where the direction of change is uncertain.

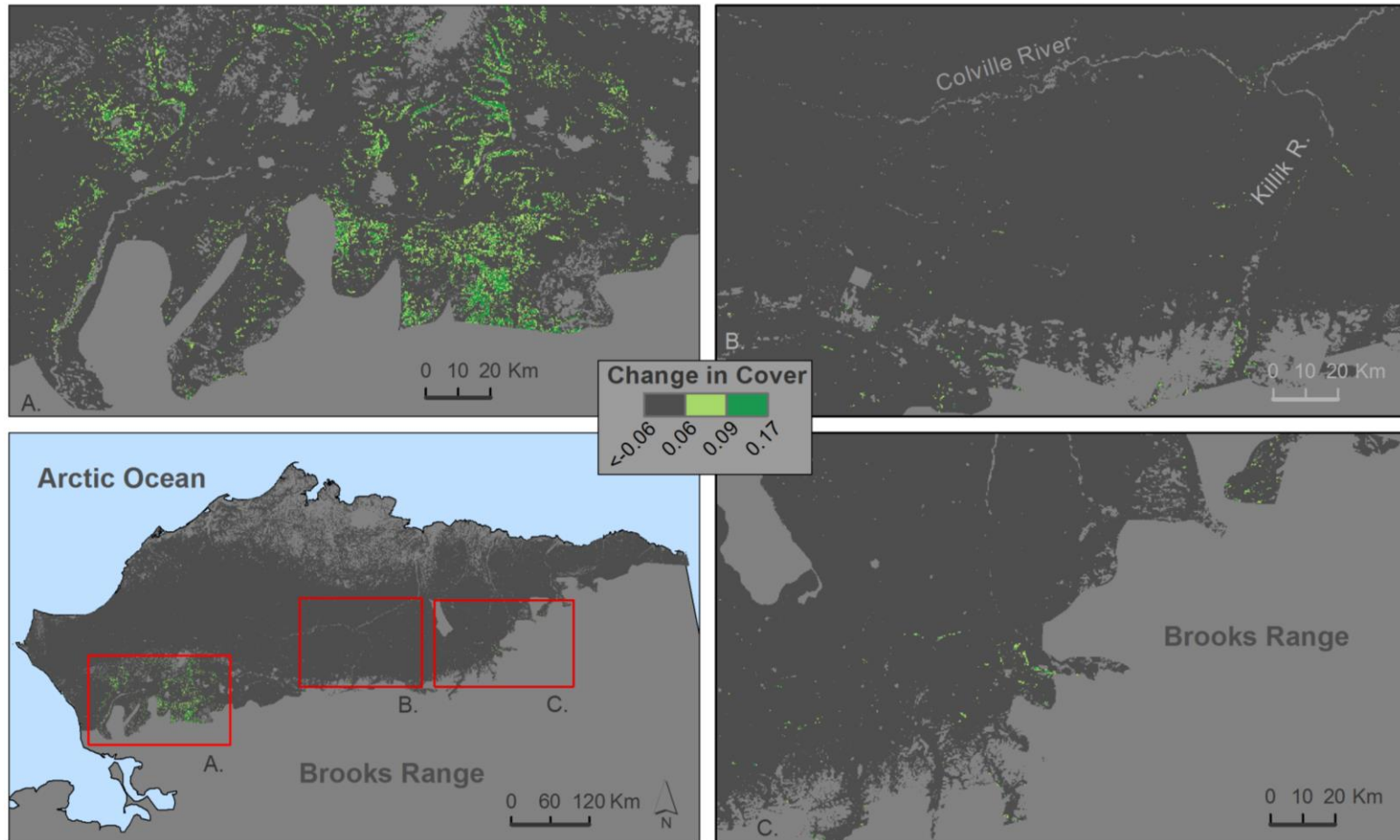


Figure 5-5. Change in tall shrub cover (CSC) depicting increase of tall vegetation. In the legend, the region between -0.06 and 0.06 represents locations where the direction of change is uncertain. A. Noakat River and surrounding areas, B. Floodplains and river terraces, C. Southern boundary of the North Slope of Alaska.

slopes. For instance, the map shows a small proliferation of shrubs on the northern portion of the Colville River and in the floodplains of the Killik River (Fig. 5-5). A possible reason is that the increase in soil temperature may have produced the thawing of permafrost, thus increasing groundwater transport and making nutrients available in those areas (Raynolds et al., 2013).

The decrease in shrub cover was limited to a few areas in the North Slope of Alaska (Fig 5-6). In two of them it seems that it corresponded to a residual effect of the compositing technique in the 2000 MISR map (Fig 5-6). This might have been the result of only having one orbit available passing through that region. Besides the aforementioned specific events, the other few cases of decrease in shrub cover were mainly along the Colville River and its surrounding areas and in the northern portion of the Kiruktagiak River. This area is dominated by erect dwarf-shrub tundra and low-shrub tundra (Walker et al., 2003). At least four hypotheses may explain declines in shrub cover: changes in stream channels (Raynolds et al., 2013), wildfires (Verbyla, 2008), shrub mortality from insects and diseases (Soja et al., 2007), and changes in carbon allocation—a decrease in leaf production and a proliferation of roots—due to a dryer environment (Verbyla, 2008). Changes in stream channels seem to be a localized effect (small patches less than 100 m², Raynolds et al., 2013), which may be the case here as some areas of decrease are only a couple of pixels in size (250 m/ pixel). The location of fires during the period 2000-2010 and the occurrence of shrub cover declines do not correspond, thus, it is unlikely that fires led to a decline in shrub abundance (Fig 5-6).

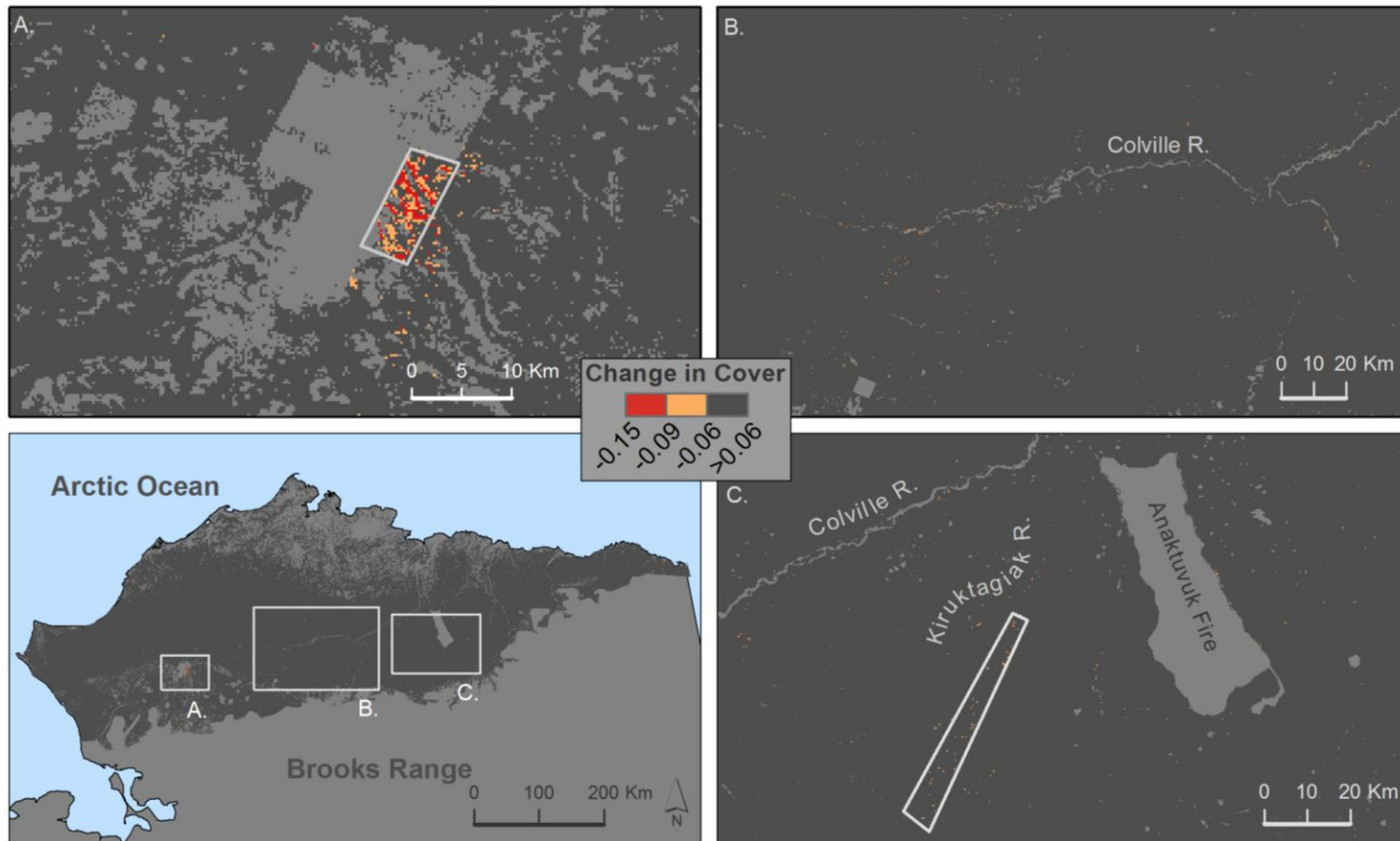


Figure 5-6. Change in tall shrub cover (CSC) depicting decrease of tall vegetation. In the legend, the region between -0.06 and 0.06 represents locations where the direction of change is uncertain. A. Residual effect of compositing technique in white polygon, B. Decrease in a few patches along the Colville River, C. Residual effect of compositing technique within the white polygon and decrease in tall shrub cover along the Kiruktagiak River.

Changes in carbon allocation have been documented in the Russian forests where warmer but dryer conditions have led to an increase in roots and a decrease in leaves and needles (Lapenis et al., 2005). If similar conditions apply to the North Slope of Alaska, then the decrease in shrub cover should be widespread and it is not. Another plausible option, although this theory is not confirmed, is an insect invasion or disease affecting the canopy of the shrubs. Cases of infestation have been reported in interior Alaska (Furniss et al., 2001; Nossov et al., 2011; Ruess et al., 2006; Snyder et al., 2007). For example, willows (*Salix* spp.) in drainages of the Kuskokwim and Yukon Rivers were infested by a leafblotch miner (*Micrurapteryx salicifoliella*) twice in the 1990s (Furniss et al., 2001). Birch have also been infested by three nonnative leaf mining sawflies that were introduced to Alaska around 1997, the most harmful of them being *Profenusa thomsoni*. *P. thomsoni* was found in Anchorage, Fairbanks, and in some remote areas of the Kenai Peninsula that were only accessible by float plane (Snyder et al., 2007).

The annual expansion rate for the plots that experienced an increase in shrub cover greater than 0.06 between the years 2000 and 2010 varied between 0.006 yr⁻¹ and 0.017 yr⁻¹ (Fig. 5-7). These rates are reasonable considering that Naito et al. (2014) found that the annual percent change in tall shrub cover within river valleys of the Brooks Range and North Slope uplands was about 1.2% per year. Tape et al. (2006) found a lower annual shrub expansion rate (0.4% per year), but this included all shrubs, tall and low ones. Expansion rate may be affected by site-specific factors such as soil condition and hydrology. For example, in a warming experiment, tall shrubs' expansion was enhanced in moist to wet soils (Elmendorf et al., 2012). Another aspect of consideration is the scale

of analysis; while this study used a moderate spatial resolution (250 m), a finer spatial scale may reveal micro-site differences (Tape et al., 2012; Reynolds et al., 2013). Factors not accounted for in the estimation of the expansion rate in this study and that may have an effect on it are the kind of plant community and type of shrubs. While in alpine plant communities deciduous shrubs concentrate in increasing cover, the Low Arctic plant community concentrates in vertical growth (Walker et al. 2006). There are also differences in the expansion rates between evergreen and deciduous shrubs. For example, Hudson and Henry (2009) found that in a High Arctic heath community, during the period 1981 to 2008, evergreen shrubs' cover increased, while deciduous shrub cover did not.

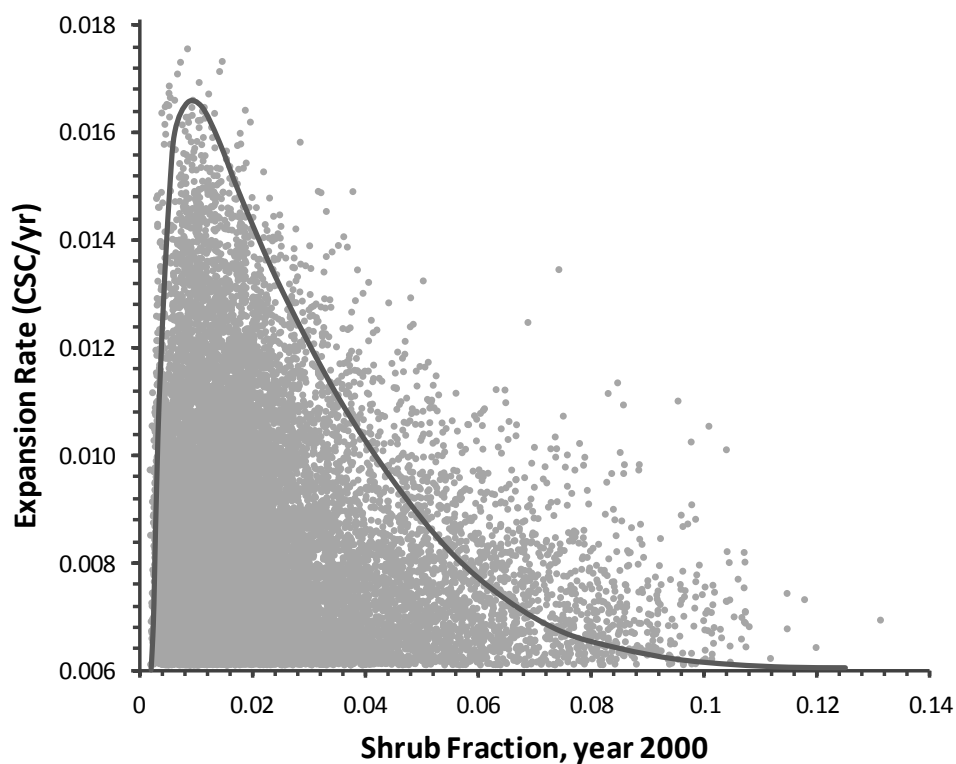


Figure 5-7. Tall shrub expansion rate against the initial fractional cover in year 2000.

The minimum initial fractional cover value necessary to see at least an increase greater than 0.06 in cover after a 10 year period was 0.001. It seems that tall shrubs tend to expand faster in areas where the initial shrub cover was very low, yet not zero. The fastest expansion rate was seen when the initial shrub cover was about 0.01, after which the expansion rate decreased rapidly. This may be due to the presence of large herbivores and the availability of more palatable food. Cahoon et al. (2012) found that the presence of large herbivores led to reductions in leaf-area index and net carbon dioxide uptake. He explained that the mechanism by which large herbivores like caribou and muskoxen reduce the shrub cover is by feeding on the leaves of deciduous shrubs early in the season. Their preference for grazing on freshly emergent leaves reduces the number of axillary and apical meristems in the shrub that would have provided canopy area (Cahoon et al., 2012).

5.4 Conclusion

As of 2010, tall shrub (> 0.5 m) fractional cover in the North Slope of Alaska was found to be very low at a spatial resolution of 250 m. Tall shrubs were more abundant in the floodplains, river terraces, and hill slopes, as well as on the tree-shrub transition zone along the northern boundary of the Brooks Range. Shrub cover considerably decreased northward, where harsh climatic conditions prevail. Comparisons of shrub cover between the years 2000 and 2010 revealed that the increase in shrub cover is not widespread but rather it is focused on a few landscape features. Areas where shrubs proliferated were located in the central and southern region of the North Slope, while there was no major

expansion in the High Arctic. The fastest expansion rate was experienced when shrub cover was about 0.01, after which the rate declined rapidly, which may indicate that when cover increases, abiotic and biotic factors may slow down the shrub expansion. Since the length of this study is relatively short (10 years), the results may reflect the influence of natural variations such as the Arctic Oscillation (time scale of 5-7 years). Thus, it would be necessary to continue extending the length of study period to include several Arctic Oscillation phases. This study focused only on shrubs taller than 0.5 m in height, which are often associated with riparian communities. However, shrubs less than 0.5 m, abundant in upland communities, are predicted to become increasingly dominant. Therefore, future work should aim to also quantify the magnitude and direction of the expansion of low shrub communities. In the face of climate change and the potential implications of a shrub expansion on the climate and ecology of the region, this study provided evidence of the site-specific tall shrub expansion and its rate in the North Slope during the period 2000-2010. Also, this study has demonstrated the efficacy of the MISR sensor to provide good coverage of the region considering the short window of time for data collection and it also has shown that machine learning algorithms, in particular, the boosted regression tree, are robust canopy models to predict tall shrub cover in spite of the low shrub cover values and low contrast between the target shrub population and background vegetation. More research is necessary to infer the potential impacts of canopy-forming shrubs on the regional climate and ecological processes in view of the findings in this study.

5.5 References

- Bhatt, U., Walker, D., Raynolds, M., Bieniek, P., Epstein, H., Comiso, J., . . . , & Polyakov, I. (2013). Recent declines in warming and vegetation greening trends over pan-Arctic tundra. *Remote Sensing*, 5(9), 4229–4254.
- Beck, P. S. A., Horning, N., Goetz, S. J., Loranty, M. M., & Tape, K. D. (2011). Shrub Cover on the North Slope of Alaska: a circa 2000 Baseline Map. *Arctic, Antarctic, and Alpine Research*, 43(3), 355–363.
- Cahoon, S. M., Sullivan, P. F., Post, E., & Welker, J. M. (2012). Large herbivores limit CO₂ uptake and suppress carbon cycle responses to warming in West Greenland. *Global Change Biology*, 18(2), 469-479.
- Chapin, F. S. (1983). Direct and indirect effects of temperature on arctic plants. *Polar Biology*, 2, 47-52.
- Chapin, F. S., Sturm, M., Serreze, M. C., McFadden, J. P., Key, J. R., Lloyd, A. H., . . . , & Welker, J. M. (2005). Role of land-surface changes in arctic summer warming. *Science (New York, N.Y.)*, 310(5748), 657–660.
- Duchesne, R.R., Chopping, M.J., & Tape, K.D. (2015). NACP woody vegetation characteristics of 1,039 sites across the North Slope, Alaska. Data set. Available online [<http://daac/ornl.gov/>] from Oak Ridge National Laboratory Distributed Active Archive Center, Oak Ridge, Tennessee, USA.
- Elith, J., & Leathwick, J. R. (2008). Tutorial for running boosted regression trees. [Appendix S3 of the article *A working guide to boosted regression trees*, by J. Elith, J. R. Leathwick, and T. Hastie]. *Journal of Animal Ecology*, 77(4), 1-15.

- Elmendorf, S. C., Henry, Gregory H. R., Hollister, R. D., Björk, R. G., Boulanger-Lapointe, N., Cooper, E. J., . . . , & Wipf, S. (2012). Plot-scale evidence of tundra vegetation change and links to recent summer warming. *Nature Climate Change*, 2(6), 453–457.
- Epstein, H. E., Beringer, J., Gould, W. A., Lloyd, A. H., Thompson, C. D., Chapin, F. S., . . . , & Walker, D. A. (2004). The nature of spatial transitions in the Arctic. *Journal of Biogeography*, 31(12), 1917–1933.
- Forbes, B. C., Fauria, M. M., & Zetterberg, P. (2010). Russian Arctic warming and ‘greening’ are closely tracked by tundra shrub willows. *Global Change Biology*, 16(5), 1542–1554.
- Furniss, M. M., Holsten, E. H., Foote, M. J., and Bertram, M. (2001). Biology of a willow leafblotch miner, *Micrurapteryx salicifoliella*, (Lepidoptera: Gracillariidae) in Alaska. *Environmental Entomology*, 30(4), 736–741.
- Griffith, B., Douglas, D. C., Walsh, N. E., Young, D. D., McCabe, T. R., Russell, D. E., White, R. G., Cameron, R. D., & Whitten, K. R. (2002). ‘The Porcupine caribou herd’, in Douglas, D. C., Reynolds, P. E. and Rhode, E. B. (eds.), *Arctic Refuge Coastal Plain Terrestrial Wildlife Research Summaries*, U. S. Geological Survey, Biological Resources Division, *Biological Science Report USGS/BRD BSR-2002-0001*, pp. 8–37.
- Higuera, P. E., Brubaker, L. B., Anderson, P. M., Brown, T. A., Kennedy, A. T., & Hu, F. S. (2008). Frequent fires in ancient shrub tundra: implications of paleorecords for arctic environmental change. *PloS one*, 3(3), e0001744.

- Hinzman, L. D., Bettez, N. D., Bolton, W. R., Chapin, F. S., Dyurgerov, M. B., Fastie, C. L., . . . , & Yoshikawa, K. (2005). Evidence and implications of recent climate change in northern Alaska and other Arctic regions. *Climatic Change*, 72(3), 251–298.
- Hudson, J. M. G., & Henry, G. H. R. (2009). Increased plant biomass in a High Arctic heath community from 1981 to 2008. *Ecology*, 90(10), 2657–2663.
- Jia, G. J., & Howard, E. E. (2003). Greening of arctic Alaska, 1981–2001. *Geophysical Research Letters*, 30(20).
- Lapenis, A., Shvidenko A., Shepaschenko, D., Nilsson S., & Aiyyer, A. (2005). Acclimation of Russian forest to recent changes in climate. *Global Change Biology*, 11, 2090-2102.
- Liston, G. E., Mcfadden, J. P., Sturm, M., & Pielke, R. A. (2002). Modelled changes in arctic tundra snow, energy and moisture fluxes due to increased shrubs. *Global Change Biology*, 8(1), 17–32.
- Macdonald, R. W., Harner, T., & Fyfe, J. (2005). Recent climate change in the Arctic and its impact on contaminant pathways and interpretation of temporal trend data. *The Science of the total environment*, 342(1-3), 5–86.
- McGuire, A. D., Chapin, F. S., Walsh, J. E., & Wirth, C. (2006). Integrated regional changes in Arctic climate feedbacks: implications for the global climate system. *Annual Review of Environment and Resources*, 31(1), 61–91.

- Myers-Smith, I. H., Forbes, B., Wilmking, M., Hallinger, M., Lantz, T., Blok, D., Tape, K., ..., & Hik, D.S. (2011). Shrub expansion in tundra ecosystems: dynamics, impacts, and research priorities. *Environmental Research Letters*, 6(4), 045509.
- Myneni, R. B., Keeling, C. D., Tucker, C. J., Asrar, G., & Nemani, R. R. (1997). Increased plant growth in the northern high latitudes from 1981 to 1991. *Nature*, 386(6626), 698–702.
- Naito, A. T., & Cairns, D. M. (2015). Patterns of shrub expansion in Alaskan arctic river corridors suggest phase transition. *Ecology and Evolution*, 5(1), 87–101.
- Nossov, D., Hollingsworth, T. N., Ruess, R. W., & Kielland, K. (2011). Development of *Alnus tenuifolia* stands on an Alaskan floodplain: patterns of recruitment, disease, and succession. *Journal of Ecology*, 99, 621-633.
- Pattison, R. R., Jorgenson, J. C., Reynolds, M. K., & Welker, J. M. (2015). Trends in NDVI and tundra community composition in the Arctic of NE Alaska between 1984 and 2009. *Ecosystems*, 18(4), 707–719.
- R Core Team. (2013). R: A language and environment for statistical computing. R Foundation for Statistical Computing. (Version 3.0.1) [Software]. Available from <http://www.R-project.org>.
- Reynolds, M. K., Walker, D. A., Verbyla, D., & Munger, C. A. (2013). Patterns of change within a tundra landscape: 22-year Landsat NDVI trends in an area of the northern Foothills of the Brooks Range, Alaska. *Arctic, Antarctic, and Alpine Research*, 45(2), 249–260.

- Ridgeway, G. (2006). Generalized boosted models: a guide to the gbm package.
Retrieved from <http://citeseerx.ist.psu.edu/viewdoc/summary?doi=10.1.1.113.9298>
- Ruess, R. W., Anderson, M. D., Mitchell, J. S., & McFarland, J. W. (2006). Effects of defoliation on growth and N fixation in *Alnus tenuifolia*: consequences for changing disturbance regimes at high latitudes. *Ecoscience*, 13(3), 404-412.
- Sellers, P. J. (1985). Vegetation-canopy spectral reflectance and biophysical processes. In G. Asrar (Ed.), *Theory and applications of optical remote sensing* (pp. 297– 335). New York: Wiley, Ch. 8.
- Selkowitz, D. J. (2010). A comparison of multi-spectral, multi-angular, and multi-temporal remote sensing datasets for fractional shrub canopy mapping in Arctic Alaska. *Remote Sensing of Environment*, 114(7), 1338–1352.
- Snyder, C., MacQuarrie, C. J. K., Zogas, K., Kruse, J.J., & Hard, J. (2007). Invasive species in the last frontier: distribution and phenology of birch leaf mining sawflies in Alaska. *Journal of Forestry*, 105(3), 113-119.
- Soja, A. J., Tchebakova, N. M., French, N. H.F., Flannigan, M. D., Shugart, H. H., Stocks, B. J., Sukhinin, A. I., Parfenova, E.I., Chapin III, F. S., & Stackhouse, Jr. P. W. (2007). Climate-induced boreal forest change: predictions versus current observations, *Global and Planetary Change*, 56(3–4), 274-296.
- Stow, D. A., Hope, A., McGuire, D., Verbyla, D., Gamon, J., Huemrich, F., ..., & Myneni, R. (2004). Remote sensing of vegetation and land-cover change in Arctic tundra ecosystems. *Remote Sensing of Environment*, 89(3), 281–308.

- Sturm, M., Racine, C., & Tape, K. (2001). Climate change: increasing shrub abundance in the Arctic. *Nature*, 411(6837), 546–547.
- Sturm, M., Schimel, J., Michaelson, G., Welker, J., Oberbauer, S. F., Liston, G. E. Fahnestock, J., & Romanovsky V. (2005). Winter biological processes could help convert Arctic tundra to shrubland. *Bioscience*, 55(1), 17-26.
- Suarez, F., Binkley, D., Kaye, M. W., & Stottlemyer R. (1999). Expansion of forest stands into tundra in the Noatak National Preserve, northwest Alaska. *Ecoscience*, 6, 465-470.
- Tape, K., Sturm, M., & Racine, C. (2006). The evidence for shrub expansion in northern Alaska and the Pan-Arctic. *Global Change Biology*, 12(4), 686–702.
- Tape, K. D., Hallinger, M., Welker J. M., & Ruess, R. (2012). Landscape heterogeneity of shrub expansion in Arctic Alaska. *Ecosystems*, 15(5), 711-724.
- Verbyla, D. (2008). The greening and browning of Alaska based on 1982–2003 satellite data. *Global Ecology and Biogeography*, 17(4), 547–555.
- Wanner, W., Li, X., & Strahler, A. H. (1995). On the derivation of kernels for kernel-driven models of bidirectional reflectance. *Journal of Geophysical Research*, 100(D10), 21077-21089.
- Walker, D.A., Jia, G.J, Epstein, H.E., Reynolds, M.K., Chapin, F.S., III, Copass, C., Hinzman, L.D., Kane, D., Knudson, J.A., Maier, H., Michaelson, G.J., Nelson, F., Ping, C.L., Romanovsky, V.E., Shiklomanov, N. & Shur, Y. (2003).Vegetation-soil-thaw depth relationships along a Low-Arctic bioclimate gradient, Alaska: synthesis of

information from the ATLAS studies. *Permafrost and Periglacial Processes*, 14, 103–123.

Walker, M. D., Wahren, C. H., Hollister, R. D., Henry, G. H. R., Ahlquist, L. E., Alatalo, J. M., ..., & Wookey, P.A. (2006). Plant community responses to experimental warming across the tundra biome. *Proceedings of the National Academy of Science (USA)*, 103: 1342-1346.

Wingfield, J. C., Owen-Ashley, N. T., Benowitz-Fredericks, Z. M., Lynn, S. E., Hahn, T. P., Wada, H., Breuner, C. M., Meddle, S. L. & Romero, L. M. (2004). Arctic spring: the arrival biology of migrant birds. *Acta Zool. Sin.* 50, 948–60.

REFERENCES

- Adams, J.M., Faure, H., Faure-Denard, L., Mcglade, J.M., & Woodward, F.L. (1990). Increases in terrestrial carbon storage from the Last Glacial Maximum to the present. *Nature*, 348, 711-714.
- Arctic Climate Impact Assessment (ACIA). (2004). Scientific Report. Cambridge University Press. 1020p
- Anderson, P. M., Bartlein, P. J., & Brubaker, L. B. (1994). Late quaternary history of tundra vegetation in northwestern Alaska. *Quaternary Research*, 41(3), 306–315.
- Asner, G. P., & Heidebrecht, K. B. (2002). Spectral unmixing of vegetation, soil and dry carbon cover in arid regions: comparing multispectral and hyperspectral observations. *International Journal of Remote Sensing*, 23(19), 3939-3958.
- Bhatt, U., Walker, D., Raynolds, M., Bieniek, P., Epstein, H., Comiso, J., . . . , & Polyakov, I. (2013). Recent declines in warming and vegetation greening trends over pan-Arctic tundra. *Remote Sensing*, 5(9), 4229–4254.
- Beck, P. S. A., Horning, N., Goetz, S. J., Loranty, M. M., & Tape, K. D. (2011). Shrub cover on the North Slope of Alaska: a circa 2000 baseline map. *Arctic, Antarctic, and Alpine Research*, 43(3), 355–363.
- Berner, L. T., Alexander, H. D., Loranty, M. M., Ganzlin, P., Mack, M., Davydov, S. P., & Goetz, S. J. (2015). Biomass allometry for alder, dwarf birch, and willow in boreal forest and tundra ecosystems of far northeastern Siberia and north-central Alaska. *Forest Ecology and Management*, 337, 110-118.

- Bi, J., Xu, L., Samanta, A., Zhu, Z., & Myneni, R. (2013). Divergent Arctic-Boreal vegetation changes between North America and Eurasia over the past 30 years. *Remote Sensing*, 5(5), 2093–2112.
- Blok, D., Schaepman-Strub, G., Bartholomeus, H., Heijmans, M. M. P. D., Maximov, T., & Berendse, F. (2011). The response of Arctic vegetation to the summer climate: relation between shrub cover, NDVI, surface albedo, and temperature. *Environmental Research Letters*, 6(3), 035502.
- Boelman, N. T., Gough, L., McLaren, J. R., & Greaves, H. (2011). Does NDVI reflect variation in the structural attributes associated with increasing shrub dominance in arctic tundra? *Environmental Research Letters*, 6(3), 35501.
- Bonan, G. B., Pollard, D., & Thompson, S. L. (1992). Effects of boreal forest vegetation on global climate. *Nature*, 359, 716-718.
- Breiman, L. (2001). Statistical modeling: the two cultures. *Statistical Science*, 16, 199–215.
- Bubier, J., Rock, B., & Crill, P. (1997). Spectral reflectance of boreal wetland and forest mosses. *Journal of Geophysical Research*, 102(D24), 29483-29494.
- Cahoon, S. M., Sullivan, P. F., Post, E., & Welker, J. M. (2012). Large herbivores limit CO₂ uptake and suppress carbon cycle responses to warming in West Greenland. *Global Change Biology*, 18(2), 469-479.
- CAVM Team. (2003). Circumpolar Arctic Vegetation Map. (1:7,500,000 scale), Conservation of Arctic Flora and Fauna (CAFF) Map No. 1. U.S. Fish and Wildlife Service, Anchorage, Alaska. ISBN: 0-9767525-0-6.

- Chapin, F. S. (1983). Direct and indirect effects of temperature on arctic plants. *Polar Biology*, 2, 47-52.
- Chapin, F. S., Shaver, G. R., Giblin, A. E., Nadelhoffer, K. J., & Laundre, J. A. (1995). Responses of Arctic tundra to experimental and observed changes in climate. *Ecology*, 76(3), 694.
- Chapin, F. S. III., Eugster, W., McFadden, J. P., Lynch, A. H., & Walter, D. A. (2000). Summer differences among Arctic ecosystems in regional climate forcing. *J. Climate*, 13, 2002-2010.
- Chapin, F. S., Sturm, M., Serreze, M. C., McFadden, J. P., Key, J. R., Lloyd, A. H., . . . , & Welker, J. M. (2005). Role of land-surface changes in arctic summer warming. *Science (New York, N.Y.)*, 310(5748), 657–660.
- Chapman, W.L., & Walsh, J.E. (1993). Recent variations of sea ice and air temperatures in high latitudes. *Bulletin American Meteorological Society*, 74: 33-47.
- Chen, J. M., Liu, J., Leblanc, S. G., Lacaze, R., & Roujean, J-L. (2003). Multi-angular optical remote sensing for assessing vegetation structure and carbon absorption. *Remote Sensing of Environment*, 84(4), 516–525.
- Chopping, M.J., Rango, A., Havstad, K.M., Schiebe, F., Ritchie, J., Schmutge, T., ... & Davis, M.R. (2003). Canopy attributes of desert grassland and transition communities derived from multiangular airborne imagery. *Remote Sensing of Environment*, 85: 339-354.

- Chopping, M. J., Su, L., Laliberte, A., Rango, A., Peters, D. P. C., & Martonchik, J. V. (2006). Mapping woody plant cover in desert grasslands using canopy reflectance modeling and MISR data. *Geophysical Research Letters*, 33, L17402.
- Chopping, M., Su, L., Kollikkathara, N., & Urena, L. (2007). Advances in mapping woody plant canopies using the NASA's MISR instrument on Terra. Proceedings *IEEE International Geoscience and Remote Sensing Symposium*. Barcelona, Spain.
- Chopping, M., Moisen, G., Su, L., Laliberte, A., Rango, A., Martonchik, J., & Peters, D. (2008). Large area mapping of southwestern forest crown cover, canopy height, and biomass using MISR. *Remote Sensing of Environment*, 112, 2051-2063.
- Chopping, M. (2011). CANAPI: canopy analysis with panchromatic imagery. *Remote Sensing Letters*, 2(1), 21-29.
- Chopping, M., North, M., Chen, J., Schaaf, C. B., Blair, J. B., Martonchik, J. V., & Bull, M. A. (2012). Forest canopy cover and height from MISR in topographically complex southwestern US landscapes assessed with high quality reference data. *IEEE Journal of Selected Topics in Applied Earth Observations and Remote Sensing*, 5(1), 44-58.
- De'Ath, G. (2007). Boosted trees for ecological modeling and prediction. *Ecology*, 88(1), 243-251.
- Diner, D. J., Asner, G. P., Davies, R., Knyazikhin, Y., Muller, J. P., Nolin, A. W., Pinty, B., Schaaf, C., & Stroeve, J. (1999). New directions in Earth observing: scientific applications of multi-angle remote sensing. *Bulletin of the American Meteorological Society*, 80 (11), 2209-2229.

- Duchesne, R.R., Chopping, M.J., & Tape, K.D. (2015). NACP woody vegetation characteristics of 1,039 sites across the North Slope, Alaska. Data set. Available online [<http://daac/ornl.gov/>] from Oak Ridge National Laboratory Distributed Active Archive Center, Oak Ridge, Tennessee, USA.
- Duchesne, R.R., Chopping, M.J., & Tape, K.D. (2015). Capability of the CANAPI algorithm to derive shrub structural parameters from satellite imagery in the Alaskan Arctic. *Polar Record*. [In press].
- Elith, J., Leathwick, J. R., & Hastie, T. (2008). A working guide to boosted regression trees. *Journal of Animal Ecology*, 77(4), 802–813.
- Elith, J., & Leathwick, J. R. (2008). Tutorial for running boosted regression trees. [Appendix S3 of the article *A working guide to boosted regression trees*, by J. Elith, J. R. Leathwick, and T. Hastie]. *Journal of Animal Ecology*, 77(4), 1-15.
- Elmendorf, S. C., Henry, Gregory H. R., Hollister, R. D., Björk, R. G., Boulanger-Lapointe, N., Cooper, E. J., . . . , & Wipf, S. (2012). Plot-scale evidence of tundra vegetation change and links to recent summer warming. *Nature Climate Change*, 2(6), 453–457.
- Elmhagen, B., Kindberg, J., & Hellstrom, P. (2015). A boreal invasion in response to climate change? Range shifts and community effects in the borderland between forest and tundra. *AMBIO*, 44(1), 39-50.
- Elzinga, C.L., Salzer, D.W., & Willoughby, J. W. (1998). Measuring and monitoring plant populations. BLM Technical Reference 1730-1.

- Epstein, H. E., Beringer, J., Gould, W. A., Lloyd, A. H., Thompson, C. D., Chapin, F. S., . . ., & Walker, D. A. (2004). The nature of spatial transitions in the Arctic. *Journal of Biogeography*, 31(12), 1917–1933.
- Euskirchen, E. S., McGuire, A. D., Chapin, F. S. III, Yi, S., & Thompson, C. C. (2009). Changes in vegetation in northern Alaska under scenarios of climate change, 2003-2100: Implications for Climate Feedbacks. *Ecological Applications*, 19(4), 1022-1043.
- Fahnestock, J.T., Jones, M.H., Brooks, P.D., Walker, D. A., & Welker, J.M. (1998). Winter and early spring CO₂ flux from tundra communities of northern Alaska. *Journal of Geophysical Research*, 102, 29925-29931.
- Forbes, B. C., Fauria, M. M., & Zetterberg, P. (2010). Russian Arctic warming and ‘greening’ are closely tracked by tundra shrub willows. *Global Change Biology*, 16(5), 1542–1554.
- Friedman, J.H., Hastie, T., & Tibshirani, R. (2000). Additive logistic regression: a statistical view of boosting. *Annals of Statistics*, 28, 337–407.
- Furniss, M. M., Holsten, E. H., Foote, M. J., and Bertram, M. (2001). Biology of a willow leafblotch miner, *Micrurapteryx salicifoliella*, (Lepidoptera: Gracillariidae) in Alaska. *Environmental Entomology*, 30(4), 736–741.
- Gamon, J. A., Huemmrich, K. F., Stone, R. S., & Tweedie, C. E. (2013). Spatial and temporal variation in primary productivity (NDVI) of coastal Alaskan tundra: Decreased vegetation growth following earlier snowmelt. *Remote Sensing of Environment*, 129, 144–153.

- Glenn, E., Huete, A., Nagler, P., & Nelson, S. G. (2008). Relationship between remotely sensed vegetation indices, canopy attributes and plant physiological processes: what vegetation indices can and cannot tell us about the landscape. *Sensors*, 8, 2136-2160.
- Griffith, B., Douglas, D. C., Walsh, N. E., Young, D. D., McCabe, T. R., Russell, D. E., White, R. G., Cameron, R. D., & Whitten, K. R. (2002). 'The Porcupine caribou herd', in Douglas, D. C., Reynolds, P. E. and Rhode, E. B. (eds.), *Arctic Refuge Coastal Plain Terrestrial Wildlife Research Summaries, U. S. Geological Survey, Biological Resources Division, Biological Science Report USGS/BRD BSR-2002-0001*, pp. 8–37.
- Hill D., Fasham M., Tucker G., Shewry M., & Shaw P. (Eds.). (2005). *Handbook of Biodiversity Methods: Survey, Evaluation, and Monitoring*. New York, NY: Cambridge University Press.
- Higuera, P. E., Brubaker, L. B., Anderson, P. M., Brown, T. A., Kennedy, A. T., & Hu, F. S. (2008). Frequent fires in ancient shrub tundra: implications of paleorecords for arctic environmental change. *PloS one*, 3(3), e0001744.
- Hinzman, L. D., Kane, D. L., Benson, C. S., & Everett, K. R. (1996). Energy balance and hydrological processes in an Arctic watershed. Vol. 120. *Ecologica Studies*. Reynolds, J.F. & Tenhunen, J.D. Eds., Springer-Verlag, 131-154.
- Hinzman, L. D., Bettez, N. D., Bolton, W. R., Chapin, F. S., Dyurgerov, M. B., Fastie, C. L., . . . , & Yoshikawa, K. (2005). Evidence and implications of recent climate change in northern Alaska and other Arctic regions. *Climatic Change*, 72(3), 251–298.

- Hope, A., & Stow, D. (1995). Shortwave reflectance properties of Arctic tundra. In Reynolds J. and Tenhunen J. (Eds.), *Landscape function and disturbance in Arctic tundra*. Ecological Studies 120: 155– 164. Heidelberg: Springer.
- Hopkinson, C., Chasmer, L. E., Sass, G., Creed, I. F., Sitar, M., Kalbfleisch, W., & Treitz, P. (2005). Vegetation class dependent errors in lidar ground elevation and canopy height estimates in a boreal wetland environment. *Canadian Journal of Remote Sensing*, 31(2), 191-206.
- Hudson, J. M. G., & Henry, G. H. R. (2009). Increased plant biomass in a High Arctic heath community from 1981 to 2008. *Ecology*, 90(10), 2657–2663.
- Huemmrich, K., Gamon, J. A., Tweedie, C. E., Oberbauer, S. F., Kinoshita, G., Houston, S., . . . , & Mano, M. (2010). Remote sensing of tundra gross ecosystem productivity and light use efficiency under varying temperature and moisture conditions. *Remote Sensing of Environment*, 114(3), 481–489.
- Intergovernmental Panel on Climate Change. (2014). *Climate change 2013: the physical science basis: working group I contribution. IPCC Fifth Assessment Report*. Cambridge: Cambridge University Press.
- Jia, G. J., & Howard, E. E. (2003). Greening of arctic Alaska, 1981–2001. *Geophysical Research Letters*, 30(20).
- Kasischke, E. S., Goetz, S. J., Kimball, J. S., & Mack, M. M. (2010). *The Arctic-Boreal Vulnerability Experiment (ABoVE): A concise plan for a NASA-sponsored field campaign. Final Report on the VuRSAL/ABoVE Scoping Study*.

- Lacaze, R., Chen, J.M., Roujean, J.L., & Leblanc, S.G. (2002). Retrieval of vegetation clumping index using hotspot signatures measured by POLDER instrument. *Remote Sensing of Environment*, 79(1), 84-95.
- Lapenis, A., Shvidenko A., Shepaschenko, D., Nilsson S., & Aiyyer, A. (2005). Acclimation of Russian forest to recent changes in climate. *Global Change Biology*, 11, 2090-2102.
- Leathwick, J.R., Elith, J., Francis, M.P., Hastie, T., & Taylor, P. (2006). Variation in demersal fish species richness in the oceans surrounding New Zealand: an analysis using boosted regression trees. *Marine Ecology Progress Series*, 321, 267–281.
- Li, X., & Strahler, A. H. (1992). Geometric-optical bidirectional reflectance modeling of the discrete crown vegetation canopy: Effect of crown shape and mutual shadowing. *IEEE Transactions on Geoscience and Remote Sensing*, 30, 276-292.
- Liston, G. E., Mcfadden, J. P., Sturm, M., & Pielke, R. A. (2002). Modelled changes in arctic tundra snow, energy and moisture fluxes due to increased shrubs. *Global Change Biology*, 8(1), 17–32.
- Lloyd, A., Rupp, T., Fastie, C., & Starfield, A. (2003). Patterns and dynamics of treeline advance in the Seward Peninsula, Alaska. *Journal of Geophysical Research*, 108(8161).
- Macdonald, R. W., Harner, T., & Fyfe, J. (2005). Recent climate change in the Arctic and its impact on contaminant pathways and interpretation of temporal trend data. *The Science of the total environment*, 342(1-3), 5–86.

- Mack, M.C., Bret-Harte, M.S., Hollingsworth, T. N., Jandt, R. R., Shuur, E. A. G., Shaver, G. R., & Verbyla, D. L. (2011). Carbon loss from an unprecedented Arctic tundra wildfire. *Nature*, 475, 489-492.
- Martonchik, J.V., Diner, D.J., Pinty, B., Verstraete, M.M., Myneni, R.B., Knyazikhin, Y., & Gordon, H.R. (1998). Determination of land and ocean reflective, radiative, and biophysical properties using multiangle imaging. *IEEE Transactions on Geoscience and Remote Sensing*, 36, 1266–1281.
- Matveyeva, N. & Chernov, Y. (2000). Biodiversity of terrestrial ecosystems. In: M. Nuttall and T.V. Callaghan (eds.). *The Arctic: Environment, People, Policy*, pp. 233–274. Harwood Academic Publishers.
- McGuire, A. D., Chapin, F. S., Walsh, J. E., & Wirth, C. (2006). Integrated regional changes in Arctic climate feedbacks: implications for the global climate system *Annual Review of Environment and Resources*, 31(1), 61–91.
- McManus, K. M., Morton, D. C., Masek, J. G., Wang, D., Sexton, J. O., Nagol, J. R., Ropars, P. & Boudreau, S. (2012). Satellite-based evidence for shrub and graminoid tundra expansion in northern Quebec from 1986 to 2010. *Global Change Biology*, 18, 2313–2323.
- Meyer T., & Okin G. S. (2015). Evaluation of spectral unmixing techniques using MODIS in a structural complex savanna environment for retrieval of green vegetation, non photosynthetic vegetation, and soil fractional cover. *Remote Sensing of Environment*, 161, 122-130.

- Muller, S. V., Racoviteanu, A. E., & Walker, D. A. (1999). Landsat MSS-derived land-cover map of northern Alaska: Extrapolation methods and a comparison with photointerpreted and AVHRR-derived maps. *International Journal of Remote Sensing*, 20, 2921–2946.
- Myers-Smith, I. H., Forbes, B., Wilmking, M., Hallinger, M., Lantz, T., Blok, D., Tape K., ..., & Hik, D.S. (2011). Shrub expansion in tundra ecosystems: dynamics, impacts, and research priorities. *Environmental Research Letters*, 6(4), 045509.
- Myneni, R. B., Keeling, C. D., Tucker, C. J., Asrar, G., & Nemani, R. R. (1997). Increased plant growth in the northern high latitudes from 1981 to 1991. *Nature*, 386(6626), 698–702.
- Naito, A. T., & Cairns, D. M. (2015). Patterns of shrub expansion in Alaskan arctic river corridors suggest phase transition. *Ecology and Evolution*, 5(1), 87–101.
- NASA Land Processes Distributed Active Archive Center (LP DAAC). (2001). MODIS Land Cover Type Product. USGS/Earth Resources Observation and Science (EROS) Center, Sioux Falls, South Dakota. Retrieved on April 2015 from https://lpdaac.usgs.gov/products/modis_products_table/mcd12q1.
- Nicodemus, F. E., Richmond, J. C., Hsia, J. J., Ginsberg, I. W., & Limperis, T. (1977). Geometrical considerations and nomenclature for reflectance. *U.S.A. Department of Commerce/ National Bureau of Standards, NBS Monogr.*, No. 160, 1-52.
- Nolin, A. (2004). Towards retrieval of forest cover density over snow from the Multi-angle Imaging SpectroRadiometer (MISR). *Hydrological Processes*, 18(18), 3623 – 3636.

- Nossov, D., Hollingsworth, T. N., Ruess, R. W., & Kielland, K. (2011). Development of *Alnus tenuifolia* stands on an Alaskan floodplain: patterns of recruitment, disease, and succession. *Journal of Ecology*, 99, 621-633.
- Oke, T.R. (1987). *Boundary layer climates*. Methuen, London, UK.
- Overpeck, J., Hughen, K., Hardy, D., Bradley, R., Case, R., Douglas, M., . . . , & Zielinski, G. (1997). Arctic environmental change of the last four centuries. *Science*, 278, 1251-1256.
- Pattison, R. R., Jorgenson, J. C., Raynolds, M. K., & Welker, J. M. (2015). Trends in NDVI and tundra community composition in the Arctic of NE Alaska between 1984 and 2009. *Ecosystems*, 18(4), 707–719.
- Popescu, S. C., Zhao, K., Neuenschwander, A., & Lin, C. (2011). Satellite lidar vs. small footprint airborne lidar: comparing the accuracy of aboveground biomass estimates and forest structure metrics at footprint level. *Remote Sensing of Environment*, 115, 2786-2797.
- Post, W. M., Emanuel, W.R., Zinke, P.J., & Stangenberger, A.J. (1982). Soil carbon pools and world life zones. *Nature*, 298, 156-159.
- R Core Team. (2013). *R: A language and environment for statistical computing*. R Foundation for Statistical Computing. (Version 3.0.1) [Software]. Available from <http://www.R-project.org>.
- Raynolds, M. K., Walker, D. A., Verbyla, D., & Munger, C. A. (2013). Patterns of change within a tundra landscape: 22-year Landsat NDVI trends in an area of the

- northern Foothills of the Brooks Range, Alaska. *Arctic, Antarctic, and Alpine Research*, 45(2), 249–260.
- Read, C., Duncan, D., Vesk, P., & Elith, J. (2011). Surprisingly fast recover of biological soil crusts following livestock removal in southern Australia. *Journal of Vegetation Science*, 22, 905-916.
- Ridgeway, G. (2006). Generalized boosted models: a guide to the gbm package. Retrieved from <http://citeseerx.ist.psu.edu/viewdoc/summary?doi=10.1.1.113.9298>
- Romanovsky, V. E. & Osterkamp, T. E. (2000). Effects of unfrozen water on heat and mass transport processes in the active layer and permafrost. *Permafrost Periglacial Process*, 11, 219–239.
- Rosette, J.A.B., North, P. R. J., & Suarez, J. C. (2008). Vegetation height estimates for a mixed temperate forest using satellite laser altimetry. *International Journal of Remote Sensing*, 29(5), 1475-1493.
- Roujean, J., Leroy, M., & Deschamps, P. (1992). A bidirectional reflectance model of the Earth's surface for the correction of remote sensing data. *Journal of Geophysical Research*, 97(D18), 20455-20468.
- Ruess, R. W., Anderson, M. D., Mitchell, J. S., & McFarland, J. W. (2006). Effects of defoliation on growth and N fixation in *Alnus tenuifolia*: Consequences for changing disturbance regimes at high latitudes. *Ecoscience*, 13(3), 404-412.
- Selkowitz, D. (2010). A comparison of multi-spectral, multi-angular, and multi-temporal remote sensing datasets for fractional shrub canopy mapping in Arctic Alaska. *Remote Sensing of Environment*, 114 (2010), 1338–1352.

- Sellers, P.J. (1985). Vegetation-canopy spectral reflectance and biophysical processes. In: Asrar G. (Ed.), *Theory and Applications of Optical Remote Sensing* (p 297-335). New York: Wiley, Ch. 8
- Silapaswan, C.S., Verbyla, D.L., & McGuire, A.D (2001). Land cover change on the Seward Peninsula: the use of remote sensing to evaluate the potential influences of climate warming on historical vegetation dynamics. *Canadian Journal of Remote Sensing*, 27, 542-554.
- Snyder, C., MacQuarrie, C. J. K., Zogas, K., Kruse, J.J., & Hard, J. (2007). Invasive species in the last frontier: distribution and phenology of birch leaf mining sawflies in Alaska. *Journal of Forestry*, 105(3), 113-119.
- Soja, A. J., Tchebakova, N. M., French, N. H.F., Flannigan, M. D., Shugart, H. H., Stocks, B. J., Sukhinin, A. I., Parfenova, E.I., Chapin III, F. S., & Stackhouse, Jr. P. W. (2007). Climate-induced boreal forest change: predictions versus current observations, *Global and Planetary Change*, 56(3–4), 274-296.
- Stow, D., Daeschner, S., Hope, A., Douglas, D., Petersen, A., Myneni, R., Zhou, L., & Oechel, W. (2003). Variability of the seasonally integrated normalized difference vegetation index across the North Slope of Alaska in the 1990s. *International Journal of Remote Sensing*, 24(5), 1111 – 1117.
- Stow, D., Hope, A., McGuire, D., Verbyla, D., Gamon, J., Huemrich, F., . . . , & Myneni, R. (2004). Remote sensing of vegetation and land-cover change in Arctic tundra ecosystems. *Remote Sensing of Environment*, 89, 281–308.

- Strahler, A., Jupp, D., Woodcock, C., & Li, X. (2005). The discrete-object scene model and its application in remote sensing. *Proceedings 9th International Symposium on Physical Measurements and Signatures in Remote Sensing*, 1, 166 -168.
- Streutker, D., & Glenn, N. F. (2006). LiDAR measurement of sagebrush steppe vegetation height. *Remote Sensing of Environment*, 102(1-2), 135-145.
- Sturm, M., McFadden, J., Liston, G., Chapin, S. III., Racine, C., & Holmgren, J. (2001a). Snow-shrub interactions in Arctic tundra: a hypothesis with climatic implications. *Journal of Climate*, 14(3), 336–344.
- Sturm, M., Racine, C., & Tape, K. (2001b). Climate change: increasing shrub abundance in the Arctic. *Nature*, 411(6837), 546–547.
- Sturm, M., Douglas, T., Racine, R., & Liston, G. (2005). Changing snow and shrub conditions affect albedo with global implications. *Journal of Geophysical Research*, 110(G01004.), 1–13.
- Suarez, F., Binkley, D., Kaye, M. W., & Stottlemeyer R. (1999). Expansion of forest stands into tundra in the Noatak National Preserve, northwest Alaska. *Ecoscience*, 6, 465-470.
- Tape, K., Sturm, M., & Racine, C. (2006). The evidence for shrub expansion in Northern Alaska and the Pan-Arctic. *Global Change Biology*, 12(4), 686–702.
- Tape, K. D., Hallinger, M., Welker, J. M., & Ruess, R. (2012). Landscape heterogeneity of shrub expansion in Arctic Alaska. *Ecosystems*, 15(5), 711-724.
- Tazik, D., Warren, S., Diersing, V., Shaw, R., Brozka, R., Bagley, C., & Whitworth, W. (1992). U.S. Army Land Condition-Trend Analysis (LCTA) Plot Inventory Field

- Methods. Champaign, IL. US Army Corps of Engineers: Construction Engineering Research Laboratory Technical Report N-92/03.
- U.S. Geological Survey. (2001). NLCD 2001 Land cover Alaska - National Geospatial Data Asset (NGDA) Land Use Land Cover. Edition 1.0.
- Verbyla, D. (2008). The greening and browning of Alaska based on 1982–2003 satellite data. *Global Ecology and Biogeography*, 17(4), 547–555
- Vierling, L., Deering, D., & Eck, T. (1997). Differences in Arctic tundra type and phenology as seen using bidirectional radiometry in the early growing season. *Remote Sensing of Environment*, 60(1), 71-82.
- Walker, D.A., Jia, G.J, Epstein, H.E., Raynolds, M.K., Chapin, F.S., III, Copass, C., Hinzman, L.D., Kane, D., Knudson, J.A., Maier, H., Michaelson, G.J., Nelson, F., Ping, C.L., Romanovsky, V.E., Shiklomanov, N. & Shur, Y. (2003).Vegetation-soil-thaw depth relationships along a Low-Arctic bioclimate gradient, Alaska: synthesis of information from the ATLAS studies. *Permafrost and Periglacial Processes*, 14, 103–123.
- Walker, M. D., Wahren, C. H., Hollister, R. D., Henry, G. H. R., Ahlquist, L. E., Alatalo, J. M., ..., & Wookey, P.A. (2006). Plant community responses to experimental warming across the tundra biome. *Proceedings of the National Academy of Science (USA)*, 103, 1342-1346.
- Wanner, W., Li, X., & Strahler, A. H. (1995). On the derivation of kernels for kernel-driven models of bidirectional reflectance. *Journal of Geophysical Research*, 100(D10), 21077-21089.

- Wanner, W., Strahler, A. H., Hu, B., Lewis, P., Muller, J. P., Li, X., Schaaf, C. L. B., & Barnsley, M. J. (1997). Global retrieval of bidirectional reflectance and albedo over land from EOS MODIS and MISR data: theory and algorithm. *Journal of Geophysical Research*, 102(D14), 17143-17161.
- Wingfield, J. C., Owen-Ashley, N. T., Benowitz-Fredericks, Z. M., Lynn, S. E., Hahn, T. P., Wada, H., Breuner, C. M., Meddle, S. L. & Romero, L. M. (2004). Arctic spring: the arrival biology of migrant birds. *Acta Zool. Sin.*, 50, 948–60.
- Wofsy, S. C., & Harriss, R. C. (2002). The North American Carbon Program (NACP). Report of the NACP Committee of the US Interagency Carbon Cycle Science Program. US Global Change Research Program, Washington, DC, 59.
- Zhou, L., Tucker, C. J., Kaufmann, R. K., Slayback, D., Shabanov, N. V., & Myneni, R. B. (2001). Variations in northern vegetation activity inferred from satellite data of vegetation index during 1981 to 1999. *Journal of Geophysical Research*, 106, 20069– 20083.

LIST OF APPENDICES

Appendix A: Projection parameters for Chapter 1

Appendix B: Reference Database for Chapter 2

Appendix C: Downloaded MISR data for Chapter 3

Appendix D: Downloaded MISR data for Chapter 4

Appendix E: Downloaded MISR data for Chapter 5

Appendix F: Preface

Appendix A

A.1. Parameters of the Albers Conical Equal Area projection used for field sites as well as for all imagery and map products. Units: meters.

Projection Type	Albers Conical Equal Area
Spheroid Name	WGS 84
Datum Name	WGS 84
Latitude of 1st Standard Parallel	55 N
Latitude of 2nd Standard Parallel	65 N
Longitude of Central Meridian	154 W
Latitude of Origin of Projection	50 N
False Easting at Central Meridian	0.0 meters
False Northing at Origin	0.0 meters

Appendix B

B.1. Shrub structural parameters collected during field campaign along the Colville River in 2010. The column headers mean: *Site*, field site surveyed; *Sp_genus*, species genus; *X* and *Y*, the coordinate location of the shrub in UTM, Zone 5N.

Site	Sp_genus	Canopy_height (m)	Crown_radius (m)	X (m)	Y (m)
Colville-01	<i>Alnus sp.</i>	1.32	0.73	558010	7729420
Colville-01	<i>Alnus sp.</i>	1.34	1.05	558010	7729420
Colville-01	<i>Alnus sp.</i>	1.27	0.7	558022	7729439
Colville-01	<i>Alnus sp.</i>	1.18	1.35	558055	7729407
Colville-01	<i>Alnus sp.</i>	1.42	1.02	558043	7729464
Colville-01	<i>Alnus sp.</i>	1.07	2.3	558048	7729455
Colville-01	<i>Alnus sp.</i>	1.3	0.84	558099	7729300
Colville-01	<i>Alnus sp.</i>	1.19	1.11	557971	7729273
Colville-01	<i>Alnus sp.</i>	1.18	0.94	557974	7729280
Colville-01	<i>Alnus sp.</i>	1.51	1.12	557978	7729289
Colville-01	<i>Alnus sp.</i>	1.37	0.75	557965	7729298
Colville-01	<i>Alnus sp.</i>	1.52	1.74	557968	7729348
Colville-01	<i>Alnus sp.</i>	1.15	1.31	557929	7729335
Colville-01	<i>Alnus sp.</i>	1.15	0.78	557929	7729335
Colville-01	<i>Alnus sp.</i>	1	1.46	557922	7729316
Colville-01	<i>Alnus sp.</i>	0.96	1.07	557941	7729315
Colville-01	<i>Alnus sp.</i>	0.94	1.01	557937	7729306
Colville-01	<i>Alnus sp.</i>	1.08	1.28	557937	7729292
Colville-02	<i>Alnus sp.</i>	2.03	1.37	562042	7726370
Colville-02	<i>Alnus sp.</i>	1.78	1.36	562103	7726386
Colville-02	<i>Alnus sp.</i>	1.6	1.27	562182	7726371
Colville-02	<i>Alnus sp.</i>	1.9	2.42	562195	7726375
Colville-02	<i>Alnus sp.</i>	2.37	2.07	562220	7726379
Colville-02	<i>Salix sp.</i>	0.82	2.23	562245	7726374
Colville-02	<i>Salix sp.</i>	1.32	0.54	562234	7726400

Site	Sp_genus	Canopy_height (m)	Crown_radius (m)	X (m)	Y (m)
Colville-02	<i>Alnus sp.</i>	1.8	0.62	562225	7726402
Colville-02	<i>Alnus sp.</i>	2.41	1.65	562205	7726405
Colville-02	<i>Alnus sp.</i>	1.67	2.8	562185	7726402
Colville-02	<i>Alnus sp.</i>	1.41	0.7	562173	7726401
Colville-02	<i>Alnus sp.</i>	1.42	1.38	562165	7726400
Colville-02	<i>Alnus sp.</i>	1.26	1.68	562159	7726399
Colville-02	<i>Alnus sp.</i>	1.2	1.49	562127	7726398
Colville-02	<i>Alnus sp.</i>	2.27	2.3	562077	7726392
Colville-02	<i>Alnus sp.</i>	1.54	0.99	562042	7726391
Colville-02	<i>Alnus sp.</i>	2.27	1.42	562030	7726392
Colville-02	<i>Alnus sp.</i>	1.48	0.46	562020	7726389
Colville-02	<i>Alnus sp.</i>	1.81	1.57	561995	7726427
Colville-02	<i>Alnus sp.</i>	2.4	0.76	562000	7726429
Colville-02	<i>Alnus sp.</i>	1.37	0.48	562006	7726432
Colville-02	<i>Alnus sp.</i>	1.19	0.44	562054	7726438
Colville-02	<i>Alnus sp.</i>	2.03	1.04	562075	7726443
Colville-02	<i>Alnus sp.</i>	1.42	0.53	562085	7726443
Colville-02	<i>Alnus sp.</i>	2	2.01	562093	7726444
Colville-02	<i>Alnus sp.</i>	1.34	0.99	562097	7726445
Colville-02	<i>Alnus sp.</i>	0.79	1.41	562105	7726445
Colville-02	<i>Alnus sp.</i>	1.88	1.62	562111	7726441
Colville-02	<i>Alnus sp.</i>	1.88	0.64	562130	7726435
Colville-02	<i>Alnus sp.</i>	1.96	0.81	562130	7726435
Colville-02	<i>Alnus sp.</i>	1.51	1.56	562151	7726431
Colville-02	<i>Alnus sp.</i>	1.78	0.63	562195	7726431
Colville-02	<i>Alnus sp.</i>	1.11	0.64	562230	7726429
Colville-02	<i>Alnus sp.</i>	2.34	1.7	562241	7726427
Colville-02	<i>Alnus sp.</i>	1.51	0.79	562241	7726427
Colville-02	<i>Alnus sp.</i>	1.73	1.25	562243	7726446
Colville-02	<i>Alnus sp.</i>	1.99	1.25	562235	7726448
Colville-02	<i>Alnus sp.</i>	1.73	0.81	562235	7726448
Colville-02	<i>Alnus sp.</i>	1.92	1.05	562229	7726448
Colville-02	<i>Alnus sp.</i>	2.05	1.58	562212	7726442
Colville-02	<i>Alnus sp.</i>	1.9	1.58	562157	7726439
Colville-02	<i>Alnus sp.</i>	1.47	0.55	562152	7726439
Colville-02	<i>Alnus sp.</i>	1.82	0.86	562146	7726438
Colville-02	<i>Alnus sp.</i>	2.24	0.69	562135	7726438

Site	Sp_genus	Canopy_height (m)	Crown_radius (m)	X (m)	Y (m)
Colville-02	<i>Alnus sp.</i>	1.81	0.5	562131	7726437
Colville-02	<i>Alnus sp.</i>	1.07	0.49	562116	7726436
Colville-02	<i>Alnus sp.</i>	1.37	0.47	562112	7726434
Colville-02	<i>Alnus sp.</i>	1.53	0.53	562112	7726434
Colville-02	<i>Alnus sp.</i>	1.66	0.64	562106	7726437
Colville-02	<i>Alnus sp.</i>	1.56	1.51	562099	7726438
Colville-02	<i>Alnus sp.</i>	1.85	0.44	562094	7726438
Colville-02	<i>Alnus sp.</i>	1.08	0.49	562084	7726439
Colville-02	<i>Alnus sp.</i>	1.85	0.96	562078	7726439
Colville-02	<i>Alnus sp.</i>	1.12	0.44	562056	7726439
Colville-02	<i>Alnus sp.</i>	1.08	0.49	562039	7726447
Colville-02	<i>Alnus sp.</i>	1.43	1.14	562034	7726447
Colville-02	<i>Alnus sp.</i>	1.34	0.46	562034	7726447
Colville-02	<i>Alnus sp.</i>	0.86	0.33	562028	7726448
Colville-02	<i>Alnus sp.</i>	1.12	1.37	562008	7726475
Colville-02	<i>Alnus sp.</i>	1.12	0.42	562054	7726479
Colville-02	<i>Alnus sp.</i>	1.61	1.41	562062	7726479
Colville-02	<i>Alnus sp.</i>	1.54	1.25	562073	7726482
Colville-02	<i>Alnus sp.</i>	2.68	1.94	562085	7726483
Colville-02	<i>Alnus sp.</i>	1.37	1.02	562101	7726479
Colville-02	<i>Alnus sp.</i>	1.5	1.45	562119	7726473
Colville-02	<i>Alnus sp.</i>	1.32	1.16	562119	7726475
Colville-02	<i>Alnus sp.</i>	1.07	0.68	562124	7726474
Colville-02	<i>Alnus sp.</i>	1.75	0.63	562133	7726476
Colville-02	<i>Alnus sp.</i>	2.21	1.48	562152	7726469
Colville-02	<i>Alnus sp.</i>	1.87	1.5	562180	7726467
Colville-02	<i>Alnus sp.</i>	2.26	1.07	562198	7726468
Colville-02	<i>Alnus sp.</i>	1.44	1.02	562195	7726502
Colville-02	<i>Alnus sp.</i>	1.84	0.81	562179	7726501
Colville-02	<i>Alnus sp.</i>	1.55	0.72	562169	7726500
Colville-02	<i>Alnus sp.</i>	2.05	1.26	562153	7726505
Colville-02	<i>Alnus sp.</i>	1.72	2.71	562133	7726498
Colville-02	<i>Alnus sp.</i>	2.57	1.79	562118	7726493
Colville-02	<i>Alnus sp.</i>	1.21	1.06	562107	7726491
Colville-02	<i>Alnus sp.</i>	2	1.39	562099	7726492
Colville-02	<i>Alnus sp.</i>	1.42	1.02	562086	7726488
Colville-02	<i>Alnus sp.</i>	1.75	5.08	562071	7726494

Site	Sp_genus	Canopy_height (m)	Crown_radius (m)	X (m)	Y (m)
Colville-02	<i>Alnus sp.</i>	0.92	0.54	562071	7726494
Colville-02	<i>Alnus sp.</i>	1.81	1.06	562065	7726491
Colville-02	<i>Alnus sp.</i>	1.23	0.49	562065	7726491
Colville-02	<i>Alnus sp.</i>	1.28	0.38	562053	7726494
Colville-02	<i>Alnus sp.</i>	1.17	0.63	562022	7726533
Colville-02	<i>Alnus sp.</i>	0.96	0.66	562041	7726531
Colville-02	<i>Alnus sp.</i>	1.46	1.02	562084	7726530
Colville-02	<i>Alnus sp.</i>	2	1.46	562098	7726529
Colville-02	<i>Alnus sp.</i>	1.48	1.44	562106	7726532
Colville-02	<i>Alnus sp.</i>	1.12	1.32	562109	7726533
Colville-02	<i>Alnus sp.</i>	0.93	0.26	562109	7726533
Colville-02	<i>Alnus sp.</i>	1.29	0.49	562121	7726533
Colville-02	<i>Alnus sp.</i>	0.85	0.28	562121	7726533
Colville-02	<i>Alnus sp.</i>	0.93	0.61	562128	7726535
Colville-02	<i>Alnus sp.</i>	1.13	1.06	562142	7726537
Colville-02	<i>Alnus sp.</i>	2.22	1.93	562158	7726534
Colville-02	<i>Alnus sp.</i>	1.58	0.96	562158	7726534
Colville-02	<i>Alnus sp.</i>	1.26	0.49	562165	7726532
Colville-02	<i>Alnus sp.</i>	1.44	0.48	562172	7726531
Colville-02	<i>Alnus sp.</i>	1.18	0.38	562177	7726530
Colville-02	<i>Alnus sp.</i>	1.62	1.09	562177	7726530
Colville-02	<i>Alnus sp.</i>	1.24	1.91	562218	7726527
Colville-02	<i>Alnus sp.</i>	1.65	1.31	562230	7726546
Colville-02	<i>Alnus sp.</i>	1.06	0.69	562225	7726549
Colville-02	<i>Alnus sp.</i>	1.07	0.32	562225	7726549
Colville-02	<i>Alnus sp.</i>	0.77	0.42	562225	7726549
Colville-02	<i>Alnus sp.</i>	1.53	1.49	562218	7726549
Colville-02	<i>Alnus sp.</i>	1.83	0.94	562202	7726548
Colville-02	<i>Alnus sp.</i>	1.08	0.42	562202	7726548
Colville-02	<i>Alnus sp.</i>	1.15	0.62	562186	7726549
Colville-02	<i>Alnus sp.</i>	1.22	0.65	562178	7726548
Colville-02	<i>Alnus sp.</i>	1.09	0.36	562160	7726552
Colville-02	<i>Alnus sp.</i>	1.09	0.82	562154	7726551
Colville-02	<i>Alnus sp.</i>	1.79	0.84	562140	7726548
Colville-02	<i>Alnus sp.</i>	2.17	1.59	562125	7726548
Colville-02	<i>Alnus sp.</i>	2.41	2	562071	7726546
Colville-02	<i>Alnus sp.</i>	1.14	0.58	562034	7726552

Site	Sp_genus	Canopy_height (m)	Crown_radius (m)	X (m)	Y (m)
Colville-02	<i>Alnus sp.</i>	1.32	1.5	561995	7726548
Colville-02	<i>Alnus sp.</i>	1.62	0.71	561999	7726575
Colville-02	<i>Alnus sp.</i>	2	2.18	562005	7726575
Colville-02	<i>Alnus sp.</i>	1.88	3.27	562017	7726579
Colville-02	<i>Alnus sp.</i>	2.2	0.9	562017	7726579
Colville-02	<i>Alnus sp.</i>	2.45	0.33	562017	7726579
Colville-02	<i>Alnus sp.</i>	2.62	1.46	562029	7726578
Colville-02	<i>Alnus sp.</i>	1.69	3.64	562047	7726573
Colville-02	<i>Alnus sp.</i>	2	2.08	562065	7726580
Colville-02	<i>Alnus sp.</i>	1.57	0.75	562079	7726576
Colville-02	<i>Alnus sp.</i>	1.8	1.32	562131	7726578
Colville-02	<i>Alnus sp.</i>	1.59	0.6	562149	7726577
Colville-02	<i>Alnus sp.</i>	1.61	0.5	562163	7726577
Colville-02	<i>Alnus sp.</i>	2.03	1.67	562172	7726578
Colville-02	<i>Alnus sp.</i>	1.1	4.91	562184	7726578
Colville-02	<i>Alnus sp.</i>	1.52	0.87	562197	7726576
Colville-02	<i>Alnus sp.</i>	1.02	0.41	562215	7726573
Colville-02	<i>Alnus sp.</i>	1.85	2.16	562206	7726604
Colville-02	<i>Alnus sp.</i>	1.75	2.25	562195	7726606
Colville-02	<i>Alnus sp.</i>	1.76	0.87	562171	7726602
Colville-02	<i>Alnus sp.</i>	2.57	1.88	562162	7726602
Colville-02	<i>Alnus sp.</i>	1.83	1.42	562131	7726599
Colville-02	<i>Alnus sp.</i>	1.57	1.48	562114	7726597
Colville-02	<i>Alnus sp.</i>	1.39	0.74	562114	7726597
Colville-02	<i>Alnus sp.</i>	1.88	0.67	562105	7726627
Colville-02	<i>Alnus sp.</i>	1.25	1.08	562096	7726613
Colville-02	<i>Alnus sp.</i>	0.95	0.65	562096	7726613
Colville-02	<i>Alnus sp.</i>	1.45	0.65	562096	7726613
Colville-02	<i>Alnus sp.</i>	0.82	0.73	562071	7726606
Colville-02	<i>Alnus sp.</i>	1.28	0.65	562024	7726595
Colville-02	<i>Alnus sp.</i>	1.64	1.05	562013	7726596
Colville-02	<i>Alnus sp.</i>	1.79	1.36	562005	7726596
Colville-02	<i>Alnus sp.</i>	1.92	1.85	561996	7726600
Colville-03	<i>Salix sp.</i>	1.19	0.9	557214	7711231
Colville-03	<i>Alnus sp.</i>	1.39	1.29	557249	7711230
Colville-03	<i>Alnus sp.</i>	1.38	0.64	557249	7711230
Colville-03	<i>Salix sp.</i>	1.35	1.39	557267	7711232

Site	Sp_genus	Canopy_height (m)	Crown_radius (m)	X (m)	Y (m)
Colville-03	<i>Alnus sp.</i>	0.81	0.94	557277	7711232
Colville-03	<i>Alnus sp.</i>	0.88	0.92	557310	7711251
Colville-03	<i>Alnus sp.</i>	1.17	1.5	557280	7711245
Colville-03	<i>Alnus sp.</i>	1.48	0.51	557272	7711246
Colville-03	<i>Alnus sp.</i>	1.07	0.98	557272	7711246
Colville-03	<i>Alnus sp.</i>	0.61	0.4	557263	7711249
Colville-03	<i>Alnus sp.</i>	1.14	1.27	557257	7711246
Colville-03	<i>Alnus sp.</i>	1.11	1	557250	7711247
Colville-03	<i>Alnus sp.</i>	1.31	0.49	557250	7711247
Colville-03	<i>Alnus sp.</i>	1.19	1.28	557250	7711247
Colville-03	<i>Alnus sp.</i>	1.33	1.08	557250	7711247
Colville-03	<i>Salix sp.</i>	1.01	0.84	557216	7711244
Colville-03	<i>Alnus sp.</i>	1.68	0.95	557208	7711244
Colville-03	<i>Salix sp.</i>	1.16	1.46	557168	7711248
Colville-03	<i>Alnus sp.</i>	1.53	0.95	557184	7711273
Colville-03	<i>Salix sp.</i>	1.1	1.19	557218	7711271
Colville-03	<i>Salix sp.</i>	1.14	0.66	557218	7711271
Colville-03	<i>Salix sp.</i>	0.77	0.71	557230	7711270
Colville-03	<i>Alnus sp.</i>	1.13	0.6	557346	7711300
Colville-03	<i>Alnus sp.</i>	1.05	1.12	557268	7711293
Colville-03	<i>Alnus sp.</i>	0.8	0.51	557256	7711293
Colville-03	<i>Alnus sp.</i>	1	0.73	557246	7711290
Colville-03	<i>Alnus sp.</i>	1.72	1.25	557241	7711291
Colville-03	<i>Alnus sp.</i>	1.35	0.65	557235	7711291
Colville-03	<i>Salix sp.</i>	1.04	0.69	557231	7711290
Colville-03	<i>Alnus sp.</i>	1.78	2.67	557209	7711289
Colville-03	<i>Alnus sp.</i>	1.11	0.87	557135	7711295
Colville-03	<i>Alnus sp.</i>	1.2	1.18	557135	7711295
Colville-03	<i>Salix sp.</i>	1.12	0.89	557251	7711330
Colville-03	<i>Alnus sp.</i>	1.3	1.64	557257	7711328
Colville-03	<i>Alnus sp.</i>	1.06	0.58	557314	7711328
Colville-03	<i>Alnus sp.</i>	1.17	1	557324	7711326
Colville-03	<i>Alnus sp.</i>	1.04	1.35	557378	7711349
Colville-03	<i>Alnus sp.</i>	1.04	0.81	557358	7711348
Colville-03	<i>Alnus sp.</i>	0.96	0.82	557313	7711345
Colville-03	<i>Alnus sp.</i>	0.96	0.72	557307	7711345
Colville-03	<i>Alnus sp.</i>	1.16	0.85	557307	7711345

Site	Sp_genus	Canopy_height (m)	Crown_radius (m)	X (m)	Y (m)
Colville-03	<i>Alnus sp.</i>	1.36	0.85	557301	7711343
Colville-03	<i>Alnus sp.</i>	1.47	1	557280	7711340
Colville-03	<i>Salix sp.</i>	0.92	1.22	557275	7711345
Colville-03	<i>Alnus sp.</i>	1.17	0.89	557207	7711373
Colville-03	<i>Salix sp.</i>	0.94	0.91	557236	7711371
Colville-03	<i>Salix sp.</i>	1.54	1.37	557277	7711370
Colville-03	<i>Salix sp.</i>	2.13	1.33	557290	7711371
Colville-03	<i>Alnus sp.</i>	1.14	0.77	557353	7711376
Colville-03	<i>Alnus sp.</i>	0.69	1.08	557373	7711378
Colville-03	<i>Alnus sp.</i>	1.13	0.6	557377	7711403
Colville-03	<i>Alnus sp.</i>	1.08	0.5	557355	7711400
Colville-03	<i>Alnus sp.</i>	1.21	1.18	557350	7711401
Colville-03	<i>Alnus sp.</i>	1.37	1.07	557344	7711400
Colville-03	<i>Salix sp.</i>	2.65	2.28	557308	7711398
Colville-03	<i>Salix sp.</i>	1.34	1.75	557131	7711424
Colville-03	<i>Salix sp.</i>	1.07	1.69	557140	7711422
Colville-03	<i>Salix sp.</i>	1.31	2.39	557175	7711421
Colville-03	<i>Salix sp.</i>	1.32	1.75	557229	7711423
Colville-03	<i>Alnus sp.</i>	1.18	1.1	557253	7711425
Colville-03	<i>Salix sp.</i>	2.34	1.31	557315	7711426
Colville-03	<i>Alnus sp.</i>	1.14	1.45	557324	7711426
Colville-03	<i>Alnus sp.</i>	0.96	0.83	557353	7711425
Colville-03	<i>Alnus sp.</i>	0.98	0.82	557367	7711426
Colville-03	<i>Alnus sp.</i>	1.13	0.8	557376	7711424
Colville-03	<i>Alnus sp.</i>	0.93	0.79	557387	7711423
Colville-03	<i>Alnus sp.</i>	2	2.32	557331	7711451
Colville-03	<i>Alnus sp.</i>	1.15	1.1	557251	7711447
Colville-03	<i>Salix sp.</i>	1.15	1.24	557245	7711446
Colville-03	<i>Salix sp.</i>	1.12	1.81	557192	7711441
Colville-03	<i>Salix sp.</i>	1.98	1.86	557159	7711445
Colville-03	<i>Salix sp.</i>	1.85	1.29	557154	7711449
Colville-04	<i>Salix sp.</i>	2.58	1.49	557283	7710176
Colville-04	<i>Salix sp.</i>	1.19	1.21	557269	7710174
Colville-04	<i>Salix sp.</i>	1.07	0.98	557251	7710179
Colville-04	<i>Salix sp.</i>	0.59	1.23	557226	7710180
Colville-04	<i>Salix sp.</i>	1.05	1.82	557213	7710180
Colville-04	<i>Alnus sp.</i>	2.33	3.6	557204	7710181

Site	Sp_genus	Canopy_height (m)	Crown_radius (m)	X (m)	Y (m)
Colville-04	<i>Salix sp.</i>	2.65	2.41	557192	7710178
Colville-04	<i>Alnus sp.</i>	2.21	2.23	557157	7710171
Colville-04	<i>Alnus sp.</i>	1.33	1.18	557147	7710174
Colville-04	<i>Salix sp.</i>	1.22	0.92	557141	7710176
Colville-04	<i>Salix sp.</i>	1.23	1.02	557133	7710177
Colville-04	<i>Salix sp.</i>	1.14	1.57	557127	7710176
Colville-04	<i>Salix sp.</i>	1.03	1.15	557129	7710121
Colville-04	<i>Salix sp.</i>	1.55	1.18	557152	7710122
Colville-04	<i>Salix sp.</i>	1.79	1.86	557160	7710125
Colville-04	<i>Salix sp.</i>	1.18	0.71	557165	7710125
Colville-04	<i>Salix sp.</i>	1.04	0.9	557172	7710124
Colville-04	<i>Salix sp.</i>	1.44	1.23	557178	7710122
Colville-04	<i>Salix sp.</i>	1.2	1.16	557178	7710122
Colville-04	<i>Salix sp.</i>	1.5	1.41	557181	7710123
Colville-04	<i>Salix sp.</i>	1.17	2.03	557198	7710120
Colville-04	<i>Salix sp.</i>	1.48	0.41	557208	7710118
Colville-04	<i>Salix sp.</i>	0.71	1.41	557208	7710118
Colville-04	<i>Salix sp.</i>	1.43	1.12	557214	7710115
Colville-04	<i>Salix sp.</i>	1.48	1.62	557223	7710113
Colville-04	<i>Salix sp.</i>	3.68	3.59	557255	7710113
Colville-04	<i>Salix sp.</i>	3.07	0.86	557262	7710124
Colville-04	<i>Alnus sp.</i>	1.89	2.6	557295	7710120
Colville-04	<i>Salix sp.</i>	0.83	0.95	557325	7710119
Colville-04	<i>Salix sp.</i>	0.9	0.86	557337	7710119
Colville-04	<i>Salix sp.</i>	1.52	1.8	557369	7710074
Colville-04	<i>Salix sp.</i>	1.02	2.45	557252	7710075
Colville-04	<i>Salix sp.</i>	1.89	1.85	557236	7710075
Colville-04	<i>Alnus sp.</i>	2.47	1.1	557229	7710078
Colville-04	<i>Salix sp.</i>	2.08	1.17	557217	7710075
Colville-04	<i>Salix sp.</i>	0.88	0.87	557213	7710074
Colville-04	<i>Salix sp.</i>	1.41	1.03	557206	7710076
Colville-04	<i>Salix sp.</i>	1.51	2.44	557197	7710078
Colville-04	<i>Salix sp.</i>	1.98	1.81	557192	7710078
Colville-04	<i>Salix sp.</i>	0.69	0.46	557186	7710078
Colville-04	<i>Salix sp.</i>	0.92	1	557186	7710078
Colville-04	<i>Salix sp.</i>	0.84	0.56	557180	7710078
Colville-04	<i>Salix sp.</i>	0.92	0.72	557180	7710078

Site	Sp_genus	Canopy_height (m)	Crown_radius (m)	X (m)	Y (m)
Colville-04	<i>Salix sp.</i>	1.02	0.41	557180	7710078
Colville-04	<i>Salix sp.</i>	1.07	0.36	557180	7710078
Colville-04	<i>Alnus sp.</i>	2.69	5.69	557150	7710081
Colville-04	<i>Salix sp.</i>	1.12	1.44	557131	7710077
Colville-04	<i>Salix sp.</i>	1.12	1.69	557124	7710029
Colville-04	<i>Salix sp.</i>	1.13	1.18	557136	7710027
Colville-04	<i>Salix sp.</i>	1.3	1.72	557143	7710026
Colville-04	<i>Salix sp.</i>	0.91	1.13	557164	7710023
Colville-04	<i>Salix sp.</i>	1.35	1.63	557175	7710024
Colville-04	<i>Salix sp.</i>	0.89	0.74	557178	7710024
Colville-04	<i>Salix sp.</i>	1.12	1.2	557190	7710024
Colville-04	<i>Salix sp.</i>	1.17	1.32	557200	7710026
Colville-04	<i>Salix sp.</i>	1.06	1.48	557224	7710025
Colville-04	<i>Salix sp.</i>	1.12	0.93	557233	7710024
Colville-04	<i>Salix sp.</i>	1.75	1.71	557243	7710022
Colville-04	<i>Salix sp.</i>	1.72	2.04	557252	7710022
Colville-04	<i>Salix sp.</i>	1.3	2.71	557261	7710022
Colville-04	<i>Salix sp.</i>	1.2	2.1	557268	7710021
Colville-04	<i>Salix sp.</i>	0.75	1.48	557364	7709984
Colville-04	<i>Salix sp.</i>	1.31	1.54	557294	7709974
Colville-04	<i>Salix sp.</i>	3.54	3.75	557284	7709973
Colville-04	<i>Salix sp.</i>	2.46	2.48	557266	7709964
Colville-04	<i>Alnus sp.</i>	1.96	2.08	557253	7710012
Colville-04	<i>Salix sp.</i>	1.04	0.79	557243	7709985
Colville-04	<i>Salix sp.</i>	0.93	1.22	557243	7709985
Colville-04	<i>Salix sp.</i>	1.41	1.19	557251	7710039
Colville-04	<i>Alnus sp.</i>	2.2	1.25	557222	7709966
Colville-04	<i>Alnus sp.</i>	2.15	1.55	557212	7709970
Colville-04	<i>Salix sp.</i>	1.85	1.6	557209	7709967
Colville-04	<i>Alnus sp.</i>	2.18	1.82	557204	7709967
Colville-04	<i>Alnus sp.</i>	2.83	1.01	557198	7709967
Colville-04	<i>Alnus sp.</i>	2.17	1.96	557194	7709966
Colville-04	<i>Alnus sp.</i>	1.82	0.54	557187	7709966
Colville-04	<i>Salix sp.</i>	0.9	0.35	557183	7709965
Colville-04	<i>Salix sp.</i>	1.04	0.97	557183	7709965
Colville-04	<i>Salix sp.</i>	1.93	2.01	557117	7709968
Colville-04	<i>Salix sp.</i>	1.58	1.9	557117	7709968

Site	Sp_genus	Canopy_height (m)	Crown_radius (m)	X (m)	Y (m)
Colville-04	<i>Salix sp.</i>	1.68	1.28	557117	7709968
Colville-05	<i>Alnus sp.</i>	2.12	1.17	546727	7667525
Colville-05	<i>Alnus sp.</i>	1.42	0.83	546741	7667532
Colville-05	<i>Alnus sp.</i>	2.21	1.71	546753	7667534
Colville-05	<i>Alnus sp.</i>	2.19	1.07	546770	7667533
Colville-05	<i>Alnus sp.</i>	1.63	0.87	546795	7667534
Colville-05	<i>Alnus sp.</i>	2.16	1.8	546810	7667533
Colville-05	<i>Alnus sp.</i>	2.31	0.87	546824	7667531
Colville-05	<i>Alnus sp.</i>	1.95	1.08	546831	7667541
Colville-05	<i>Alnus sp.</i>	1.75	0.55	546846	7667536
Colville-05	<i>Alnus sp.</i>	1.95	0.67	546846	7667536
Colville-05	<i>Alnus sp.</i>	1.69	0.68	546853	7667532
Colville-05	<i>Alnus sp.</i>	2.2	2.05	546859	7667532
Colville-05	<i>Alnus sp.</i>	2.53	1.13	546866	7667532
Colville-05	<i>Alnus sp.</i>	2.21	1.3	546870	7667531
Colville-05	<i>Alnus sp.</i>	2.28	1.33	546870	7667531
Colville-05	<i>Alnus sp.</i>	1.97	0.87	546879	7667531
Colville-05	<i>Alnus sp.</i>	2.24	1.77	546885	7667528
Colville-05	<i>Alnus sp.</i>	2.04	1.04	546890	7667528
Colville-05	<i>Alnus sp.</i>	1.81	0.79	546890	7667528
Colville-05	<i>Alnus sp.</i>	1.8	1.31	546897	7667530
Colville-05	<i>Alnus sp.</i>	2.34	1.57	546911	7667529
Colville-05	<i>Alnus sp.</i>	2.78	1.35	546911	7667529
Colville-05	<i>Alnus sp.</i>	2.2	0.78	546921	7667530
Colville-05	<i>Alnus sp.</i>	1.57	0.4	546938	7667527
Colville-05	<i>Alnus sp.</i>	2.16	1.58	546943	7667527
Colville-05	<i>Alnus sp.</i>	1.93	0.76	546948	7667529
Colville-05	<i>Alnus sp.</i>	2.04	0.63	546952	7667529
Colville-05	<i>Alnus sp.</i>	2.18	1.14	546952	7667529
Colville-05	<i>Alnus sp.</i>	1.75	0.88	546955	7667528
Colville-05	<i>Alnus sp.</i>	1.43	0.93	546961	7667526
Colville-05	<i>Alnus sp.</i>	1.91	0.86	546966	7667526
Colville-05	<i>Alnus sp.</i>	1.93	1.02	546969	7667526
Colville-05	<i>Alnus sp.</i>	1.76	0.78	546978	7667473
Colville-05	<i>Alnus sp.</i>	1.52	0.79	546965	7667472
Colville-05	<i>Alnus sp.</i>	1.48	0.68	546958	7667470
Colville-05	<i>Alnus sp.</i>	1.86	0.45	546958	7667470

Site	Sp_genus	Canopy_height (m)	Crown_radius (m)	X (m)	Y (m)
Colville-05	<i>Alnus sp.</i>	1.24	0.37	546953	7667469
Colville-05	<i>Alnus sp.</i>	1.91	1.8	546946	7667471
Colville-05	<i>Alnus sp.</i>	2.67	0.69	546941	7667471
Colville-05	<i>Alnus sp.</i>	2.53	0.74	546927	7667471
Colville-05	<i>Alnus sp.</i>	2.41	1.53	546921	7667473
Colville-05	<i>Alnus sp.</i>	2.52	2.41	546906	7667472
Colville-05	<i>Alnus sp.</i>	1.71	0.83	546900	7667474
Colville-05	<i>Alnus sp.</i>	1.47	0.77	546896	7667473
Colville-05	<i>Alnus sp.</i>	2.2	0.81	546896	7667473
Colville-05	<i>Alnus sp.</i>	3.1	2.11	546878	7667478
Colville-05	<i>Alnus sp.</i>	2.11	0.96	546867	7667475
Colville-05	<i>Alnus sp.</i>	1.47	0.84	546850	7667478
Colville-05	<i>Alnus sp.</i>	2.73	1.74	546835	7667475
Colville-05	<i>Alnus sp.</i>	2.28	1.63	546824	7667474
Colville-05	<i>Alnus sp.</i>	2.16	0.75	546817	7667474
Colville-05	<i>Alnus sp.</i>	1.53	0.76	546801	7667475
Colville-05	<i>Alnus sp.</i>	2.01	0.87	546782	7667473
Colville-05	<i>Alnus sp.</i>	1.38	0.61	546770	7667472
Colville-05	<i>Alnus sp.</i>	1.15	0.67	546762	7667475
Colville-05	<i>Alnus sp.</i>	2.21	1.28	546755	7667477
Colville-05	<i>Alnus sp.</i>	1.86	0.79	546724	7667421
Colville-05	<i>Alnus sp.</i>	2.04	0.4	546733	7667420
Colville-05	<i>Alnus sp.</i>	2.14	0.73	546733	7667420
Colville-05	<i>Alnus sp.</i>	1.87	0.36	546772	7667422
Colville-05	<i>Alnus sp.</i>	2.32	1.01	546772	7667422
Colville-05	<i>Alnus sp.</i>	2.12	0.97	546780	7667424
Colville-05	<i>Alnus sp.</i>	1.92	1.44	546817	7667435
Colville-05	<i>Alnus sp.</i>	2.33	0.71	546856	7667428
Colville-05	<i>Alnus sp.</i>	2	0.87	546856	7667428
Colville-05	<i>Alnus sp.</i>	1.74	1	546862	7667428
Colville-05	<i>Alnus sp.</i>	1.85	1.86	546875	7667427
Colville-05	<i>Alnus sp.</i>	1.82	0.95	546886	7667426
Colville-05	<i>Alnus sp.</i>	1.26	0.89	546886	7667426
Colville-05	<i>Alnus sp.</i>	2.17	0.85	546886	7667426
Colville-05	<i>Alnus sp.</i>	1.56	1.14	546896	7667425
Colville-05	<i>Alnus sp.</i>	1.62	0.61	546899	7667424
Colville-05	<i>Alnus sp.</i>	2.03	1.21	546908	7667423

Site	Sp_genus	Canopy_height (m)	Crown_radius (m)	X (m)	Y (m)
Colville-05	<i>Alnus sp.</i>	1.28	0.48	546908	7667423
Colville-05	<i>Alnus sp.</i>	1.47	0.75	546963	7667428
Colville-05	<i>Alnus sp.</i>	1.38	0.71	546963	7667428
Colville-05	<i>Alnus sp.</i>	2.27	0.83	546975	7667427
Colville-05	<i>Alnus sp.</i>	2.4	1.59	546971	7667382
Colville-05	<i>Alnus sp.</i>	2.13	1.78	546962	7667380
Colville-05	<i>Alnus sp.</i>	1.69	0.69	546952	7667380
Colville-05	<i>Alnus sp.</i>	1.42	1.15	546937	7667378
Colville-05	<i>Alnus sp.</i>	1.88	0.91	546921	7667377
Colville-05	<i>Alnus sp.</i>	2.23	1.14	546906	7667376
Colville-05	<i>Alnus sp.</i>	2.16	1.76	546906	7667376
Colville-05	<i>Alnus sp.</i>	1.92	1.16	546892	7667376
Colville-05	<i>Alnus sp.</i>	1.69	0.7	546885	7667373
Colville-05	<i>Alnus sp.</i>	0.96	0.54	546874	7667373
Colville-05	<i>Alnus sp.</i>	1.49	0.48	546867	7667374
Colville-05	<i>Alnus sp.</i>	2.05	1.54	546911	7667379
Colville-05	<i>Alnus sp.</i>	2.81	1.76	546793	7667382
Colville-05	<i>Alnus sp.</i>	1.19	0.69	546733	7667379
Colville-05	<i>Alnus sp.</i>	1.39	1.03	546733	7667379
Colville-05	<i>Alnus sp.</i>	1.76	1.78	546740	7667322
Colville-05	<i>Alnus sp.</i>	1.39	0.96	546872	7667332
Colville-05	<i>Alnus sp.</i>	1.99	1.51	546890	7667333
Colville-05	<i>Alnus sp.</i>	1.73	0.79	546890	7667333
Colville-05	<i>Alnus sp.</i>	1.43	1.22	546890	7667333
Colville-05	<i>Alnus sp.</i>	1.2	0.98	546890	7667333
Colville-05	<i>Alnus sp.</i>	1.99	1.54	546923	7667332
Colville-06	<i>Alnus sp.</i>	1.32	1.64	545733	7667027
Colville-06	<i>Alnus sp.</i>	1.42	1.06	545738	7667030
Colville-06	<i>Alnus sp.</i>	1.09	0.54	545748	7667031
Colville-06	<i>Alnus sp.</i>	1.71	1.17	545755	7667030
Colville-06	<i>Alnus sp.</i>	1.78	1.36	545763	7667031
Colville-06	<i>Alnus sp.</i>	1.78	1.19	545768	7667031
Colville-06	<i>Alnus sp.</i>	1.95	0.72	545781	7667032
Colville-06	<i>Alnus sp.</i>	1.73	1.34	545781	7667032
Colville-06	<i>Alnus sp.</i>	2.44	1.85	545794	7667032
Colville-06	<i>Alnus sp.</i>	1.61	0.52	545803	7667034
Colville-06	<i>Alnus sp.</i>	1.77	0.31	545803	7667034

Site	Sp_genus	Canopy_height (m)	Crown_radius (m)	X (m)	Y (m)
Colville-06	<i>Alnus sp.</i>	2.12	1.12	545803	7667034
Colville-06	<i>Alnus sp.</i>	2.32	1.34	545813	7667034
Colville-06	<i>Alnus sp.</i>	1.31	1.23	545850	7667034
Colville-06	<i>Alnus sp.</i>	1.17	0.84	545850	7667034
Colville-06	<i>Alnus sp.</i>	1.57	0.66	545867	7667034
Colville-06	<i>Alnus sp.</i>	1.52	1	545867	7667034
Colville-06	<i>Alnus sp.</i>	1.4	0.73	545876	7667034
Colville-06	<i>Alnus sp.</i>	1.46	1.46	545886	7667032
Colville-06	<i>Alnus sp.</i>	1.09	1.05	545931	7667030
Colville-06	<i>Alnus sp.</i>	1.21	0.85	545987	7667022
Colville-06	<i>Alnus sp.</i>	0.92	0.83	545965	7666998
Colville-06	<i>Alnus sp.</i>	1.33	1.06	545959	7666997
Colville-06	<i>Alnus sp.</i>	1.85	0.73	545929	7666994
Colville-06	<i>Alnus sp.</i>	1.48	0.76	545929	7666994
Colville-06	<i>Alnus sp.</i>	1.55	2.13	545925	7666992
Colville-06	<i>Alnus sp.</i>	1.35	0.48	545916	7666989
Colville-06	<i>Alnus sp.</i>	1.24	1.03	545916	7666989
Colville-06	<i>Alnus sp.</i>	1.35	0.5	545916	7666989
Colville-06	<i>Alnus sp.</i>	1.3	1.67	545906	7666989
Colville-06	<i>Alnus sp.</i>	1.61	1.52	545906	7666989
Colville-06	<i>Alnus sp.</i>	1.12	1.07	545886	7666985
Colville-06	<i>Alnus sp.</i>	1.12	0.53	545886	7666985
Colville-06	<i>Alnus sp.</i>	1.46	0.68	545886	7666985
Colville-06	<i>Alnus sp.</i>	1.16	0.85	545844	7666981
Colville-06	<i>Alnus sp.</i>	1	0.96	545844	7666981
Colville-06	<i>Alnus sp.</i>	1.19	0.68	545817	7666983
Colville-06	<i>Alnus sp.</i>	1.9	1.51	545806	7666988
Colville-06	<i>Alnus sp.</i>	2.17	1.91	545798	7666990
Colville-06	<i>Alnus sp.</i>	2.08	2.14	545785	7666992
Colville-06	<i>Alnus sp.</i>	1.81	1.63	545773	7666992
Colville-06	<i>Alnus sp.</i>	2.33	2.52	545732	7666976
Colville-06	<i>Alnus sp.</i>	2.02	1.76	545814	7667004
Colville-06	<i>Alnus sp.</i>	1.71	1.39	545809	7666986
Colville-06	<i>Alnus sp.</i>	2.18	1.14	545809	7666986
Colville-06	<i>Alnus sp.</i>	1.49	1.48	545812	7666982
Colville-06	<i>Alnus sp.</i>	0.86	1.4	545818	7666981
Colville-06	<i>Alnus sp.</i>	1.24	1.15	545824	7666979

Site	Sp_genus	Canopy_height (m)	Crown_radius (m)	X (m)	Y (m)
Colville-06	<i>Alnus sp.</i>	1.28	0.62	545841	7666977
Colville-06	<i>Alnus sp.</i>	1.33	0.56	545841	7666977
Colville-06	<i>Alnus sp.</i>	1.64	0.75	545865	7666978
Colville-06	<i>Alnus sp.</i>	2.01	0.57	545865	7666978
Colville-06	<i>Alnus sp.</i>	1.9	1.69	545883	7666978
Colville-06	<i>Alnus sp.</i>	2.13	1.13	545903	7666977
Colville-06	<i>Alnus sp.</i>	2.05	1.09	545903	7666977
Colville-06	<i>Alnus sp.</i>	1.87	0.61	545928	7666976
Colville-06	<i>Alnus sp.</i>	1.5	0.51	545936	7666975
Colville-06	<i>Alnus sp.</i>	1.74	1.43	545946	7666979
Colville-06	<i>Alnus sp.</i>	2.1	1.46	545952	7666978
Colville-06	<i>Alnus sp.</i>	1.24	0.75	545959	7666979
Colville-06	<i>Alnus sp.</i>	1.77	1.22	545959	7666979
Colville-06	<i>Alnus sp.</i>	2.1	1.3	545966	7666978
Colville-06	<i>Alnus sp.</i>	1.13	1.04	545970	7666980
Colville-06	<i>Alnus sp.</i>	1.74	0.63	545987	7666975
Colville-06	<i>Alnus sp.</i>	1.6	0.54	545970	7666953
Colville-06	<i>Alnus sp.</i>	1.95	0.83	545957	7666951
Colville-06	<i>Alnus sp.</i>	1.57	0.96	545951	7666950
Colville-06	<i>Alnus sp.</i>	1.26	1.28	545937	7666951
Colville-06	<i>Alnus sp.</i>	1.54	0.81	545924	7666950
Colville-06	<i>Alnus sp.</i>	1.37	0.42	545917	7666948
Colville-06	<i>Alnus sp.</i>	1.58	0.68	545908	7666947
Colville-06	<i>Alnus sp.</i>	1.1	0.3	545895	7666945
Colville-06	<i>Alnus sp.</i>	1.33	0.53	545895	7666945
Colville-06	<i>Alnus sp.</i>	1.12	0.52	545891	7666944
Colville-06	<i>Alnus sp.</i>	2.18	1.28	545880	7666945
Colville-06	<i>Alnus sp.</i>	2.45	0.88	545880	7666945
Colville-06	<i>Alnus sp.</i>	1.21	0.82	545875	7666946
Colville-06	<i>Alnus sp.</i>	1.15	0.5	545867	7666948
Colville-06	<i>Alnus sp.</i>	1.23	0.62	545863	7666947
Colville-06	<i>Alnus sp.</i>	1.79	0.56	545859	7666946
Colville-06	<i>Alnus sp.</i>	1.3	0.59	545830	7666947
Colville-06	<i>Alnus sp.</i>	2.24	1.39	545830	7666947
Colville-06	<i>Alnus sp.</i>	2.15	0.99	545822	7666946
Colville-06	<i>Alnus sp.</i>	1.81	0.71	545817	7666947
Colville-06	<i>Alnus sp.</i>	2.04	1.67	545811	7666945

Site	Sp_genus	Canopy_height (m)	Crown_radius (m)	X (m)	Y (m)
Colville-06	<i>Alnus sp.</i>	1.48	0.91	545793	7666920
Colville-06	<i>Alnus sp.</i>	1.59	1.22	545793	7666920
Colville-06	<i>Alnus sp.</i>	2.13	0.74	545824	7666920
Colville-06	<i>Alnus sp.</i>	1.63	0.31	545833	7666923
Colville-06	<i>Alnus sp.</i>	1.24	0.69	545833	7666923
Colville-06	<i>Alnus sp.</i>	1.74	1.19	545842	7666924
Colville-06	<i>Alnus sp.</i>	2.08	2.25	545851	7666916
Colville-06	<i>Alnus sp.</i>	2.56	1.44	545851	7666916
Colville-06	<i>Alnus sp.</i>	1.93	0.89	545857	7666910
Colville-06	<i>Alnus sp.</i>	1.81	0.89	545857	7666910
Colville-06	<i>Alnus sp.</i>	1.86	0.64	545867	7666917
Colville-06	<i>Alnus sp.</i>	1.87	0.81	545874	7666918
Colville-06	<i>Alnus sp.</i>	1.67	0.6	545892	7666921
Colville-06	<i>Alnus sp.</i>	2.14	0.92	545892	7666921
Colville-06	<i>Alnus sp.</i>	1.84	0.72	545897	7666922
Colville-06	<i>Alnus sp.</i>	1.87	0.92	545902	7666925
Colville-06	<i>Alnus sp.</i>	1.7	0.71	545914	7666929
Colville-06	<i>Alnus sp.</i>	1.63	0.78	545925	7666929
Colville-06	<i>Alnus sp.</i>	1.84	0.45	545935	7666931
Colville-06	<i>Alnus sp.</i>	2.12	0.7	545935	7666931
Colville-06	<i>Alnus sp.</i>	1.87	0.86	545951	7666929
Colville-06	<i>Alnus sp.</i>	0.89	1.34	545985	7666926
Colville-06	<i>Alnus sp.</i>	2.15	1.73	545983	7666897
Colville-06	<i>Alnus sp.</i>	1.23	0.73	545974	7666898
Colville-06	<i>Alnus sp.</i>	2.12	1.44	545855	7666886
Colville-06	<i>Alnus sp.</i>	1.87	3.11	545732	7666874
Colville-06	<i>Alnus sp.</i>	1.25	1.74	545755	7666878
Colville-06	<i>Alnus sp.</i>	2.05	1.99	545866	7666897
Colville-06	<i>Alnus sp.</i>	1.48	0.99	545924	7667504
Colville-06	<i>Alnus sp.</i>	1.72	0.58	545984	7666847
Colville-06	<i>Alnus sp.</i>	1.82	0.67	545984	7666847
Colville-06	<i>Alnus sp.</i>	1.22	0.58	545973	7666844
Colville-06	<i>Alnus sp.</i>	1.46	0.6	545973	7666844
Colville-06	<i>Alnus sp.</i>	1.11	0.47	545959	7666843
Colville-06	<i>Alnus sp.</i>	1.1	0.38	545951	7666843
Colville-06	<i>Alnus sp.</i>	0.95	0.26	545951	7666843
Colville-06	<i>Alnus sp.</i>	1.2	0.57	545941	7666841

Site	Sp_genus	Canopy_height (m)	Crown_radius (m)	X (m)	Y (m)
Colville-06	<i>Alnus sp.</i>	1.16	0.5	545932	7666842
Colville-06	<i>Alnus sp.</i>	1	0.65	545932	7666842
Colville-06	<i>Alnus sp.</i>	1.36	0.5	545921	7666843
Colville-06	<i>Alnus sp.</i>	1.31	0.86	545914	7666842
Colville-06	<i>Alnus sp.</i>	2.27	1.57	545908	7666842
Colville-06	<i>Alnus sp.</i>	1.13	0.2	545902	7666843
Colville-06	<i>Alnus sp.</i>	1.1	0.33	545902	7666843
Colville-06	<i>Alnus sp.</i>	1.12	0.21	545902	7666843
Colville-06	<i>Alnus sp.</i>	2.21	1.98	545893	7666842
Colville-06	<i>Alnus sp.</i>	1.91	1.45	545884	7666841
Colville-06	<i>Alnus sp.</i>	1.88	1.04	545876	7666836
Colville-06	<i>Alnus sp.</i>	1.89	1.66	545835	7666833
Colville-06	<i>Alnus sp.</i>	1.84	1.04	545838	7666822
Colville-06	<i>Alnus sp.</i>	1.61	0.91	545861	7666827
Colville-06	<i>Alnus sp.</i>	1.89	1.38	545883	7666826
Colville-06	<i>Alnus sp.</i>	1.92	1.51	545893	7666825
Colville-06	<i>Alnus sp.</i>	1.38	1.77	545903	7666823
Colville-06	<i>Alnus sp.</i>	2.12	1.09	545908	7666825
Colville-06	<i>Alnus sp.</i>	1.62	0.94	545918	7666823
Colville-06	<i>Alnus sp.</i>	2.08	1.25	545923	7666823
Colville-06	<i>Alnus sp.</i>	1.31	0.62	545932	7666821
Colville-06	<i>Alnus sp.</i>	2.18	0.89	545932	7666821
Colville-06	<i>Alnus sp.</i>	1.14	0.74	545951	7666821
Colville-06	<i>Alnus sp.</i>	2.08	0.96	545956	7666822
Colville-06	<i>Alnus sp.</i>	1.6	0.67	545968	7666823
Colville-06	<i>Alnus sp.</i>	2.19	1.41	545976	7666824
Colville-06	<i>Alnus sp.</i>	1.91	1.34	545984	7666800
Colville-06	<i>Alnus sp.</i>	2.29	1.34	545970	7666798
Colville-06	<i>Alnus sp.</i>	1.54	0.86	545965	7666798
Colville-06	<i>Alnus sp.</i>	1.63	1.21	545957	7666797
Colville-06	<i>Alnus sp.</i>	2.34	1.53	545951	7666802
Colville-06	<i>Alnus sp.</i>	1.48	1.05	545940	7666801
Colville-06	<i>Alnus sp.</i>	1.79	1.11	545927	7666805
Colville-06	<i>Alnus sp.</i>	2.06	1.93	545915	7666803
Colville-06	<i>Alnus sp.</i>	2.26	0.87	545905	7666800
Colville-06	<i>Alnus sp.</i>	1.4	1.51	545879	7666794
Colville-06	<i>Alnus sp.</i>	1.88	1.17	545872	7666793

Site	Sp_genus	Canopy_height (m)	Crown_radius (m)	X (m)	Y (m)
Colville-07	<i>Alnus sp.</i>	0.92	0.83	548660	7658614
Colville-07	<i>Alnus sp.</i>	1.3	0.98	548640	7658627
Colville-07	<i>Alnus sp.</i>	2.98	1.92	548646	7658629
Colville-07	<i>Alnus sp.</i>	0.93	0.57	548643	7658578
Colville-07	<i>Alnus sp.</i>	0.72	0.97	548646	7658577
Colville-07	<i>Alnus sp.</i>	3.05	2.1	548655	7658574
Colville-07	<i>Alnus sp.</i>	1	0.87	548604	7658527
Colville-07	<i>Alnus sp.</i>	1.15	0.57	548592	7658545
Colville-07	<i>Alnus sp.</i>	0.57	0.51	548592	7658545
Colville-07	<i>Alnus sp.</i>	0.94	0.57	548640	7658530
Colville-07	<i>Alnus sp.</i>	0.9	1.02	548646	7658530
Colville-07	<i>Alnus sp.</i>	0.84	0.92	548646	7658530
Colville-07	<i>Alnus sp.</i>	1.55	0.59	548646	7658530
Colville-07	<i>Alnus sp.</i>	0.96	1.14	548671	7658533
Colville-07	<i>Alnus sp.</i>	1.41	1.34	548671	7658533
Colville-07	<i>Alnus sp.</i>	2.22	1.34	548691	7658543
Colville-07	<i>Alnus sp.</i>	1.12	0.89	548731	7658769
Colville-07	<i>Alnus sp.</i>	1.1	0.58	548731	7658769
Colville-07	<i>Alnus sp.</i>	1.06	0.6	548706	7658542
Colville-07	<i>Alnus sp.</i>	0.81	0.4	548706	7658542
Colville-07	<i>Alnus sp.</i>	0.75	0.45	548811	7658533
Colville-07	<i>Alnus sp.</i>	1.05	0.73	548811	7658533
Colville-07	<i>Alnus sp.</i>	1.49	0.84	548832	7658526
Colville-07	<i>Alnus sp.</i>	1.25	1.22	548755	7658631
Colville-07	<i>Alnus sp.</i>	1.67	0.93	548755	7658631
Colville-07	<i>Alnus sp.</i>	0.97	1.04	548755	7658631
Colville-07	<i>Alnus sp.</i>	0.93	0.56	548788	7658568
Colville-07	<i>Alnus sp.</i>	1.01	0.61	548805	7658567
Colville-07	<i>Alnus sp.</i>	1	0.56	548813	7658569
Colville-07	<i>Alnus sp.</i>	0.95	0.65	548831	7658572
Colville-07	<i>Alnus sp.</i>	0.86	0.44	548831	7658572
Colville-07	<i>Alnus sp.</i>	0.88	1.65	548729	7658471
Colville-07	<i>Alnus sp.</i>	0.91	1.04	548729	7658471
Colville-07	<i>Alnus sp.</i>	1.46	2.8	548709	7658468
Colville-07	<i>Alnus sp.</i>	2.26	1.51	548700	7658469
Colville-07	<i>Alnus sp.</i>	3.45	2.4	548691	7658470
Colville-07	<i>Alnus sp.</i>	1.53	1.63	548685	7658464

Site	Sp_genus	Canopy_height (m)	Crown_radius (m)	X (m)	Y (m)
Colville-07	<i>Alnus sp.</i>	1.08	0.63	548617	7658469
Colville-07	<i>Alnus sp.</i>	0.77	1.19	548677	7658417
Colville-07	<i>Alnus sp.</i>	0.9	0.45	548677	7658417
Colville-07	<i>Alnus sp.</i>	1	0.89	548684	7658415
Colville-07	<i>Alnus sp.</i>	0.93	0.73	548689	7658413
Colville-07	<i>Alnus sp.</i>	2.09	2.08	548710	7658410
Colville-07	<i>Alnus sp.</i>	2.2	2.15	548723	7658417
Colville-07	<i>Alnus sp.</i>	0.83	0.26	548723	7658417
Colville-07	<i>Alnus sp.</i>	1.37	0.53	548736	7658418
Colville-07	<i>Alnus sp.</i>	1.28	1.12	548736	7658418
Colville-07	<i>Alnus sp.</i>	0.99	1.58	548742	7658417
Colville-07	<i>Alnus sp.</i>	0.81	0.52	548742	7658417
Colville-07	<i>Alnus sp.</i>	1.21	1.6	548760	7658414
Colville-08	<i>Alnus sp.</i>	1.29	0.8	548348	7657625
Colville-08	<i>Alnus sp.</i>	1.66	0.63	548370	7657631
Colville-08	<i>Alnus sp.</i>	1	1.23	548379	7657627
Colville-08	<i>Alnus sp.</i>	1.7	0.73	548381	7657627
Colville-08	<i>Alnus sp.</i>	1.14	0.89	548388	7657628
Colville-08	<i>Alnus sp.</i>	1.21	1.24	548388	7657628
Colville-08	<i>Alnus sp.</i>	1.63	1.24	548388	7657628
Colville-08	<i>Alnus sp.</i>	1.21	0.66	548404	7657628
Colville-08	<i>Alnus sp.</i>	1.23	1.68	548404	7657628
Colville-08	<i>Alnus sp.</i>	1.1	0.89	548450	7657626
Colville-08	<i>Alnus sp.</i>	1.32	0.74	548461	7657625
Colville-08	<i>Alnus sp.</i>	1.23	0.65	548461	7657625
Colville-08	<i>Alnus sp.</i>	1.16	0.8	548475	7657621
Colville-08	<i>Alnus sp.</i>	0.55	0.33	548475	7657621
Colville-08	<i>Alnus sp.</i>	0.92	0.57	548491	7657615
Colville-08	<i>Alnus sp.</i>	0.76	0.45	548491	7657615
Colville-08	<i>Alnus sp.</i>	1.27	0.65	548515	7657609
Colville-08	<i>Alnus sp.</i>	1.51	1.12	548486	7657581
Colville-08	<i>Alnus sp.</i>	1.28	0.83	548486	7657581
Colville-08	<i>Alnus sp.</i>	1.23	1.01	548486	7657581
Colville-08	<i>Alnus sp.</i>	1.24	0.6	548388	7657553
Colville-08	<i>Alnus sp.</i>	0.98	0.51	548388	7657553
Colville-08	<i>Alnus sp.</i>	0.74	0.38	548388	7657553
Colville-08	<i>Alnus sp.</i>	1.14	0.52	548386	7657525

Site	Sp_genus	Canopy_height (m)	Crown_radius (m)	X (m)	Y (m)
Colville-08	<i>Alnus sp.</i>	0.92	0.92	548342	7657527
Colville-08	<i>Alnus sp.</i>	0.64	0.32	548342	7657527
Colville-08	<i>Alnus sp.</i>	0.85	0.6	548347	7657525
Colville-08	<i>Alnus sp.</i>	0.7	0.7	548347	7657525
Colville-08	<i>Alnus sp.</i>	1.02	0.7	548347	7657525
Colville-08	<i>Alnus sp.</i>	0.7	0.6	548360	7657524
Colville-08	<i>Alnus sp.</i>	0.91	0.56	548367	7657526
Colville-08	<i>Alnus sp.</i>	1.34	2.29	548472	7657454
Colville-08	<i>Alnus sp.</i>	1.26	2.11	548445	7657456
Colville-08	<i>Alnus sp.</i>	1	0.5	548445	7657456
Colville-08	<i>Alnus sp.</i>	0.94	0.84	548434	7657457
Colville-08	<i>Alnus sp.</i>	0.7	0.49	548434	7657457
Colville-08	<i>Alnus sp.</i>	0.84	0.69	548429	7657457
Colville-08	<i>Alnus sp.</i>	0.65	0.39	548429	7657457
Colville-08	<i>Alnus sp.</i>	0.78	0.32	548429	7657457
Colville-08	<i>Alnus sp.</i>	1.25	1.31	548415	7657460
Colville-08	<i>Alnus sp.</i>	0.73	0.77	548415	7657460
Colville-08	<i>Alnus sp.</i>	1.11	0.89	548371	7657466
Colville-08	<i>Alnus sp.</i>	1.01	0.38	548371	7657466
Colville-08	<i>Alnus sp.</i>	1.04	0.5	548331	7657422
Colville-08	<i>Alnus sp.</i>	0.77	0.81	548380	7657424
Colville-08	<i>Alnus sp.</i>	0.92	0.65	548391	7657429
Colville-08	<i>Alnus sp.</i>	1.1	0.69	548400	7657428
Colville-08	<i>Alnus sp.</i>	0.76	1.3	548406	7657426
Colville-08	<i>Alnus sp.</i>	1.27	1.01	548526	7657425
Colville-08	<i>Alnus sp.</i>	0.6	0.74	548526	7657425
Colville-08	<i>Alnus sp.</i>	1.09	0.74	548538	7657425
Colville-08	<i>Alnus sp.</i>	1.25	0.92	548538	7657425
Colville-09	<i>Alnus sp.</i>	0.89	0.78	540362	7633985
Colville-09	<i>Alnus sp.</i>	0.72	0.55	540301	7633974
Colville-09	<i>Alnus sp.</i>	0.56	0.34	540301	7633974
Colville-09	<i>Alnus sp.</i>	0.75	0.36	540290	7633974
Colville-09	<i>Alnus sp.</i>	1.13	0.67	540276	7633969
Colville-09	<i>Alnus sp.</i>	0.62	0.49	540227	7633965
Colville-09	<i>Alnus sp.</i>	1	0.55	540192	7633965
Colville-09	<i>Alnus sp.</i>	0.72	1.01	540214	7633956
Colville-09	<i>Alnus sp.</i>	1	0.43	540287	7633958

Site	Sp_genus	Canopy_height (m)	Crown_radius (m)	X (m)	Y (m)
Colville-09	<i>Alnus sp.</i>	0.7	0.37	540325	7633959
Colville-09	<i>Alnus sp.</i>	0.72	0.56	540331	7633958
Colville-09	<i>Alnus sp.</i>	0.72	0.34	540337	7633958
Colville-09	<i>Alnus sp.</i>	1.01	0.56	540352	7633956
Colville-09	<i>Alnus sp.</i>	1	0.82	540355	7633955
Colville-09	<i>Alnus sp.</i>	0.8	0.66	540351	7633934
Colville-09	<i>Alnus sp.</i>	0.66	0.21	540351	7633934
Colville-09	<i>Alnus sp.</i>	0.75	0.43	540323	7633931
Colville-09	<i>Alnus sp.</i>	0.62	0.39	540316	7633932
Colville-09	<i>Alnus sp.</i>	0.66	0.56	540287	7633931
Colville-09	<i>Alnus sp.</i>	0.89	0.64	540265	7633936
Colville-09	<i>Alnus sp.</i>	0.91	0.34	540233	7633937
Colville-09	<i>Alnus sp.</i>	0.63	0.69	540198	7633940
Colville-09	<i>Alnus sp.</i>	0.68	0.34	540198	7633940
Colville-09	<i>Alnus sp.</i>	0.55	0.27	540198	7633940
Colville-09	<i>Alnus sp.</i>	0.79	0.76	540166	7633937
Colville-09	<i>Alnus sp.</i>	0.92	0.65	540153	7633937
Colville-09	<i>Alnus sp.</i>	0.79	0.53	540121	7633908
Colville-09	<i>Alnus sp.</i>	0.79	0.35	540169	7633908
Colville-09	<i>Alnus sp.</i>	0.72	0.92	540239	7633912
Colville-09	<i>Alnus sp.</i>	0.79	0.55	540258	7633912
Colville-09	<i>Alnus sp.</i>	0.74	0.45	540268	7633915
Colville-09	<i>Alnus sp.</i>	0.96	0.36	540326	7633912
Colville-09	<i>Alnus sp.</i>	0.86	0.86	540332	7633913
Colville-09	<i>Alnus sp.</i>	1.05	0.46	540370	7633904
Colville-09	<i>Alnus sp.</i>	0.82	0.64	540326	7633877
Colville-09	<i>Alnus sp.</i>	0.71	0.48	540326	7633877
Colville-09	<i>Alnus sp.</i>	0.79	0.54	540307	7633878
Colville-09	<i>Alnus sp.</i>	1.04	0.34	540307	7633878
Colville-09	<i>Alnus sp.</i>	1.25	0.63	540307	7633878
Colville-09	<i>Alnus sp.</i>	0.68	0.32	540307	7633878
Colville-09	<i>Alnus sp.</i>	1.53	0.77	540293	7633876
Colville-09	<i>Alnus sp.</i>	1.07	0.61	540285	7633875
Colville-09	<i>Alnus sp.</i>	0.87	0.75	540274	7633874
Colville-09	<i>Alnus sp.</i>	1.27	0.57	540256	7633876
Colville-09	<i>Alnus sp.</i>	0.99	0.79	540215	7633880
Colville-09	<i>Alnus sp.</i>	0.65	0.38	540215	7633880

Site	Sp_genus	Canopy_height (m)	Crown_radius (m)	X (m)	Y (m)
Colville-09	<i>Alnus sp.</i>	0.68	0.66	540155	7633885
Colville-09	<i>Alnus sp.</i>	0.78	0.52	540142	7633879
Colville-09	<i>Alnus sp.</i>	0.74	0.43	540153	7633848
Colville-09	<i>Alnus sp.</i>	0.91	0.84	540177	7633853
Colville-09	<i>Alnus sp.</i>	0.96	0.87	540280	7633849
Colville-09	<i>Alnus sp.</i>	0.93	0.65	540298	7633850
Colville-09	<i>Alnus sp.</i>	0.66	0.63	540311	7633851
Colville-09	<i>Alnus sp.</i>	0.77	0.5	540361	7633826
Colville-09	<i>Alnus sp.</i>	0.93	0.95	540347	7633826
Colville-09	<i>Alnus sp.</i>	0.62	0.3	540347	7633826
Colville-09	<i>Alnus sp.</i>	0.82	1.05	540241	7633819
Colville-09	<i>Alnus sp.</i>	1.06	0.92	540228	7633818
Colville-09	<i>Alnus sp.</i>	0.85	0.92	540228	7633818
Colville-09	<i>Alnus sp.</i>	0.89	0.33	540191	7633820
Colville-09	<i>Alnus sp.</i>	0.64	0.84	540151	7633823
Colville-09	<i>Alnus sp.</i>	0.82	0.65	540158	7633805
Colville-09	<i>Alnus sp.</i>	0.86	0.93	540171	7633806
Colville-09	<i>Alnus sp.</i>	0.77	0.95	540196	7633807
Colville-09	<i>Alnus sp.</i>	0.8	1.31	540202	7633805
Colville-09	<i>Alnus sp.</i>	0.66	0.16	540202	7633805
Colville-09	<i>Alnus sp.</i>	0.85	0.61	540213	7633807
Colville-09	<i>Alnus sp.</i>	0.94	1.31	540235	7633811
Colville-09	<i>Alnus sp.</i>	1.03	1.4	540247	7633809
Colville-09	<i>Alnus sp.</i>	1.15	0.78	540323	7633816
Colville-09	<i>Alnus sp.</i>	1.04	0.6	540339	7633818
Colville-09	<i>Alnus sp.</i>	1.27	1.2	540344	7633813
Colville-09	<i>Alnus sp.</i>	1.19	0.49	540358	7633808
Colville-09	<i>Alnus sp.</i>	2.21	1.14	540369	7633802
Colville-09	<i>Alnus sp.</i>	1.18	0.93	540364	7633777
Colville-09	<i>Alnus sp.</i>	2.39	2.97	540357	7633778
Colville-09	<i>Alnus sp.</i>	2.6	1.32	540354	7633777
Colville-09	<i>Alnus sp.</i>	1.47	1.02	540348	7633777
Colville-09	<i>Alnus sp.</i>	1.48	0.71	540337	7633781
Colville-09	<i>Alnus sp.</i>	1.05	0.73	540316	7633780
Colville-09	<i>Alnus sp.</i>	0.75	0.67	540311	7633783
Colville-09	<i>Alnus sp.</i>	1.11	0.51	540269	7633777
Colville-09	<i>Alnus sp.</i>	0.74	0.37	540187	7633749

Site	Sp_genus	Canopy_height (m)	Crown_radius (m)	X (m)	Y (m)
Colville-09	<i>Alnus sp.</i>	1.23	1.08	540213	7633746
Colville-09	<i>Alnus sp.</i>	0.57	0.19	540213	7633746
Colville-09	<i>Alnus sp.</i>	1.23	0.58	540226	7633746
Colville-09	<i>Alnus sp.</i>	0.57	0.33	540226	7633746
Colville-09	<i>Alnus sp.</i>	1.31	0.46	540251	7633746
Colville-09	<i>Alnus sp.</i>	1.61	1.52	540300	7633744
Colville-09	<i>Alnus sp.</i>	1.39	0.93	540320	7633744
Colville-09	<i>Alnus sp.</i>	2.29	0.87	540329	7633744
Colville-09	<i>Alnus sp.</i>	1.49	1.01	540339	7633745
Colville-09	<i>Alnus sp.</i>	2.73	1.31	540343	7633745
Colville-09	<i>Alnus sp.</i>	1.67	1.12	540355	7633744
Colville-09	<i>Alnus sp.</i>	1.6	0.8	540367	7633754
Colville-10	<i>Alnus sp.</i>	1.47	1.02	539601	7630441
Colville-10	<i>Alnus sp.</i>	1.11	0.45	539604	7630418
Colville-10	<i>Alnus sp.</i>	1.05	0.74	539603	7630404
Colville-10	<i>Alnus sp.</i>	0.9	0.75	539603	7630404
Colville-10	<i>Alnus sp.</i>	2.52	1.19	539601	7630337
Colville-10	<i>Alnus sp.</i>	1.28	0.73	539606	7630321
Colville-10	<i>Alnus sp.</i>	2	1.27	539607	7630305
Colville-10	<i>Alnus sp.</i>	3.05	1.99	539603	7630295
Colville-10	<i>Alnus sp.</i>	1.69	1.99	539603	7630295
Colville-10	<i>Alnus sp.</i>	0.82	0.89	539603	7630268
Colville-10	<i>Alnus sp.</i>	1.15	1.67	539603	7630268
Colville-10	<i>Alnus sp.</i>	1.25	3.65	539604	7630237
Colville-10	<i>Alnus sp.</i>	1.3	1.31	539601	7630225
Colville-10	<i>Salix sp.</i>	2.07	1.82	539653	7630206
Colville-10	<i>Alnus sp.</i>	1.48	1.08	539805	7630461
Colville-10	<i>Alnus sp.</i>	1.73	1.24	539806	7630453
Colville-10	<i>Alnus sp.</i>	0.88	0.91	539803	7630442
Colville-10	<i>Alnus sp.</i>	1.29	0.72	539804	7630437
Colville-10	<i>Alnus sp.</i>	1.28	0.79	539804	7630420
Colville-10	<i>Alnus sp.</i>	1.8	0.73	539801	7630371
Colville-10	<i>Alnus sp.</i>	1.24	0.84	539800	7630366
Colville-10	<i>Alnus sp.</i>	2.22	2.45	539800	7630353
Colville-10	<i>Alnus sp.</i>	2.49	1.13	539795	7630343
Colville-10	<i>Alnus sp.</i>	1.62	0.96	539797	7630328
Colville-10	<i>Alnus sp.</i>	1.29	2.06	539794	7630315

Site	Sp_genus	Canopy_height (m)	Crown_radius (m)	X (m)	Y (m)
Colville-10	<i>Alnus sp.</i>	2.79	1.23	539794	7630315
Colville-10	<i>Alnus sp.</i>	2.33	1.16	539804	7630284
Colville-10	<i>Alnus sp.</i>	1.29	1.39	539804	7630284
Colville-10	<i>Alnus sp.</i>	2.45	1.58	539806	7630272
Colville-10	<i>Alnus sp.</i>	1.63	1.38	539804	7630265
Colville-10	<i>Alnus sp.</i>	1.91	1.11	539803	7630259
Colville-10	<i>Alnus sp.</i>	1.21	1.18	539803	7630232
Colville-10	<i>Alnus sp.</i>	0.86	0.96	539801	7630214
Colville-10	<i>Alnus sp.</i>	1.18	0.79	539750	7630218
Colville-10	<i>Alnus sp.</i>	1.58	1.41	539750	7630240
Colville-10	<i>Alnus sp.</i>	2.22	1.29	539751	7630250
Colville-10	<i>Salix sp.</i>	1.52	1.01	539750	7630260
Colville-10	<i>Alnus sp.</i>	2.71	1.87	539747	7630275
Colville-10	<i>Alnus sp.</i>	2.79	1.01	539745	7630287
Colville-10	<i>Alnus sp.</i>	1.81	1.38	539745	7630307
Colville-10	<i>Alnus sp.</i>	0.86	0.85	539745	7630307
Colville-10	<i>Alnus sp.</i>	2.65	2.12	539744	7630329
Colville-10	<i>Alnus sp.</i>	1.92	1.18	539749	7630353
Colville-10	<i>Alnus sp.</i>	2.82	2.77	539747	7630374
Colville-10	<i>Alnus sp.</i>	1.23	0.96	539745	7630382
Colville-10	<i>Alnus sp.</i>	1.42	0.88	539744	7630399
Colville-10	<i>Alnus sp.</i>	0.98	0.89	539742	7630429
Colville-10	<i>Alnus sp.</i>	0.72	0.51	539746	7630447
Colville-10	<i>Alnus sp.</i>	1.22	0.94	539746	7630447
Colville-10	<i>Alnus sp.</i>	1.62	1.15	539746	7630454
Colville-10	<i>Alnus sp.</i>	1.1	1.17	539749	7630463
Colville-10	<i>Alnus sp.</i>	1.58	1.05	539698	7630465
Colville-10	<i>Alnus sp.</i>	1.26	1.46	539698	7630465
Colville-10	<i>Alnus sp.</i>	1.66	1.96	539696	7630431
Colville-10	<i>Alnus sp.</i>	1.03	1.01	539696	7630387
Colville-10	<i>Alnus sp.</i>	0.83	1.21	539696	7630384
Colville-10	<i>Alnus sp.</i>	2.38	2.24	539694	7630362
Colville-10	<i>Alnus sp.</i>	2.01	1.04	539696	7630345
Colville-10	<i>Alnus sp.</i>	1.18	1.08	539696	7630345
Colville-10	<i>Salix sp.</i>	3.21	3.68	539693	7630330
Colville-10	<i>Alnus sp.</i>	1.32	1.37	539689	7630304
Colville-10	<i>Alnus sp.</i>	2.26	2.28	539687	7630276

Site	Sp_genus	Canopy_height (m)	Crown_radius (m)	X (m)	Y (m)
Colville-10	<i>Alnus sp.</i>	0.82	1.19	539680	7630262
Colville-10	<i>Alnus sp.</i>	1.49	2.37	539699	7630209
Colville-10	<i>Alnus sp.</i>	1.37	3.95	539647	7630215
Colville-10	<i>Alnus sp.</i>	3.35	1.95	539655	7630267
Colville-10	<i>Alnus sp.</i>	1.58	1.66	539655	7630267
Colville-10	<i>Alnus sp.</i>	2.62	0.94	539651	7630281
Colville-10	<i>Alnus sp.</i>	2.54	1.4	539651	7630281
Colville-10	<i>Alnus sp.</i>	2.53	0.81	539652	7630289
Colville-10	<i>Alnus sp.</i>	1.86	1.1	539652	7630289
Colville-10	<i>Alnus sp.</i>	1.29	1.21	539655	7630326
Colville-10	<i>Alnus sp.</i>	1.13	2.98	539653	7630338
Colville-10	<i>Alnus sp.</i>	1.22	1.19	539656	7630346
Colville-10	<i>Alnus sp.</i>	0.67	0.75	539654	7630351
Colville-10	<i>Alnus sp.</i>	1.56	0.9	539657	7630414
Colville-10	<i>Alnus sp.</i>	0.79	1.13	539655	7630431
Colville-10	<i>Alnus sp.</i>	1.43	0.39	539653	7630453
Colville-10	<i>Alnus sp.</i>	1.27	0.79	539652	7630462
Colville-11	<i>Salix sp.</i>	4.18	2.76	536830	7630770
Colville-11	<i>Alnus sp.</i>	1.17	1.36	536808	7630776
Colville-11	<i>Alnus sp.</i>	1.75	1.69	536730	7630779
Colville-11	<i>Alnus sp.</i>	1.03	1	536730	7630779
Colville-11	<i>Alnus sp.</i>	1.12	0.37	536659	7630774
Colville-11	<i>Alnus sp.</i>	1.86	1	536659	7630774
Colville-11	<i>Alnus sp.</i>	1.71	1.05	536642	7630774
Colville-11	<i>Alnus sp.</i>	1.35	0.74	536638	7630775
Colville-11	<i>Alnus sp.</i>	1	0.38	536638	7630775
Colville-11	<i>Alnus sp.</i>	1.41	2.02	536629	7630804
Colville-11	<i>Alnus sp.</i>	1.13	0.68	536632	7630802
Colville-11	<i>Alnus sp.</i>	1.01	1.34	536648	7630806
Colville-11	<i>Alnus sp.</i>	1.54	1.24	536658	7630803
Colville-11	<i>Alnus sp.</i>	1.39	0.49	536662	7630804
Colville-11	<i>Alnus sp.</i>	1.46	1.04	536662	7630804
Colville-11	<i>Salix sp.</i>	4.67	1.77	536665	7630804
Colville-11	<i>Salix sp.</i>	4.35	7.34	536793	7630816
Colville-11	<i>Alnus sp.</i>	0.86	0.75	536782	7630838
Colville-11	<i>Alnus sp.</i>	2.06	1.47	536749	7630839
Colville-11	<i>Alnus sp.</i>	2.14	1.28	536749	7630839

Site	Sp_genus	Canopy_height (m)	Crown_radius (m)	X (m)	Y (m)
Colville-11	<i>Alnus sp.</i>	0.77	0.53	536699	7630833
Colville-11	<i>Alnus sp.</i>	0.91	0.53	536699	7630833
Colville-11	<i>Alnus sp.</i>	1.05	0.37	536680	7630830
Colville-11	<i>Alnus sp.</i>	1.69	0.49	536664	7630829
Colville-11	<i>Alnus sp.</i>	0.98	0.9	536664	7630829
Colville-11	<i>Alnus sp.</i>	1.44	0.96	536636	7630828
Colville-11	<i>Alnus sp.</i>	1.28	0.82	536627	7630824
Colville-11	<i>Alnus sp.</i>	0.77	0.71	536619	7630823
Colville-11	<i>Alnus sp.</i>	1.55	0.57	536619	7630823
Colville-11	<i>Alnus sp.</i>	1.66	1.07	536646	7630852
Colville-11	<i>Alnus sp.</i>	1.32	0.73	536663	7630855
Colville-11	<i>Alnus sp.</i>	0.88	0.93	536675	7630852
Colville-11	<i>Alnus sp.</i>	1.11	1.28	536694	7630848
Colville-11	<i>Alnus sp.</i>	0.9	0.97	536702	7630850
Colville-11	<i>Salix sp.</i>	4.06	1.31	536723	7630851
Colville-11	<i>Salix sp.</i>	4.16	2.7	536723	7630851
Colville-11	<i>Salix sp.</i>	1.81	1.48	536776	7630845
Colville-11	<i>Alnus sp.</i>	1.18	0.46	536774	7630880
Colville-11	<i>Alnus sp.</i>	1.18	0.59	536774	7630880
Colville-11	<i>Alnus sp.</i>	1.18	0.79	536774	7630880
Colville-11	<i>Alnus sp.</i>	1.05	0.61	536704	7630883
Colville-11	<i>Alnus sp.</i>	1.01	0.61	536692	7630883
Colville-11	<i>Alnus sp.</i>	1.18	0.56	536678	7630881
Colville-11	<i>Alnus sp.</i>	1.15	0.4	536678	7630881
Colville-11	<i>Alnus sp.</i>	0.93	0.31	536678	7630881
Colville-11	<i>Alnus sp.</i>	0.88	0.95	536650	7630882
Colville-11	<i>Alnus sp.</i>	0.96	0.42	536648	7630918
Colville-11	<i>Alnus sp.</i>	1.32	0.4	536661	7630901
Colville-11	<i>Alnus sp.</i>	1.81	1.5	536661	7630901
Colville-11	<i>Alnus sp.</i>	0.98	0.35	536669	7630903
Colville-11	<i>Alnus sp.</i>	1.24	0.92	536669	7630903
Colville-11	<i>Alnus sp.</i>	1.29	0.92	536669	7630905
Colville-11	<i>Alnus sp.</i>	1.45	0.99	536678	7630904
Colville-11	<i>Alnus sp.</i>	1.29	1.01	536684	7630907
Colville-11	<i>Alnus sp.</i>	1.51	0.7	536690	7630907
Colville-11	<i>Alnus sp.</i>	0.96	0.84	536691	7630904
Colville-11	<i>Alnus sp.</i>	2.67	2.34	536714	7630905

Site	Sp_genus	Canopy_height (m)	Crown_radius (m)	X (m)	Y (m)
Colville-11	<i>Alnus sp.</i>	1.13	1.73	536743	7630907
Colville-11	<i>Alnus sp.</i>	2.17	1.36	536750	7630915
Colville-11	<i>Alnus sp.</i>	1.88	1.55	536747	7630919
Colville-11	<i>Alnus sp.</i>	1.21	1.85	536753	7630915
Colville-11	<i>Alnus sp.</i>	1.61	1.35	536701	7630916
Colville-11	<i>Alnus sp.</i>	1.31	0.38	536692	7630919
Colville-11	<i>Alnus sp.</i>	1.24	0.49	536692	7630919
Colville-11	<i>Alnus sp.</i>	1.66	1.41	536684	7630915
Colville-11	<i>Alnus sp.</i>	1.5	0.92	536657	7630917
Colville-11	<i>Alnus sp.</i>	1.08	0.47	536647	7630917
Colville-11	<i>Alnus sp.</i>	0.83	0.41	536640	7630957
Colville-11	<i>Alnus sp.</i>	1.13	0.82	536659	7630954
Colville-11	<i>Alnus sp.</i>	1.62	1.01	536693	7630953
Colville-11	<i>Salix sp.</i>	4.43	2.9	536704	7630951
Colville-11	<i>Alnus sp.</i>	1.47	0.97	536736	7630952
Colville-11	<i>Alnus sp.</i>	1.55	0.95	536847	7630961
Colville-11	<i>Alnus sp.</i>	1.26	1.39	536860	7630957
Colville-11	<i>Alnus sp.</i>	1.17	1.04	536863	7630956
Colville-11	<i>Alnus sp.</i>	0.94	1.41	536837	7630974
Colville-11	<i>Alnus sp.</i>	1.26	1.35	536837	7630974
Colville-11	<i>Alnus sp.</i>	1.42	0.81	536858	7631004
Colville-11	<i>Alnus sp.</i>	1.69	2.19	536832	7631000
Colville-11	<i>Alnus sp.</i>	2.77	2.08	536780	7631000
Colville-11	<i>Alnus sp.</i>	0.84	1.32	536725	7631000
Colville-11	<i>Alnus sp.</i>	0.8	0.83	536695	7630994
Colville-11	<i>Alnus sp.</i>	1.25	0.82	536682	7630994
Colville-11	<i>Alnus sp.</i>	1.09	0.82	536682	7630994
Colville-11	<i>Alnus sp.</i>	0.86	0.8	536666	7630993
Colville-11	<i>Alnus sp.</i>	1.31	0.79	536635	7630994
Colville-11	<i>Alnus sp.</i>	0.88	0.41	536625	7630997
Colville-11	<i>Alnus sp.</i>	0.86	0.59	536735	7631045
Colville-11	<i>Alnus sp.</i>	1.13	0.76	536670	7630924
Colville-11	<i>Alnus sp.</i>	1.24	1.48	536681	7630919
Colville-11	<i>Alnus sp.</i>	1.82	0.62	536664	7630975
Colville-11	<i>Alnus sp.</i>	5.05	1.09	536693	7630971
Colville-11	<i>Alnus sp.</i>	4.91	1.9	536693	7630971
Colville-12	<i>Alnus sp.</i>	0.92	1.21	528809	7628879

Site	Sp_genus	Canopy_height (m)	Crown_radius (m)	X (m)	Y (m)
Colville-12	<i>Alnus sp.</i>	0.78	0.88	528818	7628878
Colville-12	<i>Salix sp.</i>	0.85	1.07	528833	7628880
Colville-12	<i>Salix sp.</i>	2.63	0.66	528846	7628877
Colville-12	<i>Salix sp.</i>	2.6	1.76	528846	7628877
Colville-12	<i>Salix sp.</i>	2.9	0.87	528862	7628883
Colville-12	<i>Alnus sp.</i>	1.26	0.74	528866	7628881
Colville-12	<i>Alnus sp.</i>	1.24	1.12	528892	7628879
Colville-12	<i>Salix sp.</i>	2.32	1.66	528911	7628881
Colville-12	<i>Alnus sp.</i>	1.58	1.29	528924	7628876
Colville-12	<i>Alnus sp.</i>	1.9	2.26	528941	7628874
Colville-12	<i>Alnus sp.</i>	1.93	1.54	528933	7628928
Colville-12	<i>Alnus sp.</i>	2.41	2.09	528917	7628933
Colville-12	<i>Alnus sp.</i>	1.41	2.56	528900	7628934
Colville-12	<i>Alnus sp.</i>	1.74	1.38	528886	7628930
Colville-12	<i>Salix sp.</i>	1.28	1.1	528852	7628929
Colville-12	<i>Alnus sp.</i>	1.34	1.36	528848	7628930
Colville-12	<i>Alnus sp.</i>	1.75	1.53	528808	7628931
Colville-12	<i>Alnus sp.</i>	2.05	1.1	528798	7628927
Colville-12	<i>Alnus sp.</i>	1.64	1.47	528795	7628929
Colville-12	<i>Salix sp.</i>	1.19	1.23	528771	7628931
Colville-12	<i>Alnus sp.</i>	1.73	1	528765	7628927
Colville-12	<i>Alnus sp.</i>	2.2	1.03	528753	7628921
Colville-12	<i>Alnus sp.</i>	2.2	1.3	528746	7628922
Colville-12	<i>Alnus sp.</i>	1.69	1.13	528686	7628929
Colville-12	<i>Alnus sp.</i>	1.55	0.94	528720	7628920
Colville-12	<i>Alnus sp.</i>	2.33	1.99	528711	7628921
Colville-12	<i>Salix sp.</i>	1.89	1.49	528698	7628920
Colville-12	<i>Alnus sp.</i>	2.54	1.81	528692	7628925
Colville-12	<i>Alnus sp.</i>	1.25	0.62	528687	7628923
Colville-12	<i>Alnus sp.</i>	1.64	2.12	528737	7628976
Colville-12	<i>Salix sp.</i>	1.43	0.96	528739	7628980
Colville-12	<i>Alnus sp.</i>	1.2	1.25	528759	7628991
Colville-12	<i>Alnus sp.</i>	0.76	1.58	528775	7628982
Colville-12	<i>Alnus sp.</i>	0.64	0.45	528783	7628980
Colville-12	<i>Alnus sp.</i>	0.87	0.64	528783	7628980
Colville-12	<i>Alnus sp.</i>	1.17	0.89	528787	7628982
Colville-12	<i>Alnus sp.</i>	1.16	0.87	528807	7628984

Site	Sp_genus	Canopy_height (m)	Crown_radius (m)	X (m)	Y (m)
Colville-12	<i>Alnus sp.</i>	1	1.35	528823	7628982
Colville-12	<i>Salix sp.</i>	1.31	1.83	528843	7628972
Colville-12	<i>Salix sp.</i>	1.71	1.19	528859	7628980
Colville-12	<i>Alnus sp.</i>	1.85	1.14	528868	7628979
Colville-12	<i>Salix sp.</i>	1.77	0.66	528937	7629033
Colville-12	<i>Alnus sp.</i>	1.94	1.34	528937	7629036
Colville-12	<i>Alnus sp.</i>	1.69	0.97	528916	7629044
Colville-12	<i>Alnus sp.</i>	2.44	1.34	528916	7629044
Colville-12	<i>Alnus sp.</i>	2.35	1.51	528896	7629043
Colville-12	<i>Alnus sp.</i>	1.75	1.97	528887	7629043
Colville-12	<i>Alnus sp.</i>	2.41	0.9	528886	7629043
Colville-12	<i>Alnus sp.</i>	1.42	0.65	528886	7629043
Colville-12	<i>Alnus sp.</i>	2.65	0.49	528878	7629040
Colville-12	<i>Alnus sp.</i>	1.99	1.06	528878	7629040
Colville-12	<i>Alnus sp.</i>	1.96	0.99	528866	7629035
Colville-12	<i>Alnus sp.</i>	1.07	2.45	528862	7629037
Colville-12	<i>Salix sp.</i>	2.18	1.22	528838	7629036
Colville-12	<i>Alnus sp.</i>	1.16	1.11	528812	7629032
Colville-12	<i>Alnus sp.</i>	1.54	2.08	528800	7629033
Colville-12	<i>Alnus sp.</i>	1.28	1.26	528760	7629024
Colville-12	<i>Alnus sp.</i>	1.64	1.38	528748	7629022
Colville-12	<i>Alnus sp.</i>	1.31	0.95	528748	7629022
Colville-12	<i>Alnus sp.</i>	1.91	0.91	528737	7629018
Colville-12	<i>Alnus sp.</i>	0.78	0.63	528724	7629019
Colville-12	<i>Alnus sp.</i>	1.22	0.43	528720	7629016
Colville-12	<i>Alnus sp.</i>	1.51	1.8	528779	7629077
Colville-12	<i>Alnus sp.</i>	2.34	1.97	528812	7629077
Colville-12	<i>Alnus sp.</i>	2.4	0.57	528820	7629082
Colville-12	<i>Alnus sp.</i>	1.5	1.3	528820	7629082
Colville-12	<i>Alnus sp.</i>	1.1	0.8	528858	7629082
Colville-12	<i>Alnus sp.</i>	1.03	0.8	528858	7629082
Colville-12	<i>Alnus sp.</i>	0.92	0.4	528858	7629082
Colville-12	<i>Alnus sp.</i>	0.72	1.05	528868	7629078
Colville-12	<i>Alnus sp.</i>	1.22	1.37	528879	7629075
Colville-12	<i>Alnus sp.</i>	1.87	1.55	528908	7629039
Colville-12	<i>Salix sp.</i>	2.15	1.51	528907	7629083
Colville-12	<i>Alnus sp.</i>	2.48	1.98	528913	7629079

Site	Sp_genus	Canopy_height (m)	Crown_radius (m)	X (m)	Y (m)
Colville-12	<i>Alnus sp.</i>	2.71	1.38	528922	7629078
Colville-12	<i>Alnus sp.</i>	0.57	0.48	528700	7628879
Colville-12	<i>Alnus sp.</i>	0.81	0.72	528700	7628879
Colville-12	<i>Alnus sp.</i>	0.87	1.06	528735	7628881
Colville-12	<i>Alnus sp.</i>	1.45	0.84	528745	7628880
Colville-12	<i>Alnus sp.</i>	1.22	0.87	528751	7628874
Colville-13	<i>Betula sp.</i>	0.99	1.04	528649	7628604
Colville-13	<i>Alnus sp.</i>	1.53	1.71	528457	7628611
Colville-13	<i>Alnus sp.</i>	1.8	1.88	528445	7628612
Colville-13	<i>Alnus sp.</i>	1.91	1.75	528428	7628576
Colville-13	<i>Alnus sp.</i>	2.47	1.36	528433	7628574
Colville-13	<i>Alnus sp.</i>	2.73	3.43	528439	7628573
Colville-13	<i>Salix sp.</i>	0.75	1.17	528590	7628574
Colville-13	<i>Alnus sp.</i>	1.32	0.79	528593	7628547
Colville-13	<i>Alnus sp.</i>	1.39	0.76	528558	7628548
Colville-13	<i>Alnus sp.</i>	2.25	2.27	528558	7628548
Colville-13	<i>Alnus sp.</i>	2.2	1.31	528468	7628546
Colville-13	<i>Alnus sp.</i>	2.28	0.97	528468	7628546
Colville-13	<i>Alnus sp.</i>	1.41	1.06	528468	7628546
Colville-13	<i>Salix sp.</i>	2.59	3.69	528445	7628549
Colville-13	<i>Alnus sp.</i>	2.66	1.93	528440	7628548
Colville-13	<i>Salix sp.</i>	1.37	1.46	528431	7628549
Colville-13	<i>Alnus sp.</i>	3	1.63	528430	7628552
Colville-13	<i>Alnus sp.</i>	1.23	0.63	528428	7628521
Colville-13	<i>Alnus sp.</i>	2.67	0.66	528428	7628521
Colville-13	<i>Alnus sp.</i>	1.58	0.83	528437	7628521
Colville-13	<i>Alnus sp.</i>	1.9	1.21	528441	7628520
Colville-13	<i>Alnus sp.</i>	1.22	1.34	528452	7628522
Colville-13	<i>Alnus sp.</i>	1.87	0.88	528461	7628517
Colville-13	<i>Alnus sp.</i>	2.48	1.79	528487	7628517
Colville-13	<i>Salix sp.</i>	2.66	2.3	528496	7628515
Colville-13	<i>Alnus sp.</i>	1.89	0.61	528512	7628513
Colville-13	<i>Alnus sp.</i>	2.19	1.25	528512	7628513
Colville-13	<i>Salix sp.</i>	2.08	2.64	528559	7628506
Colville-13	<i>Salix sp.</i>	4.37	2.52	528584	7628519
Colville-13	<i>Alnus sp.</i>	3.18	3.27	528589	7628508
Colville-13	<i>Betula sp.</i>	1.19	1.02	528617	7628513

Site	Sp_genus	Canopy_height (m)	Crown_radius (m)	X (m)	Y (m)
Colville-13	<i>Alnus sp.</i>	1.3	2.82	528578	7628498
Colville-13	<i>Salix sp.</i>	3.25	2.37	528571	7628510
Colville-13	<i>Salix sp.</i>	1.87	1.53	528559	7628509
Colville-13	<i>Salix sp.</i>	0.9	1.76	528533	7628509
Colville-13	<i>Alnus sp.</i>	2.62	1.68	528501	7628475
Colville-13	<i>Alnus sp.</i>	3.01	2.44	528492	7628480
Colville-13	<i>Salix sp.</i>	1.69	1.48	528485	7628483
Colville-13	<i>Salix sp.</i>	1.74	1.03	528437	7628500
Colville-13	<i>Alnus sp.</i>	1.63	1.28	528427	7628499
Colville-13	<i>Alnus sp.</i>	2.14	1.04	528427	7628499
Colville-13	<i>Alnus sp.</i>	2.7	2.07	528425	7628476
Colville-13	<i>Alnus sp.</i>	3.09	2.02	528469	7628471
Colville-13	<i>Alnus sp.</i>	2.65	1.81	528478	7628468
Colville-13	<i>Salix sp.</i>	1.71	1.12	528487	7628466
Colville-13	<i>Salix sp.</i>	2.17	2.01	528515	7628464
Colville-13	<i>Salix sp.</i>	1.9	2.29	528521	7628459
Colville-13	<i>Salix sp.</i>	0.78	1.84	528593	7628456
Colville-13	<i>Salix sp.</i>	2.2	2.98	528515	7628457
Colville-13	<i>Salix sp.</i>	2.37	1.52	528505	7628460
Colville-13	<i>Alnus sp.</i>	1.53	0.92	528492	7628458
Colville-13	<i>Alnus sp.</i>	1.23	2.1	528482	7628457
Colville-13	<i>Alnus sp.</i>	2.57	0.77	528474	7628456
Colville-13	<i>Alnus sp.</i>	2.43	2.51	528439	7628423
Colville-13	<i>Salix sp.</i>	1.98	1.71	528444	7628418
Colville-13	<i>Alnus sp.</i>	2	1.45	528450	7628418
Colville-13	<i>Alnus sp.</i>	1.94	1.49	528461	7628414
Colville-13	<i>Alnus sp.</i>	1.56	1.21	528471	7628411
Colville-13	<i>Alnus sp.</i>	1.42	1.49	528480	7628410
Colville-13	<i>Alnus sp.</i>	1.42	1.52	528480	7628410
Colville-13	<i>Salix sp.</i>	1.27	0.93	528589	7628407
Colville-13	<i>Salix sp.</i>	2.15	0.97	528599	7628405
Colville-13	<i>Salix sp.</i>	1.25	1.35	528614	7628401
Colville-13	<i>Alnus sp.</i>	1.81	1.13	528481	7628390
Colville-13	<i>Alnus sp.</i>	1.42	1.26	528470	7628399
Colville-13	<i>Alnus sp.</i>	1.79	1.19	528462	7628400
Colville-13	<i>Alnus sp.</i>	1.59	1.28	528453	7628401
Colville-13	<i>Alnus sp.</i>	1.7	2.07	528441	7628400

Site	Sp_genus	Canopy_height (m)	Crown_radius (m)	X (m)	Y (m)
Colville-13	<i>Alnus sp.</i>	2.87	2.01	528458	7628414
Colville-13	<i>Alnus sp.</i>	2.37	1.74	528457	7628365
Colville-13	<i>Salix sp.</i>	2.22	1.28	528478	7628372
Colville-13	<i>Salix sp.</i>	1.43	2.01	528486	7628369
Colville-13	<i>Alnus sp.</i>	3.02	3.14	528576	7628383
Colville-13	<i>Alnus sp.</i>	2.44	1.3	528660	7628378
Colville-13	<i>Alnus sp.</i>	1.91	1.63	528677	7628355
Colville-13	<i>Salix sp.</i>	1.47	0.79	528658	7628347
Colville-13	<i>Salix sp.</i>	1.86	0.38	528658	7628347
Colville-13	<i>Alnus sp.</i>	1.91	1.64	528651	7628348
Colville-13	<i>Salix sp.</i>	2	1.11	528546	7628339
Colville-13	<i>Salix sp.</i>	1.07	1.94	528515	7628319
Colville-13	<i>Salix sp.</i>	2.14	1.25	528508	7628339
Colville-14	<i>Alnus sp.</i>	0.8	0.35	528152	7626827
Colville-14	<i>Alnus sp.</i>	0.9	0.61	528133	7626824
Colville-14	<i>Alnus sp.</i>	0.93	0.27	528113	7626824
Colville-14	<i>Alnus sp.</i>	0.69	0.56	528068	7626820
Colville-14	<i>Alnus sp.</i>	0.62	0.36	528029	7626829
Colville-14	<i>Alnus sp.</i>	0.67	0.71	528006	7626827
Colville-14	<i>Alnus sp.</i>	0.75	1.16	527977	7626830
Colville-14	<i>Alnus sp.</i>	0.92	0.42	527975	7626828
Colville-14	<i>Alnus sp.</i>	0.67	0.9	527960	7626826
Colville-14	<i>Alnus sp.</i>	0.69	0.78	527953	7626827
Colville-14	<i>Alnus sp.</i>	0.75	0.55	527953	7626827
Colville-14	<i>Alnus sp.</i>	1.32	1.01	527964	7626802
Colville-14	<i>Alnus sp.</i>	0.83	0.7	527968	7626802
Colville-14	<i>Alnus sp.</i>	0.88	1.11	527978	7626803
Colville-14	<i>Alnus sp.</i>	0.77	0.87	527998	7626803
Colville-14	<i>Alnus sp.</i>	0.73	0.41	528033	7626802
Colville-14	<i>Alnus sp.</i>	0.69	0.72	528065	7626805
Colville-14	<i>Alnus sp.</i>	0.97	0.86	528077	7626805
Colville-14	<i>Alnus sp.</i>	0.96	0.93	528110	7626807
Colville-14	<i>Alnus sp.</i>	0.69	0.58	528114	7626808
Colville-14	<i>Alnus sp.</i>	0.71	0.56	528157	7626805
Colville-14	<i>Alnus sp.</i>	0.5	0.92	528158	7626779
Colville-14	<i>Alnus sp.</i>	0.62	0.93	528090	7626778
Colville-14	<i>Alnus sp.</i>	0.58	0.44	528078	7626778

Site	Sp_genus	Canopy_height (m)	Crown_radius (m)	X (m)	Y (m)
Colville-14	<i>Alnus sp.</i>	0.57	0.97	528074	7626777
Colville-14	<i>Alnus sp.</i>	0.5	1.54	527992	7626772
Colville-14	<i>Alnus sp.</i>	0.59	0.86	527907	7626779
Colville-14	<i>Alnus sp.</i>	0.85	0.93	527924	7626748
Colville-14	<i>Alnus sp.</i>	0.83	0.44	528063	7626749
Colville-14	<i>Alnus sp.</i>	0.61	0.75	528094	7626747
Colville-14	<i>Alnus sp.</i>	0.64	0.59	528063	7626731
Colville-14	<i>Alnus sp.</i>	0.61	0.51	528063	7626731
Colville-14	<i>Alnus sp.</i>	0.9	0.65	527961	7626701
Colville-14	<i>Alnus sp.</i>	0.69	0.26	528089	7626678
Colville-14	<i>Alnus sp.</i>	0.79	0.74	527975	7626685
Colville-14	<i>Alnus sp.</i>	0.78	1	527913	7626678
Colville-14	<i>Alnus sp.</i>	0.75	0.56	527928	7626652
Colville-14	<i>Alnus sp.</i>	0.57	0.37	527979	7626649
Colville-14	<i>Alnus sp.</i>	1.22	0.77	528087	7626648
Colville-14	<i>Alnus sp.</i>	0.77	0.48	528145	7626639
Colville-14	<i>Salix sp.</i>	0.87	1.1	528103	7626628
Colville-14	<i>Alnus sp.</i>	0.64	0.59	527996	7626627
Colville-14	<i>Alnus sp.</i>	1.09	0.64	528015	7626590
Colville-14	<i>Alnus sp.</i>	0.81	1.04	528015	7626590
Colville-14	<i>Salix sp.</i>	1.09	1.05	528049	7626595
Colville-14	<i>Salix sp.</i>	1.14	1	528102	7626598
Colville-14	<i>Salix sp.</i>	0.79	0.88	528109	7626599
Colville-14	<i>Salix sp.</i>	1.18	0.79	528109	7626599
Colville-14	<i>Salix sp.</i>	0.7	0.79	528127	7626600
Colville-14	<i>Alnus sp.</i>	1.05	0.49	528140	7626603
Colville-14	<i>Alnus sp.</i>	0.87	1.31	528161	7626608

B.2. Shrub structural parameters collected during field campaign along the Dalton Highway in 2011. The column headers mean: *Site*, field site surveyed; *Sp_genus*, species genus; *X* and *Y*, the coordinate location of the shrub in UTM, Zone 5N. A value of -999 represents no shrubs surveyed at that site.

Site	Sp_genus	Canopy_height (m)	Crown_radius (m)	X (m)	Y (m)
Dalton-01	<i>Willow sp.</i>	0.53	0.5	431147	7750248
Dalton-01	<i>Willow sp.</i>	0.68	0.45	431102	7750251
Dalton-01	<i>Willow sp.</i>	0.52	0.38	430980	7750350
Dalton-01	<i>Willow sp.</i>	0.6	0.27	431094	7750394
Dalton-02	<i>Willow sp.</i>	0.61	0.36	431380	7750454
Dalton-03	<i>Willow sp.</i>	0.51	0.53	434854	7705571
Dalton-03	<i>Willow sp.</i>	0.5	0.66	434854	7705571
Dalton-03	<i>Willow sp.</i>	0.57	0.66	434871	7705570
Dalton-03	<i>Willow sp.</i>	0.55	0.85	434888	7705572
Dalton-03	<i>Willow sp.</i>	0.51	0.68	434936	7705573
Dalton-03	<i>Willow sp.</i>	0.6	0.48	434972	7705572
Dalton-03	<i>Willow sp.</i>	0.71	1.16	434991	7705571
Dalton-03	<i>Willow sp.</i>	0.51	0.55	434991	7705571
Dalton-03	<i>Willow sp.</i>	0.5	0.36	435071	7705573
Dalton-03	<i>Birch sp.</i>	0.5	0.73	435062	7705528
Dalton-03	<i>Willow sp.</i>	0.57	0.69	435032	7705527
Dalton-03	<i>Willow sp.</i>	0.6	0.45	435026	7705528
Dalton-03	<i>Willow sp.</i>	0.5	0.81	435022	7705523
Dalton-03	<i>Willow sp.</i>	0.56	0.38	435010	7705524
Dalton-03	<i>Willow sp.</i>	0.57	0.42	435000	7705521
Dalton-03	<i>Willow sp.</i>	0.83	0.3	434996	7705523
Dalton-03	<i>Willow sp.</i>	0.53	0.26	434990	7705526
Dalton-03	<i>Willow sp.</i>	0.54	0.47	434979	7705522
Dalton-03	<i>Willow sp.</i>	0.56	0.57	434972	7705523
Dalton-03	<i>Willow sp.</i>	0.53	0.54	434972	7705523
Dalton-03	<i>Willow sp.</i>	0.55	0.64	434966	7705526
Dalton-03	<i>Willow sp.</i>	0.57	0.89	434957	7705524
Dalton-03	<i>Willow sp.</i>	0.75	0.57	434953	7705525
Dalton-03	<i>Willow sp.</i>	0.67	0.42	434948	7705523
Dalton-03	<i>Willow sp.</i>	0.5	0.67	434942	7705526

Site	Sp_genus	Canopy_height (m)	Crown_radius (m)	X (m)	Y (m)
Dalton-03	<i>Willow sp.</i>	0.5	0.25	434923	7705526
Dalton-03	<i>Willow sp.</i>	0.54	1.02	434923	7705526
Dalton-03	<i>Willow sp.</i>	0.65	0.42	434914	7705523
Dalton-03	<i>Willow sp.</i>	0.57	0.75	434907	7705521
Dalton-03	<i>Willow sp.</i>	0.57	0.44	434904	7705524
Dalton-03	<i>Willow sp.</i>	0.6	0.3	434895	7705523
Dalton-03	<i>Willow sp.</i>	0.53	0.22	434856	7705521
Dalton-03	<i>Willow sp.</i>	0.58	0.3	434865	7705474
Dalton-03	<i>Willow sp.</i>	0.54	0.58	434899	7705475
Dalton-03	<i>Willow sp.</i>	0.51	0.36	434899	7705475
Dalton-03	<i>Willow sp.</i>	0.62	0.61	434907	7705472
Dalton-03	<i>Willow sp.</i>	0.53	0.48	434912	7705475
Dalton-03	<i>Willow sp.</i>	0.53	0.73	434912	7705475
Dalton-03	<i>Willow sp.</i>	0.51	0.41	434921	7705476
Dalton-03	<i>Willow sp.</i>	0.59	0.38	434928	7705473
Dalton-03	<i>Willow sp.</i>	0.5	0.3	434928	7705473
Dalton-03	<i>Willow sp.</i>	0.51	0.34	434994	7705473
Dalton-03	<i>Willow sp.</i>	0.57	0.21	435006	7705470
Dalton-03	<i>Willow sp.</i>	0.58	0.28	435006	7705470
Dalton-03	<i>Willow sp.</i>	0.54	0.32	435006	7705470
Dalton-03	<i>Willow sp.</i>	0.58	0.24	435058	7705475
Dalton-03	<i>Willow sp.</i>	0.5	0.46	435060	7705475
Dalton-03	<i>Willow sp.</i>	0.6	0.18	435060	7705475
Dalton-03	<i>Willow sp.</i>	0.57	1	435071	7705423
Dalton-03	<i>Willow sp.</i>	0.68	0.41	435053	7705420
Dalton-03	<i>Willow sp.</i>	0.5	0.39	435053	7705420
Dalton-03	<i>Willow sp.</i>	0.52	0.34	435038	7705419
Dalton-03	<i>Willow sp.</i>	0.56	0.34	435032	7705418
Dalton-03	<i>Willow sp.</i>	0.6	0.35	435032	7705418
Dalton-03	<i>Willow sp.</i>	0.5	0.53	435032	7705418
Dalton-03	<i>Willow sp.</i>	0.67	0.55	435006	7705419
Dalton-03	<i>Willow sp.</i>	0.57	0.26	434993	7705418
Dalton-03	<i>Willow sp.</i>	0.67	0.46	434986	7705419
Dalton-03	<i>Willow sp.</i>	0.51	0.55	434986	7705419
Dalton-03	<i>Willow sp.</i>	0.72	0.45	434965	7705419
Dalton-03	<i>Willow sp.</i>	0.52	0.51	434947	7705418
Dalton-03	<i>Willow sp.</i>	0.52	0.57	434947	7705418

Site	Sp_genus	Canopy_height (m)	Crown_radius (m)	X (m)	Y (m)
Dalton-03	<i>Willow sp.</i>	0.64	0.93	434937	7705417
Dalton-03	<i>Willow sp.</i>	0.6	0.23	434932	7705417
Dalton-03	<i>Willow sp.</i>	0.6	0.28	434932	7705417
Dalton-03	<i>Willow sp.</i>	0.53	0.27	434932	7705417
Dalton-03	<i>Willow sp.</i>	0.66	0.52	434932	7705417
Dalton-03	<i>Willow sp.</i>	0.67	0.4	434932	7705417
Dalton-03	<i>Willow sp.</i>	0.5	0.59	434932	7705417
Dalton-03	<i>Willow sp.</i>	0.58	0.15	434871	7705420
Dalton-03	<i>Willow sp.</i>	0.67	0.16	434871	7705420
Dalton-03	<i>Willow sp.</i>	0.6	0.46	434356	7705418
Dalton-03	<i>Willow sp.</i>	0.55	0.74	434356	7705418
Dalton-03	<i>Willow sp.</i>	0.54	0.69	434356	7705418
Dalton-03	<i>Willow sp.</i>	0.61	0.4	434356	7705418
Dalton-03	<i>Willow sp.</i>	0.59	1.15	434859	7705375
Dalton-03	<i>Willow sp.</i>	0.53	0.43	434895	7705374
Dalton-03	<i>Willow sp.</i>	0.67	0.76	434947	7705373
Dalton-03	<i>Willow sp.</i>	0.53	0.67	434986	7705376
Dalton-03	<i>Willow sp.</i>	0.51	0.42	435013	7705375
Dalton-03	<i>Willow sp.</i>	0.55	0.64	435013	7705375
Dalton-03	<i>Willow sp.</i>	0.59	0.6	435029	7705372
Dalton-03	<i>Willow sp.</i>	0.59	0.33	735048	7705370
Dalton-04	<i>Willow sp.</i>	0.57	0.89	435083	7705302
Dalton-04	<i>Willow sp.</i>	0.58	0.67	435104	7705298
Dalton-04	<i>Willow sp.</i>	0.75	0.95	435116	7705299
Dalton-04	<i>Willow sp.</i>	0.6	0.5	435120	7705297
Dalton-04	<i>Willow sp.</i>	0.5	0.18	435120	7705297
Dalton-04	<i>Willow sp.</i>	0.5	0.75	435120	7705297
Dalton-04	<i>Willow sp.</i>	0.63	0.66	435120	7705297
Dalton-04	<i>Willow sp.</i>	0.52	0.26	435140	7705298
Dalton-04	<i>Willow sp.</i>	0.65	0.58	435140	7705298
Dalton-04	<i>Willow sp.</i>	0.56	0.3	435140	7705298
Dalton-04	<i>Willow sp.</i>	0.71	0.38	435179	7705298
Dalton-04	<i>Willow sp.</i>	0.51	0.45	435216	7705299
Dalton-04	<i>Willow sp.</i>	0.68	0.34	435282	7705249
Dalton-04	<i>Willow sp.</i>	0.5	0.15	435282	7705249
Dalton-04	<i>Willow sp.</i>	0.59	0.89	435282	7705249
Dalton-04	<i>Willow sp.</i>	0.67	1	435282	7705249

Site	Sp_genus	Canopy_height (m)	Crown_radius (m)	X (m)	Y (m)
Dalton-04	<i>Willow sp.</i>	0.6	0.39	435269	7705250
Dalton-04	<i>Willow sp.</i>	0.7	0.75	435250	7705248
Dalton-04	<i>Willow sp.</i>	0.56	0.39	435236	7705248
Dalton-04	<i>Willow sp.</i>	0.51	0.24	435232	7705247
Dalton-04	<i>Willow sp.</i>	0.51	0.3	435216	7705247
Dalton-04	<i>Willow sp.</i>	0.69	0.47	435190	7705249
Dalton-04	<i>Willow sp.</i>	0.58	0.49	435168	7705251
Dalton-04	<i>Willow sp.</i>	0.61	0.43	435168	7705251
Dalton-04	<i>Willow sp.</i>	0.52	0.55	435110	7705251
Dalton-04	<i>Willow sp.</i>	0.58	0.46	435106	7705249
Dalton-04	<i>Willow sp.</i>	0.58	0.48	435098	7705248
Dalton-04	<i>Willow sp.</i>	0.75	0.53	435078	7705249
Dalton-04	<i>Willow sp.</i>	0.63	0.27	435078	7705249
Dalton-04	<i>Willow sp.</i>	0.6	0.25	435078	7705249
Dalton-04	<i>Willow sp.</i>	0.92	1.22	435071	7705202
Dalton-04	<i>Willow sp.</i>	0.63	0.73	435071	7705202
Dalton-04	<i>Willow sp.</i>	0.76	0.22	435076	7705202
Dalton-04	<i>Willow sp.</i>	0.53	0.5	435076	7705202
Dalton-04	<i>Willow sp.</i>	0.52	0.25	435091	7705205
Dalton-04	<i>Willow sp.</i>	0.53	0.51	435102	7705200
Dalton-04	<i>Willow sp.</i>	0.5	0.63	435102	7705200
Dalton-04	<i>Willow sp.</i>	0.5	0.23	435102	7705200
Dalton-04	<i>Willow sp.</i>	0.54	0.43	435155	7705202
Dalton-04	<i>Willow sp.</i>	0.58	0.52	435155	7705202
Dalton-04	<i>Willow sp.</i>	0.59	0.6	435160	7705199
Dalton-04	<i>Willow sp.</i>	0.51	0.41	435168	7705201
Dalton-04	<i>Willow sp.</i>	0.57	0.54	435221	7705198
Dalton-04	<i>Willow sp.</i>	0.64	0.38	435221	7705198
Dalton-04	<i>Willow sp.</i>	0.58	0.54	435228	7705200
Dalton-04	<i>Willow sp.</i>	0.51	0.54	435228	7705200
Dalton-04	<i>Willow sp.</i>	0.55	1.13	435251	7705198
Dalton-04	<i>Willow sp.</i>	0.5	0.3	435251	7705198
Dalton-04	<i>Willow sp.</i>	0.63	0.49	435251	7705198
Dalton-04	<i>Willow sp.</i>	0.57	0.6	435251	7705198
Dalton-04	<i>Willow sp.</i>	0.56	0.35	435278	7705199
Dalton-04	<i>Willow sp.</i>	0.65	0.43	435278	7705199
Dalton-04	<i>Willow sp.</i>	0.54	0.49	435278	7705199

Site	Sp_genus	Canopy_height (m)	Crown_radius (m)	X (m)	Y (m)
Dalton-04	<i>Willow sp.</i>	0.64	0.71	435283	7705202
Dalton-04	<i>Willow sp.</i>	0.5	0.19	435283	7705152
Dalton-04	<i>Willow sp.</i>	0.54	0.12	435278	7705152
Dalton-04	<i>Willow sp.</i>	0.56	0.61	435269	7705150
Dalton-04	<i>Willow sp.</i>	0.56	0.47	435253	7705150
Dalton-04	<i>Willow sp.</i>	0.53	0.29	435253	7705150
Dalton-04	<i>Willow sp.</i>	0.5	0.22	435245	7705149
Dalton-04	<i>Willow sp.</i>	0.52	0.23	435223	7705149
Dalton-04	<i>Willow sp.</i>	0.8	0.51	435223	7705149
Dalton-04	<i>Willow sp.</i>	0.89	0.29	435223	7705149
Dalton-04	<i>Willow sp.</i>	0.94	0.83	435223	7705149
Dalton-04	<i>Willow sp.</i>	0.62	0.58	435075	7705100
Dalton-04	<i>Willow sp.</i>	0.6	0.37	435095	7705097
Dalton-04	<i>Willow sp.</i>	0.56	0.59	435095	7705097
Dalton-04	<i>Willow sp.</i>	0.71	0.71	435095	7705097
Dalton-04	<i>Willow sp.</i>	0.75	0.74	435090	7705097
Dalton-04	<i>Willow sp.</i>	0.77	0.49	435090	7705097
Dalton-04	<i>Birch sp.</i>	0.54	0.36	435090	7705097
Dalton-04	<i>Willow sp.</i>	0.85	1.55	435092	7705099
Dalton-04	<i>Birch sp.</i>	0.64	0.39	435092	7705099
Dalton-04	<i>Willow sp.</i>	0.51	0.22	435094	7705094
Dalton-04	<i>Willow sp.</i>	0.55	0.29	435094	7705094
Dalton-04	<i>Birch sp.</i>	0.51	0.92	435096	7705097
Dalton-04	<i>Willow sp.</i>	0.57	0.56	435107	7705094
Dalton-04	<i>Willow sp.</i>	0.56	0.13	435122	7705095
Dalton-04	<i>Willow sp.</i>	0.57	0.56	435128	7705097
Dalton-04	<i>Birch sp.</i>	0.76	2.84	435128	7705097
Dalton-04	<i>Birch sp.</i>	0.51	2.01	435142	7705096
Dalton-04	<i>Willow sp.</i>	0.55	0.81	435155	7705093
Dalton-05	<i>Willow sp.</i>	0.77	0.28	426126	7660750
Dalton-05	<i>Willow sp.</i>	0.57	0.39	426114	7660750
Dalton-05	<i>Willow sp.</i>	0.53	0.44	426114	7660750
Dalton-05	<i>Willow sp.</i>	0.55	0.24	426094	7660747
Dalton-05	<i>Willow sp.</i>	0.85	0.3	426089	7660748
Dalton-05	<i>Willow sp.</i>	0.5	0.45	426089	7660748
Dalton-05	<i>Willow sp.</i>	0.62	0.22	426081	7660746
Dalton-05	<i>Willow sp.</i>	0.66	0.48	426075	7660749

Site	Sp_genus	Canopy_height (m)	Crown_radius (m)	X (m)	Y (m)
Dalton-05	<i>Birch sp.</i>	0.59	0.14	426071	7660747
Dalton-05	<i>Willow sp.</i>	0.65	0.46	426065	7660744
Dalton-05	<i>Willow sp.</i>	0.5	0.53	426057	7660743
Dalton-05	<i>Willow sp.</i>	0.6	0.59	426034	7660744
Dalton-05	<i>Willow sp.</i>	0.5	0.39	426020	7660742
Dalton-05	<i>Willow sp.</i>	0.5	0.32	426025	7660804
Dalton-05	<i>Willow sp.</i>	0.55	0.17	426045	7660804
Dalton-05	<i>Willow sp.</i>	0.54	0.28	426049	7660803
Dalton-05	<i>Willow sp.</i>	0.59	0.44	426079	7660802
Dalton-05	<i>Willow sp.</i>	0.57	0.29	426079	7660802
Dalton-05	<i>Willow sp.</i>	0.51	0.52	426116	7660855
Dalton-05	<i>Willow sp.</i>	0.5	0.24	426030	7660906
Dalton-06	<i>Birch sp.</i>	0.51	1.08	426587	7660447
Dalton-06	<i>Willow sp.</i>	0.63	1.1	426587	7660447
Dalton-06	<i>Willow sp.</i>	0.93	0.34	426583	7660447
Dalton-06	<i>Willow sp.</i>	0.87	0.87	426583	7660447
Dalton-06	<i>Willow sp.</i>	0.87	0.36	426583	7660447
Dalton-06	<i>Willow sp.</i>	0.71	0.44	426578	7660450
Dalton-06	<i>Willow sp.</i>	0.79	0.34	426578	7660450
Dalton-06	<i>Willow sp.</i>	0.79	0.36	426578	7660450
Dalton-06	<i>Willow sp.</i>	0.81	0.67	426578	7660450
Dalton-06	<i>Willow sp.</i>	0.81	0.59	426578	7660450
Dalton-06	<i>Willow sp.</i>	0.51	0.57	426578	7660450
Dalton-06	<i>Willow sp.</i>	0.85	0.57	426578	7660450
Dalton-06	<i>Willow sp.</i>	0.76	0.28	426578	7660450
Dalton-06	<i>Willow sp.</i>	0.75	1.26	426572	7660452
Dalton-06	<i>Willow sp.</i>	0.83	0.74	426572	7660452
Dalton-06	<i>Willow sp.</i>	0.62	0.47	426572	7660452
Dalton-06	<i>Willow sp.</i>	0.9	0.74	426573	7660448
Dalton-06	<i>Willow sp.</i>	0.61	0.87	426573	7660448
Dalton-06	<i>Willow sp.</i>	1.02	0.79	426569	7660448
Dalton-06	<i>Willow sp.</i>	0.78	0.67	426569	7660448
Dalton-06	<i>Willow sp.</i>	1.18	0.54	426569	7660448
Dalton-06	<i>Willow sp.</i>	0.91	1.07	426569	7660452
Dalton-06	<i>Willow sp.</i>	0.88	1.48	426569	7660452
Dalton-06	<i>Willow sp.</i>	0.96	0.66	426459	7660451
Dalton-06	<i>Willow sp.</i>	0.99	0.58	426459	7660451

Site	Sp_genus	Canopy_height (m)	Crown_radius (m)	X (m)	Y (m)
Dalton-06	<i>Willow sp.</i>	1.11	1.77	426459	7660451
Dalton-06	<i>Willow sp.</i>	0.67	0.42	426511	7660495
Dalton-06	<i>Willow sp.</i>	0.84	0.74	426514	7660497
Dalton-06	<i>Willow sp.</i>	1.01	2.83	426520	7660497
Dalton-06	<i>Willow sp.</i>	0.82	0.96	426520	7660494
Dalton-06	<i>Willow sp.</i>	0.75	1.5	426529	7660496
Dalton-06	<i>Birch sp.</i>	0.64	1.21	426529	7660496
Dalton-06	<i>Birch sp.</i>	0.89	1.34	426529	7660496
Dalton-06	<i>Birch sp.</i>	0.84	0.99	426531	7660495
Dalton-06	<i>Birch sp.</i>	0.9	0.9	426531	7660495
Dalton-06	<i>Birch sp.</i>	0.59	2.1	426531	7660495
Dalton-06	<i>Birch sp.</i>	0.7	1.25	426543	7660494
Dalton-06	<i>Willow sp.</i>	0.68	0.3	426593	7660552
Dalton-06	<i>Birch sp.</i>	0.58	0.88	426467	7660552
Dalton-06	<i>Birch sp.</i>	0.77	1.75	426465	7660551
Dalton-06	<i>Birch sp.</i>	0.82	0.67	426464	7660552
Dalton-06	<i>Birch sp.</i>	0.65	0.83	426464	7660552
Dalton-06	<i>Birch sp.</i>	0.62	0.6	426464	7660552
Dalton-06	<i>Willow sp.</i>	1.1	1.23	426461	7660552
Dalton-06	<i>Willow sp.</i>	0.74	0.39	426461	7660552
Dalton-06	<i>Willow sp.</i>	0.8	0.26	426461	7660552
Dalton-06	<i>Willow sp.</i>	0.87	0.86	426454	7660554
Dalton-06	<i>Willow sp.</i>	1	0.99	426454	7660554
Dalton-06	<i>Willow sp.</i>	0.92	0.86	426454	7660554
Dalton-06	<i>Willow sp.</i>	0.68	0.7	426454	7660554
Dalton-06	<i>Birch sp.</i>	0.77	0.95	426449	7660552
Dalton-06	<i>Willow sp.</i>	1.07	0.73	426449	7660552
Dalton-06	<i>Willow sp.</i>	1.27	1.47	426449	7660552
Dalton-06	<i>Willow sp.</i>	0.79	1.96	426445	7660554
Dalton-06	<i>Willow sp.</i>	1.31	2.24	426445	7660554
Dalton-06	<i>Willow sp.</i>	1.1	2.05	426445	7660554
Dalton-06	<i>Willow sp.</i>	1.18	2.2	426441	7660555
Dalton-06	<i>Willow sp.</i>	0.76	1.1	426441	7660555
Dalton-06	<i>Willow sp.</i>	0.87	1.36	426435	7660560
Dalton-06	<i>Willow sp.</i>	0.9	1.64	426435	7660560
Dalton-06	<i>Willow sp.</i>	0.72	1.68	426435	7660560
Dalton-06	<i>Birch sp.</i>	0.58	0.86	426428	7660562

Site	Sp_genus	Canopy_height (m)	Crown_radius (m)	X (m)	Y (m)
Dalton-06	<i>Willow sp.</i>	0.7	1.39	426428	7660562
Dalton-06	<i>Willow sp.</i>	0.51	0.72	426409	7660601
Dalton-06	<i>Willow sp.</i>	0.7	1.3	426413	7660600
Dalton-06	<i>Willow sp.</i>	0.67	1.32	426413	7660600
Dalton-06	<i>Willow sp.</i>	0.63	1.03	426413	7660600
Dalton-06	<i>Willow sp.</i>	0.64	1.3	426418	7660598
Dalton-06	<i>Willow sp.</i>	1.01	1.29	426418	7660598
Dalton-06	<i>Willow sp.</i>	0.73	0.71	426424	7660597
Dalton-06	<i>Willow sp.</i>	0.69	0.9	426424	7660597
Dalton-06	<i>Willow sp.</i>	0.68	0.59	426506	7660591
Dalton-06	<i>Birch sp.</i>	0.6	0.12	426511	7660589
Dalton-06	<i>Willow sp.</i>	0.61	0.29	426590	7660651
Dalton-06	<i>Willow sp.</i>	0.53	0.3	426460	7660649
Dalton-06	<i>Willow sp.</i>	0.67	1.05	426460	7660649
Dalton-06	<i>Willow sp.</i>	0.83	1.13	426432	7660650
Dalton-06	<i>Willow sp.</i>	0.71	1.15	426425	7660650
Dalton-06	<i>Willow sp.</i>	0.77	1.12	426425	7660650
Dalton-06	<i>Birch sp.</i>	0.52	1.79	426421	7660649
Dalton-06	<i>Birch sp.</i>	0.66	0.84	426410	7660650
Dalton-07	<i>Birch sp.</i>	0.5	0.81	426159	7643100
Dalton-07	<i>Birch sp.</i>	0.68	0.78	426159	7643100
Dalton-07	<i>Birch sp.</i>	0.54	0.56	426027	7643050
Dalton-07	<i>Birch sp.</i>	0.56	0.59	426016	7643048
Dalton-07	<i>Willow sp.</i>	0.59	0.25	426010	7643047
Dalton-07	<i>Birch sp.</i>	0.57	0.21	426090	7643001
Dalton-07	<i>Birch sp.</i>	0.5	0.27	426144	7643000
Dalton-07	<i>Willow sp.</i>	0.58	0.23	426150	7643001
Dalton-07	<i>Willow sp.</i>	0.65	0.54	426164	7643002
Dalton-07	<i>Willow sp.</i>	0.56	0.62	426174	7643003
Dalton-07	<i>Willow sp.</i>	0.75	0.51	426179	7643001
Dalton-07	<i>Willow sp.</i>	0.53	0.18	426182	7643001
Dalton-07	<i>Willow sp.</i>	0.63	0.16	426182	7643001
Dalton-07	<i>Willow sp.</i>	0.59	0.16	426188	7643001
Dalton-07	<i>Willow sp.</i>	0.58	0.43	426212	7642998
Dalton-07	<i>Willow sp.</i>	0.56	0.37	426217	7642997
Dalton-07	<i>Willow sp.</i>	0.56	0.26	426222	7643000
Dalton-07	<i>Willow sp.</i>	0.59	0.61	426222	7643000

Site	Sp_genus	Canopy_height (m)	Crown_radius (m)	X (m)	Y (m)
Dalton-07	<i>Willow sp.</i>	0.53	0.74	426207	7642945
Dalton-07	<i>Willow sp.</i>	0.72	0.57	426207	7642945
Dalton-07	<i>Willow sp.</i>	0.56	0.47	426207	7642945
Dalton-07	<i>Willow sp.</i>	0.58	0.51	426206	7642945
Dalton-07	<i>Willow sp.</i>	0.53	0.25	426207	7642947
Dalton-07	<i>Willow sp.</i>	0.61	0.25	426205	7642948
Dalton-07	<i>Willow sp.</i>	0.54	0.46	426166	7642948
Dalton-07	<i>Willow sp.</i>	0.59	0.27	426158	7642950
Dalton-07	<i>Willow sp.</i>	0.51	1.37	426153	7642944
Dalton-07	<i>Willow sp.</i>	0.57	0.72	426149	7642949
Dalton-07	<i>Willow sp.</i>	0.64	0.91	426143	7642950
Dalton-08	<i>Willow sp.</i>	0.52	0.18	425953	7642448
Dalton-08	<i>Willow sp.</i>	0.62	0.47	425976	7642444
Dalton-08	<i>Willow sp.</i>	0.55	0.3	425982	7642443
Dalton-08	<i>Willow sp.</i>	0.72	0.65	425986	7642443
Dalton-08	<i>Willow sp.</i>	0.76	0.25	425989	7642447
Dalton-08	<i>Willow sp.</i>	0.65	0.44	426053	7642437
Dalton-08	<i>Willow sp.</i>	0.66	0.28	426056	7642436
Dalton-08	<i>Willow sp.</i>	0.74	0.75	426056	7642436
Dalton-08	<i>Willow sp.</i>	0.56	0.25	426092	7642438
Dalton-08	<i>Willow sp.</i>	0.62	0.22	426131	7642436
Dalton-08	<i>Willow sp.</i>	0.72	0.63	426131	7642436
Dalton-08	<i>Willow sp.</i>	0.58	0.29	426131	7642436
Dalton-08	<i>Willow sp.</i>	0.8	0.5	426131	7642436
Dalton-08	<i>Willow sp.</i>	0.51	0.77	426131	7642436
Dalton-08	<i>Willow sp.</i>	0.53	0.49	426134	7642437
Dalton-08	<i>Willow sp.</i>	0.69	0.56	426138	7642436
Dalton-08	<i>Willow sp.</i>	0.6	0.24	426143	7642433
Dalton-08	<i>Birch sp.</i>	0.62	0.52	426143	7642433
Dalton-08	<i>Willow sp.</i>	0.55	0.49	426143	7642433
Dalton-08	<i>Willow sp.</i>	0.51	0.3	426143	7642433
Dalton-08	<i>Birch sp.</i>	0.69	0.39	426143	7642433
Dalton-08	<i>Birch sp.</i>	0.71	0.52	426143	7642433
Dalton-08	<i>Willow sp.</i>	0.67	0.61	426145	7642435
Dalton-08	<i>Willow sp.</i>	0.51	0.32	426150	7642437
Dalton-08	<i>Willow sp.</i>	0.67	0.35	426150	7642437
Dalton-08	<i>Willow sp.</i>	0.51	0.2	426156	7642432

Site	Sp_genus	Canopy_height (m)	Crown_radius (m)	X (m)	Y (m)
Dalton-08	<i>Willow sp.</i>	0.69	0.34	426162	7642434
Dalton-08	<i>Willow sp.</i>	0.87	0.35	426162	7642434
Dalton-08	<i>Willow sp.</i>	0.9	0.2	426162	7642434
Dalton-08	<i>Willow sp.</i>	0.73	0.37	426162	7642434
Dalton-08	<i>Willow sp.</i>	0.62	0.47	426167	7642433
Dalton-08	<i>Willow sp.</i>	0.5	0.41	426036	7642496
Dalton-08	<i>Willow sp.</i>	0.62	0.34	425953	7642504
Dalton-08	<i>Willow sp.</i>	0.64	0.61	425977	7642546
Dalton-08	<i>Willow sp.</i>	0.6	0.13	426051	7642551
Dalton-08	<i>Willow sp.</i>	0.58	0.32	426051	7642551
Dalton-08	<i>Willow sp.</i>	0.61	0.46	426063	7642553
Dalton-08	<i>Willow sp.</i>	0.72	0.36	426126	7642553
Dalton-08	<i>Willow sp.</i>	0.67	0.2	426140	7642557
Dalton-08	<i>Alder sp.</i>	0.91	1.06	426168	7642558
Dalton-08	<i>Alder sp.</i>	0.73	1.37	426168	7642558
Dalton-08	<i>Alder sp.</i>	0.78	1.14	426175	7642557
Dalton-08	<i>Willow sp.</i>	0.58	0.17	426161	7642603
Dalton-08	<i>Willow sp.</i>	0.53	0.41	426158	7642602
Dalton-08	<i>Willow sp.</i>	0.52	0.21	426150	7642601
Dalton-08	<i>Willow sp.</i>	0.57	0.26	426150	7642601
Dalton-08	<i>Willow sp.</i>	0.6	0.19	426150	7642601
Dalton-08	<i>Willow sp.</i>	0.55	0.26	426143	7642602
Dalton-08	<i>Willow sp.</i>	0.5	0.36	426140	7642600
Dalton-08	<i>Willow sp.</i>	0.57	0.2	426140	7642600
Dalton-08	<i>Willow sp.</i>	0.52	0.4	426138	7642602
Dalton-08	<i>Willow sp.</i>	0.59	0.22	426131	7642606
Dalton-08	<i>Willow sp.</i>	0.65	0.66	426131	7642606
Dalton-08	<i>Willow sp.</i>	0.52	0.45	426131	7642606
Dalton-08	<i>Alder sp.</i>	0.85	1.38	426131	7642606
Dalton-08	<i>Willow sp.</i>	0.57	0.23	426131	7642606
Dalton-08	<i>Willow sp.</i>	0.68	0.25	426131	7642606
Dalton-08	<i>Willow sp.</i>	0.71	0.65	426131	7642606
Dalton-08	<i>Willow sp.</i>	0.52	0.52	426131	7642606
Dalton-08	<i>Willow sp.</i>	0.74	0.56	426131	7642606
Dalton-08	<i>Willow sp.</i>	0.54	0.22	426131	7642606
Dalton-08	<i>Willow sp.</i>	0.73	0.41	426116	7642601
Dalton-08	<i>Willow sp.</i>	0.55	0.41	426105	7642600

Site	Sp_genus	Canopy_height (m)	Crown_radius (m)	X (m)	Y (m)
Dalton-08	<i>Willow sp.</i>	0.71	0.53	426099	7642600
Dalton-08	<i>Willow sp.</i>	0.59	0.47	426099	7642600
Dalton-08	<i>Willow sp.</i>	0.54	0.31	426094	7642596
Dalton-08	<i>Willow sp.</i>	0.6	0.42	426088	7642594
Dalton-08	<i>Willow sp.</i>	0.69	0.31	426068	7642598
Dalton-08	<i>Willow sp.</i>	0.5	0.18	425981	7642599
Dalton-08	<i>Willow sp.</i>	0.52	0.23	425963	7642601
Dalton-08	<i>Willow sp.</i>	0.59	0.74	425969	7642653
Dalton-08	<i>Willow sp.</i>	0.59	0.94	426035	7642647
Dalton-08	<i>Willow sp.</i>	0.64	1.37	426040	7642648
Dalton-08	<i>Willow sp.</i>	0.57	0.46	426046	7642651
Dalton-08	<i>Willow sp.</i>	0.7	1.35	426046	7642651
Dalton-08	<i>Willow sp.</i>	0.79	0.97	426051	7642651
Dalton-08	<i>Willow sp.</i>	0.86	0.7	426051	7642649
Dalton-08	<i>Willow sp.</i>	0.53	0.57	426051	7642649
Dalton-08	<i>Birch sp.</i>	0.63	0.8	426065	7642652
Dalton-08	<i>Willow sp.</i>	0.79	1.25	426069	7642650
Dalton-08	<i>Willow sp.</i>	0.82	0.26	426072	7642652
Dalton-08	<i>Willow sp.</i>	0.53	0.4	426100	7642653
Dalton-08	<i>Willow sp.</i>	0.53	0.51	426107	7642652
Dalton-08	<i>Willow sp.</i>	0.7	0.4	426111	7642651
Dalton-08	<i>Willow sp.</i>	0.65	0.55	426113	7642649
Dalton-08	<i>Willow sp.</i>	0.7	0.51	426113	7642649
Dalton-08	<i>Willow sp.</i>	0.55	0.51	426116	7642651
Dalton-08	<i>Willow sp.</i>	0.68	0.43	426144	7642650
Dalton-08	<i>Willow sp.</i>	0.58	0.15	426145	7642649
Dalton-08	<i>Willow sp.</i>	0.6	0.24	426152	7642649
Dalton-08	<i>Willow sp.</i>	0.74	0.67	426163	7642648
Dalton-09	<i>Willow sp.</i>	0.94	4.55	396638	7617201
Dalton-09	<i>Willow sp.</i>	0.71	4.43	396655	7617200
Dalton-09	<i>Willow sp.</i>	1.52	2.17	396658	7617201
Dalton-09	<i>Willow sp.</i>	1.94	3.79	396658	7617201
Dalton-09	<i>Willow sp.</i>	1.13	2.62	396687	7617199
Dalton-09	<i>Willow sp.</i>	0.89	1.66	396700	7617198
Dalton-09	<i>Birch sp.</i>	0.84	0.93	396707	7617197
Dalton-09	<i>Willow sp.</i>	0.88	2.14	396707	7617197
Dalton-09	<i>Birch sp.</i>	0.63	2.9	396712	7617199

Site	Sp_genus	Canopy_height (m)	Crown_radius (m)	X (m)	Y (m)
Dalton-09	<i>Willow sp.</i>	0.66	2.45	396712	7617199
Dalton-09	<i>Willow sp.</i>	0.85	3.13	396727	7617196
Dalton-09	<i>Willow sp.</i>	1.05	3.33	396736	7617195
Dalton-09	<i>Birch sp.</i>	0.63	2.53	396746	7617200
Dalton-09	<i>Willow sp.</i>	0.56	3.79	396768	7617202
Dalton-09	<i>Birch sp.</i>	0.68	3.2	396777	7617202
Dalton-09	<i>Birch sp.</i>	0.7	2.63	396784	7617202
Dalton-09	<i>Birch sp.</i>	0.8	1.38	396788	7617202
Dalton-09	<i>Willow sp.</i>	0.74	1.45	396802	7617202
Dalton-09	<i>Willow sp.</i>	0.83	1.41	396829	7617199
Dalton-09	<i>Willow sp.</i>	0.65	1.25	396844	7617199
Dalton-09	<i>Willow sp.</i>	0.62	2.1	396848	7617200
Dalton-09	<i>Willow sp.</i>	0.64	0.43	396858	7617248
Dalton-09	<i>Willow sp.</i>	0.75	0.28	396858	7617248
Dalton-09	<i>Birch sp.</i>	0.52	0.56	396838	7617242
Dalton-09	<i>Willow sp.</i>	0.62	0.92	396831	7617239
Dalton-09	<i>Willow sp.</i>	0.68	0.88	396831	7617239
Dalton-09	<i>Willow sp.</i>	0.69	1.01	396822	7617238
Dalton-09	<i>Willow sp.</i>	0.68	2.68	396812	7617236
Dalton-09	<i>Willow sp.</i>	0.85	0.82	396806	7617235
Dalton-09	<i>Willow sp.</i>	0.69	1.21	396806	7617235
Dalton-09	<i>Willow sp.</i>	0.97	1.59	396806	7617235
Dalton-09	<i>Willow sp.</i>	1.09	1.38	396806	7617235
Dalton-09	<i>Willow sp.</i>	0.57	0.77	396806	7617235
Dalton-09	<i>Willow sp.</i>	0.75	1.39	396801	7617234
Dalton-09	<i>Willow sp.</i>	0.86	1.31	396796	7617235
Dalton-09	<i>Willow sp.</i>	1.1	2.06	396781	7617232
Dalton-09	<i>Willow sp.</i>	0.61	0.55	396768	7617231
Dalton-09	<i>Willow sp.</i>	0.58	0.49	396768	7617231
Dalton-09	<i>Willow sp.</i>	0.69	0.41	396768	7617231
Dalton-09	<i>Willow sp.</i>	0.74	2.18	396764	7617232
Dalton-09	<i>Willow sp.</i>	0.68	2.03	396754	7617232
Dalton-09	<i>Willow sp.</i>	0.62	1.22	396739	7617229
Dalton-09	<i>Willow sp.</i>	0.7	2.34	396679	7617245
Dalton-09	<i>Birch sp.</i>	0.53	0.56	396659	7617248
Dalton-09	<i>Birch sp.</i>	0.85	0.73	396666	7617307
Dalton-09	<i>Birch sp.</i>	0.53	3.27	396749	7617323

Site	Sp_genus	Canopy_height (m)	Crown_radius (m)	X (m)	Y (m)
Dalton-09	<i>Willow sp.</i>	0.5	1.93	396752	7617321
Dalton-09	<i>Birch sp.</i>	0.59	2.41	396769	7617320
Dalton-09	<i>Birch sp.</i>	0.5	0.71	396807	7617310
Dalton-09	<i>Birch sp.</i>	0.53	0.81	396807	7617310
Dalton-09	<i>Birch sp.</i>	0.69	0.86	396806	7617307
Dalton-09	<i>Birch sp.</i>	0.5	0.64	396828	7617307
Dalton-09	<i>Willow sp.</i>	0.57	0.35	396835	7617305
Dalton-09	<i>Willow sp.</i>	0.58	2.18	396840	7617301
Dalton-09	<i>Willow sp.</i>	0.79	1.47	396845	7617302
Dalton-09	<i>Willow sp.</i>	0.53	1	396848	7617301
Dalton-09	<i>Willow sp.</i>	0.51	1.27	396857	7617300
Dalton-09	<i>Willow sp.</i>	0.53	3.05	396848	7617348
Dalton-09	<i>Birch sp.</i>	0.69	0.46	396811	7617347
Dalton-09	<i>Birch sp.</i>	0.5	0.58	396773	7617344
Dalton-09	<i>Birch sp.</i>	0.51	1.95	396771	7617347
Dalton-09	<i>Birch sp.</i>	0.58	0.79	396760	7617346
Dalton-09	<i>Willow sp.</i>	0.55	0.49	396759	7617343
Dalton-09	<i>Willow sp.</i>	0.51	0.78	396752	7617344
Dalton-09	<i>Birch sp.</i>	0.56	1.96	396741	7617345
Dalton-09	<i>Willow sp.</i>	0.61	0.99	396739	7617349
Dalton-09	Not identified	0.8	0.41	396735	7617347
Dalton-09	<i>Willow sp.</i>	0.81	2.59	396729	7617347
Dalton-09	<i>Willow sp.</i>	0.64	1.83	396720	7617346
Dalton-09	<i>Birch sp.</i>	0.57	1.63	396697	7617345
Dalton-09	<i>Birch sp.</i>	0.87	0.43	396648	7617402
Dalton-09	<i>Birch sp.</i>	0.59	1.05	396657	7617399
Dalton-09	<i>Willow sp.</i>	0.5	0.47	396687	7617394
Dalton-09	<i>Willow sp.</i>	0.52	0.67	396706	7617393
Dalton-09	<i>Willow sp.</i>	0.5	1.2	396719	7617393
Dalton-09	<i>Willow sp.</i>	0.65	2.04	396724	7617394
Dalton-09	<i>Birch sp.</i>	0.53	1.02	396734	7617393
Dalton-09	<i>Willow sp.</i>	0.58	1.25	396747	7617394
Dalton-09	<i>Birch sp.</i>	0.55	0.48	396788	7617394
Dalton-09	<i>Birch sp.</i>	0.55	1.49	396791	7617392
Dalton-09	<i>Birch sp.</i>	0.57	1.68	396799	7617394
Dalton-09	<i>Birch sp.</i>	0.56	1.04	396819	7617392
Dalton-09	<i>Willow sp.</i>	0.56	1.16	396828	7617394

Site	Sp_genus	Canopy_height (m)	Crown_radius (m)	X (m)	Y (m)
Dalton-09	<i>Willow sp.</i>	0.86	2.23	396828	7617394
Dalton-09	<i>Birch sp.</i>	0.6	2.52	396836	7617395
Dalton-09	<i>Willow sp.</i>	0.55	1.88	396846	7617395
Dalton-09	<i>Birch sp.</i>	0.57	2.12	396850	7617398
Dalton-10	<i>Willow sp.</i>	0.69	1.09	402627	7615752
Dalton-10	<i>Willow sp.</i>	0.73	1.13	402627	7615752
Dalton-10	<i>Willow sp.</i>	0.65	1.79	402627	7615752
Dalton-10	<i>Willow sp.</i>	0.66	2.39	402610	7615755
Dalton-10	<i>Birch sp.</i>	1	0.48	402610	7615755
Dalton-10	<i>Birch sp.</i>	0.88	0.34	402610	7615755
Dalton-10	<i>Willow sp.</i>	0.63	1.39	402597	7615753
Dalton-10	<i>Willow sp.</i>	0.61	0.51	402592	7615754
Dalton-10	<i>Birch sp.</i>	0.58	0.71	402592	7615754
Dalton-10	<i>Willow sp.</i>	0.64	0.7	402537	7615750
Dalton-10	<i>Willow sp.</i>	0.64	0.44	402492	7615753
Dalton-10	<i>Willow sp.</i>	0.86	0.51	402449	7615696
Dalton-10	<i>Willow sp.</i>	0.57	0.81	402455	7615695
Dalton-10	<i>Willow sp.</i>	0.65	0.33	402461	7615694
Dalton-10	<i>Willow sp.</i>	0.78	1.27	402475	7615696
Dalton-10	<i>Willow sp.</i>	0.89	1.07	402475	7615696
Dalton-10	<i>Birch sp.</i>	0.55	0.74	402485	7615699
Dalton-10	<i>Birch sp.</i>	0.67	0.34	402488	7615698
Dalton-10	<i>Willow sp.</i>	0.72	0.35	402492	7615698
Dalton-10	<i>Birch sp.</i>	0.79	0.86	402604	7615692
Dalton-10	<i>Birch sp.</i>	0.6	0.65	402604	7615692
Dalton-10	<i>Birch sp.</i>	0.53	1.17	402609	7615693
Dalton-10	<i>Willow sp.</i>	0.63	0.93	402609	7615693
Dalton-10	<i>Birch sp.</i>	0.53	1.38	402614	7615694
Dalton-10	<i>Birch sp.</i>	0.67	0.62	402649	7615694
Dalton-10	<i>Willow sp.</i>	0.53	0.55	402628	7615650
Dalton-10	<i>Willow sp.</i>	0.68	0.66	402619	7615652
Dalton-10	<i>Willow sp.</i>	0.6	0.48	402619	7615652
Dalton-10	<i>Willow sp.</i>	0.5	0.28	402619	7615652
Dalton-10	<i>Willow sp.</i>	0.65	0.81	402586	7615652
Dalton-10	<i>Willow sp.</i>	0.5	1.43	402441	7615651
Dalton-10	<i>Willow sp.</i>	0.54	1.23	402441	7615651
Dalton-10	<i>Birch sp.</i>	0.63	1.34	402441	7615602

Site	Sp_genus	Canopy_height (m)	Crown_radius (m)	X (m)	Y (m)
Dalton-10	<i>Willow sp.</i>	0.67	0.4	402441	7615602
Dalton-10	<i>Birch sp.</i>	0.9	1.06	402441	7615602
Dalton-10	<i>Birch sp.</i>	0.52	1.08	402450	7615599
Dalton-10	<i>Birch sp.</i>	0.56	0.41	402464	7615599
Dalton-10	<i>Willow sp.</i>	0.56	0.32	402537	7615602
Dalton-10	<i>Birch sp.</i>	0.5	0.6	402584	7615600
Dalton-10	<i>Willow sp.</i>	0.74	0.75	402601	7615600
Dalton-10	<i>Birch sp.</i>	0.72	0.53	402601	7615600
Dalton-10	<i>Birch sp.</i>	0.5	0.45	402601	7615600
Dalton-10	<i>Willow sp.</i>	0.71	1.1	402601	7615600
Dalton-10	<i>Willow sp.</i>	0.58	1.43	402601	7615600
Dalton-10	<i>Birch sp.</i>	0.66	0.69	402605	7615599
Dalton-10	<i>Birch sp.</i>	0.74	0.79	402605	7615599
Dalton-10	<i>Willow sp.</i>	0.69	0.83	402657	7615601
Dalton-10	<i>Birch sp.</i>	0.86	0.77	402563	7615555
Dalton-10	<i>Birch sp.</i>	0.8	0.76	402563	7615555
Dalton-10	<i>Birch sp.</i>	0.78	0.76	402563	7615555
Dalton-10	<i>Birch sp.</i>	0.65	1.09	402556	7615556
Dalton-10	<i>Birch sp.</i>	0.53	0.74	402556	7615556
Dalton-10	<i>Birch sp.</i>	0.5	0.38	402556	7615556
Dalton-10	<i>Willow sp.</i>	0.57	0.68	402445	7615551
Dalton-10	<i>Willow sp.</i>	0.54	0.45	402445	7615551
Dalton-10	<i>Birch sp.</i>	0.57	0.55	402445	7615551
Dalton-10	<i>Birch sp.</i>	0.78	0.4	402439	7615549
Dalton-11	<i>Dasiphora sp.</i>	0.54	0.3	396444	7616981
Dalton-11	<i>Birch sp.</i>	0.5	0.51	396444	7616978
Dalton-11	<i>Willow sp.</i>	0.58	0.42	396461	7616984
Dalton-11	<i>Birch sp.</i>	0.51	0.5	396517	7616979
Dalton-11	<i>Birch sp.</i>	0.6	1.14	396521	7616980
Dalton-11	<i>Birch sp.</i>	0.55	0.68	396534	7616976
Dalton-11	<i>Willow sp.</i>	0.82	0.99	396543	7616976
Dalton-11	<i>Willow sp.</i>	0.54	0.69	396548	7616980
Dalton-11	<i>Willow sp.</i>	0.52	0.3	396560	7616980
Dalton-11	<i>Willow sp.</i>	0.68	0.82	396563	7616980
Dalton-11	<i>Willow sp.</i>	0.55	0.43	396576	7616979
Dalton-11	<i>Birch sp.</i>	0.53	0.87	396586	7616981
Dalton-11	<i>Birch sp.</i>	0.7	0.37	396589	7616981

Site	Sp_genus	Canopy_height (m)	Crown_radius (m)	X (m)	Y (m)
Dalton-11	<i>Birch sp.</i>	0.79	0.62	396589	7616983
Dalton-11	<i>Willow sp.</i>	0.59	1.08	396448	7617015
Dalton-11	<i>Birch sp.</i>	0.68	0.75	396384	7617081
Dalton-11	<i>Birch sp.</i>	0.51	0.7	396384	7617079
Dalton-11	<i>Birch sp.</i>	0.69	1.04	396384	7617079
Dalton-11	<i>Willow sp.</i>	0.62	0.54	396393	7617079
Dalton-11	<i>Willow sp.</i>	0.86	1.27	396561	7617063
Dalton-11	<i>Willow sp.</i>	0.67	0.94	396565	7617063
Dalton-11	<i>Willow sp.</i>	0.73	0.65	396383	7617181
Dalton-11	<i>Willow sp.</i>	0.61	0.75	396437	7617169
Dalton-11	<i>Willow sp.</i>	0.53	0.15	396437	7617169
Dalton-11	<i>Willow sp.</i>	0.58	0.7	396442	7617168
Dalton-11	<i>Willow sp.</i>	0.76	0.39	396510	7617170
Dalton-11	<i>Willow sp.</i>	0.62	0.29	396519	7617168
Dalton-11	<i>Willow sp.</i>	0.53	0.76	396521	7617170
Dalton-11	<i>Willow sp.</i>	0.84	1.17	396596	7617129
Dalton-11	<i>Birch sp.</i>	0.72	0.58	396591	7617127
Dalton-11	<i>Willow sp.</i>	0.8	0.54	396587	7617131
Dalton-11	<i>Willow sp.</i>	0.56	0.52	396513	7617125
Dalton-11	<i>Willow sp.</i>	0.54	0.57	396506	7617123
Dalton-11	<i>Birch sp.</i>	0.78	0.96	396487	7617127
Dalton-11	<i>Birch sp.</i>	0.51	0.39	396475	7617126
Dalton-11	<i>Birch sp.</i>	0.53	0.84	396474	7617123
Dalton-12	-999	-999	-999	-999	-999

B.3. Field data estimates per site after using the belt transect equations. The column headers mean: *Site*, field site surveyed; *X* and *Y*, the coordinate location of the site center in Albers Conical Equal Area grid, . A value of -999 represents that there were no shrubs to survey at that site.

Site	Number_of_Shrubs_per_unit_area	Canopy_height_mean	Crown_radius_mean	Shrub_area_fraction	X	Y
Colville-01	18	1.22	1.142	0.001	98250	2190000
Colville-02	1520	1.582	1.007	0.126	102500	2187250
Colville-03	365	1.231	0.986	0.026	97750	2172250
Colville-04	810	1.516	1.205	0.097	97750	2171000
Colville-05	990	1.919	0.982	0.064	87750	2128750
Colville-06	795	1.648	0.958	0.051	86750	2128250
Colville-07	500	1.267	0.819	0.034	89750	2120000
Colville-08	540	1.028	0.787	0.021	89500	2119000
Colville-09	480	0.999	0.669	0.014	81500	2095500
Colville-10	810	1.659	1.077	0.081	81000	2092000
Colville-11	465	1.581	0.939	0.033	78000	2092500
Colville-12	810	1.595	1.029	0.071	70000	2090500
Colville-13	405	1.983	1.184	0.055	69750	2090000
Colville-14	280	0.765	0.75	0.009	69250	2088250
Dalton-01	40	0.583	0.398	0	203250	2216500
Dalton-02	10	0.61	0.36	0	203500	2216750
Dalton-03	830	0.572	0.502	0.013	213750	2178750
Dalton-04	820	0.603	0.504	0.018	214000	2179000
Dalton-05	200	0.583	0.357	0.001	207750	2128250
Dalton-06	810	0.796	0.523	0.05	208250	2128000
Dalton-07	290	0.583	0.417	0.004	209750	2110750
Dalton-08	910	0.637	0.452	0.014	209750	2110250
Dalton-09	870	0.695	0.919	0.118	183000	2082250
Dalton-10	570	0.656	0.529	0.023	189000	2081250
Dalton-11	360	0.63	0.67	0.009	182750	2082000
Dalton-12	0	0	0	0	188500	2081250

Appendix C

C.1. List of paths, orbits, and blocks of MISR imagery, downloaded for the period June15 - July 31 for the year 2010, used for the training and validation of the BRT model.

Path	Orbit	Blocks
065	55913	35-38
	56146	35-38
	56379	35-38
066	56015	34-38
	56248	34-38
067	55884	34-38
	56117	34-38
	56350	34-38
068	55986	34-38
	56219	34-38
	56452	34-38
069	55855	34-38
	56088	34-38
	56321	34-38
070	55957	34-38
	56190	34-38
	56423	34-38
071	55826	33-38
	56059	33-38
	56292	33-38
072	55928	33-38
	56161	33-38
	56394	33-38
073	56263	33-38
074	55899	33-38
	56132	33-38
	56365	33-38
075	56001	33-38
	56234	33-38
	56467	33-38

Path	Orbit	Blocks
076	55870	33-38
	56103	33-38
	56336	33-38
077	55972	33-38
	56205	33-38
	56438	33-38
078	55841	33-38
	56074	33-38
	56307	33-38
079	55943	33-38
	56176	33-38
	56409	33-38
080	55812	32-38
	56045	32-38
	56278	32-38
081	55914	32-38
	56147	32-38
	56380	32-38
082	56016	32-38
	56249	32-38
083	55885	32-38
	56118	32-38
	56351	32-38
084	55987	32-38
	56220	32-38
	56453	32-38
085	56322	33-35

Appendix D

D.1. List of paths, orbits, and blocks of MISR imagery, downloaded for the period June 1 - August 15 for the year 2000, used for construction of the 2000 fractional cover map.

Path	Block	Orbits (Good imagery available out of five potential orbits)
065	35-38	2556, 3022
066	34-38	2658, 2891, 3124
067	34-38	2527, 2760, 2993, 3226, 3459
068	34-38	2862, 3095, 3328
069	34-38	2498, 2731, 2964, 3430
070	34-38	2833, 3299
071	33-38	2469, 2702, 2935, 3168
072	33-38	3037, 3270, 3503
073	33-38	2906, 3139
074	33-38	2542, 2775, 3008, 3241
075	33-38	n/a
076	33-38	2513, 2746, 2979, 3212
077	33-38	2615, 2848, 3314
078	33-38	2717, 2950
079	33-38	2819, 3052
080	32-38	2688, 2921, 3154
081	32-38	2557, 3023, 3256
082	32-38	2659, 2892, 3125
083	32-38	2528, 2761, 2994, 3227
084	32-38	3096
085	33-35	2499, 2732, 2965
086	33-35	2834

D.2. List of paths, orbits, and blocks of MISR imagery, downloaded for the period June 1 - August 15 for the year 2001, used for construction of the 2000 fractional cover map.

Path	Block	Orbits (Good imagery available out of five potential orbits)
065	35-38	8148, 8381, 8614
066	34-38	8017, 8250, 8483, 8716
067	34-38	7886, 8119, 8352, 8585
068	34-38	7755, 8221, 8687
069	34-38	7857, 8090, 8323, 8556, 8789
070	34-38	7959, 8192, 8425, 8658
071	33-38	7828, 8061, 8294, 8527
072	33-38	8163, 8396, 8629
073	33-38	7799, 8032, 8265, 8498, 8731
074	33-38	7901, 8134, 8367, 8600
075	33-38	7770, 8469, 8702
076	33-38	7872, 8105, 8338
077	33-38	7741, 8207, 8673
078	33-38	7813, 8076, 8309, 8542
079	33-38	7945, 8178, 8411, 8644
080	32-38	7814, 8047, 8280, 8513, 8746
081	32-38	7916, 8149
082	32-38	8018, 8484, 8717
083	32-38	7887, 8120, 8353, 8586, 8819
084	32-38	7756, 8455, 8688
085	33-35	7858, 8324
086	33-35	7727, 8426

D.3. List of paths, orbits, and blocks of MISR imagery, downloaded for the period June 1

- August 15 for the year 2002, used for construction of the 2000 fractional cover map.

Path	Block	Orbits (Good imagery available out of five potential orbits)
065	35-38	13274, 13507, 13740, 13973
066	34-38	13143, 13376, 13609, 13842, 14075
067	34-38	13245, 13478, 13711, 13944
068	34-38	13114, 13347, 13580, 13813, 14046
069	34-38	13216, 13682, 13915
070	34-38	13318, 13551, 13784, 14017
071	33-38	13187, 13420, 13653, 13886, 14119
072	33-38	13056, 13289, 13522, 13755, 13988
073	33-38	13158, 13391, 13624, 14090
074	33-38	13260, 13493, 13726, 13959
075	33-38	13129, 13362, 13828
076	33-38	13231, 13464, 13697, 13930
077	33-38	13100, 13333, 14032
078	33-38	13202, 13668, 13901, 14134
079	33-38	13071, 13304, 13770, 14003
080	32-38	13173, 13406, 13639, 13872, 14105
081	32-38	13275, 13508, 13741, 13974
082	32-38	13377, 13610, 13843, 14076
083	32-38	13246, 13479, 13712, 13945
084	32-38	13115, 13348, 13581, 13814
085	33-35	13683, 13916
086	33-35	13086, 13319

Appendix E

E.1. List of paths, orbits, and blocks of MISR imagery, downloaded for the period June 1 - August 15 for the year 2010, used for construction of the 2010 fractional cover map.

Path	Block	Orbits (Good imagery available out of five potential orbits)
065	35-38	55680, 55913, 56146, 56612
066	34-38	55782, 56015, 56481
067	34-38	55651, 55884, 56117, 56350
068	34-38	55753, 55986, 56685
069	34-38	55622, 55855, 56088
070	34-38	55724, 55957, 56190, 56423
071	33-38	56059, 56525
072	33-38	55695, 55928, 56161, 56394
073	33-38	55797, 56030, 56496
074	33-38	55666, 55899, 56365
075	33-38	55768, 56001
076	33-38	55637, 55870, 56336
077	33-38	55739, 55972, 56205
078	33-38	55608, 55841, 56074
079	33-38	55710, 55943, 56176, 56409
080	32-38	55812, 56045, 56511
081	32-38	55681, 55914, 56147, 56380, 56613
082	32-38	55783, 56016, 56249, 56482
083	32-38	55652, 55885, 56118
084	32-38	55754, 55987, 56220
085	33-35	55623, 55856, 56322
086	33-35	None

E.2. List of paths, orbits, and blocks of MISR imagery, downloaded for the period June 1

- August 15 for the year 2011, used for construction of the 2010 fractional cover map.

Path	Block	Orbits (Good imagery available out of five potential orbits)
065	35-38	61039, 61272, 61505, 61971
066	34-38	61141, 61374, 61607, 61840
067	34-38	61010, 61243, 61476
068	34-38	61112
069	34-38	60981, 61447, 61680
070	34-38	61316, 61549
071	33-38	60952, 61185, 61418, 61651, 61884
072	33-38	61054, 61287, 61753
073	33-38	60923, 61156, 61389, 61622, 61855
074	33-38	61025, 61258, 61491, 61724, 61957
075	33-38	61127
076	33-38	60996, 61229, 61462, 61695, 61928
077	33-38	61098, 61331, 61564
078	33-38	60967, 61200, 61433, 61666
079	33-38	61069, 61302, 62001
080	32-38	60938, 61171, 61404, 61637
081	32-38	61040, 61273, 61506, 61739
082	32-38	61142, 61608
083	32-38	61011, 61477, 61710
084	32-38	61113, 61346
085	33-35	60982, 61448, 61681
086	33-35	61084, 61317, 61783

APPENDIX F

PREFACE

“This Doctoral Dissertation was produced in accordance with guidelines which permit the inclusion as part of the Doctoral Dissertation the text of an original paper, or papers, submitted for publication. Doctoral Dissertation must still conform to all other requirements explained in the “Guide for the Preparation of the Doctoral Dissertation at The Montclair State University.” It must include a comprehensive abstract, a full introduction and literature review, and a final overall conclusion. Additional material (procedural and design data as well as descriptions of equipment) must be provided in sufficient detail to allow a clear and precise judgment to be made of the importance and originality of the research reported.

It is acceptable for this Doctoral Dissertation to include as chapters authentic copies of papers already published, provided these meet type size, margin, and legibility requirements. In such cases, connecting texts, which provide logical bridges between different manuscripts, are mandatory. Where the student is not the sole author of a manuscript, the student is required to make an explicit statement in the introductory material to that manuscript describing the student’s contribution to the work and acknowledging the contribution of the other author(s). The signatures of the Supervising Committee which precede all other material in the Doctoral Dissertation attest to the accuracy of this statement.”

Duchesne, R.R., Chopping, M.J., & Tape, K.D. (2015). NACP woody vegetation characteristics of 1,039 sites across the North Slope, Alaska. Data set. Available online [<http://daac/ornl.gov/>] from Oak Ridge National Laboratory Distributed Active Archive Center, Oak Ridge, Tennessee, USA.

Duchesne, R.R., Chopping, M.J., & Tape, K.D. (2015). Capability of the CANAPI algorithm to derive shrub structural parameters from satellite imagery in the Alaskan Arctic. *Polar Record*. [Accepted].

VITA

Ms. Duchesne-Onoro was born in Barranquilla, Colombia. She earned a B.S. in Biology from the Universidad del Atlantico, Colombia in 2005, and an M.S. in Statistics from Montclair State University in 2010. She joined the Environmental Management doctoral program at Montclair State University in 2010. Her research focused on mapping shrub expansion in Arctic tundra using remote sensing. Ms. Duchesne-Onoro's research was possible thanks to a NASA-sponsored research project in which Professor Mark Chopping was the Principal Investigator. As part of the project, she has participated in two field expeditions to Alaska, the most recent of which was partially funded by a grant she received from the Geological Society of America. Ms. Duchesne-Onoro was also a teaching assistant at Montclair State University and an adjunct faculty at Sussex County Community College. She has written several chapters that have been published in the *Biomes and Ecosystems: An Encyclopedia*. She has also authored a data product for the North America Carbon Program and one peer-reviewed journal article. In addition, Ms. Duchesne-Onoro has presented at several national and international conferences. She is currently a member of the Geological Society of America and is working as an assistant professor in the Department of Geography and Geology at the University of Wisconsin-Whitewater.

This Page Intentionally Left Blank